delivering benefits through evidence

source   pathway   receptor

Coastal flood boundary conditions for UK mainland and islands

Project: SC060064/TR3: Design swell waves

Flood and Coastal Erosion Risk Management Research and Development Programme

The Environment Agency is the leading public body protecting and improving the environment in England and Wales.

It's our job to make sure that air, land and water are looked after by everyone in today's society, so that tomorrow's generations inherit a cleaner, healthier world.

Our work includes tackling flooding and pollution incidents, reducing industry's impacts on the environment, cleaning up rivers, coastal waters and contaminated land, and improving wildlife habitats.

This report is the result of research commissioned by the Environment Agency's Evidence Directorate and funded by the joint Environment Agency/Defra Flood and Coastal Erosion Risk Management Research and Development Programme.
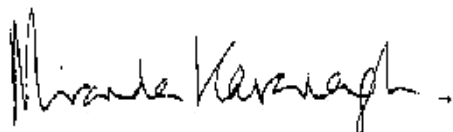
Evidence at the Environment Agency

Evidence underpins the work of the Environment Agency. It provides an up-to-date understanding of the world about us, helps us to develop tools and techniques to monitor and manage our environment as efficiently and effectively as possible. It also helps us to understand how the environment is changing and to identify what the future pressures may be.

The work of the Environment Agency's Evidence Directorate is a key ingredient in the partnership between research, guidance and operations that enables the Environment Agency to protect and restore our environment.

The Research & Innovation programme focuses on four main areas of activity:

- **Setting the agenda**, by providing the evidence for decisions;

- **Maintaining scientific credibility**, by ensuring that our programmes and projects are fit for purpose and executed according to international standards;

- **Carrying out research**, either by contracting it out to research organisations and consultancies or by doing it ourselves;

- **Delivering information, advice, tools and techniques**, by making appropriate products available.

Miranda Kavanagh

Director of Evidence

Executive summary

Successful risk-based flood and coastal erosion risk management requires the best available information on coastal flood boundary conditions, such as for sea levels and swell waves. Current information is not consistent around the country and is becoming out of date.

In April 2008 the Environment Agency took on the strategic overview of coasts in England, giving it an overarching role in the management of the English coastline.

The Environment Agency R&D project *Coastal flood boundary conditions for UK mainland and islands* was set up to develop and apply improved methods to update these important datasets, using a longer data record.

The aims of the project were to:

- Provide a consistent set of swell wave designs around the coasts of England, Wales and Scotland, updating earlier advice given in the 1997 HR Wallingford report SR409, *Swell and bi-model wave climate around the coast of England and Wales*[1].

- Practice guidance on how to use this new dataset.

This report presents the findings from the swell wave studies, together with a description of the data used and methodology applied. The detailed results are available in GIS format. The practical guidance can be found in a separate document (R&D SC060064/TR5 - *Practical guidance swell waves*).

Key outputs from the project may be summarised as follows:

- Swell wave heights of annual exceedance probability from 100 to 0.1 per cent (average return period one in one year to one in 1,000 years) related to six sectors of wave direction.

- A relationship between swell wave height and the corresponding wave period.

The above parameters are given at points along a chainage line around the UK coast. The points are set broadly along a contour line of 50-m water depth, though in the shallower waters of the North Sea an approximate contour line of 20-m water depth is used.

For flooding and coastal protection, both wind waves and swell waves need to be considered when identifying the worst case scenario for flooding or damage due to wave action. This project only considered swell waves; however, analysis of wind waves should also be taken into consideration.

Data for this project was obtained from the UK Met Office and UK Coastal Monitoring and Forecasting (UKCMF); the latter data was sourced via the Cefas Wavenet[3] website. The Met Office data was hindcast model data, providing a continuous record of modelled wave data around the coastline. The UKCMF data was observed wave buoy data from a number of wave buoys deployed around the coastline. Ideally, observed data would be the primary data used for this analysis. However, given the limited coverage and sporadic wave data records at most sites, it was not possible to provide swell wave conditions with any degree of confidence using observed data only.

In practice we used the Met Office data for our analysis, though we compared Met Office data with observed data where possible. In doing so, we checked that the respective wave buoys were deployed in suitably deep water to be consistent with the Met Office data used here.

Estimates of design swell wave characteristics were made by statistical analysis of the eight years Met Office hindcast modelled data. This gave values at three-hour intervals on a 12-km

grid. We did not analyse the data from every grid point, but chose those points that matched our intention of providing deep water values along a single chainage line around the UK coast.

The analysis used a distribution specifically tailored to represent the upper tail, specifically the Generalised Pareto Distribution (GPD). In this process, a threshold is selected to determine the boundary between typical values and the upper tail, with the GPD used to model the distribution of values greater than the threshold.

The statistical method was developed using eight test sites around the coast of England, Scotland and Wales, each of which represented a site at which swell would be significant.

We did not remove any data which show high variability compared to neighbouring sites. Instead, we analysed the number of occurrences of swell, depth at the location, regional geography and statistical fit to the tail of the data and provided comments for the user to decide whether to use the data.

The results naturally vary around the coastline due to factors such as depth, sheltering effects, prevailing weather directions and number of swell occurrences used to fit the statistical distribution. Another factor that is inherited in the results is the accuracy of the modelled data used to create these results.

In the future when data from the new Met Office model configuration, Wavewatch III, becomes available, there is an opportunity to assess whether the current model data can be pooled with the new model data. It is reasonable to expect that our selected GPD model for the tail of wave heights will be a good choice of statistical model for the new dataset, given its theoretical justification.

Acknowledgements

Contents

List of figures

1 Introduction

1.1 Background

Successful risk-based flood and coastal erosion risk management requires the best available information on coastal flood boundary conditions, such as sea levels and swell waves. Current information is not consistent around the country and is becoming out of date.

In April 2008, the Environment Agency took on the strategic overview of coasts in England, giving it an overarching role in the management of the English coastline.

The Environment Agency R&D project *Coastal flood boundary conditions for UK mainland and islands* was set up to develop and apply improved methods to update these important dataset, using a longer data record.

The aims of the project were to:

- Provide a consistent set of swell wave extremes around the coasts of England, Wales and Scotland, updating earlier information given in the 1997 HR Wallingford report SR409, *Swell and bi-model wave climate around the coast of England and Wales*[1].
- Offer practical guidance on how to use this new dataset.

This report presents the findings from the swell wave studies, together with a description of the data used and methodology applied. The detailed results are available in GIS format. The practical guidance can be found in a separate document (R&D SC060064/TR5 - *Practical guidance swell waves*).

This project was carried out as part of the Environment Agency/Department for Environment, Food and Rural Affairs joint Flood and Coastal Risk Research and Development programme.

The work was conducted by a project team led by Royal Haskoning in collaboration with Professor Jonathan Tawn.

The Environment Agency Project Executive was Angela Scott; the Environment Agency's Business User was Tim Hunt and the Environment Agency Project Manager was Stefan Laeger.

The Project Director for Royal Haskoning was Fola Ogunyoye; their Project Manager was Alastair McMillan.

The project was supported by the Scottish Environment Protection Agency (SEPA).

1.2 Current practices and the need for change

Existing nationally available information on swell waves is found in the HR Wallingford report SR409.

The information provided in Report SR409 was based on four years of wave data. We felt it appropriate to improve on the previous work using a longer wave record, simultaneously taking advantage of better statistical techniques now available.

The work reported here provides the intended improvements. It also extends the coverage of swell wave information around the UK coast by including Scotland.

Swell wave values generated by this project, and the associated methodology used to derive them, update the findings given in Report SR409 and provide, at the time of writing, the best available information on a national scale.

The outputs of this project provide improved information on offshore swell wave parameters around the coast. This information is needed to support successful risk-based management of flooding and coastal erosion. It can inform a wide range of decisions, including:

- coastal design
- flood forecasting
- flood risk mapping
- spatial planning.

1.3   Study area

This project has produced swell wave parameters for a sequence of points along a chainage around the coast of England, Scotland and Wales.

Discrete chainages have also been included for the following locations:

- Shetland Isles
- Inner Hebrides
- West Coast of the Isle of Man
- Bristol Channel.

Figure 1.1 shows the main coastal chainages and the discrete chainages for these locations. These figures can be found at the end of this document.

1.4   Summary of outputs

Key outputs from the project may be summarised as follows:

- Swell wave heights of annual exceedence probability ranging from 100 to 0.1 per cent (average return period one in one year to one in 1,000 years) related to six sectors of wave direction.
- A relationship between swell wave height and the corresponding wave period.
- The above parameters are given at points along a chainage line around the UK coast. The points are set broadly along a contour line of 50-m water depth, though in the shallower waters of the North Sea an approximate contour line of 20-m water depth is used.

This project provides estimates of swell wave height and period for relatively deep water offshore. As the waves propagate inshore, shallow water effects will become significant. It is these shallow water effects that cause the waves to break. Therefore, the user must consider the transformation process as the waves move from deep water conditions to shallow water conditions near the shoreline.

For flooding and coastal protection, both wind waves and swell waves need to be considered when identifying the worst case scenario for flooding or damage due to wave action. This project only considered swell waves; however, analysis of wind waves should also be taken into consideration.

It is important to account for both components of the wave process in coastal design. Larger waves (in terms of wave height) will typically be wind waves, whereas waves with the longest

period will typically be swell waves. Given these different characteristics, consideration of individual components is required rather than the use of a combined, resultant wave in design.

Note 1

Extreme swell wave heights are considered accurate to one decimal place

Extreme swell wave heights provided in this project can be considered accurate to one decimal place. Two decimal places have been provided to differentiate between nodes on the chainage. This does not infer greater accuracy and the user should be mindful of this when selecting a node for an extreme swell wave height.

Note 2

Definition of annual exceedance probability

Annual exceedance probabilities (AEP) describe the likelihood of being exceeded in any given year. AEPs can also be expressed as chance. For instance an AEP of one per cent has a chance of being exceeded of one in 100 in any given year. In coastal design this often termed 'return period'.

Note 3

How to obtain the data

The data produced by this project can be obtained for *Environment Agency statutory purposes* under licence through the Environment Agency Customer Contact Centre (www.environment-agency.gov.uk/contactus/default.aspx).

1.5   Definition of wave characteristics and swell

Through observation of waves, a number of features can be easily measured. These are summarised over a time interval by the following statistics:

- significant wave height;
- zero crossing wave period;
- mean wave direction.

Throughout the report, we term these statistics **wave height**, **wave period** and **wave direction**.

When a wind starts blowing on the sea surface wind energy is transferred to the sea, creating waves. The waves will first appear as ripples, having a short wave period, before gradually develop in height and period depending on the strength and duration of the wind. There is a continuum from ripples to small waves to large waves as they grow and similarly as they decay.

Waves are commonly divided into wind waves and swell waves. A standard interpretation of these waves is that wind waves are generated by local winds, while swell waves are generated

over a larger region and are due to energy transfer to lower frequency waves as wind-sea wave events decay. The swell waves are created by wind blowing over an area some distance away for some hours prior to travelling to the area of interest. When the characteristics of both wind-sea and swell waves are combined, the net characteristics are termed the resultant wave.

Readers should note that the term "wind waves" is used in this report as the more common parlance for what are also called "wind-sea" waves.

Swell can be identified by examining the frequency spectrum (Joosten and Noteborn, 2009)[2], where wind-sea waves and swell show up as two distinct peaks or 'modes' (see the example shown as **Figure 1.2**). Each frequency mode will in general have a direction which helps identify it as a separate wave field. In Figure 1.2, the wind-sea waves come from the east, whereas the swell direction is northwest. There is a sharp transition at 0.12 Hz (eight-second wave period) and the frequency bimodality is seen.
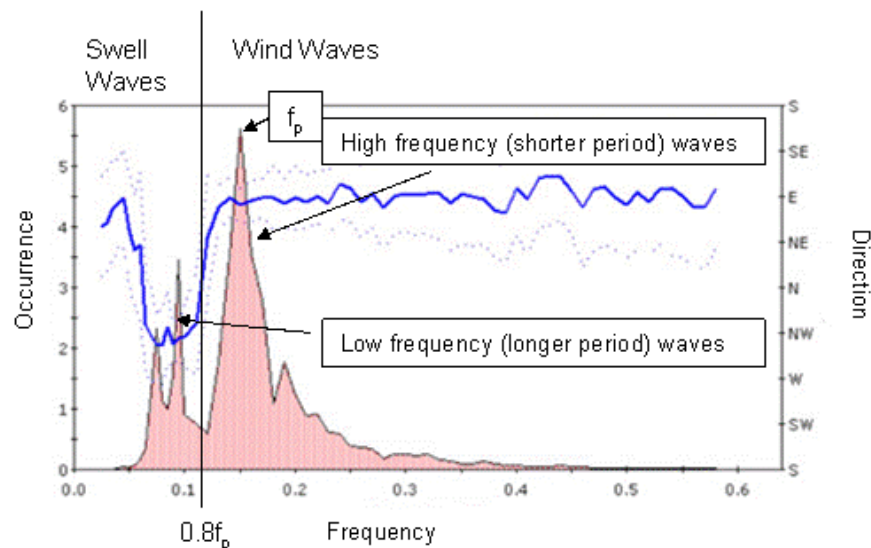

Figure 1.2 Typical bi-modal wave spectra

This project used Met Office hindcast model data on swell, wind and resultant wave characteristics based on pre-determined Met Office definitions. The UK Met Office (UKMO) Wave Model uses the following definition for the separation of wind-sea from swell, where f and f_p are the individual spectral frequency and spectral peak frequency respectively, see **Figure 1.2**, and α is the difference between the wave direction and the wind direction:

- UKMO Definition 1: $f > 0.8f_p$

Waves with a frequency greater than 80 per cent of the peak frequency are classed as wind waves. This can also be expressed as waves with a period shorter than 125 per cent of the most frequent wave period.

- UKMO Definition 2: $|\alpha| < 90°$

Waves where the difference between the wave direction and wind direction is less than 90° are classed as wind waves.

"UKMO Definition 2" introduces a possibility that waves classified as wind waves may include long-period waves (swell) if the direction of real swell is the same as the direction of the local wind. This is particularly the case along the UK west coast where the swell from Atlantic Ocean shares the same direction as the predominant wind. This finding is reflected in the analysis of wave roses, as shown in **Appendix 1**.

The Met Office classifies waves as swell if both of the criteria set out above apply.

The UK Met Office does not archive results of wave forecasts in full spectra. Without re-running their model, it is not possible to change the above inherited definitions.

1.6   Importance of swell

The relevance of swell waves to coastal flood risk and the design of coastal structures arises from their wave period, which is longer than for wind waves. Associated with the longer period is an increase in the power of waves. Thus, swell waves can be very damaging to coastal structures. Their long wave period also means that wave run-up and wave overtopping will be much greater than for wind waves of equivalent wave height.

A notable example of the damage caused by swell arose in Lyme Bay, Dorset, on 13 February 1979. The prevailing wind was an easterly breeze and the sea was fairly calm. At this time, swell waves entered the English Channel from the Atlantic Ocean, the swell having been generated by an earlier intense storm off Newfoundland, Canada. The swell was recorded as having a wave height of seven to eight metres and a period of 18 seconds. When the swell reached the eastern end of Lyme Bay, it rapidly breached the shingle mass of Chesil Beach as well as causing extensive damage to buildings and roads on the Isle of Portland. The dominant characteristic creating such extensive damage was the long wave period. Wave heights of seven to eight metres are not infrequent in the English Channel but are usually associated with wind waves of up to eight seconds in period.

It is recommended that the consequence of swell waves is taken into account alongside consideration of the (more common) wind wave conditions. It will normally be adequate to evaluate the two cases (swell waves/wind waves) separately. Joint probability scenarios can treat the occurrence of swell as having no, or low, correlation to the occurrence of wind waves, as described in **Section 3**.

1.7   Additional criteria for swell waves

Previous analysis of swell waves for Report SR 409 identified a small proportion of swell records which were considered to be inappropriate for use in coastal engineering applications, attributed to the slightly arbitrary definition of swell used by the Met Office. Therefore, additional criteria were developed and applied to validate the use of swell records.

Following a review of these criteria (see **Appendix 2**) we retained a filtering based on wave steepness but concluded that other forms of filtering were unnecessary.

2　Data

2.1　Introduction

Data for this project was obtained from the UK Met Office and UKCMF; the latter data was sourced via the Cefas Wavenet[3] website. The Met Office data was hindcast model data, providing a continuous record of modelled wave data around the coastline. The UKCMF data was observed wave buoy data from a number of wave buoys deployed around the coastline. Ideally, observed data would be the primary data used for this analysis. However, given the limited coverage and sporadic wave data records at most sites, it was not possible to provide swell wave conditions with any degree of confidence using observed data only.

In practice we used Met Office data for our analysis, though we compared Met Office data with observed data where possible. In doing this, we ensured that the respective wave buoys were deployed in suitably deep water to be consistent with the Met Office data used in this project.

2.2　Model data

The Met Office UK Waters wave model is forced using hourly surface winds from global and regional scale numerical weather prediction models. The Met Office model yields outputs at coastal and open sea points. In order to ensure we used relatively deep water output points which best represented offshore wave conditions, we used model output from open sea grid points only. Further details of the Met Office modelling on which we based our analysis can be found in **Appendix 3**.

The Met Office model provided hindcast wave data, from August 2000 to December 2008, at three-hourly intervals on a 12-km grid. The outputs of this model were wind waves, swell and resultant (wind waves and swell combined) significant wave height, mean zero crossing wave period and wave direction. The model also provided wind speeds and wind direction, as distinct to wave direction, at three-hour intervals. We are aware that there was no hindcast data for the entire month of November 2006, due to an issue identified by the Met Office.

The Met Office also has the following data which was not used in this project:

- European Wave Model 1994-2000.
- Wavewatch III North Atlantic European (NAE) Wave Model Data – Operational since January 2009.

Use of the European Wave Model data was beyond the scope of this project. The Wavewatch III data was not used because of the limited statistical benefit of incorporating this additional short data series.

2.3　Observed data

Measurement of wave data using wave buoys is particularly useful as buoys provide detailed site-specific information. However, they are rarely deployed in an appropriate location for a sufficient length of time to record the rarer, more extreme events at the point of interest. Visual observations are available from ships, but these are carried out at a single point in time rather than as more continuous information covering a wide area of sea, so this form of data was not used here.

Observed wave data was obtained for the following wave buoys:

- Scarweather (30 m depth)
- Liverpool Bay (22 m depth)
- Firth of Forth (65 m depth)
- Tyne/Tees (65 m depth)
- West Gabbard (34 m depth)
- Hastings (36 m depth).

These sites were selected because of their proximity to Met Office model data points we wished to use; thus, they would offer the best comparison between the synthetic hindcast data and observations from wave buoys. They also provide good coverage of the UK coast. Their location is shown on **Figure 2.1**.

The comparison shows a good match for significant wave height between observed and modelled wave data at the six validation sites. The peak occurrences are similar, with the largest difference of 0.4 m at West Gabbard.

The comparison shows a more variable match between modelled and observed zero crossing wave periods at the six validation sites. In general, the peak zero crossing wave period difference is up to half a second between the observed and modelled data. At West Gabbard and Hastings there is a larger difference, with the peak observed zero crossing periods one second higher than modelled data at West Gabbard and 1.5 seconds higher at Hastings.

Appendix 4 contains further details of the comparison between observed and modelled data

2.4   Data validation

Our analysis was based on Met Office hindcast modelled wave data. We carried out validation checks on this synthetic data to confirm its acceptability for the project and to identify potential weaknesses that might reduce confidence in the ultimate project output.

The validation checks were in two forms: comparison with wave conditions as observed at the six wave buoys noted earlier; and plotting wave roses to assess the general plausibility of the wave distributions these showed.

Validation of Met Office model output with wave buoy data showed a good match for significant wave height between observed and modelled data. The comparison showed a variable match between modelled and observed zero crossing wave periods at the six validation sites. In general, the zero crossing wave period difference was up to half a second between the observed and modelled data. Details of the checks can be found in **Appendix 4**.

Wave roses were plotted for eight test sites around the coast. They were used to visually check the directional spread and subsequent magnitude of swell waves. Wave roses divide wave data into direction bands and colour code by wave height. An example is presented in **Figure 2.2**, showing swell directions and magnitudes of wave height for a site off the south coast of Cornwall. This shows the dominant swell directions are from the west (270°N) and south west (240°N), that is, swell propagating from the Atlantic Ocean.
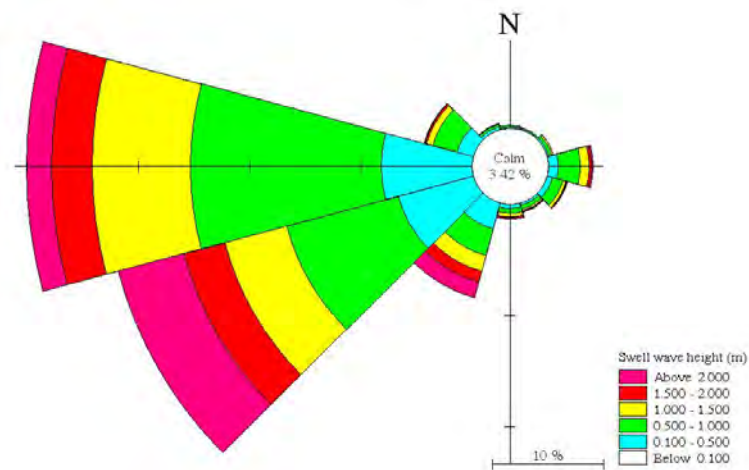
Figure 2.2 – Example of a wave rose showing magnitude and occurrence of swell wave heights for directional sectors

The wave roses show higher magnitude and frequencies of swell waves with increased exposure to long fetches, such as for sites exposed to the Atlantic Ocean and in the northern North Sea. This implies that, in principle, the model results accord with what one would expect.

In comparison, the wind wave rose in a number of locations show a higher magnitude and frequency of wind waves due to the misclassification of swell waves by the Met Office definitions (**as described in Section 1.5**); correspondingly, the swell waves show a lower frequency and magnitude than expected. This highlights the difficulties in classifying wind and swell waves from the model data.

3 Method of deriving the swell extreme characteristics

3.1 Introduction

The aim of extreme value statistical analysis is to quantify the random behaviour of a process at unusually large or small levels. In extreme analysis of physical events we are, by definition, often trying to predict an event that has not occurred, and indeed may rarely occur. The aim of this project was to estimate what swell waves might occur for return periods in excess of the eight-year dataset available as the basis of these estimates.

Given the relative shortage of data, it was necessary to use statistical analysis to derive estimates of the height and period of swell waves. For example, for a sequence of significant swell wave heights the maximum value over this period can be seen from the data. If the exact statistical behaviour of these values is known, the corresponding value of the absolute maximum wave height can be calculated exactly. In practice, the behaviour of values in a sequence is unknown, that is they haven't yet been observed, and therefore exact calculation of an absolute maximum wave height is impossible. Suitable assumptions can be applied which leads to a family of statistical models.

We need to be aware of the limitations in using models to extrapolate to higher return periods than observed in a range of data. Two limitations are particularly pertinent. Firstly, the statistical expressions with the model, although well justified, remain theoretical so they may not fully and accurately cover the distribution in values that could arise over a very long time frame. Secondly the results from the statistical model, as with other models, are dependent on the quality and quantity of the data inputs.

Overall, therefore, we cannot say the results from this project are wholly accurate and will remain valid for all time. Nevertheless, they are derived from the data using the best available techniques. Their derivation has also involved careful thought, intelligently applied, in conjunction with the mathematical analyses.

The user needs to be aware of the limitations of such statistical analysis. The results should be viewed in the context of these limitations, the limited length of dataset and limited number of observed data to validate the results.

3.2 Overview

Estimates of extreme swell wave characteristics were made by statistical analysis of the eight years Met Office hindcast modelled data. As noted earlier, this gives values at three-hour intervals on a 12-km grid. We did not analyse the data from every grid point, but chose those points that matched our intention of providing deep water values along a single chainage line around the UK coast. The points are shown on **Figure 1.1**.

The form of statistical analysis is described in **Section 3.4**.

3.3 Considerations in choice of output points

Met Office data was provided for coastal (nearshore) locations and sea (offshore) locations. We wished to use offshore values for this project to ensure the modelled data would not be affected

by shallow water effects, which can distort the model results. We therefore applied, as a minimum, a one-cell buffer to these offshore cells from the boundary with the coastal cells due to uncertainty of the data quality at this boundary.

We specified a chainage around the coastline based on the contour depth using MIKE C-MAP bathymetry data provided via Danish Hydraulics Institute (DHI). To ensure the swell wave estimates were produced for relatively deep water, the chainage was selected using modelled output points at an indicative water depth of 50-m Chart Datum where possible. In the shallow depths offshore of the East Anglian coastline, a 20-m contour was used to generate the chainage. The chainage line based on depth contours incorporates the buffering noted above. The chainage can be seen in **Figure 1.1**.

3.4 Statistical methods adopted

A number of statistical distributions are available for extreme value analysis. For this project, we used the Generalised Pareto Distribution (GPD) but also considered the Weibull distribution, which was the chosen statistical distribution for the analysis by HR Wallingford for Report SR409.

Depending on the values of parameters, the **Weibull distribution** can be used to model a variety of life behaviours. For any distribution, the parameter(s) of the distribution are estimated from the data. Most distributions used for reliability analysis are limited to a maximum of three parameters, as given below:

- Scale: defines where the bulk of the distribution lies, or how stretched out it is.
- Shape: defines the shape of a distribution.
- Location: used to shift a distribution in one direction or another, often the time shift in lifetime distributions.

Swell is caused by energy transfer to lower frequency waves as wind wave events decay due to variations in weather patterns and wind speed. The growth of swell requires energy from the weather system; generation of large swell requires a lot of energy and therefore rarely occurs. So, by their nature, extreme values are rarely observed. Consequently, the tails of the probability can be poorly defined and hence the return levels will be biased. Although as a trend the frequency of occurrence decreases with increasing wave height, the relative shortage of observations means this trend can be inconsistent. In our case, a statistical model was used to fit a smooth upper tail in order to best represent this behaviour.

The analysis used a distribution specifically tailored to represent the upper tail, specifically the GPD. In this process, a threshold is selected to determine the boundary between typical values and the upper tail, with the GPD used to model the distribution of values greater than the threshold. A typical GPD is presented in **Figure 3.1**.
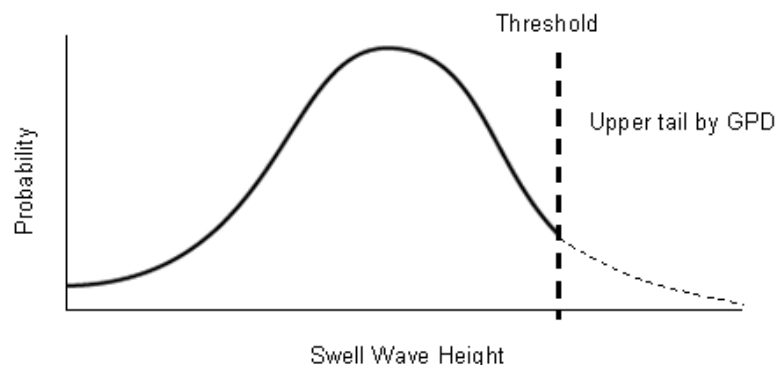
Figure 3.1 – Schematic of the Generalised Pareto Statistical Distribution

Like the Weibull distribution, the GPD has three parameters. However, the GPD tail model provides a much greater range of tail behaviour than the Weibull distribution and therefore can capture a greater range of return level curves.

We tested the Weibull and GPD statistical distributions on eight test sites, see below. In all cases the GPD provided the best fit to data in the tail of the distribution above a given threshold.

Our basis for selecting the GPD is that it is mathematically justified by asymptotic theory, the shape is stable for a high enough threshold to identify extremes, and it has been found to make an excellent fit to a range of oceanographic extremes in applications to wave heights, wave impacts, surge levels and current speeds, see Davison and Smith (1990)[4] and Coles (2001)[5].

The GPD parameters were optimised to give a best fit to the extreme swell wave heights above a specific threshold level. Since we wished to split the results by directional sector, we adopted a threshold at the 90 percentile point of the swell wave heights. In view of the limited length of data, a higher threshold would have left insufficient data above the threshold on which to perform the GPD analysis. Even with this selection, a few sectors at some points had too little data so no analysis could be made. Threshold setting followed a test of the 90, 95 and 99 percentile upper tail thresholds at the eight test sites and a visual check to determine the best fit of the data above these thresholds. Further details of this test are provided in **Appendix 6**.

3.5   Test sites

The statistical method was developed using eight test sites around the coast of England, Scotland and Wales, each of which represented sites at which swell would be significant. These sites were at the following locations, and can be seen in **Figure 3.2**.

- South Cornwall   (gl2849)
- South Coast (Isle of Wight) (gl2645)
- Anglesey   (gl1946)
- West Scotland   (gl1276)
- Orkneys   (gl0531)
- East Scotland   (gl1104)
- East Anglia   (gl1993)
- South East Coast   (gl2495)
- South Coast (Isle of Wight) (gl2645).

Further details of the tests undertaken can be found in **Appendix 6**.

This project used a single dataset for the statistical analysis, the Met Office UK hindcast wave model from 2000 to 2008. We assumed the data was stationary, in other words that it did not change its statistical characteristics (such as return period wave heights) over time.

A report (Met Office, 2007)[6] assessing homogeneity was published after questions were raised by model and data users on the homogeneity of Met Office archived wave data. This report concludes for the UK waters wave model that the significant wave height consistently has an error, or difference compared to equivalent wave buoy observations, of less than one metre. Wave periods are low, but exhibit some seasonality. In addition, the report finds that the occurrence over time of major changes to the UK and global atmospheric models, for either wind surface forcing or the resulting wave field, does not appear to generate noticeable changes in errors. Our own checks, conducted for this project, are reported in **Appendix 4**.

3.6   Software

Bespoke software was developed to carry out the extremes analysis for this project.   We developed the code using 'R' software.   R is a programming language and environment for statistical computing and graphics which is available as free software under the terms of the Free Software Foundation's GNU General Public License in source code form.   Most of the functions we required for the statistical analysis of swell waves were already available in R, so the amount of programming was reduced.   Having the methods presented in R would also make it easier to apply the code on further data in future.

3.7   Wind wave and swell joint dependence

Previous analysis, reported in SR409, estimated the joint probability of wind waves and swell waves to produce a bi-modal wave climate.   Met Office swell and wind wave data were compared to identify dependence between them.   Correlation between the two needs to be accounted for to produce a joint occurrence of swell and wind waves.   Swell wave heights were compared to wind wave heights to determine any correlation between them and therefore dependence at the same point in time.   At the eight test sites there was no, or very little, correlation between swell wave heights and wind-sea heights; thus, we concluded that the two were independent.   Further details of the tests for correlation between wind waves and swell waves are in **Appendix 7**.

This conclusion is consistent with the definitions of wind waves and swell waves.   Wind waves are generated by local winds and swell waves are generated over a larger region and are due to energy transfer to lower frequency waves as wind-sea wave events decay.   Therefore, the input meteorological conditions that lead to the wind waves and swell are physically independent, which is reflected in our statistical analysis. Given this independence, wind waves and swell should be treated separately when determining a wave climate for any site.

This conclusion is based on the definition for wind and swell waves adopted for this project.

4 Results and discussion

4.1 Introduction

This project has produced swell wave parameters for a continuous chainage of points around the coast of England, Scotland and Wales in GIS format. The swell wave results were obtained by statistical analysis of Met Office hindcast modelled offshore data.

We have supplied the GIS Shapefiles together with files which contain the results in a separate folder. The Shapefile references these files which contain the results, therefore the folder and Shapefile must remain in same relative paths.

4.2 Swell wave heights

Swell wave heights (in metres) of annual exceedance probability ranging from 100 to 0.1 per cent (average return period one in one year to one in 1,000 years), as listed below, are provided.

- 1, 5, 10, 20, 25, 50, 75, 100, 150, 200, 250, 300, 500, 1,000 years

The results files are referenced to Met Office data points to which the method was applied. The results files are in a comma separated format which can be viewed in standard spreadsheet software.

Although wave heights are quoted to two decimal places, they should not be treated as accurate to that apparent degree of precision. Wave heights should be considered accurate to one decimal place.

4.3 Directional extremes

It is important for practitioners to know the direction associated with swell. For this reason, we have split the swell wave return periods into directional sectors at sixty degree intervals, as shown in **Figure 4.1**:

North - 330° to 30°	**North East - 30° to 90°**	**South East - 90° to 150°**
South - 150° to 210°	**South West - 210° to 270°**	**North West - 270° to 330°**
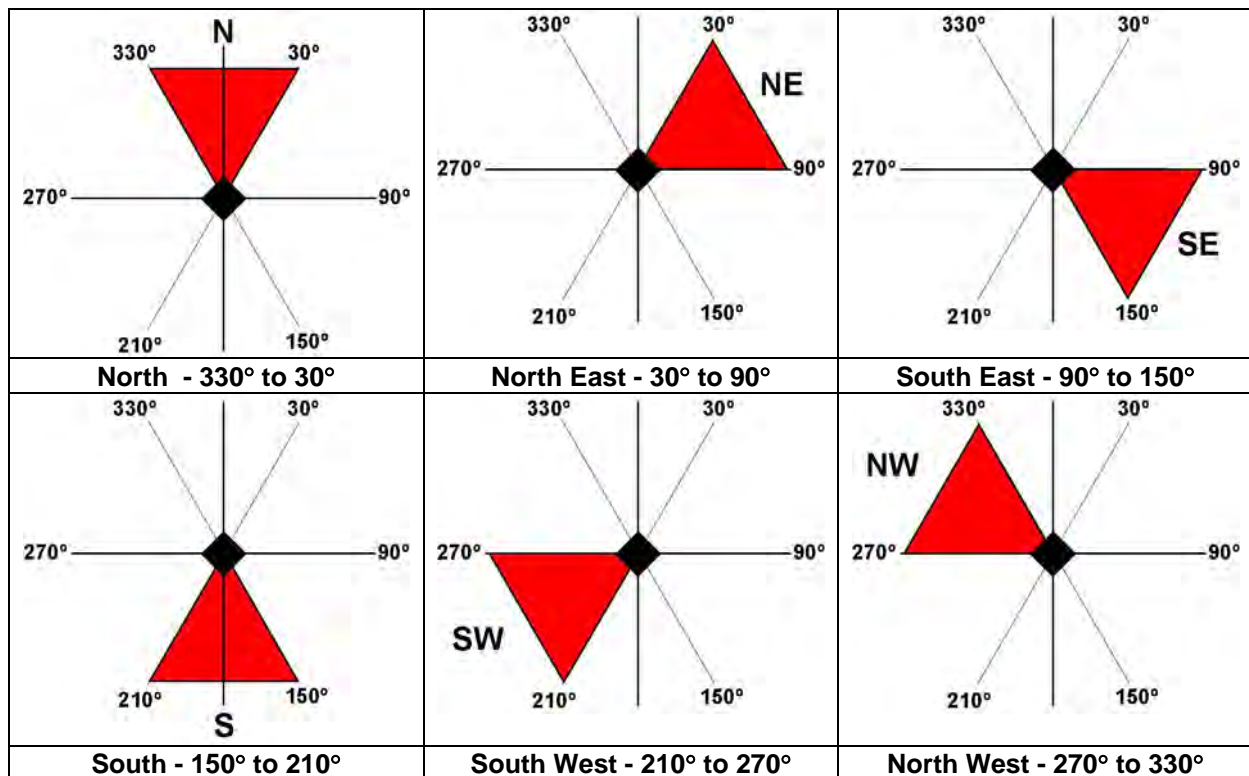
Figure 4.1 – Directional sectors for swell wave height return period results

For sites where swell estimates are not provided per direction, this is due to insufficient data records. Fifteen extreme events of swell for a particular direction were chosen as the minimum below which an extreme fit would be too unreliable.

4.4   Frequency table of periods

For any swell wave there will be a wave period associated with the significant wave height. We have provided a table of wave period (bandings) for all occurrences of significant wave height (banding) in the swell wave dataset.

The results files are referenced to Met Office data points to which the method was applied. The results files are in a comma separated format which can be viewed in a standard spreadsheet application.

This probability table was produced based on the eight years of modelled swell wave data we received from the Met Office. For higher swell wave heights beyond the range of the Met Office data, no probability could be calculated.

We therefore selecting the wave period distribution given for the highest calculated range of swell heights.

4.5   Confidence intervals

Confidence intervals are provided for each annual exceedance probability swell wave height per direction sector. Please note that confidence intervals provide uncertainty information for swell wave heights only. In this project we expressed confidence intervals as a distance ($\pm$) from the mean swell wave height estimate. For sites where not enough occurrences (15) of swell were included in the Met Office model data, this was not possible. Confidence intervals can be used to indicate the reliability of an estimate. In this project we provided the 95 per cent confidence

interval, therefore 95 per cent of the values are within these bounds. This is an arbitrary decision but a common selection in extreme statistics. The derivation of confidence intervals is discussed in greater detail in **Appendix 8**.

4.6   Discussion of swell wave height results

Appendix 8 contains a more detailed discussion of the results and graphs of results for all locations around the coastline ranging from annual exceedance probability of one to 0.001 (one to 1,000 year return periods). The results are given for all sites as shown in **Figure 1.1**. The main chainage has been split into regional chainages to view the results easily, which are shown in **Figure 4.2**.

We did not remove any data which showed high variability compared to neighbouring sites. Instead we analysed the number of occurrences of swell, depth at the location, regional geography and statistical fit to the tail of the data and provided comments for the user to decide whether to use the data.

The results naturally vary around the coastline due to factors such as depth, sheltering effects, prevailing weather directions and number of swell occurrences used to fit the statistical distribution. Another factor that is inherited in the results is the accuracy of the modelled data used to create these results.

The sheltering effect was a significant factor in the availability of data from which to devise a result. Therefore some sectors have insufficient data and results are returned as not applicable (N/A).

The chainage line for which results are given is based on the Met Office model grid points. In some locations the line is irregular with the need choose a more seaward grid point due to the alignment of the chainage relative to the land. At the more seaward grid point the depth may increase, or the site may become more exposed to swell, so it may yield higher results of swell wave height than a nearby more landward grid point.

Furthermore, the amount of data was limited to eight years. In some instances there were few events to devise a result. Therefore there may be an error in the statistical distribution. A general comment on the statistical distribution is that the method is suitable for the whole coast, although there are a few locations for which the statistical method under- or overestimates the results. These considerations are highlighted in **Appendix 9**.

5   Conclusions

We based our analysis on hindcast model data from the Met Office. We compared the Met Office data with observed data and found that the Met Office model tends to underestimate the swell wave period, though not greatly. Users are advised to be precautionary when selecting an appropriate swell wave period, by adopting a value at the higher end of the ranges advised in the project output.

This project used eight years of data; therefore, there is a high degree of uncertainty associated with the results, especially those for the lower annual probabilities (longer return period). Confidence intervals have been provided. It is possible to obtain longer datasets of hindcast model data from the Met Office to improve the confidence of the results.

In the future when data from the new Met Office model configuration, Wavewatch III, becomes available there is an opportunity to assess whether the current model data can be pooled with the new model data. It is reasonable to expect that our GPD model for the tail of wave heights will be a good choice of statistical model for the new dataset, given its theoretical justification.

In addition, the method developed for deriving extreme swell wave characteristics could also be applied to wind-wave data provided by the Met Office.

We have obtained a sample of the Wavewatch III model which contains the same parameters as the Met Office UK Waters Model, therefore the method can be applied to this new model configuration.

References

1.   HAWKES, P.J., BAGENHOLM, C., GOULDBY, B.P. AND EWING, J. 1997. Swell and bi-modal wave climate around the coast of England and Wales. HR Wallingford Report No. SR409.

2.   JOOSTEN, H., NOTEBORN, H. AND MONZÒN, O.L. 2009. Measuring separate wave fields. *International Ocean Systems*, 13 (5).

3.   CEFAS. 2009. WaveNet [online] Centre for Environment, Fisheries & Aquaculture Science (Cefas). Available from http://www.cefas.co.uk/data/wavenet.aspx [Accessed 15 May 2009].

4.   DAVIDSON, A.C. AND SMITH, R.L. 1990. Models for exceedances over high thresholds (with discussion), *Journal of the Royal Statistical Society*, Series B, 56, 393-442.

5.   COLES, S.G. 2001. *An introduction to statistical modelling of extreme values*, London: Springer-Verlag.

6.   LEONARD-WILLIAMS, A. 2007. *European and UK Wave Model Homogeneity Assessment*. Met Office
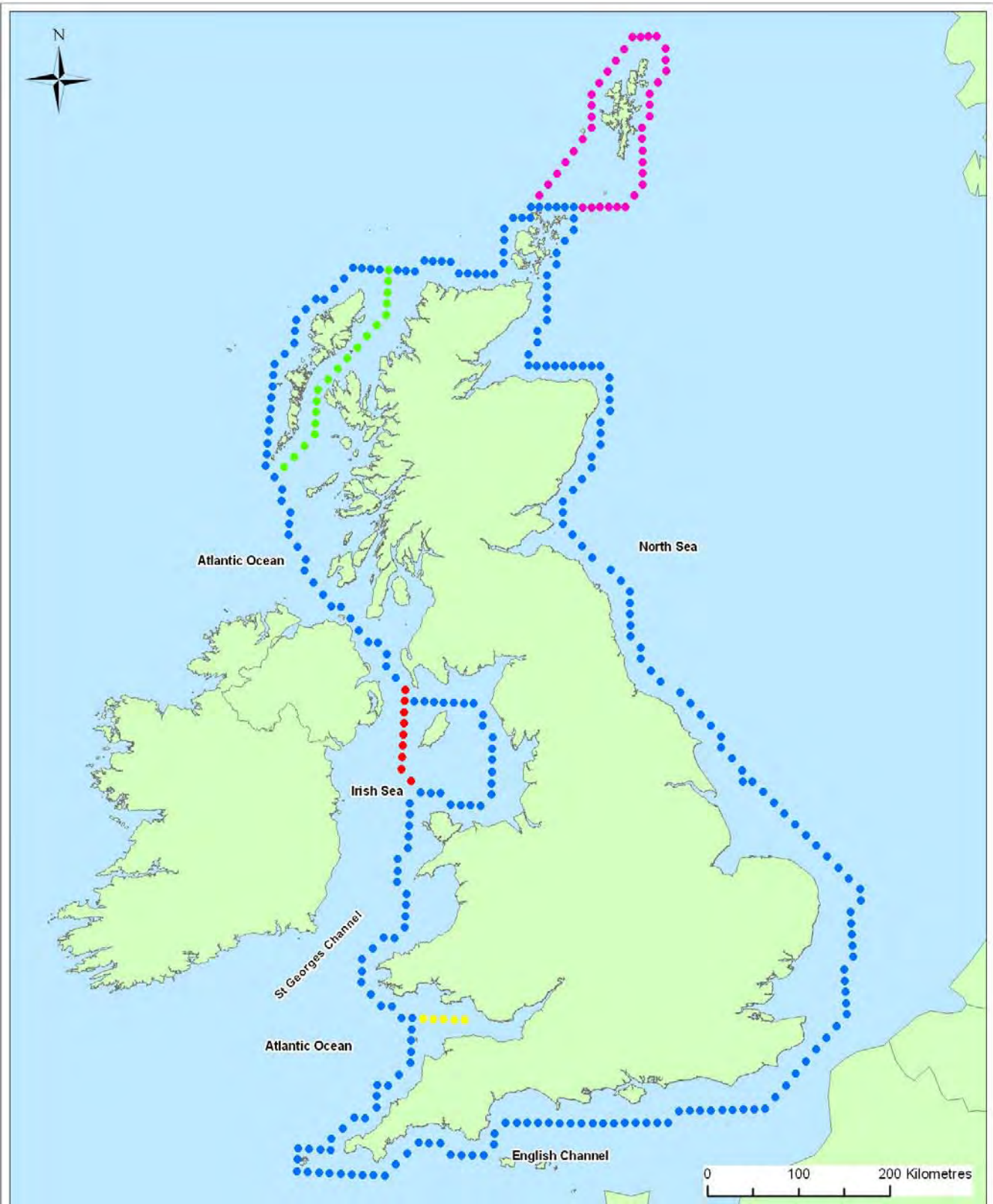
Key:

Chainage Reference

- Main
- Bristol Channel
- Hebrides
- Isle of Man
- Shetland

Source / Copyright

\\9S7299\Technical_Data\F12_GIS\Projects\Report_Figures\Extreme_Swell_Wave_Conditions

| Title: |
| Swell Wave Chainages |

| Project: |
| SC060064: Development and Dissemination of Coastal and Estuary Extremes |

| Client: |
| Environment Agency |

| Date: | Scale @A4: |
| 2010 | 1:5,500,000 |

Figure:
1.1

Key:		Title: Wave Validation Sites		Figure: 2.1
🔴 Wave Validation Sites		Project: SC060064: Development and Dissemination of Coastal and Estuary Extremes		
		Client: Environment Agency		
Source / Copyright I:\9S7299\Technical_Data\F12_GIS\Projects\Report_Figures\Extreme_Swell_Wave_Conditions		Date: 2010	Scale @A4: 1:5,500,000	

Key:		Title: Test Sites	Figure: 3.2
◆ UK Met Office Model Points		Project: SC060064: Development and Dissemination of Coastal and Estuary Extremes	
		Client: Environment Agency	
Source / Copyright i:\9S7299\Technical_Data\F12_GIS\Projects\Report_Figures\Extreme_Swell_Wave_Conditions		Date: 2010	Scale @A4: 1:4,966,350	

List of abbreviations

Cefas	Centre for Environment, Fisheries and Aquaculture Science
CD	Chart Datum
Defra	Department for Environment, Food and Rural Affairs
DHI	Danish Hydraulics Institute
GIS	Geographic Information Systems
GPD	Generalised Pareto Distribution
NAE	Wavewatch III North Atlantic European Wave Model
SEPA	Scottish Environmental Protections Agency
UKMO	United Kingdom Meteorological Office
UKCMF	United Kingdom Coastal Monitoring and Forecasting

Glossary

Annual exceedance probability:	The probability (likelihood) of being exceeded in any given year.
Bathymetry:	The study of underwater depth.
Bi-modal wave spectra:	Two distinct peaks or 'modes' shown on a wave frequency spectrum, low frequency (longer period) swell waves; high frequency (shorter period) wind-waves.
Chainage:	Continuous arbitrary line of output points around the coastline with the zero chainage at Newlyn and continuing clockwise around the UK coastline.
Generalised Pareto Distribution:	Statistical model to represent the upper tail of the distribution.
Hindcast data:	Data from retrospective forecasting. Inputs for past events are entered into the model to see how well the output matches the known results.
Mean wave direction (θ_m):	Spectrally averaged mean direction from which wave energy is coming.
MIKE C-MAP:	Source of electronic Admiralty Chart and bathymetry data.
Resultant wave:	Resultant characteristics from combining coincident wind waves and swell waves.
Significant wave height (H_s):	Standard wave height measure equal to the average wave height of the highest one-third of the waves.
Wave frequency:	Number of waves passing a given point per unit time.
Wave spectrum:	Distribution of wave energy with respect to wave frequency or period. Wave spectra assist in differentiating between wind waves and swell.
Weibull Distribution:	A statistical distribution that is widely used for matching observed data, due to the fact that the probability density function can assume different shapes based on the parameter values.
Wind waves:	Wave energy generated by "local" wind conditions, also known as wind-sea waves.
UK Coastal Monitoring and Forecasting:	A partnership of public bodies who work together to provide a comprehensive coastal flood forecasting service.
UKMO:	UK Met Office. The UK's national weather service.

Zero crossing wave period (T_z, T_{av}):   Average time interval between similar direction crossings of mean water level for a wave record. The zero crossing period can also be calculated from the moments of wave frequency spectra. Tz = square root of (m^0/m^2). Also called the mean spectral period.

Appendix 1 Wave Rose Analysis

A1.1   Introduction

The statistical methodology, applied to sites along the coastal chainage, has been developed by undertaking a number of tests on eight sites around the coast of the UK. These sites chosen as swell wave conditions at these locations will be significant. The locations of the eight test sites can be seen in **Figure 3.2**.

Wave roses have been produced for the eight test sites. These are the same test sites as those that were investigated for the possibility of joint probability. The wave roses were produced in Mike Zero package, using the Met Office Time series data for each point.

For each point four waves roses are produced. These detail the magnitude and direction of:-

- Wind speed
- Resultant wave height
- Wind wave height
- Swell wave height

From these is would be expected that the magnitude and direction of the wind roses should follow a similar shape to the wind speed as they are locally generated and quick response to the wind energy providing growth in wave height. These will both provide a shape that is similar to the prevailing weather. The swell and to a slightly lesser extent the wind waves will reflect the shape of the location so that the waves are small due to the sheltering effect of the land.

A1.2   Discussion

Considering the expected shapes, each site is discussed below.

A1.2.1   GL0531 – Orkneys (See Figures A1.1 to A1.4)

The wind rose is as expected. The wind waves are biased in a number of directions in comparison to the wind rose. The bias mirrors the bias in the swell waves suggesting it is borrowing waves that should be classified as swell waves. The swell and resultant wave roses are biased to the North, East and West cardinal points; they are understandably sheltered from the south and from the Shetlands in the north east.

A1.2.2   GL1104 – Aberdeen (See Figures A1.5 to A1.8)

The wind rose is broadly as expected, except for a slight reduction in waves from the east. The wind waves are strongly biased to the south. This may be because of the more limited fetch from the more westerly directions than from the south, but we also suspect the wind waves include some miss classified waves borrowed from the swell component, reflecting the potential for swell from the northern Atlantic. The resultant and swell waves have a strong northern component. The resultant includes the contribution of waves from the south providing a more realistic distribution of wave directions.

A1.2.3   GL1993 – Humber (See Figures A1.9 to A1.12)

The wind and wind wave roses are similar and as expected. The resultant and swell wave roses are dominated by waves from the north as expected for the lower North Sea with limited fetches from other directions.

A1.2.4   GL2495 – South Coast (See Figures A1.13 to A1.16)

The wind rose is as expected. In comparison the wind wave rose is more biased to the south and west directions. This is probably due to the miss-classification or borrowing of swell waves which happen to be propagated from the same direction as the wind. The resultant and swell waves have a heavy bias to the west and south west as expected from the shape of the English Channel.

A1.2.5   GL2645 – South Coast 2 (See Figures A1.17 to A1.20)

The wind is as expected with some sheltering to the north and south, the dominant direction is south west-to-west with a distinct element form the east and northeast. The wind waves follow a similar pattern but the dominant directions have a more significant bias than those in the wind rose. The resultant and swell roses show waves primarily from the south west. This is as expected, given that the dominant source of swell will be the western Atlantic.

A1.2.6   GL2849 – Plymouth (See Figures A1.21 to A1.24)

The wind rose is as expected. The wind waves are biased to the east and west suggesting borrowing from the swell waves. The swell and resultant wave roses are biased to the west due to the fetches across the Atlantic.

A1.2.7   GL1946 – Anglesey (See Figures A1.25 to A1.28)

The wind rose is sheltered a bit from the land to the east biasing the wind to the southwest. The wind wave rose is more balanced though there is still a sheltering effect as expected form the east. The resultant and swell waves are dominated by south westerly waves as expected due to the fetches over the southern Irish Sea and exposure to the Atlantic Ocean.

A1.2.8   Gl1276 – South Hebrides (See Figures A1.29 to A1.32)

The wind rose is as expected. The wind wave rose is slightly sheltered in comparison to the north east due to the influence of the Scottish mainland. The resultant and swell wave roses are biased to the west due to the North Atlantic fetches.

A1.3   Conclusions

The wind and resultant wave roses are as expected and provide a good indication of the distribution of wind and wave directions. In comparison, the wind wave rose in a number of locations is biased due to the misclassification of swell waves; correspondingly the swell waves

are under-biased. This highlights the difficulties in classifying wind and swell waves from the model data. We have obtained wave buoy data from the Cefas Wavenet (funded by the UK Coastal Monitoring and Forecasting) to identify differences with the wave height and wave period; this is described in **Appendix 4**.

Figures A1 – A4 for Met Office point GL0531 – ORKNEYS
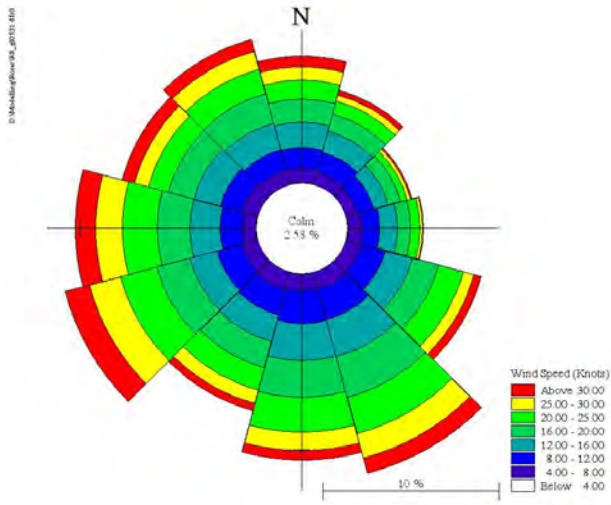
Figure A1.1 - Wind Speed

Figure A1.2 Wind Wave Height

Figure A1.3 Resultant Wave Height
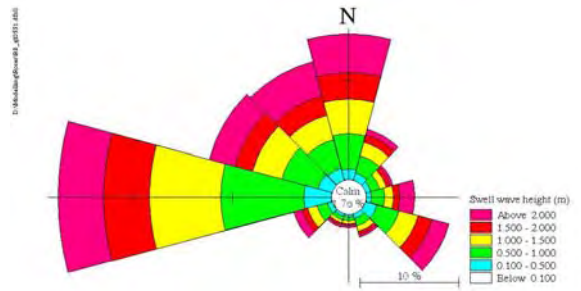
Figure A1.4 Swell Wave Height

.

Figures A1.5 to A1.8 for Met Office point GL1104 - ABERDEEN
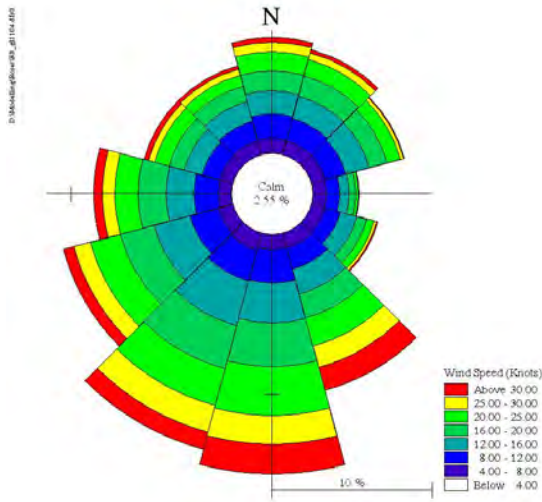
Figure A1.5 Wind Speed
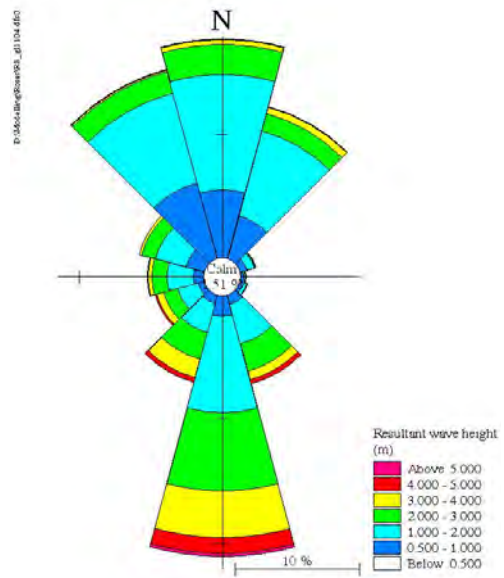
A1.7 Resultant Wave Height
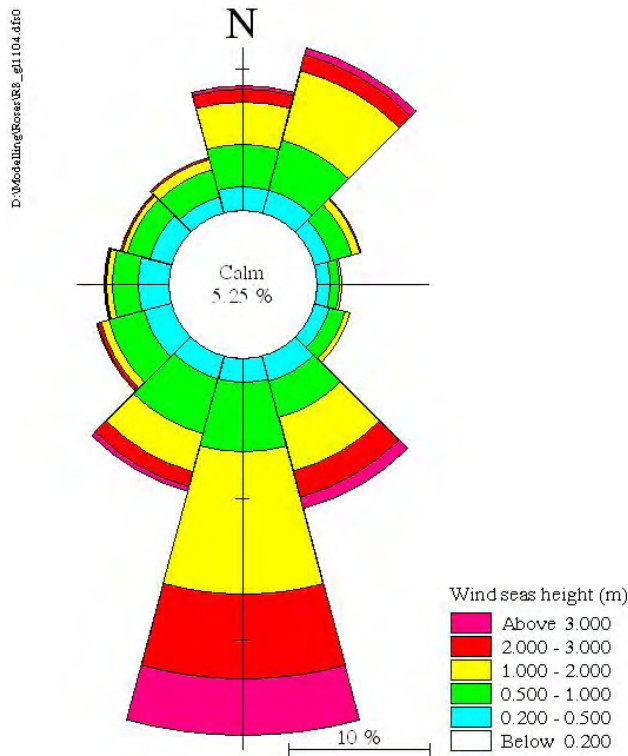
Figure A1.6 Wind Wave Height
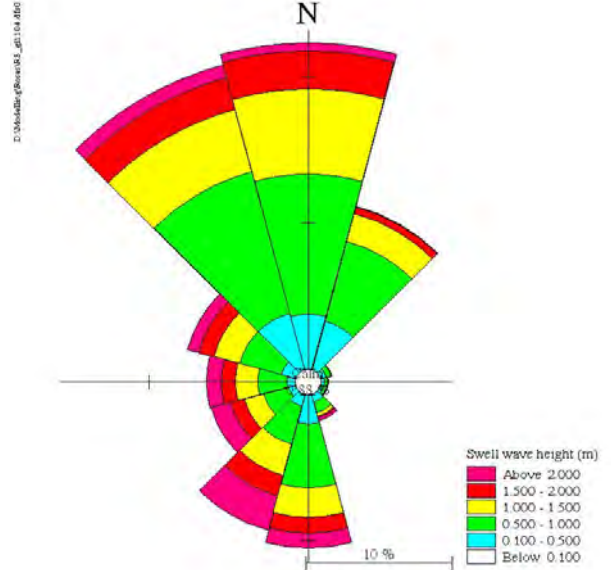
Figure A1.8 Swell Wave Height

Figures A1.9 to A1.12 for Met Office point GL1993 - HUMBER
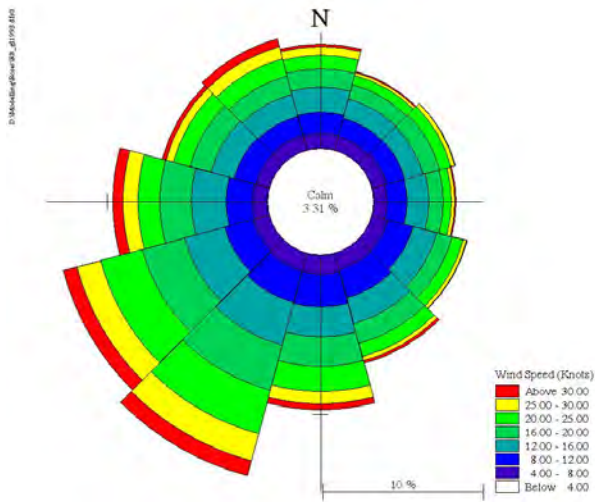
Figure A1.9 Wind Speed
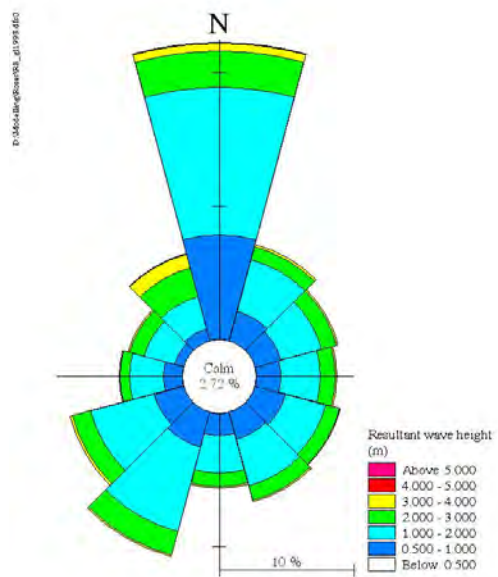
Figure A1.11 Resultant Wave Height
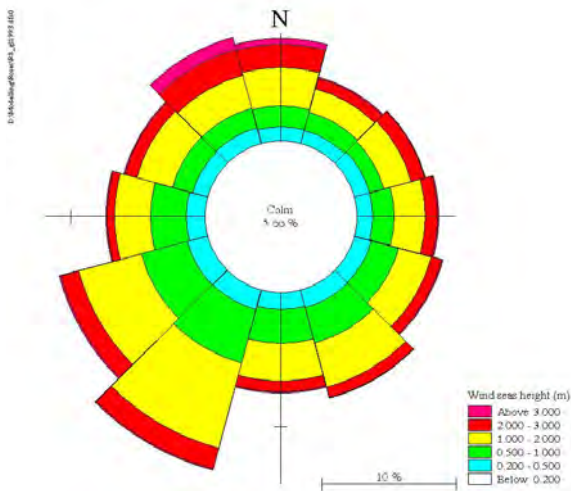
Figure A1.10 Wind Wave Height
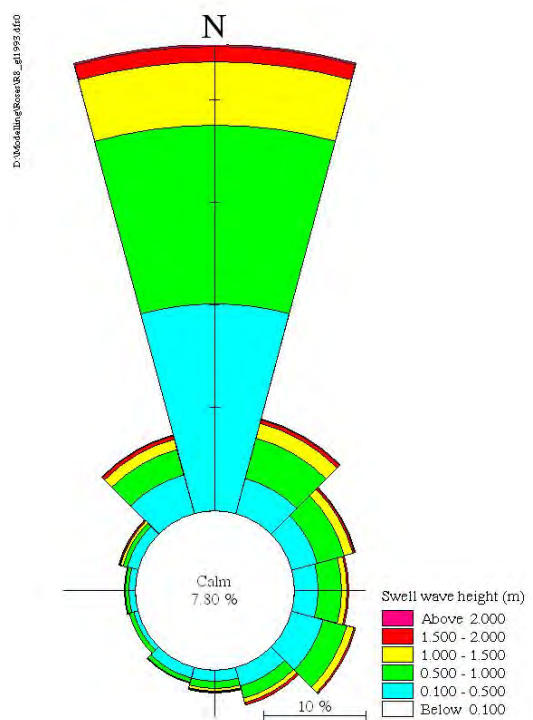
Figure A1.12 Swell Wave Height

Figures A1.13 to A1.16 for Met Office point GL2495 – SOUTH COAST
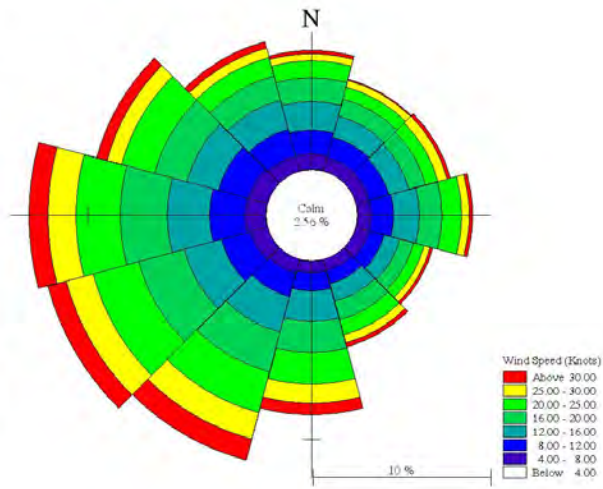
Figure A1.13 Wind Speed
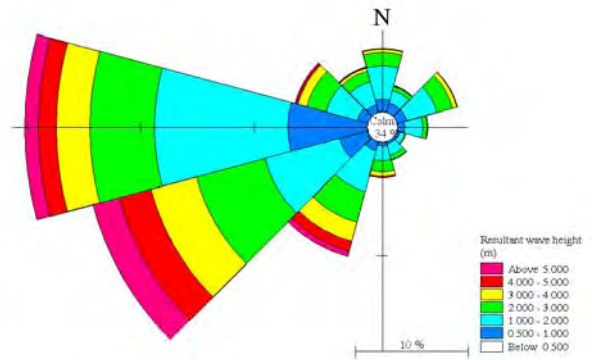
Figure A1.15 Resultant Wave Height
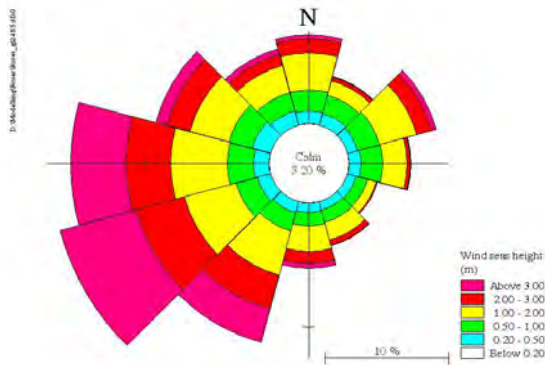
Figure A1.14 Wind Wave Height
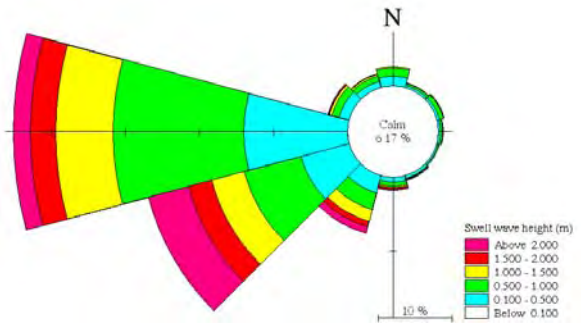
Figure A1.16 Swell Wave Height

Figures A1.17 to A1.20 for Met Office point GL2645 – SOUTH COAST (Isle of Wight)
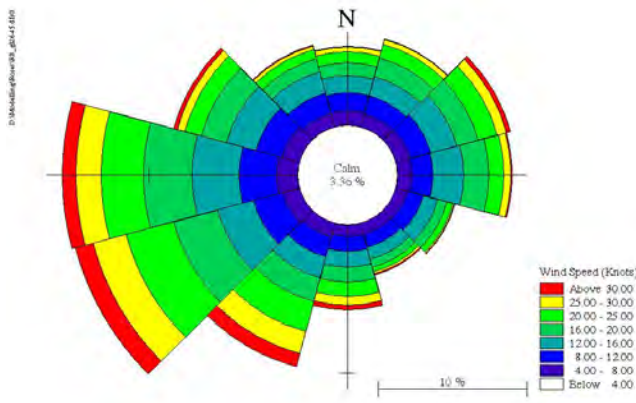
Figure A1.17 Wind Speed
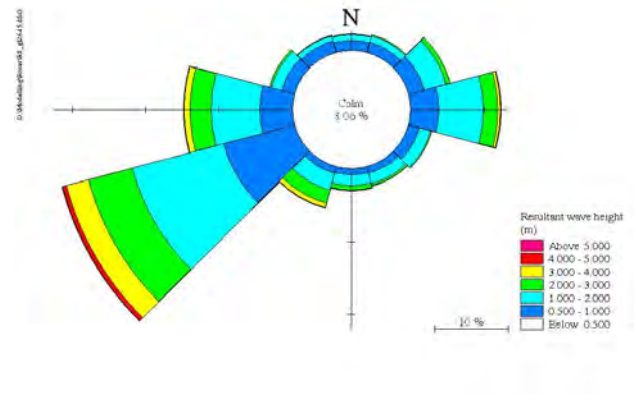
Figure A1.19 Resultant Wave Height
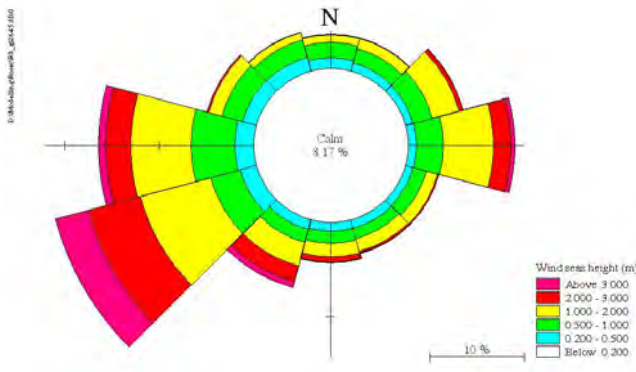
Figure A1.18 Wind Wave Height
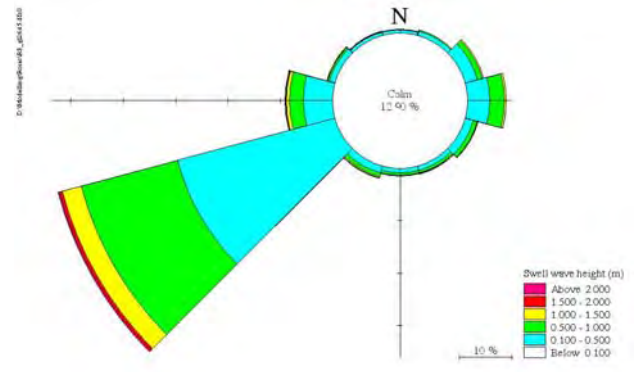
Figure A1.20 Swell Wave Height

Figures A1.21 to A1.24 for Met Office point GL2849 - PLYMOUTH
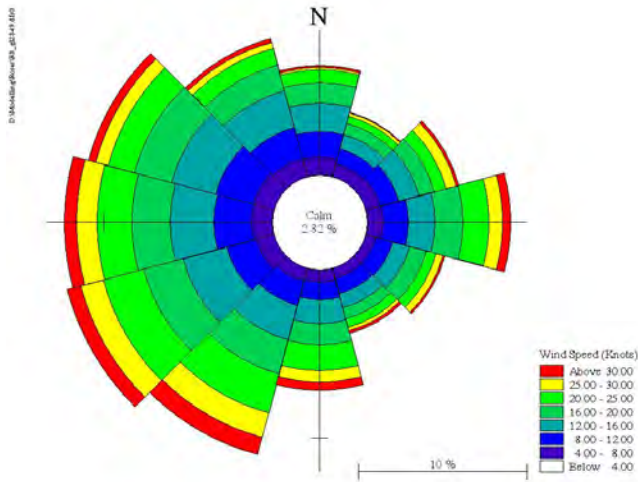
Figure A1.21 Wind Speed
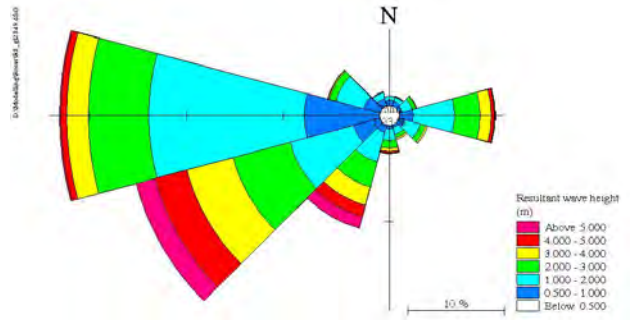
Figure A1.23 Resultant Wave Height
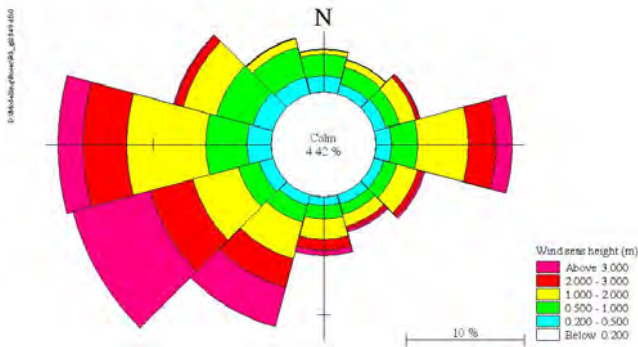
Figure A1.22 Wind Wave Height
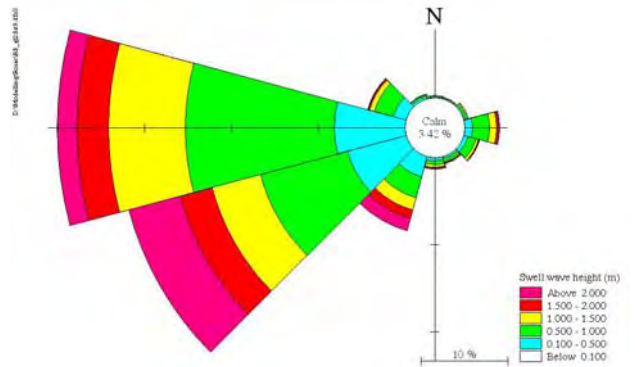
Figure A1.24 Swell Wave Height

Figures A1.25 to A1.28 for Met Office point GL1946 - ANGLESEY
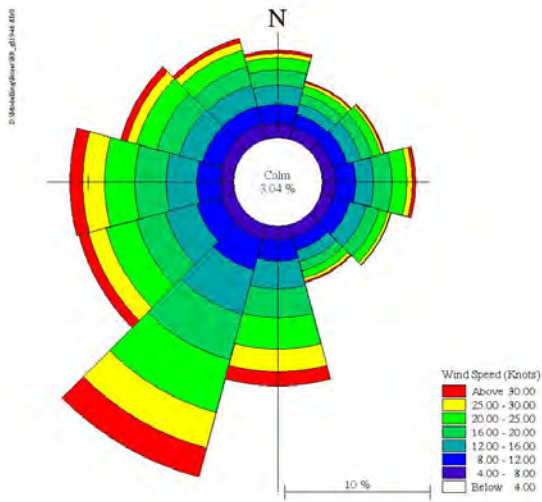
Figure A1.25 Wind Speed
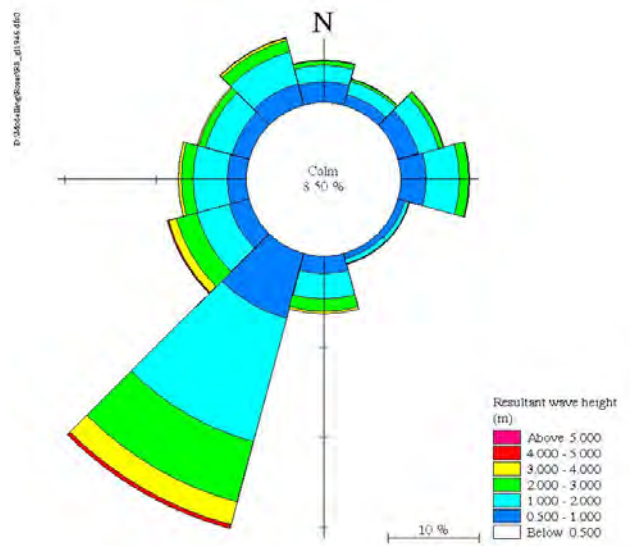
Figure A1.27 Resultant Wave Height
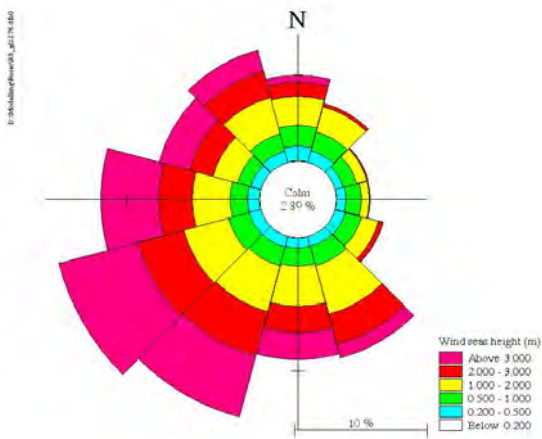
Figure A1.26 Wind Wave Height
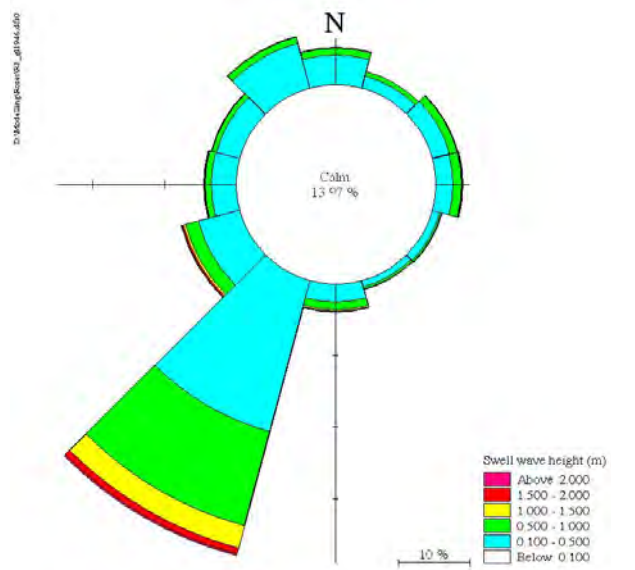
Figure A1.28 Swell Wave Height

Figures A1.9 to A1.12 for Met Office point GL1276 – S. HEBRIDES
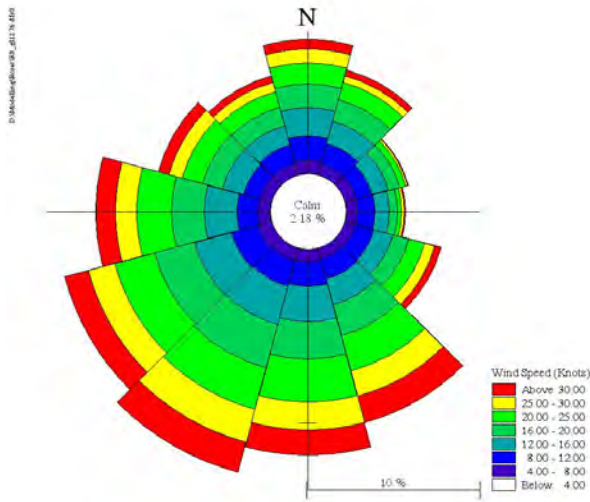
Figure A1.29 Wind Speed
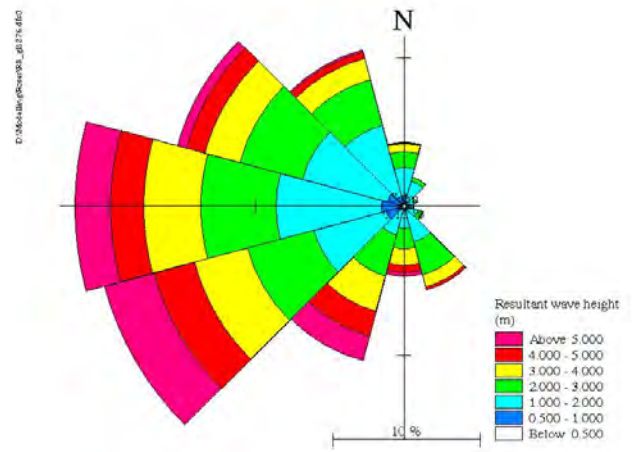
Figure A1.31 Resultant Wave Height
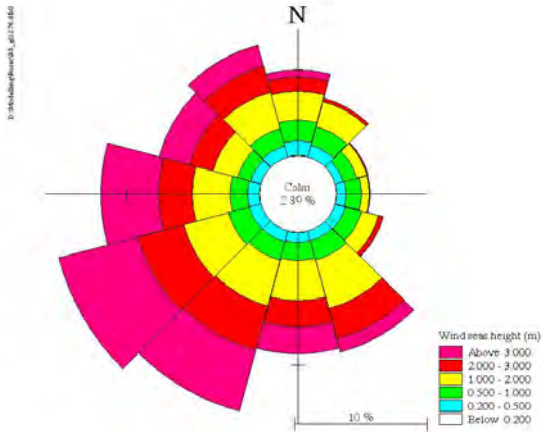
Figure A1.30 Wind Wave Height
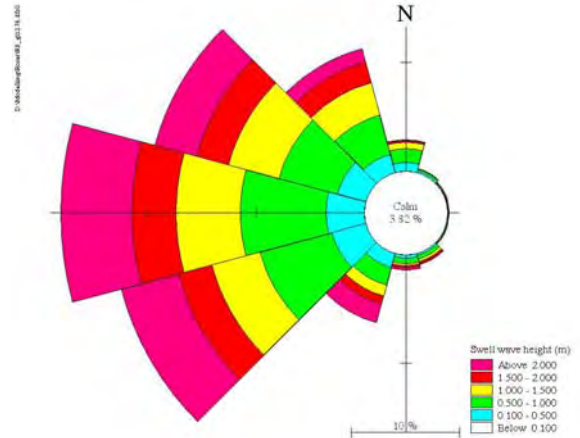
Figure A1.32 Swell Wave Height

Appendix 2 Swell Definition

A2.1 Introduction

A2.2 Definition of Swell and Modification

The UKMO Wave Model uses the following definition for the separation of wind-sea from swell:

- UKMO Definition 1: $f > 0.8f_p$

- UKMO Definition 2: $|\alpha| < 90°$

where f and f_p are the spectral frequency and spectral peak frequency respectively and α is the difference between the wave direction and the wind direction.

"UKMO Definition 2" introduces a possibility that wind-sea may include long-period waves if the direction of real swell travels the same direction of local wind. This is particularly the case along the UK west coast where the swell from Atlantic Ocean shares the same direction as the predominant wind.

The UK Met Office does not archive results of wave forecasts in their full spectrum. Without completely re-running their model, it is not possible to change the above inherited definition. Therefore, like the previous project ("Swell and Bi-model Wave Climate around the Coast of England and Wales, Report SR409 by HR Wallingford 1997), we can not change the above definition, though we can modify the swell data produced by the above definition, discussed in this Appendix.

In Coastal and Maritime engineering practice, swell is regarded as long period waves generated far away from a reference site. The UKMO definition does not fully match this engineering definition. For this reason, HR Wallingford introduced four additional criteria aiming to remove some false swell data (see Table 1).

Table A2.1 - HR Wallingford Criteria (1997) to Remove False Swell Data

	Description
HR Criterion 1	If the change of wind speed exceeds 5m/s, swell data next 12hour was removed
HR Criterion 2	Swell data with mean wave period below 8 seconds was removed
HR Criterion 3	Swell data with wave steepness above 0.02 was removed
HR Criterion 4	Swell data with wave direction propagating away from land was removed

It is important to note that introducing additional criteria can not change the UKMO definition, but removes some data. For this reason, this project team was reluctant to introduce additional criteria because it would reduce the data size and could potentially introduce a bias.

We believe that HR Criterion 1 was arbitrary, which was also recognized in the report by HR Wallingford (Report SR409). We do not believe introducing this criterion would improve the quality of the swell data. The problem HR Wallingford reported is deeply rooted from the UKMO definition; removing some false swell would not necessarily improve data quality but may introduce a bias.

About HR Criterion 2, we selected six offshore Met office model data output points representing southern, northern, western, eastern, south-western and south-eastern coastal chainages. The

swell data falling into HR Criterion 2 contributes 19.7-36.8% of the data. With less than nine years data provided for this extreme swell analysis, we do not think it is a good idea to reduce data size by introducing this criterion. Instead, the data was split into four groups according to wave periods, and probability distribution analysis was carried out for each group.

We adopted a criterion similar to HR Criterion 3 but the ceiling was increased to 0.04 instead of 0.02. This criterion removed very few data. For eight test sites, it only removed less than 0.54% of the data.

In this project, extreme swell analysis was carried out for each directional sector (each sector covers 60 degrees). We found that the number of swell waves that propagated away from land is so small that extreme value analysis using Generalized Pareto Distribution can not be exercised. Therefore, no extreme swell is available for these directional sectors. This automatically removes a need for HR Criterion 4.

A2.3   Conclusions:

1) We believe that the UKMO Definition does not fully match the swell definition used by the coastal and maritime engineering community. The extreme swell derived from the wave forecasts by the UKMO Wave Model would inherit any caveats associated with the UKMO definition.

2) We believe that the additional criterion would reduce data size and could introduce bias. After carefully studying the criteria used in the previous work by HR Wallingford (1997), this project only adopted a filter similar to HR Criterion 3 but it removed only a very small amount of the data.

Appendix 3 Met Office Modelling

A3.1   Introduction

The Met Office runs a 2nd Generation spectral wave model, with both global and nested regional configurations. The wave models are forced using hourly wind fields generated in Met Office Numerical Weather Prediction (NWP) models, which include observational data from satellite, ship and data buoy networks in their assimilation schemes. Based on the local wind speed and direction, energy is input to waves through a parameterization of the exponential growth of existing wind-sea energy (linear growth in the early development stage). Wind-sea spectral peakedness and peak frequency are used to select an appropriate member of the JONSWAP family of spectra to describe the growing wind-sea energy distribution in frequency space. Directional distribution of wind-sea energy is defined using a cosine squared distribution about the mean wind-sea direction. Frequency dependency for the rate of turn of wave energy in response to turning winds is also parameterized. As the waves grow, a balance is reached between parameterizations for the input, nonlinear transfer between frequencies and dissipation of wave energy. This ensures that for a given wind speed, with sufficient fetch and duration, the limiting Pierson-Moskowitz spectrum is reached but not exceeded.

Wave energy is advected through the model domain using a 2nd order Lax-Wendroff scheme. In the Global wave model, longer period swell energy direction of propagation is modified to ensure that the energy follows a Great Circle. In shallow water (<200m depth) wave group speed depth dependency, bottom friction and depth refraction are represented in the model physics. The UK Waters Wave Model additionally includes the effects of time-varying currents on the UK continental shelf, taking hourly currents from the ~12km Storm Surge model.

The 2nd Generation model scheme mainly differs from its 3rd Generation counterparts (e.g. WAM, WAVEWATCH III) in its use of parameterization schemes for wave growth, nonlinear transfer of energy and dissipation, where more recently devised models calculate some of these explicitly (details in Holt and Hall 1992). Nevertheless, the 2nd Generation scheme is considered robust for operational wave modeling applications and compares favourably with 3rd Generation counterparts operated by other meteorological bureau in an ongoing international data exchange (Bidlot et al., 2000, 2002). Wave model verification is undertaken daily at the Met Office and uses available networks of in-situ wave buoys, ENVISAT along-track altimeter data and ERS-2 Synthetic Aperture Radar (SAR) datasets.

A3.2   Operational Configurations

The Met Office suite of operational global and regional nested wave models produces regularly updated wave forecasts with lead times of up to five days. Operationally the models are configured with a spectral resolution of 13 frequency bins and 16 directional bins, representing waves with a range of periods between 25 seconds and 3 seconds (deep-water wavelengths from 975 m to 15 m).

Wave conditions worldwide are forecast using the Global Wave Model on a 5/9 degree latitude by 5/6 degree longitude grid (approximately. 60km square grid at mid-latitudes), with fields output at 3-hourly resolution to a lead time of 5 days (T+120). This model is forced using the Met Office's Global domain NWP 10m wind field and run twice daily based on 0000 and 1200 UTC analysis times. The extent of ice cover at high latitudes is updated daily using NWP global analysis data.

Boundary conditions from the Global Wave Model are used as input to a European Wave Model, based on a 1/4 degree latitude by 2/5 degree longitude grid (approximately 35km) covering the area from 30°.75N to 67°.00N and 14°.46W to 41°.14E and with a forecast range out to 2 days (T+48). Similarly to the Global Wave Model, this model is forced using the Met

Office Global domain NWP 10m wind field and run twice daily based on 0000 and 1200 UTC analysis times.

A further increase in resolution is made for the UK Waters Wave Model, which is nested using boundary conditions from the Global Wave Model. The UK Waters Wave Model uses a 1/9 degree latitude by 1/6 degree longitude grid (approximately 12km) covering the north-west European continental shelf from 12°W between 48°N and 63°N. Two configurations of the UK Waters Wave Model are run. The first configuration is forced by high resolution (~12km grid) Mesoscale NWP 10m winds and includes effects of time-varying currents on the UK continental shelf as generated by the Met Office's operational Storm Surge Model. This model is run four times daily using analysis times 0000, 0600, 1200 and 1800 UTC and provides hourly forecasts out to T+48. The second configuration (Extended UK Waters Wave Model) does not include current effects, and is run twice daily (0000 and 1200 UTC analyses) forced by Global NWP 10m winds to provide 3-hourly forecast data out to T+120.

Data are output from the model and variously retained in commercially available fast-access hindcast archives and research based forecast model archives. Due to data handling constraints two-dimensional (frequency-direction) spectral data are output at specific model points only and are not archived. The hindcast archives are based upon one-dimensional (frequency) spectral data output for all model grid points. These data are used to construct integrated wave parameters including significant wave height, period and direction based on the total spectrum, wind-sea and swell components. The decomposition between swell and wind-sea is made using analyses based upon archived model values of wind speed and direction. Hindcast and forecast integrated parameters (e.g. significant wave height) are generated at model run-time for each model grid point and are retained in the research forecast model archive.

A3.3   Technical Description

A published description of the wave model is provided in Golding (1983). Technical details from the wave model code are provided by Holt (1994) and Stratton et al. (1995).

Spectral Modelling of Wave Fields

The Met Office 2nd Generation Wave Model is a spectral wave model (as are 3rd Generation models, e.g. WAM, WAVEWATCH III). Spectral models work by calculating the levels of wave energy that can be assigned to a two-dimensional frequency-direction domain (termed the wave spectrum) used to describe motion of the sea-surface under waves (the sea-state). Essentially the spectrum decomposes a given sea-state into a set of constituent sine waves, each with a different direction, period (inverse of frequency) and amplitude (energy).

From the two-dimensional frequency-direction spectrum standard integrated parameters representing wave conditions are generated (.e.g. significant wave height, wave peak and zero-upcrossing period, principal wave direction). With knowledge of wind strength and direction, these integrated parameters can also be assigned to wave field components defined as wind-wave or swell (see *Wind-Wave/Swell Partitioning*).

Field experiments have established families of wave spectra appropriate to different forcing circumstances, and upon which spectral wave models have been based. In the instance of the global/regional scale 2nd Generation model, the spectra used are those derived from the JONSWAP experiment that recorded wave growth over a fetch in the North Sea (Hasselmann, 1973), including the Pierson-Moskowitz spectrum which defines a fully developed wind-sea and therefore defines the fully developed limit of a JONSWAP spectrum.

Model Grid and Forcing Data

The model runs on prescribed regular latitude-longitude spatial grids. Parameter values are derived at collocated positions corresponding to grid cell centre (i.e. the grid is not staggered). Cell types comprise 'sea points', where the full set of calculations for wind-sea growth/dissipation and wave energy advection are applied; 'land points' where no calculations are performed; and 'coast points', where advective/dissipative schemes only are applied and which act as a buffer zone for the land.

Depth information is held on the model grid using a representative average for each cell. This assumption may prove important in some near coastal grid cells where the average depth (for example taken over a 12km grid cell in the UK Waters model, 60km cell in the global model) may mask bathymetric features affecting the local distribution of wave energy. A cut-off depth is set in the model scheme at 200m, since at depths greater than this value shallow water effects are negligible even for wave energy in the lowest frequency range.

The importance of increased spatial resolution is clearest in the near coastal zone, since this allows a better representation of the coastline itself and will increasingly resolve shallow water bathymetric features. The trade off for making these resolution changes lies in run-time, with shorter calculation timesteps required for increased spatial resolution in order not to violate conditions for energy advection (see *Wave Energy Advection*).

Models are calibrated to be forced by representative 19.5m mean wind speed and direction, such that for correct wind speed, duration and fetch the wave model will attain the limiting Pierson-Moskowitz wave height. In the operational models this forcing is provided by NWP atmospheric models operated on rotated grids. As a result the winds must first be converted to the regular latitude-longitude grid prior to ingestion by the wave model. In assessing an appropriate wave model spatial grid size, the resolution at which the forcing winds are provided is an important constraint.

Wind-Sea/Swell Partitioning

Taking a simplistic view of the wave model two main processes are represented; growth/dissipation of wind-sea; and advection of wave energy in both wind-sea and swell components of the total wave field. An essential task in the model is therefore to define which parts of the two-dimensional (frequency-direction) wave energy spectrum are wind-sea, which will respond to wind forcing, and which are swell that will be permitted to propagate freely in the model (subject to swell dissipation terms).

The spectral domain occupied by wind-sea is defined in the model using a two stage process based on the wind strength and direction prescribed for each timestep and model grid point in order to generate a spectral cut-off in frequency and direction. Initially the wind-sea to swell cut-off in frequency space is defined using:

$$F_{cut-off} = 0.8 * F_{PM} ,$$

where F_{PM} is the Pierson-Moskowitz peak frequency defined by:

$$F_{PM} = 0.14 g / V_w ,$$

where g is acceleration due to gravity and V_w is wind speed at 19.5m above mean sea level and assumes neutral stability in the boundary layer. The cut-off in direction space is derived from:

$$D_{cut-off} = D_w \pm 0.63 * \pi ,$$

where D_w is wind direction in radians. The second stage of wind-sea domain definition occurs when wind-sea energy is turned, grown and recast, and is discussed in *Wind-Sea Growth/Dissipation and Spectral Reshaping*.

One drawback of this method is that there will be circumstances when the range of frequencies and directions assigned to receive wind-sea energy coincides with some frequencies and directions containing swell energy (i.e. when a strong wind is shifts and blows at a direction close to that in which swell is propagating). In such cases swell energy is appropriated into the wind-sea energy calculations. The result may include redistribution of some swell energy to higher frequencies and modified directions in the spectrum as a result of the model recasting the wind-sea (see *Wind-Sea Growth/Dissipation and Spectral Reshaping)*. This process has been termed 'poaching' by Met Office wave modelers.

Poaching can lead to enhanced wind-sea growth and excessive swell dissipation within the model scheme since swell energy is lost from comparatively low frequencies whilst the wind-sea energy present at the time is overestimated compared to reality. Under such growth conditions the wind-sea is likely to be assigned an artificially low peak frequency.

There may be some remnant sign of the old swell after poaching has occurred since wave energy at the lowest wind-sea frequencies may attain a direction some way between that of the majority of the new wind-sea and that of the old swell. This is due to the fact that where wave energy is already present the model tries to take account of this and slowly 'relaxes' that energy toward the new wind-sea direction (see *Wind-Sea Growth/Dissipation and Spectral Reshaping)*.

Wind-Sea Growth/Dissipation and Spectral Reshaping

Energy from the atmosphere is transferred to ocean waves through growth of the wind forced component of the wave spectrum (wind-sea). Calculation of the wind-sea at each model timestep comprises the following steps:

Calculate existing wave energy in new wind-sea frequency-direction (*f,θ*) range (*see Wind-Sea/Swell Partitioning*).

Turn the existing wind-sea.

Calculate source terms for linear and exponential growth of wind-sea, deep and shallow water dissipation (applied across the whole wave spectrum, i.e. inclusive of swell) and add source terms to define new wind-sea energy.

Reshape new wind-sea spectrum to parameterize nonlinear wave interaction using appropriate JONSWAP family member.

Using the model partitioning scheme described in *Wind-Sea/Swell Partitioning*, existing wind-sea energy is integrated by direction for each frequency bin. These calculations include determination of the mean wave direction associated with each frequency bin ($D_{mean,f}$). Where increasing wind includes frequency bins containing no wave energy, the mean direction is set to the wind direction for later use.

Commonly the wind will back or veer in addition to changing in speed. Wind-sea response is to follow this change in direction, but at a lag dependent upon frequency. In the model scheme turning the wind-sea follows two steps. First a frequency based relaxation factor is calculated using

$$RF = 0.0004 * f^2$$

which is then applied to produce a frequency based turn angle

$$\theta_{turn,f} = RF * \sin\left(D_w - D_{mean,f}\right) * \left(1/F_{PM}\right).$$

The turned wind-sea is then recast for each frequency based upon summed energy, a principal direction equal to

$$DP_f = D_{mean,f} + \theta_{turn,f}$$

and using a cosine squared directional spread. This process is described in further detail by Ephraums (1986).

Subsequent to creating the turned wind-sea, parameterized source terms for growth and dissipation of wave energy, plus nonlinear interaction between wave frequencies are applied. Two exceptional growth circumstances exist; where no wind-sea energy pre-exists, a linear growth parameterization inputs energy into the highest frequency bin; a parametric parameterization is used for wind-sea growth under low wind speed conditions (less than 7ms^{-1}; Holt, 1994). Otherwise exponential growth of wind-sea (Snyder, 1981) is calculated based on a growth factor:

$$GF_1 = E_{PM} / E_{WS1},$$

where E_{WS1} is the energy residing in the existing turned wind-sea and E_{PM} is Pierson-Moskowitz energy defined by

$$E_{PM} = \left(V_w / 1.4g \right)^4.$$

The growth factor is used to define both a peak frequency for the growing wind-sea based on:

$$f_p = F_{PM} * GF_1^{0.33},$$

and determine frequency based growth terms (constrained to be greater than zero) following:

a)   For all frequency bins below the top frequency,

$$GT_f = GC * f * W\left(V_w, f \right) * E_{f,\theta},$$

where $W(V_w, D_w, f, \theta)$ is a wind speed versus wave speed function defined as:

$$W\left(V_w, D_w, f, \theta \right) = \left[V_w * \cos\left(D_w - \theta \right) / c_f \right] - 1.0.$$

for which $D_w - \theta$ represents the angular difference between wind direction and the spectral direction bin, whilst c_f is wave phase speed for the given spectral frequency.

b)   For the top frequency bin

$$GT_f = GC * FP * W_T\left(V_w, D_w, f, \theta \right),$$

where $W_T(V_w, D_w, f, \theta)$ is a wind speed versus wave speed function defined as:

$$W_T\left(V_w, D_w, f, \theta \right) = \left[V_w * \cos\left(D_w - \theta \right) * f_p * 2\pi / g \right] - 1.0.$$

In both cases GC represents a growth constant calculated based on timestep and a number of other predefined constants, including a fixed value drag coefficient.

Dissipation parameterizes deep-water mechanisms for energy loss including 'whitecapping'. This is calculated using a dissipation term set up such that dissipation balances the Snyder (1981) growth term appropriately for fully developed wave conditions (Holt, 1992). The dissipation calculations are based upon the total energy existing in the entire spectrum (i.e. both wind-sea and swell), subject to hardwired upper and lower limits. For wind-sea (f,θ) bins the dissipation term (DT) is then:

$$DT = A*\left(s/s_{PM}\right)^2 * E_{f,\theta} * \left(2\pi*f\right)^2,$$

where A is a tunable constant $(4.5*10^{-5})$, and s and s_{PM} are respectively integral wave steepness terms for modelled existing energy and Pierson-Moskowitz spectral energy based on:

$$s = \left[\sum E\left(f,\theta\right)\right]^4 \Big/ g^2 .$$

Calculated source terms (including shallow water dissipation terms, see *Shallow Water Physics*) are simply added to existing (f,θ) bin energies to yield the grown-dissipated wind-sea. The final parameterization is that of nonlinear interaction between the wind-sea frequencies. This is made by fitting the grown-dissipated wind-sea to an appropriate JONSWAP spectrum family member and re-shaping the wind-sea spectrum accordingly. In the model JONSWAP members are pre-calculated for a sample set of peak frequencies (f_p, 220 in operational model) and JONSWAP gamma (γ, 24 in operational model) and stored as normalized spectral shapes following:

$$JONSWAP_{norm,f} = JONSWAP_{dim,f} \Big/ \sum JONSWAP_{dim,f} * df ,$$

Where:

$$JONSWAP_{dim,f} = \frac{1}{f^5} * \exp\left[-1.25*\left(\frac{f}{f_p}\right)^{-4}\right] * \gamma^{\left[\exp\left[\frac{\left(\frac{f}{f_p}-1\right)^2}{2\sigma^2}\right]\right]}$$

for frequencies above a spectral cut-off defined by:

$$f_{cut-off} = 0.8 * F_{PM}$$

In the operational model σ is given the constant value 0.08.

Grown-dissipated wind-sea f_p and γ for selection of the normalized JONSWAP member are defined using the growth factor for this third iteration of wind-sea energy, i.e.

$$GF_3 = E_{PM} \Big/ E_{WS3}$$

so that:

$$f_p = F_{pm} * GF_3^{0.33},$$

and:

$$\gamma = 2.3*\left[1.0 - \left(1.0/GF_3\right)^2\right] + 1.0,$$

such that the maximum value for γ is set at 3.3.

A final partition of wind-sea energy is made based upon this latest value of peak frequency to provide the frequency cut-off. The resulting wind-sea energy is reshaped using the selected normalized JONSWAP member, and applied to the appropriate frequency bins, being distributed in spectral directional space by using the turned wind-sea principal directions and a cosine squared energy distribution.

<u>Wave Energy Advection</u>

Wave energy is propagated through the ocean at wave group speed (c_g, half the wave phase speed in deep water). This process is replicated across the model grid using a numerical energy advection scheme satisfying the equation:

$$\frac{\partial E}{\partial t} + c_g \frac{\partial E}{\partial x} = 0$$

The first criterion required for a stable model advection scheme is that the condition,

$$c_g \frac{\Delta t}{\Delta x} \leq 1$$

where Δx is model grid length (which will be a minimum at high latitudes) and Δt the timestep be satisfied. Since the latitude-longitude grid is predefined, satisfying this criteria sets the timestep and as a result the calculation time involved in a model run, with a higher spatial resolution model requiring a shorter timestep and longer run-time for a given forecast period.

In order to ensure numerical stability and accuracy in model advection a Lax-Wendroff scheme (Richtmeyer and Morton, 1967; Gadd, 1978) is employed. The scheme uses a two-step approach, first making a diffusing step to an intermediate gridpoint and timestep ($\Delta t/2$), and then using these values to evaluate the next whole timestep. Applied to the simple advection equation with m representing spatial grid cells and n timesteps, the scheme is:

$$E^*_{m+1/2,n+1/2} = 1/2\left(E_{m+1,n} + E_{m,n}\right) - \left(c_g \Delta t/2\Delta x\right)\left(E_{m+1,n} - E_{m,n}\right)$$

$$E_{m,n+1} = E_{m,n} - \left(c_g \Delta t/\Delta x\right)\left(E^*_{m+1/2,n+1/2} - E^*_{m-1/2,n-1/2}\right)$$

Substituting the diffusing step into the whole timestep equation yields terms that indicate the scheme is second order in both time and space.

Within the global and large scale regional wave models it is also necessary to account for Great Circle turning of propagating wave energy for all but the highest frequencies (less than 0.15Hz, periods longer than 6 seconds). Great Circle turning is required due to the curvature of the earth, which without a correction term would be unaccounted for in the regular grid representation used by the wave model. Placing the energy advection equation in spherical co-ordinates, the result is to add an extra term for Great Circle turning, i.e.

$$\frac{\partial E'}{\partial t} + \frac{\partial E'}{\partial \varphi} + \frac{\partial E'}{\partial \lambda} + \frac{\partial E'}{\partial \beta},$$

where φ, λ and β respectively relate to terms for latitude, longitude and great circle turning. Turning is calculated using a forward difference scheme, as outlined in Stratton and Ephraums (1986).

Swell Dissipation

Swell dissipation is based on the same scheme as described for wind-sea (see *Wind-Sea Growth/Dissipation and Spectral Reshaping*). However, that parameterization scheme was designed to compensate for the fact that results from boundary layer coupled models (Chalikov and Makin, 1991; Burgers and Makin, 1993; Janssen, 1991) demonstrated an overprediction of wind-sea growth in the Snyder (1981) method employed by this model. It was therefore found that adopting the same dissipation parameterization for swell terms (for which no wind forced growth occurs) would lead to excessive dissipation of swell (Holt, 1992, 1994). As a result a reduced dissipation factor is applied to swell using:

$$DT = A * \left(s / s_{PM} \right)^2 * E_{f,\theta} * \left(2\pi * f \right)^2 * 0.33 .$$

Shallow Water Physics

In shallow water three principal processes are accounted for in the model scheme (Holt, 1993).

Wave phase and group speeds must be calculated using the full wave dispersion relationship:

$$c = \sqrt{gk * \tanh kh} ,$$

where *k* is wave number (=2*π/*wavelength*) and *h* depth, and:

$$c_g = \frac{1}{2} \left(1 + \frac{2kh}{\sinh 2kh} \right) * c .$$

At the start of a model run a look-up table of appropriate shallow water wave speeds is derived. This table can then be interrogated for calculations performed for model designated shallow water points.

Refraction is a forced redirection of wave energy due to changes in wave speed, and is discussed in detail in Golding (1983). This is dealt with in the model using a forward difference scheme.

A term is included in the model to allow additional wave energy dissipation due to bottom friction at shallow water points.

For the UK Waters wave model effects of time-variant currents on the continental shelf are also accounted for. This procedure is detailed by Buckley (1999).

Post-Processing Wind-Sea/Swell Partition

Separate from the wave model, hindcast archive data extraction also uses a wind-sea/swell partition scheme in order to produce integrated parameters (e.g. significant wave height) from archived one-dimensional (frequency) spectral data. Several of the steps used to create this partition in the model cannot be replicated from the output data, and so the approach to defining the wind-sea is in post processing is based on the initial cut-off criteria described in *Wind-Sea/Swell Partitioning*, but with some modification.

The direction cut-off uses:

$$D_{cut-off} = D_w \pm \pi / 2$$

The frequency cut-off is modified to account for the fact that in reality, the sea requires a certain length of time to respond to the wind blowing over it. Initially the relationship:

$$F_{cut-off} = 0.8 * F_{PM}$$

is used. However, the wind-sea from which this 'first-guess' was made may not have reached the theoretical fully-developed state described by the Pierson-Moskowitz spectrum. So the difference between the model actual and theoretical states is used to calculate a more realistic peak frequency for the wind-sea based on:

$$F_{cut-off} = 0.7 * 10^{(-0.04*XX)},$$

$$XX = -25 * \log\left(F_{final}\right)$$

and:

$$F_{final} = F_{PM} * \left(E_{PM} / E_{model}\right)^{0.31}$$

where E_{model} is the first-guess wind-sea energy.

References

Bidlot, J.R., Holmes-Bell, D.J., Wittmann, P.A., Lalbeharry, R., Chen, H.S., 2000. Intercomparison of the performance of operational ocean wave forecasting systems with buoy data. European Centre for Medium-Range Weather Forecasts (ECMWF) Technical Memorandum Number 315 *also* 2002, Weather and Forecasting, 17, 287-310.

Buckley, A.L., 1999. Implementation of a wave-current interaction scheme in the Met Office wave model. Unpublished Met Office Ocean Applications Internal Paper 29.

Burgers, G., Makin, V., 1993. Boundary-layer model results for wind-sea growth. Journal of Physical Oceanography, 23, 372-385.

Chalikov, D., Makin, V, 1991. Models of the wave boundary layer. Boundary Layer Meteorology, 56, 83-99.

Ephraums, J., 1986. Directional relaxation of the wave energy spectrum in turning winds. Unpublished Met O 2b Technical Note Number 105.

Gadd, A.J., 1978. A split explicit integration scheme for numerical weather prediction. Quarterly Journal Royal Meteorological Society, 104, 569-582.

Golding, B., 1983. A wave prediction system for real-time sea-state forecasting. Quarterly Journal Royal Meteorological Society, 109, 393-416.

Hasselmann, K., Barnett, T.P., Bouws, E., Carlson, H., Cartwright, D.E., Enke, K., Ewing, J.A., Gienapp, H., Hasselmann, D.E., Kruseman, P., Meerburg, A., Muller, P., Olbers, D.J., Richter, K., Sell, W., Walden, H., 1973. Measurements of wind-wave growth and swell decay during the Joint North Sea Wave Project (JONSWAP). Deutsches Hydrographisches Institut, Hamburg, UDC 551.466.31; ANE German Bight.

Haltiner, G.J., Williams, R.T., 1980. Numerical prediction and dynamic meteorology, 2nd Edition. Wiley, 477pp.

Holt, M.W., and Hall, B.J., 1992. A comparison of 2nd generation and 3rd generation wave model physics. Unpublished Met Office Short-Range Forecasting Research Division Technical Report Number 10.

Holt, M.W., 1992. A re-calibration of the Wave model. Unpublished Met Office Short-Range Forecasting Research Division Technical Report Number 26.

Holt, M.W., 1993. Running the global wave model with shallow water depth information. Unpublished Met Office Forecasting Research Division Technical Report Number 45.

Holt, M.W., 1994. Improvements to the UKMO wave model swell dissipation and performance in light winds. Unpublished Met Office Forecasting Research Division Technical Report Number 119.

Janssen, P.A.E.M., 1991. Quasi-linear theory of wind-wave generation applied to wave forecasting. Jpurnal of Physical Oceanography, 21, 1631-1642.

Richtmeyer, R.D., Morton, K.W., 1967. Difference methods for initial value problems. Interscience, 406pp.

Snyder, R.L., Dobson, F.W., Elliott, J.A., Long, R.B., 1981. Array measurements of atmospheric pressure fluctuations above surface gravity waves. Journal of Fluid Mechanics, 102, 1-60.

Stratton, R.A., Ephraums, J., 1986. Great circle turning for the operational wave model. Unpublished Met O 2b Technical Note Number 109.

Stratton, R.A., Holt, M.J., Kelsall, S., 1995 (last modification). Wave model forecast program qxglwmodel. Unpublished Met Office Wave Model Documentation Paper Number 6.

Appendix 4 Validation of Met Office Wave Model Data

A4.1   Introduction

This note compares the Met Office modelled data with observed data from wave buoys.   The intention of the comparison was to provide information on the accuracy of the modelling.   The comparison is carried out at six sites, described in **Table A4.1** and shown in **Figure A4.1**.   The parameters compared were significant wave height and zero crossing wave period of resultant waves in the observed and modelled records (See **Figures A4.2.1 to 4.2.12**).   The graphs show occurrences of wave height and wave period for a given banding for modelled and observed data.   These sites were selected as they represent sites with sufficiently deep water.   This reflects the swell wave chainage selected, based on the 20m and 50m Chart Datum depth contours.

Table A4.1 – Details of Met Office Wave Model Validation

Location	Easting (m)	Northing (m)	Depth (m)	Data Coverage	
Scarweather	265716	172255	30	3 years	1st Feb 2006 – 31st Dec 2008
Liverpool Bay	310399	405021	22	5 years	13th Nov 2002 – 31st Dec 2002 1st Jan 2004 – 31st Dec 2008
Firth of Forth	368818	699693	65	1 year	1st Jan 2008 – 31st Dec 2008
Tyne/Tees	480382	558899	65	1 year	7th Dec 2006 – 31st Dec 2007
West Gabbard	680221	239143	34	6 years	28th Aug 2002 – 31st Dec 2008
Hastings	594341	97640	36	6 years	26th Nov 2002 – 31st Dec 2008

Figure A4.1 – Location of Wave Buoys for Met Office Model Validation

A4.2　Validation Sites

A4.2.1　Scarweather
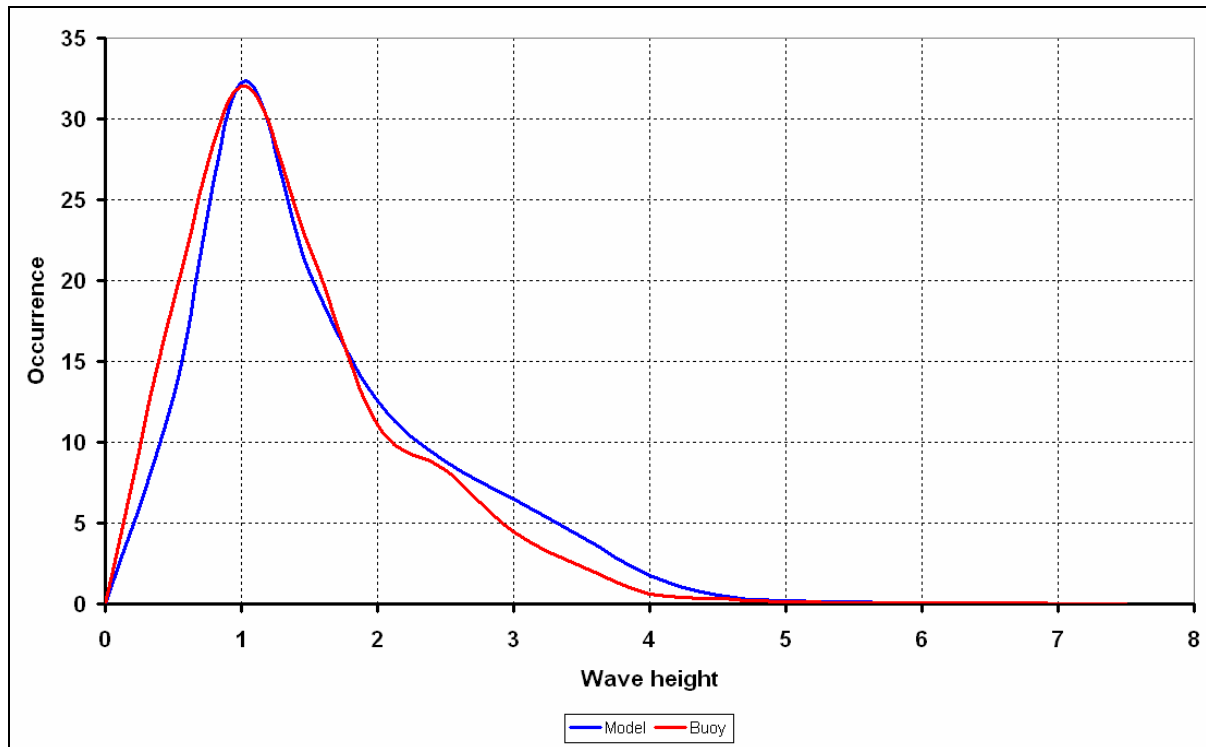
Figure A4.2.1 Scarweather Wave Height Comparison
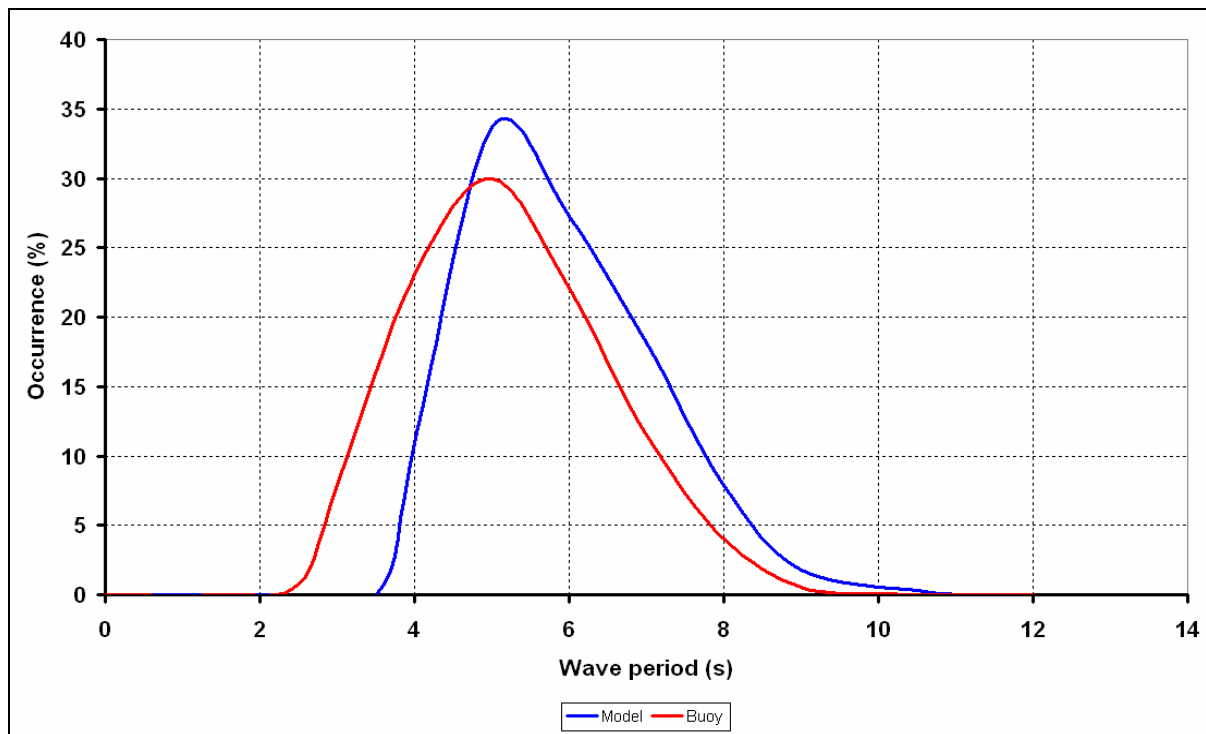
Figure A4.2.2 Scarweather Wave Period Comparison

A4.2.2 Liverpool Bay
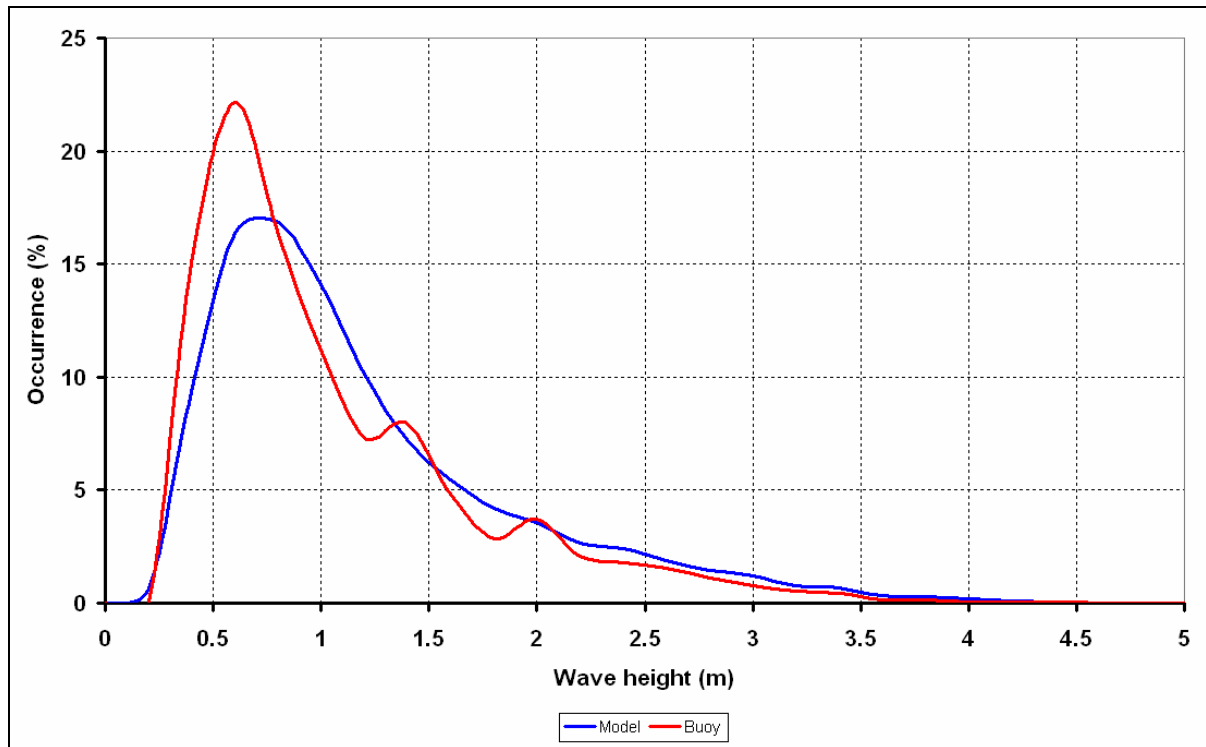
Figure A4.2.3 Liverpool Bay Wave Height Comparison
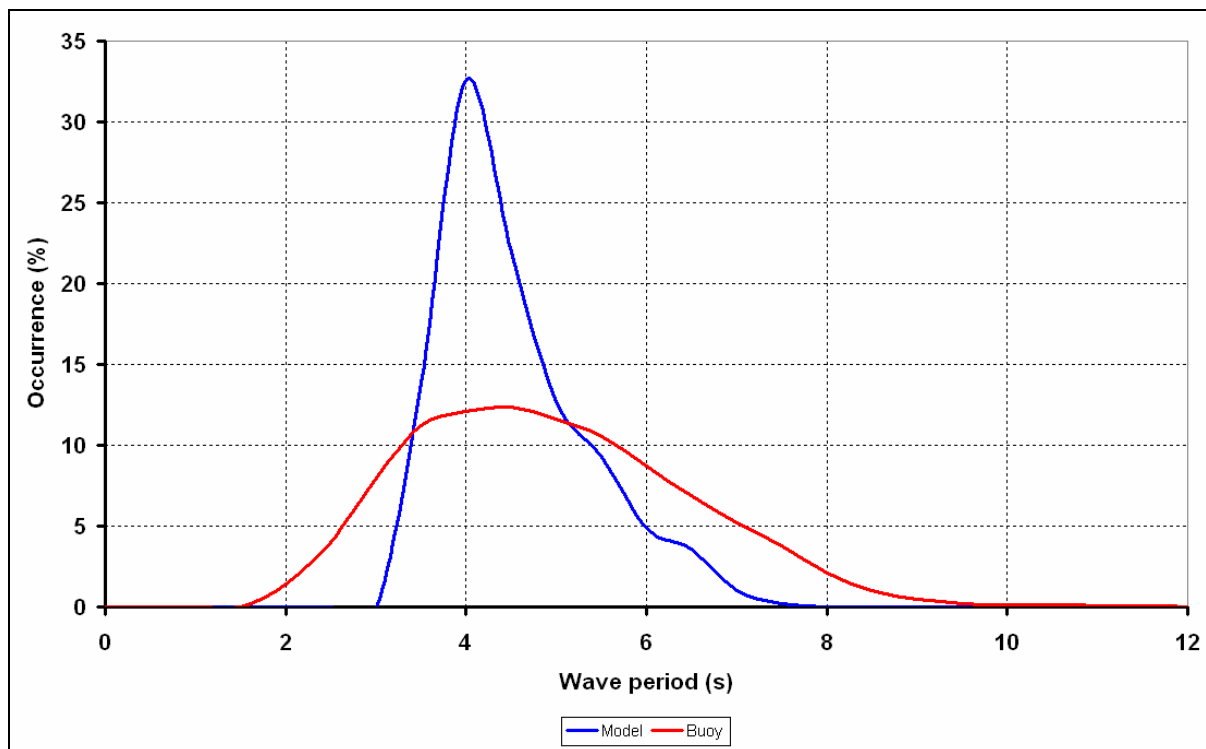
Figure A4.2.4 Liverpool Bay Wave Period Comparison

A4.2.3   Firth of Forth
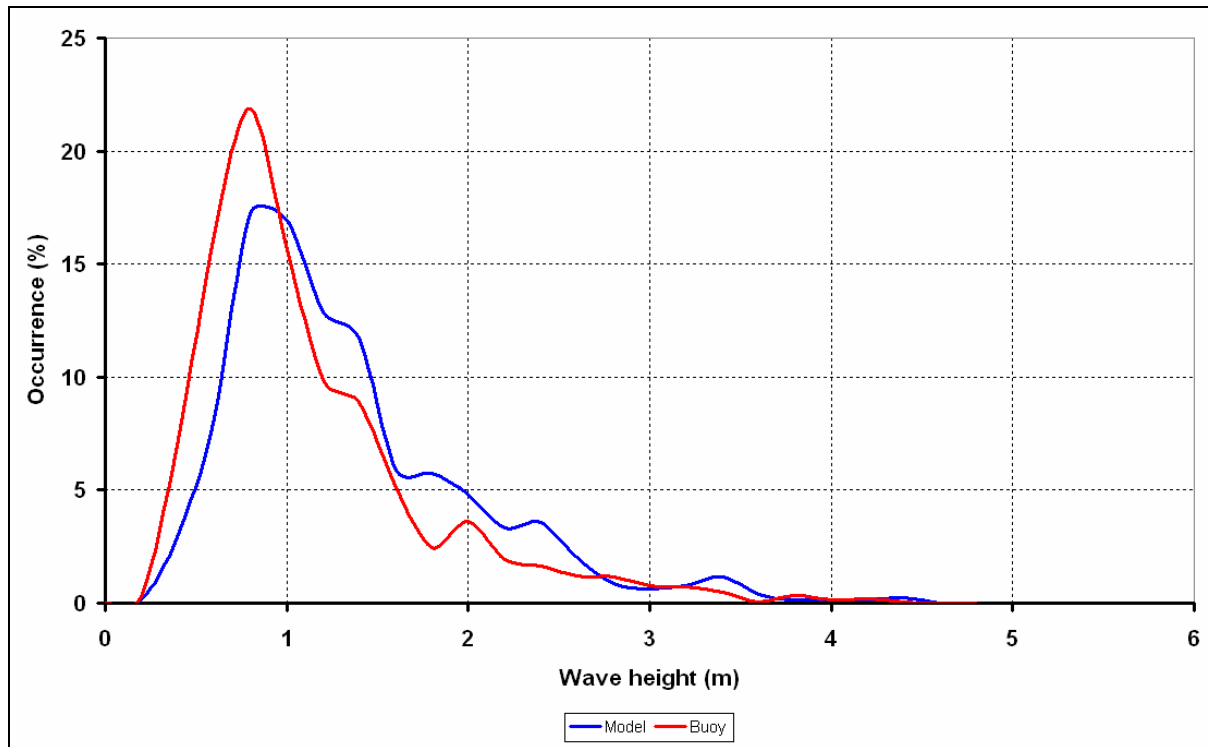
Figure A4.2.5 Firth of Forth Wave Height Comparison
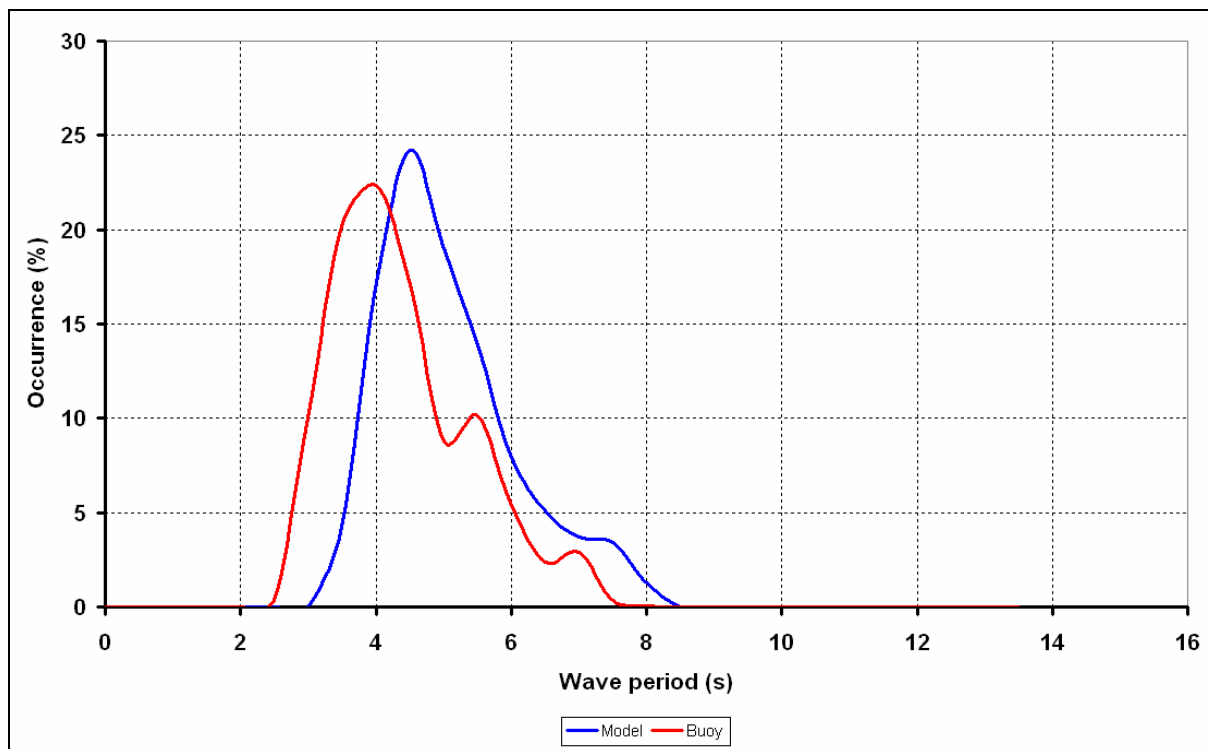
Figure A4.2.6 Firth of Forth Wave Height Comparison

A4.2.4   Tyne/Tees
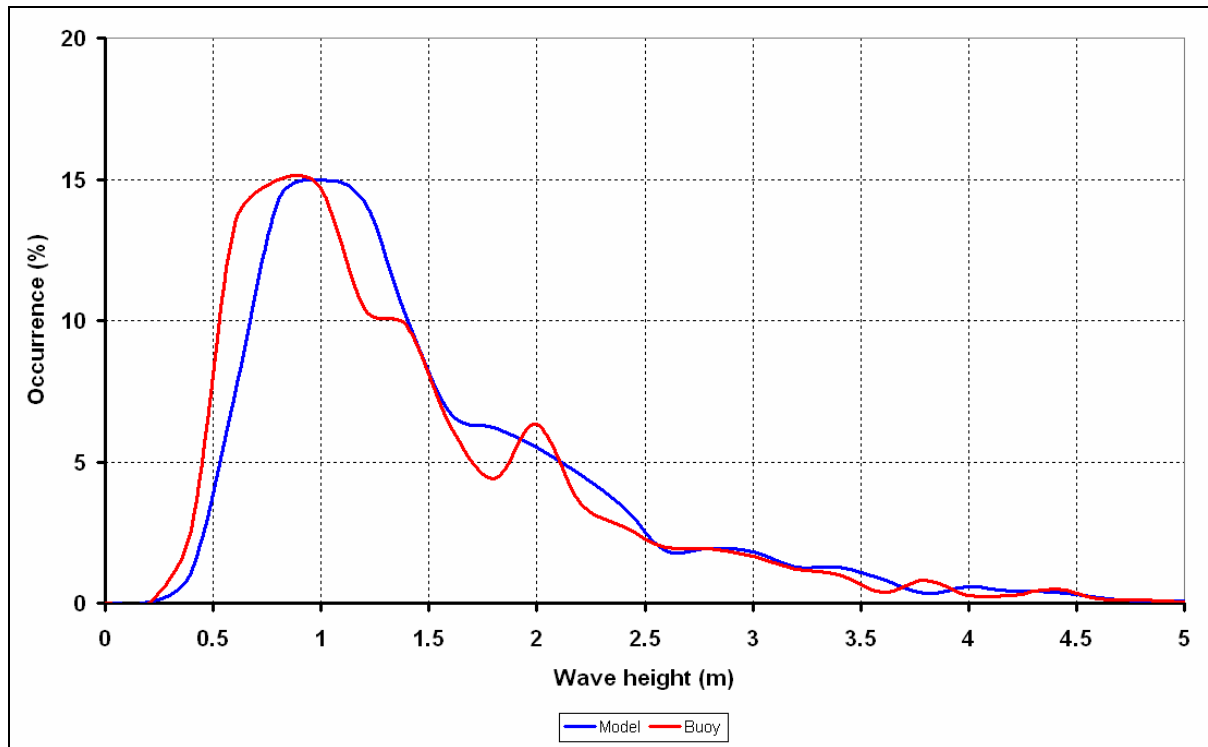
Figure A4.2.7 Tyne/Tees Wave Height Comparison
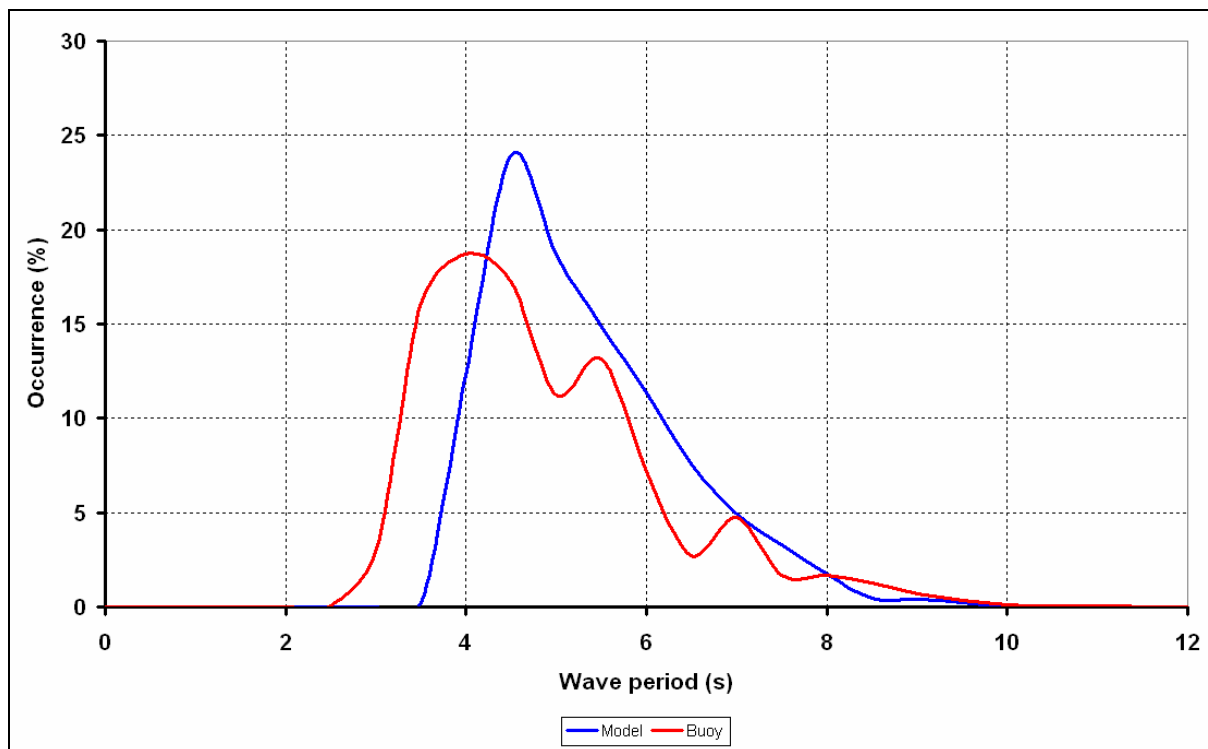
Figure A4.2.8 Tyne/Tees Wave Period Comparison

A4.2.5 West Gabbard
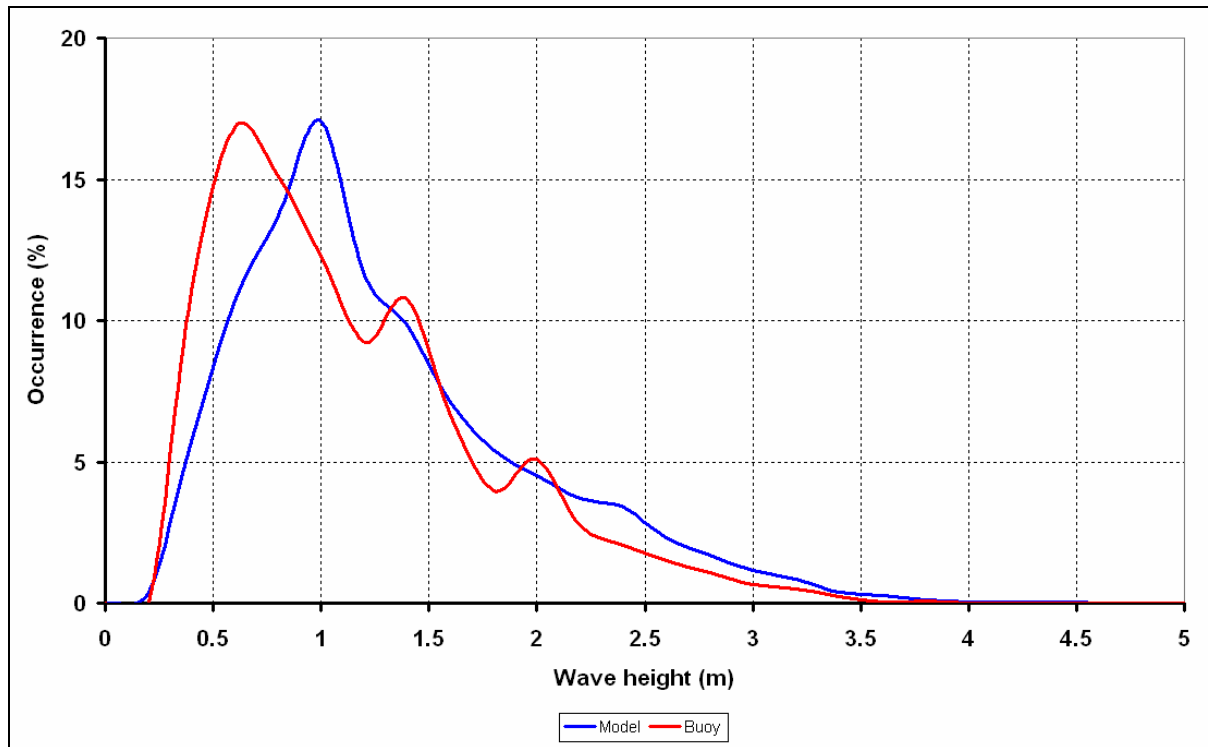
Figure A4.2.9 West Gabbard Wave Height Comparison
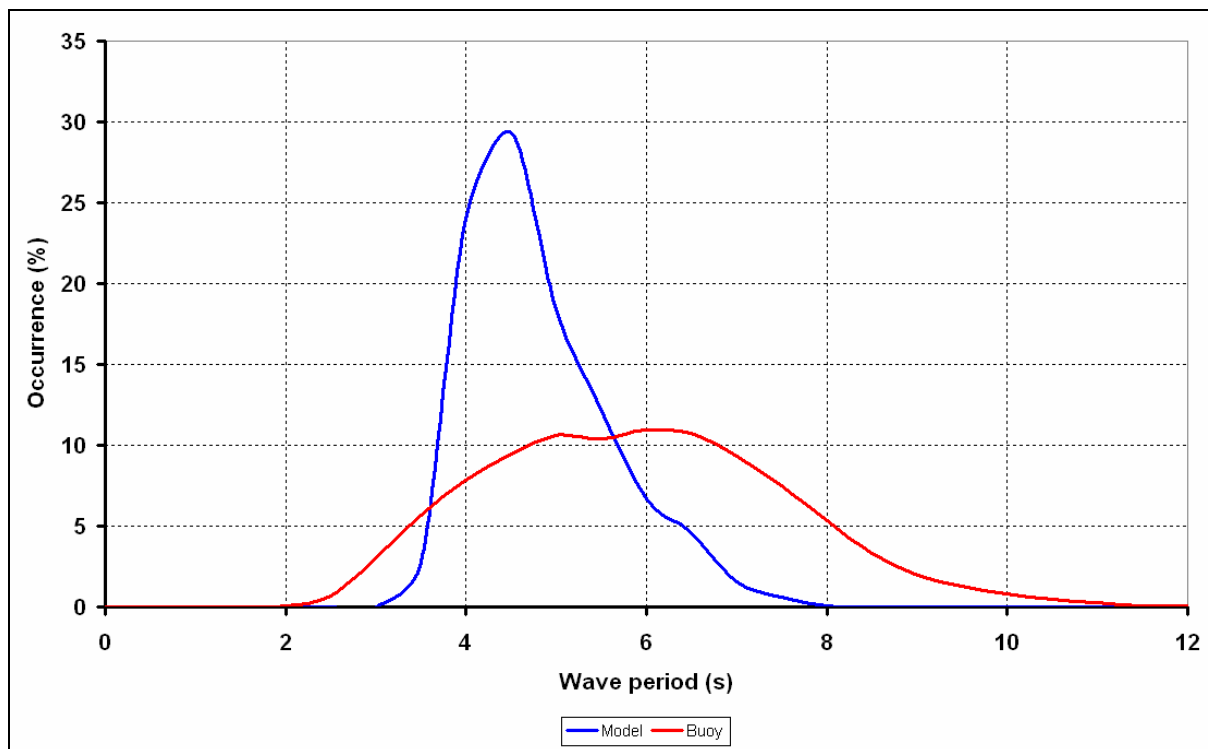
Figure A4.2.10 West Gabbard Wave Period Comparison

A4.2.6   Hastings
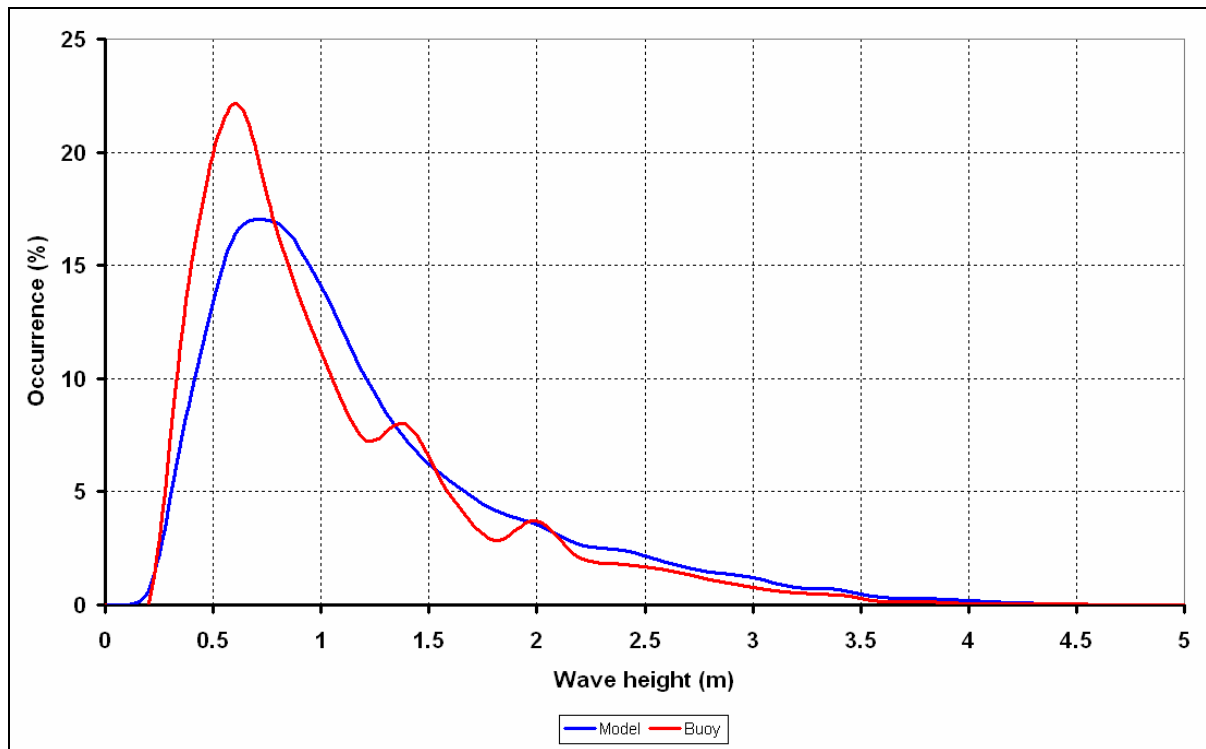
Figure A4.2.11 Hastings Wave Height Comparison
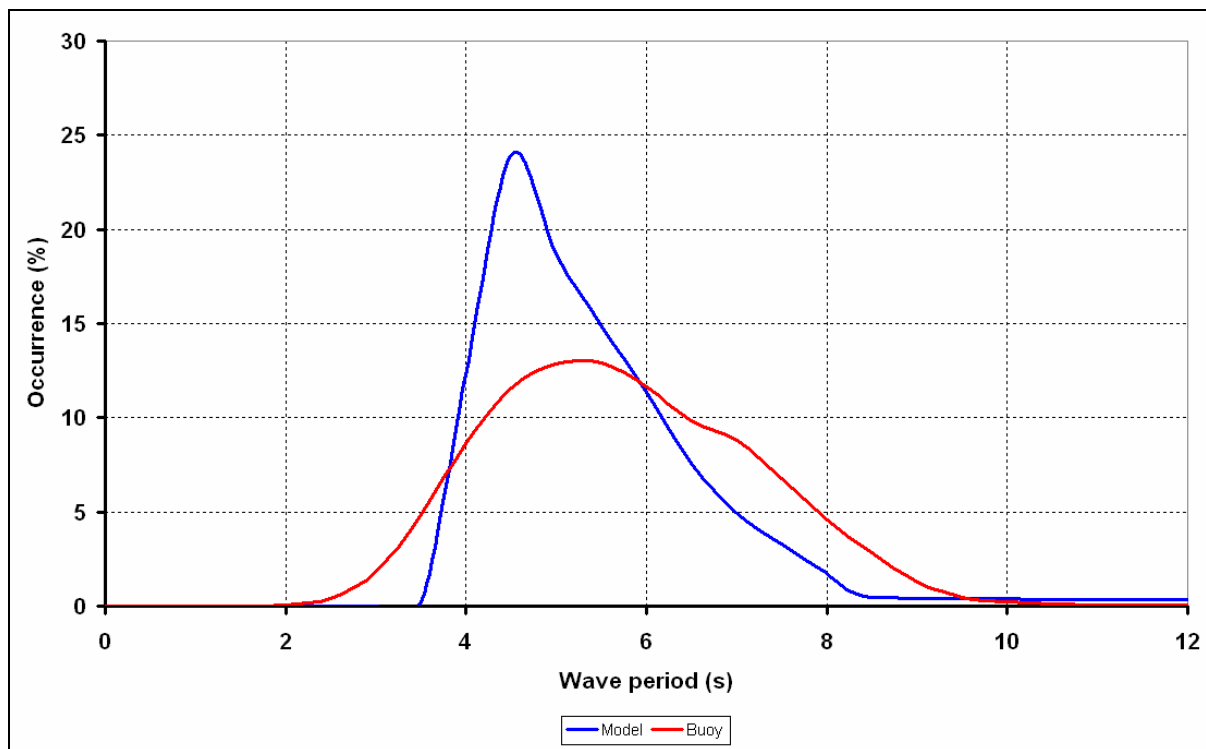
Figure A4.2.12 Hastings Wave Period Comparison

A4.3   Overview

Table A4.2 shows a comparison of peak and observed wave data characteristics.

Table A4.2 – Peak wave height and wave periods for modelled and observed wave data

	Wave Height Peak Occurrence		Wave Period Peak Occurrence	
	Model (m)	Observed (m)	Model (s)	Observed (s)
Scarweather	1.0	1.0	5.0	5.0
Liverpool Bay	0.8	0.6	4.5	4.5
Firth of Forth	0.8	0.8	4.5	4.0
Tyne/Tees	1.0	0.8	4.5	4.0
West Gabbard	1.0	0.6	4.5	5.5
Hastings	0.8	0.6	4.5	6.0

The comparison shows a good match for significant wave height between observed and modelled wave data at the six validation sites. The peak occurrences are similar with the largest difference of 0.4m at West Gabbard. The occurrence distributions are also similar.

The comparison shows a more variable match between the modelled and observed zero crossing wave periods at the six validation sites. In general the peak zero crossing wave period difference is up to half a second between the observed and modelled data. At West Gabbard and Hastings there is a larger difference with the peak observed zero crossing periods 1 second higher than modelled data at West Gabbard and 1.5 seconds higher at Hastings.

The occurrence distribution differs for the zero crossing wave period at Liverpool, West Gabbard and Hastings, with a lower peak and broader base for these sites in comparison with the model data. The model may therefore not include the higher wave periods at these sites, and potentially others; this may affect the wave periods provided in this project. Therefore, a precautionary approach should be used when selecting a wave period for a corresponding wave period for a given wave height.

Appendix 5 Statistical Method Development

A5.1   Introduction

This Appendix describes each of the functions that calculate the statistics used in this work. These functions are called in a routine to provide the information and graphs provided in this report.

The final results used the following functions:

- gpd.fit
- gpd.pp
- gdp.qq
- gpd.rtn.level

There are a number of further functions that were used in the investigations and development of the final method. These include:

- weibull.fit
- weibull.pp
- weibull.qq
- weibull.rtn.level
- weibull.to.normal
- gpd.to.normal
- bvn.fit
- bvn.sim
- normal.to.weibull
- normal.to.gpd
- ecdf.by.group
- gpd.by.group
- gpd.pp.by.group
- gpd.qq.by.group
- height.ecdf.by.group
- find.period.dist
- sim.period.above.thresh
- sim.period
- prob.period.given.height
- prob.period.given.height.2

The descriptions provide the basic mathematical explanation of the function, the required inputs (arguments) and the results (values).

Documentation for R code

Emma Eastoe

August 25, 2009

Contents

1.1 Marginal fits

`weibull.fit`
Fits the 3-parameter Weibull distribution to all non-zero data. The distribution function is

$$F(x) = 1 - \exp\left\{-\left[\frac{x - \alpha}{\beta}\right]^{\gamma}\right\}, \quad \beta > 0, \ \gamma > 0, \quad x \geq 0.$$

Fit uses Maximum Likelihood (ML) estimation.
Arguments
`data` - vector of data (*e.g.* surge wave height).
Values - list containing
`par.est` - vector of maximum likelihood estimates (MLE's) of (α, β, γ).
`covar.matrix` - estimated covariance matrix for (α, β, γ).
`data` - the data that were entered into the function (required for later functions).
`data.nonz` - the non-zero data (required for later functions).

`weibull.pp`
Produces a probability-probability (PP) plot to assess goodness of fit of the Weibull distribution. Also plots 95% confidence intervals (dashed lines) and the 45° line of perfect fit (full line).
Arguments
`fit` - output of `weibull.fit`
Values
PP-plot in existing active graphics device (will open a new one if currently none open).

`weibull.qq`
Produces a quantile-quantile (QQ) plot to assess goodness of fit of the Weibull distribution. Also plots 95% confidence intervals (dashed lines) and the 45° line of perfect fit (full line).
Arguments
`fit` - output of `weibull.fit`
Values
QQ-plot in existing active graphics device (will open a new one if currently none open).

`weibull.rtn.level`
Produces MLE's for one or more N-year return levels. Let x_N denote the N-year return level which has probability of excess $p = 1/(N \times npy)$, where npy is the number of points observed in each year, then

$$x_p = \alpha + \beta\left[-\log(p/\kappa)\right]^{1/\gamma}$$

where κ is the observed proportion of non-zeroes in the data. Also produces standard errors for each of the return levels using the ∇-method.
Arguments
`fit` - output of `weibull.fit`
`N` - number of years for return level
`npy` - observed number of points per year
Values - a list containing
`point.est` - vector of MLE's for the specified return levels. Return levels will be returned in the same order as the survival probabilities were input in `p`.
`se` - vector of standard errors associated with MLE's in `point.est`.

2

`gpd.fit`
Fits the 2-parameter generalised Pareto (GP) distribution with conditional distribution function, for $x > u$,

$$\Pr(X \leq x | X > u) = 1 - \left[1 + \xi \left(\frac{x - u}{\sigma} \right) \right]_+^{-1/\xi}, \quad \sigma > 0$$

and $z_+ = \max\{z, 0\}$. Fit is to excesses of a specified threshold and parameter estimation is by ML.
Arguments
`data` - vector of data (*e.g.* surge wave height).
`threshold` - threshold to be used in modelling.
Values - list containing
`par.est` - vector of maximum likelihood estimates (MLE's) of (σ, ξ).
`covar.matrix` - estimated covariance matrix for (σ, ξ).
`data` - the data that were entered into the function (required for later functions).

`gpd.pp`
Produces a probability-probability (PP) plot to assess goodness of fit of the GP distribution to threshold excesses used in model fit. Also plots 95% confidence intervals (dashed lines) and the 45° line of perfect fit (full line).
Arguments
`fit` - output of `gpd.fit`
Values
PP-plot in existing active graphics device (will open a new one if currently none open).

`gpd.qq`
Produces a quantile-quantile (QQ) plot to assess goodness of fit of the GP distribution to threshold excesses used in model fit. Also plots 95% confidence intervals (dashed lines) and the 45° line of perfect fit (full line).
Arguments
`fit` - output of `gpd.fit`
Values
QQ-plot in existing active graphics device (will open a new one if currently none open).

`gpd.rtn.level`
Produces MLE's for one or more N-year return levels. Let x_N denote the N-year return level which has probability of excess $p = 1/(N \times npy)$, where npy is the number of points observed in each year. If p is less than the probability of exceeding the threshold, *i.e.* $p < \lambda$ where $\lambda = \Pr[X > u]$, then

$$x_p = u + \frac{\sigma}{\xi} \left[\left(\frac{p}{\lambda} \right)^{-\xi} - 1 \right]$$

Also produces standard errors for each of the return levels using the ∇-method. Note that λ is estimated empirically using the full data series (including any observations which are zero).
Arguments
`fit` - output of `gpd.fit`
`N` - number of years for return level
`npy` - observed number of points per year
Values - a list containing
`point.est` - vector of MLE's for the specified return levels. Return levels will be returned in the same

3

order as the survival probabilities were input in `p`.

`se` - vector of standard errors associated with MLE's in `point.est`.

1.2 Bivariate normal fit

`weibull.to.normal`
Transforms data to standard normal margins, under the Weibull model fit to that data. Transformation uses the probability integral transform.
Arguments
`fit` - output of `weibull.fit`
Values - a list containing
`fit` - As input into the function.
`normal` - data transformed to have a Normal(0,1) distribution.

`gpd.to.normal`
Transforms data to standard normal margins, under the GP model fit to that data. Transformation uses the probability integral transform. For data below the modelling threshold, the empirical distribution function is used.
Arguments
`fit` - output of `gpd.fit`
Values - a list containing
`fit` - As input into the function.
`normal` - data transformed to have a Normal(0,1) distribution.

`bvn.fit`
Fits a bivariate normal (BVN) distribution to a 2-dimensional data set with standard normal margins. Since margins are Normal(0,1) the only parameter that requires estimation is the correlation ρ. Requires the R library `mvtnorm` (which may be downloaded from CRAN[1] if necessary).
Arguments
`data1` - first variable on Normal$(0,1)$ margins (may be `$normal` output of `weibull.fit` or `gpd.fit`).
`data2` - second variable on Normal$(0,1)$ margins (may be `$normal` output of `weibull.fit` or `gpd.fit`).
`threshold1` - threshold used in joint modelling for first variable (may be the same as for marginal GP model, but must be respecified).
`threshold2` - threshold used in joint modelling for second variable (may be the same as for marginal GP model, but must be respecified).
Values - a list containing
`par.est` - MLE of the correlation ρ
`se` - standard error of the estimate of ρ
`data1` - data on first variable as input.
`data2` - data on first variable as input.
`threshold1` - threshold for first variable as input.
`threshold2` - threshold for second variable as input.

---

[1] http://cran.r-project.org/web/packages/mvtnorm/index.html

1.3 Bivariate normal simulation

`bvn.sim`
Simulation from the BVN model fitted using `bvn.fit`. Margins are output on Normal(0,1) margins, so either `normal.to.weibull` or `normal.to.gpd` should be used to transform variables back to their original scale.
Arguments
`size` - size of data set to be simulated.
`fit` - output from `bvn.fit`.
Values - a list containing
`data.sim` - `size`×2 matrix containing simulated data set (first column contains the first variable, second column contains the second).

`normal.to.weibull`
Transforms data for a single variable from a standard normal margin to a Weibull margin. Transformation uses the probability integral transform. Note that this function would have to be used twice separately to transform both variables simulated using `bvn.sim`.
Arguments
`sim` - simulated data extracted from output of `bvn.fit`.
`margin` - output of `weibull.fit` for the appropriate variable
Values - a list containing
`fit` - the Weibull model fit as input as `margin`.
`weibull` - data transformed to the Weibull distribution.

`normal.to.gpd`
Transforms data for a single variable from a standard normal margin to a GP margin. Transformation uses the probability integral transform and the empirical distribution function for values below the marginal modelling threshold. As with `normal.to.weibull` this function would have to be used twice separately to transform both variables simulated using `bvn.sim`.
Arguments
`sim` - simulated data extracted from output of `bvn.fit`.
`margin` - output of `gpd.fit` for the appropriate variable
Values - a list containing
`fit` - the GP model fit as input as `margin`.
`gpd` - data transformed to the GP distribution.

1.4 Simulating period given height

1.4.1 Exploratory tools

`ecdf.by.group`
Plots the empirical cumulative distribution functions (ECDF's) of wave height where height is split into groups according to the size of the associated wave period. The ECDF for group j is defined as

$$\hat{F}_j(x_{(i)}) = \frac{i}{n_j + 1}$$

where $x_{(i)}$ is the ith largest height in that group and n_j is the total number of observations in the group.

<u>Arguments</u>
`height` - vector of heights.
`period` - vector of periods corresponding to heights.
`groups` - vector of separation points for period groups. Note that this does not include the lower end point of the first group nor the upper end point of the last group, *e.g.* to split the period into three groups would require a vector of length two.

<u>Values</u>
Returns a plot of the ECDF's for height, split by period group. Colour coding is according to group with the usual `R` colour ordering (black - group 1, red - group 2, green - group 3, dark blue - group 4 and so on).

`gpd.by.group`
Within the p period groups, fits a separate $\mathrm{GP}(\sigma_j, \xi_j)$ distribution to the heights exceeding a pre-specified threshold. The threshold is specified as a percentage, *e.g.* 0.9, 0.99, which is the same for each group. Within each group the threshold level is calculated as the empirical quantile associated with this percentage and so may vary between groups.

<u>Arguments</u>
`height` - vector of heights.
`period` - vector of periods corresponding to heights.
`groups` - vector of separation points for period groups. Note that this does not include the lower end point of the first group nor the upper end point of the last group, *e.g.* to split the period into three groups would require a vector of length two.
`q` - percentage for threshold level calculation, should be high *e.g.* 0.9, 0.95, 0.99

<u>Values</u>
`thresholds` - vector of the threshold level used for each group.
`par.est` - $p \times 2$ matrix of the MLE's $(\hat{\sigma}_j, \hat{\xi}_j)$. First column gives estimates of $\hat{\sigma}_j$ and second estimates of $\hat{\xi}_j$. Row j corresponds to estimates for group j.
`covar.matrix` - list of 2×2 covariance matrices for $(\hat{\sigma}_j, \hat{\xi}_j)$. The jth element corresponds to the covariance matrix for the jth group.

`gpd.pp.by.group`
Gives PP plots for each of the GPD height models fitted to heights split by period groups. Arguments are the same as for the function `gpd.by.group`.

Arguments
`height` - vector of heights.
`period` - vector of periods corresponding to heights.
`groups` - vector of separation points for period groups. Note that this does not include the lower end point of the first group nor the upper end point of the last group, *e.g.* to split the period into three groups would require a vector of length two.
`q` - percentage for threshold level calculation, should be high *e.g.* 0.9,0.95, 0.99

Values
Returns a plot of the p PP plots, with 45° line of exact agreement and 95% confidence intervals also indicated.

`gpd.qq.by.group`
Gives QQ plots for each of the GPD height models fitted to heights split by period groups. Arguments are the same as for the function `gpd.by.group`.

Arguments
`height` - vector of heights.
`period` - vector of periods corresponding to heights.
`groups` - vector of separation points for period groups. Note that this does not include the lower end point of the first group nor the upper end point of the last group, *e.g.* to split the period into three groups would require a vector of length two.
`q` - percentage for threshold level calculation, should be high *e.g.* 0.9,0.95, 0.99

Values
Returns a plot of the p QQ plots, with 45° line of exact agreement and 95% confidence intervals also indicated.

1.4.2 Simulation

`height.ecdf.by.group`
All heights below the maximum of the thresholds used to fit the separate GP models (according to period group) are first split into q non-overlapping bands according to their size. For each band of heights $h_1, \ldots, h_q$, the function calculates the empirical conditional probabilities $\Pr[p_j|h_k]$ of being in each of the period groups, $p_1, \ldots, p_p$.

Arguments
`height` - vector of observed heights.
`period` - vector of observed periods corresponding to heights.
`n.height` - number of observations to be contained within each height band (single number *e.g. 2000*).
`groups.period` - vector of separation points for period groups. Note that this does not include the lower end point of the first group nor the upper end point of the last group, *e.g.* to split the period into three groups would require a vector of length two.
`fit` - output of `gpd.fit.group`

Values
`cond.probs` - $q \times p$ matrix of conditional probabilities $\Pr[p_j|h_k]$. The ith row corresponds to the ith height band and the jth column to the jth period group.
`groups.height` - vector of end-points for the height bands (of length q).

8

`find.period.dist`

Estimates the probability of being in each of the period groups using the empirical proportion of points in each group.

<u>Arguments</u>

`p` - vector of observed periods.

`groups.period` - vector of separation points for period groups. Note that this does not include the lower end point of the first group nor the upper end point of the last group, *e.g.* to split the period into three groups would require a vector of length two.

<u>Values</u>

Returns a vector of probabilities.

`sim.period.above.thresh`

Let v be the maximum of the thresholds used to fit the separate GP models (according to period group). For a given height $h^* > v$ this function will simulate an associated period group as follows. First, for each of the p period groups, the conditional probabilities $\Pr[p_j|h^*]$ are calculated using the formula

$$\Pr[p_j|h^*] = \frac{f(h^*|p_j)\Pr(p_j)}{f(h^*)}$$

where $f(h^*|p_j)$ is the $\text{GP}(\sigma^j, \xi_j)$ density evaluated at h^*, $\Pr(p_j)$ is the empirical proportion of points with period j (found using `find.period.dist`) and $f(h^*)$ is calculated as a normalising constant. The period group is then sampled using these conditional probabilities.

<u>Arguments</u>

`h` - single height.

`p` - vector of observed periods.

`fit` - output of `gpd.by.groups`.

`groups.period` - vector of separation points for period groups. Note that this does not include the lower end point of the first group nor the upper end point of the last group, *e.g.* to split the period into three groups would require a vector of length two.

`period.density` - output of `find.period.dist`.

<u>Values</u>

Returns a single simulated period group from $1, \ldots, p$.

`sim.period.below.thresh`

Let v be the maximum of the thresholds used to fit the separate GP models (according to period group). For a given height $h^* \leq v$ this function will simulate an associated period group as follows. Let h_k^* be the height band to which h^* belongs. The p conditional probabilities $\Pr[p_j | h_k^*]$ are obtained from the function `height.ecdf.by.group`. The period group is then sampled using these conditional probabilities.

Arguments

`h` - single height.

`p` - vector of observed periods.

`fit2` - output of `height.ecdf.by.group`.

`groups.period` - vector of separation points for period groups. Note that this does not include the lower end point of the first group nor the upper end point of the last group, *e.g.* to split the period into three groups would require a vector of length two.

Values

Returns a single simulated period group from $1, \ldots, p$.

`sim.period`

Given a vector of simulated wave heights this function returns a vector of simulated periods, using the functions `sim.period.below.thresh` and `sim.period.above.thresh`.

Arguments

`height.sim` - vector of simulate heights.

`height` - vector of observed heights.

`p` - vector of observed periods.

`groups.period` - vector of separation points for period groups. Note that this does not include the lower end point of the first group nor the upper end point of the last group, *e.g.* to split the period into three groups would require a vector of length two.

`fit` - output of `gpd.by.groups`.

Values

`period.sim` - vector of simulated periods groups $((1, \ldots, p))$ corresponding to input vector of simulated heights `height.sim`.

`prob.period.given.height`

Given vectors of wave heights and wave period *groups* this function estimates empirically an $r \times c$ data frame containing the empirical probabilities

$$p_{ij} = \Pr[p \in p_j | h \in h_i], \quad i = 1, \ldots, r, \quad j = 1, \ldots, p.$$

Here $p_1, \ldots, p_p$ are p non-overlapping period groups (corresponding to the groups used to fit the model) and $h_1, \ldots, h_r$ are r non-overlapping height groups.

Arguments

`height` - vector of heights.

`period` - vector of period groups.

`groups.height` - vector of separation points for period groups. Note that this does not include the lower end point of the first group nor the upper end point of the last group, *e.g.* to split the period into three groups would require a vector of length two.

`groups.period` - vector of separation points for period groups. Note that this does not include the lower end point of the first group nor the upper end point of the last group, *e.g.* to split the period into three groups would require a vector of length two.

Values

`cond.probs` - $r \times p$ data frame of conditional probabilities p_{ij}.

`prob.period.given.height.2`

As `prob.period.given.height.2` except that the periods input are actual periods (rather than period groups).

<u>Arguments</u>

`height` - As `prob.period.given.height.2`.

`period` - vector of periods.

`groups.height` - As `prob.period.given.height.2`.

`groups.period` - As `prob.period.given.height.2`.

<u>Values</u>

`cond.probs` - As `prob.period.given.height.2`.

Appendix 6 Generalised Pareto Threshold Tests

A6.1 Introduction

This Appendix describes the choice of statistical method employed for this project. We first consider the Weibull distribution, used in previous analysis, before presenting our preferred distribution, the Generalised Pareto Distribution.

A6.2 Marginal Distribution

The Weibull distribution was used in the previous work (HR Wallingford Report SR409) report for the distribution of all swell wave heights W. The cumulative distribution function, F, for the Weibull is:

$$F(w) = P(W < w) = \exp\{-[(w - \alpha)/\beta]^{\gamma}]\} \text{ for } -\infty < w < \infty,$$

here α, β ($\beta > 0$) and γ are location, scale and shape parameters respectively. It is important to note that the upper tail, shown in Figure 1 for the probability density function $f(w)$ (the derivative of the function $F(w)$), is the primary focus for the generation of extreme swell wave height.
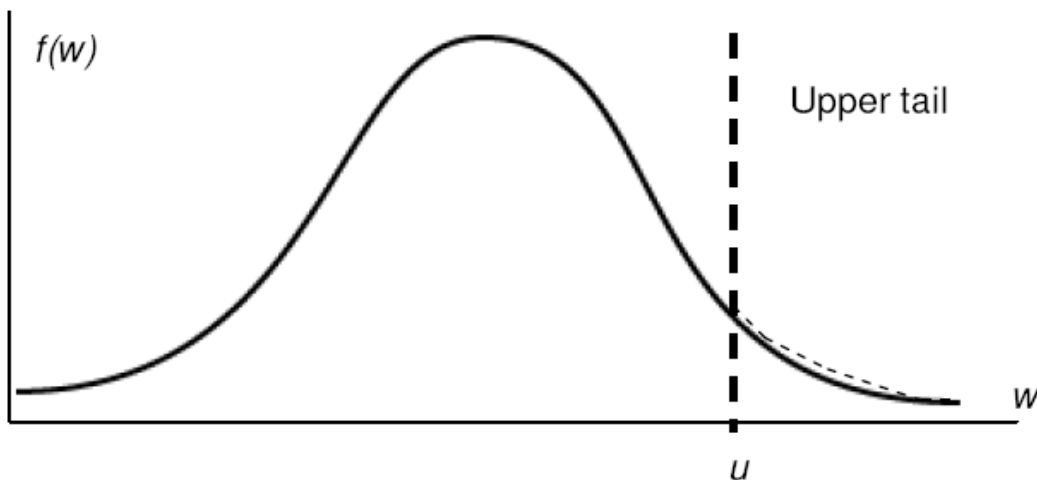
Figure A6.1 – Comparison of approaches. Solid line, a distribution fitted to all the data (e.g. a Weibull distribution) and dashed line, the Generalised Pareto Distribution fitted only to the upper tail.

There is a substantial risk when fitting a single distribution to all the data, which may introduce bias into the return level estimates. Therefore we recommend the use of a distribution specifically tailored to the upper tail, specifically the Generalised Pareto distribution (GPD). A threshold u is selected to determine the boundary between typical values and the upper tail, with the Generalised Pareto distribution being used to model the distribution of the values greater than u. The Generalised Pareto has cumulative distribution function is G_u with

$$G_u(w) = P(W < w \mid W > u) = 1 - [1 + \xi(w - u)/\sigma_u]^{-1/\xi} \text{ for } u < w < \infty,$$

where $\sigma_u > 0$ and ξ are scale and shape parameters respectively. This is a conditional distribution for the upper tail of W.

Like the Weibull distribution, the Generalised Pareto distribution has three parameters. However, the Generalised Pareto distribution tail model provides a much greater range of tail behavior than the Weibull distribution and therefore can capture a greater range of return level curves. The Weibull distribution can produce only an exponential tail decay whatever the selected parameters. In contrast, the Generalised Pareto distribution has an exponential tail decay then $\xi = 0$, but has a heavier tail than exponential when $\xi > 0$ and a lighter tail than exponential when $\xi < 0$.

To facilitate our decision on the choice of marginal distribution method, both Weibull and Generalized Pareto distributions were tested at the following sites (see **Figure A6.2**):

- Two East Coast locations (grid points: GL1104 and GL1993
- Two South Coast locations: GL2645 and GL 2849
- Southwest England (north coast): GL2523
- Wales: GL1946
- West Scotland: GL 1276
- North Scotland: GL 0531

Figure A6.2 – Statistical Distribution Test Sites

The results of Weibull fitting to wind-sea and swell are presented in **Figures A6.3** to **A6.10** and the results of the Generalised Pareto fitting are presented in **Figure A6.11** to **A6.18**. For both distributions, the maximum likelihood fitting method was used in all cases to fit wind-sea and swell from all directions.

The statistical fitting is expressed as probability-probability (PP) plots and quantile-quantile (QQ) plots. The PP plots show the relative probability distributions between the data and that given by the statistical fitting; the QQ plots show the relative wave height values.

Figures **A6.3** to **A6.10** show that the Weibull distribution fits the wind-sea poorly. This can be seen in, for example, **Figures A6.3a** and **A6.4a** where the data lies outside the confidence bounds of the Weibull fit. For the swell, the fitting to the Weibull distribution is better but the maximum likelihood estimation failed at sites GL1993, GL2645 and GL1946.

Comparing to the Weibull distribution, the Generalised Pareto distribution fits consistently well to both wind-sea and swell. Overall, the use of the exceedance of 95% for threshold performs better than the use of exceedancs of 90% and 99% with respect to fitting errors and 95% confidence intervals.

A6.3   Conclusions:

- The Weibull distribution does not fit well to the wind-sea and performs less well than the GPD for the swell.

- The GPD distribution fits consistently well to both wind-sea and swell. Therefore, we believe the use of the GPD distribution for extreme swell analysis is the better approach.
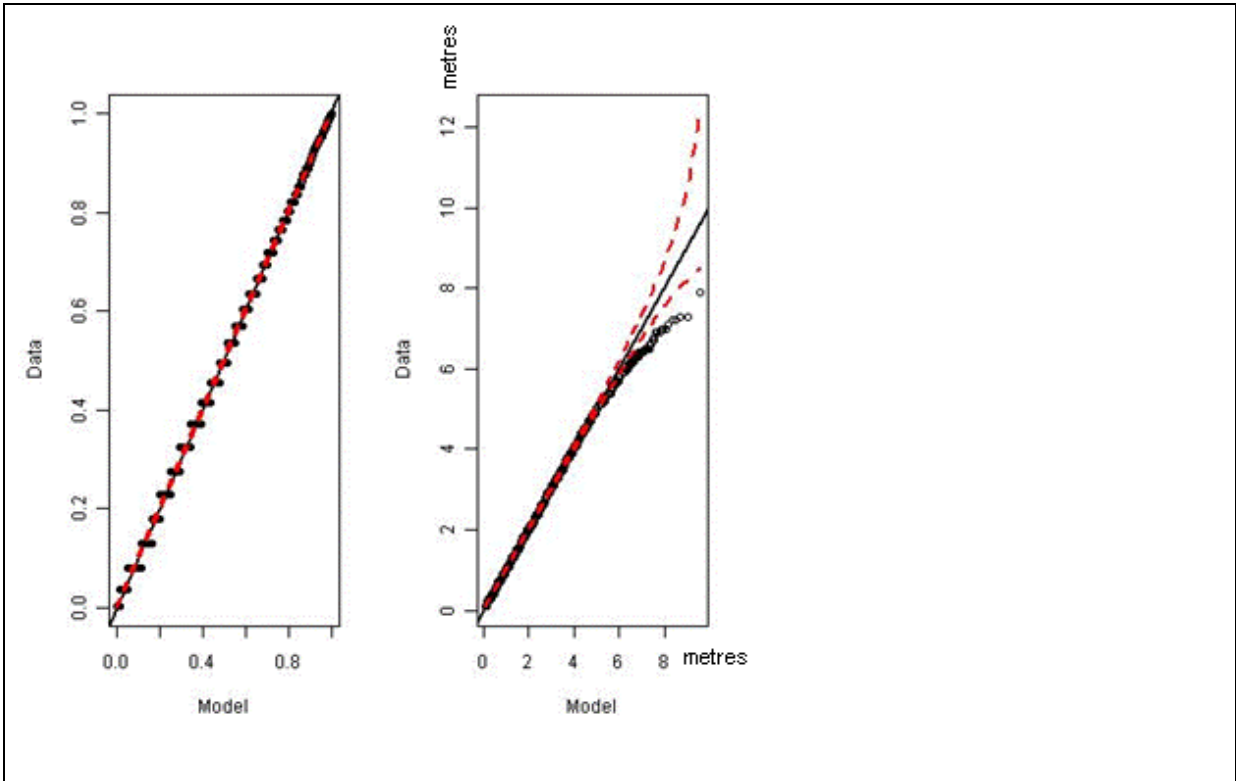
Figure A6.3a – Weibull fit for the wind-sea height (PP and QQ plots) – Test Site GL1104 (the red-dashed lines show 95% confidence bounds)
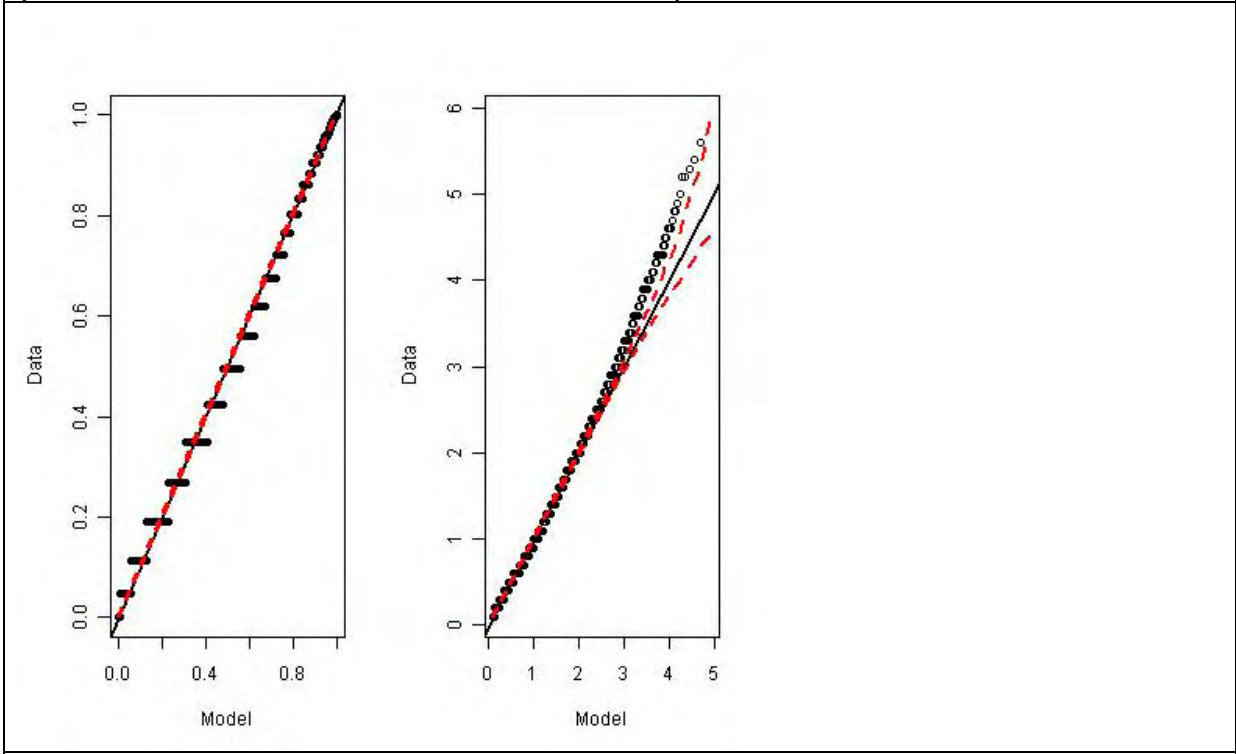
Figure A6.3b – Weibull fit for the swell height (PP and QQ plots) – Test Site GL1104 (the red-dashed lines show 95% confidence bounds)
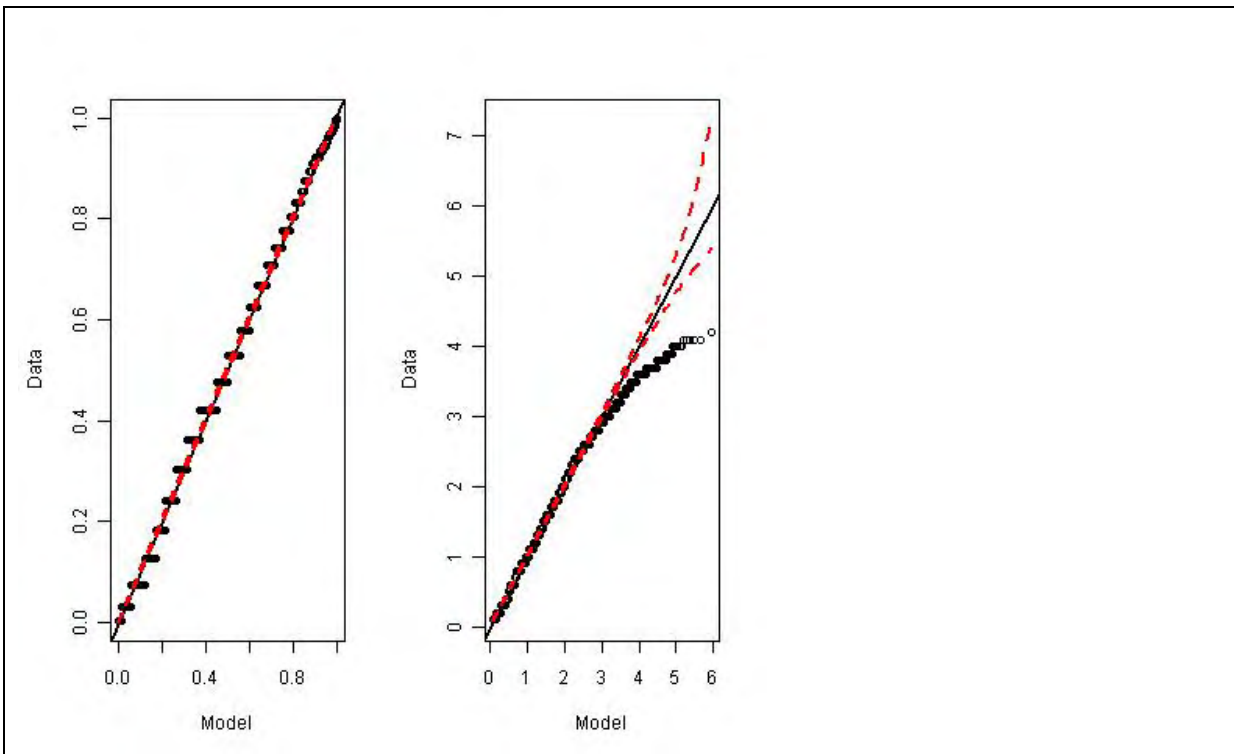
Figure A6.4a – Weibull fit for the wind-sea height (PP and QQ plots) – Test Site GL1993 (the red-dashed lines show 95% confidence bounds)
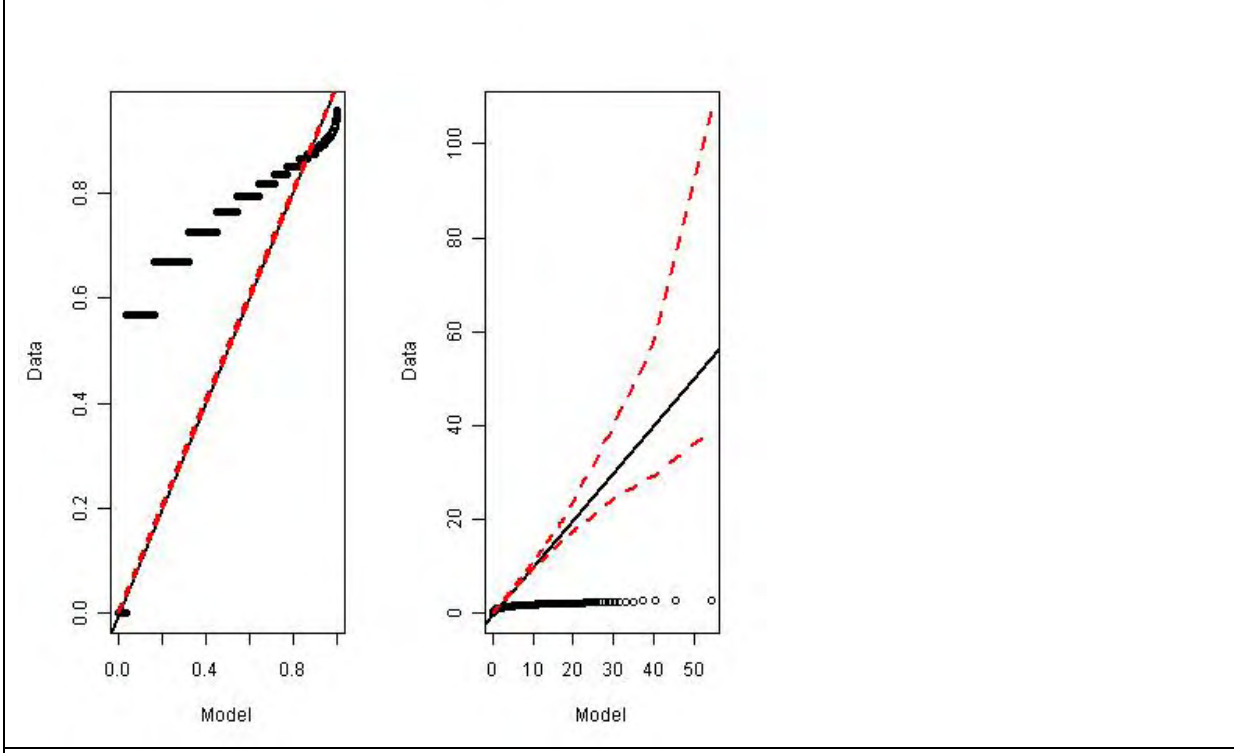
Figure A6.4b – Weibull fit for the swell height (PP and QQ plots) – Test Site GL1993 (the red-dashed lines show 95% confidence bounds)
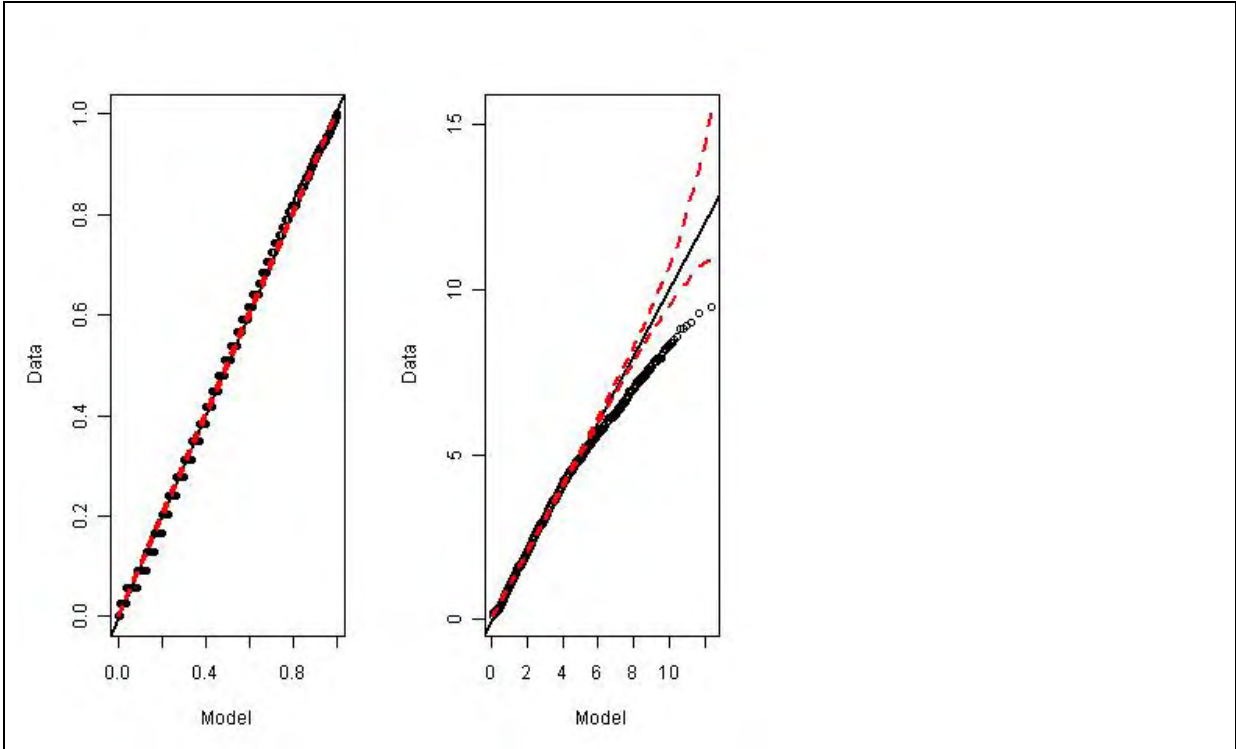
Figure A6.5a – Weibull fit for the wind-sea height (PP and QQ plots) – Test Site GL2645 (the red-dashed lines show 95% confidence bounds)
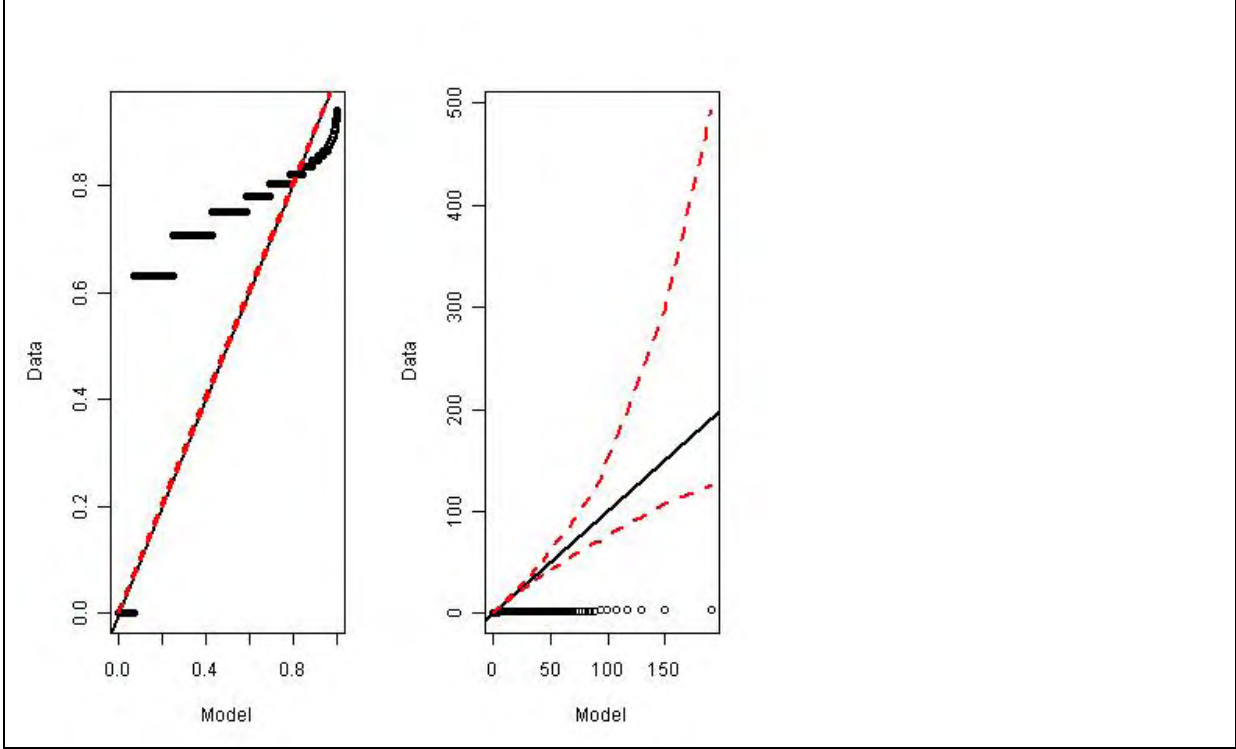
Figure A6.5b – Weibull fit for the swell height (PP and QQ plots) – Test Site GL2645 (the red-dashed lines show 95% confidence bounds)
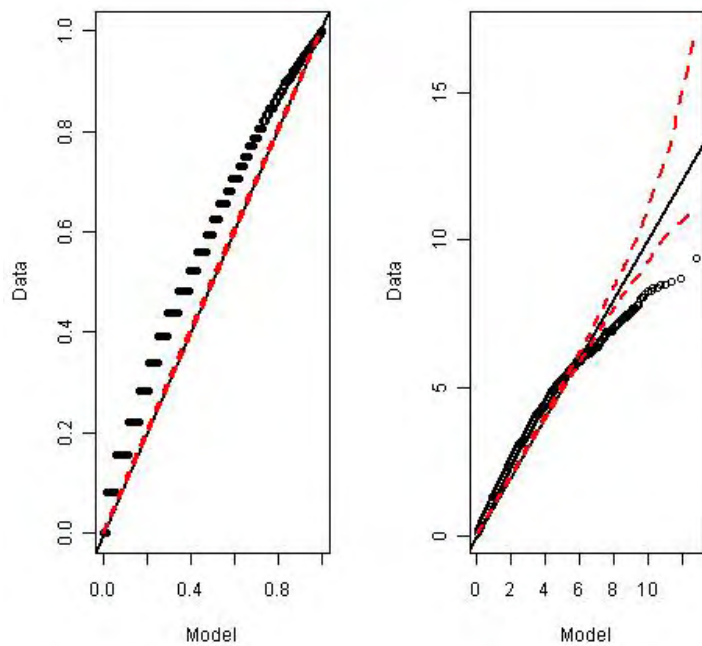
Figure A6.6a – Weibull fit for the wind-sea height (PP and QQ plots) – Test Site GL2849 (the red-dashed lines show 95% confidence bounds)
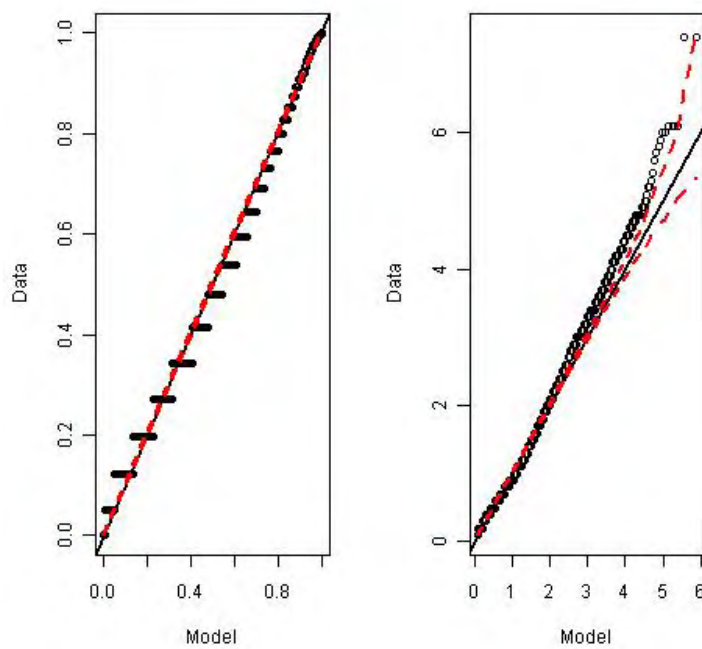
Figure A6.6b – Weibull fit for the swell height (PP and QQ plots) – Test Site GL2849 (the red-dashed lines show 95% confidence bounds)
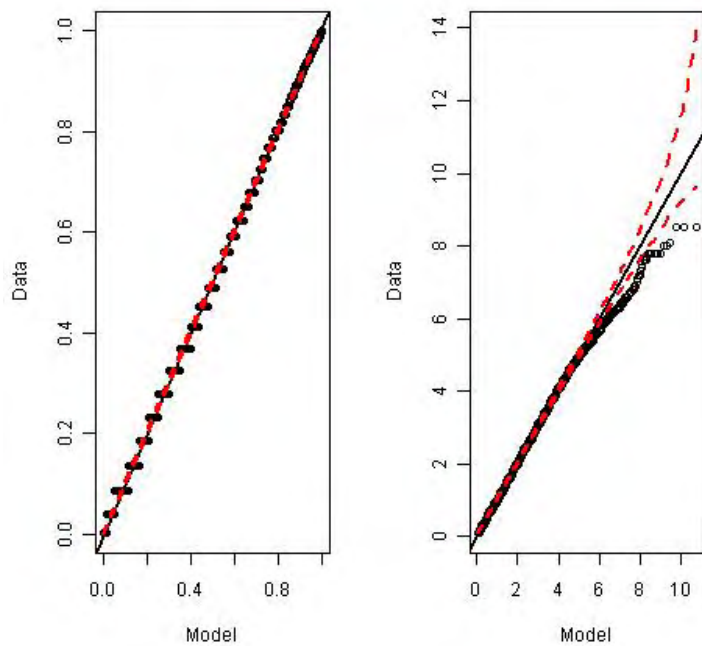
Figure A6.7a – Weibull fit for the wind-sea height (PP and QQ plots) – Test Site GL2523 (the red-dashed lines show 95% confidence bounds)
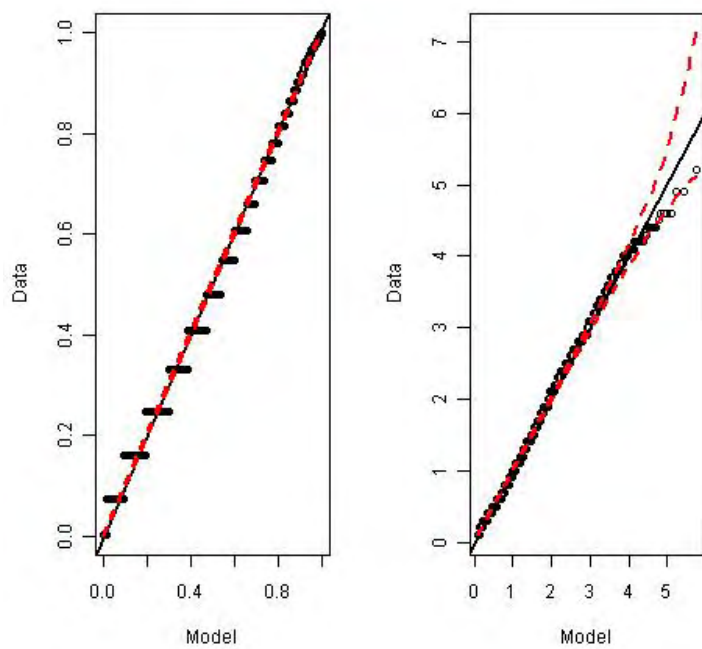
Figure A6.7b – Weibull fit for the swell height (PP and QQ plots) – Test Site GL2523 (the red-dashed lines show 95% confidence bounds)
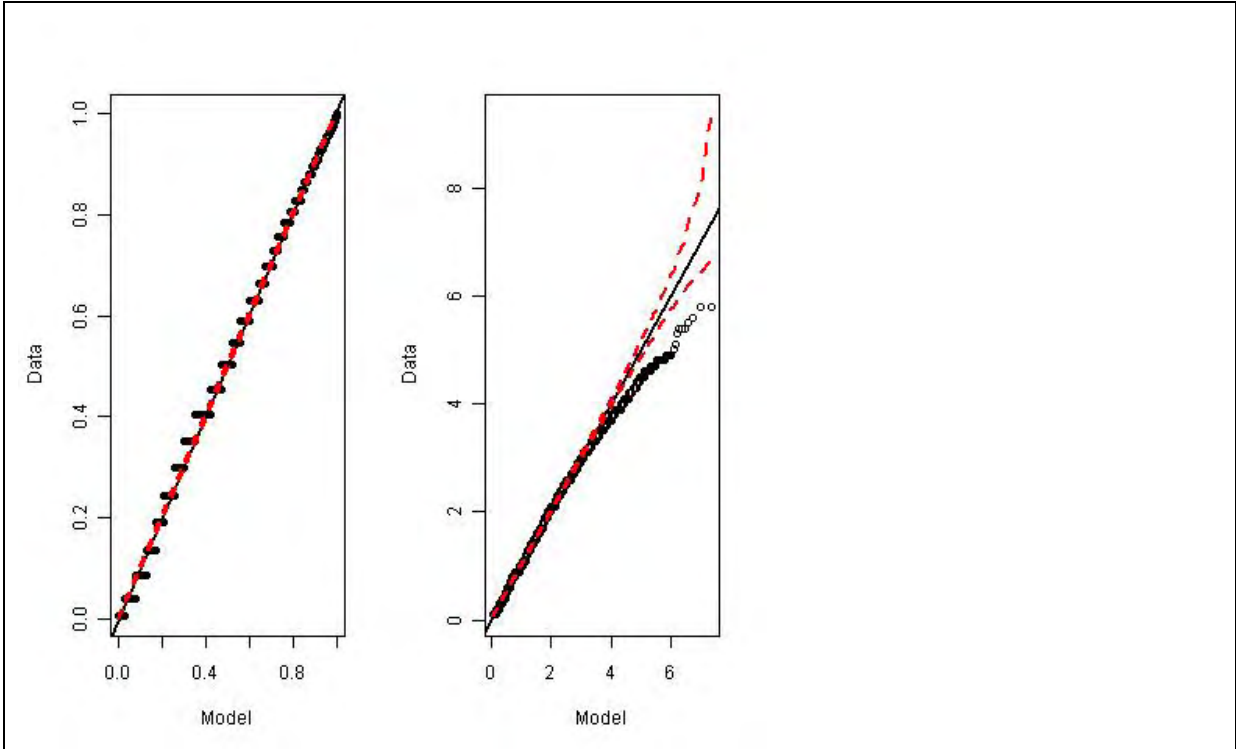
Figure A6.8a – Weibull fit for the wind-sea height (PP and QQ plots) – Test Site GL1946 (the red-dashed lines show 95% confidence bounds)
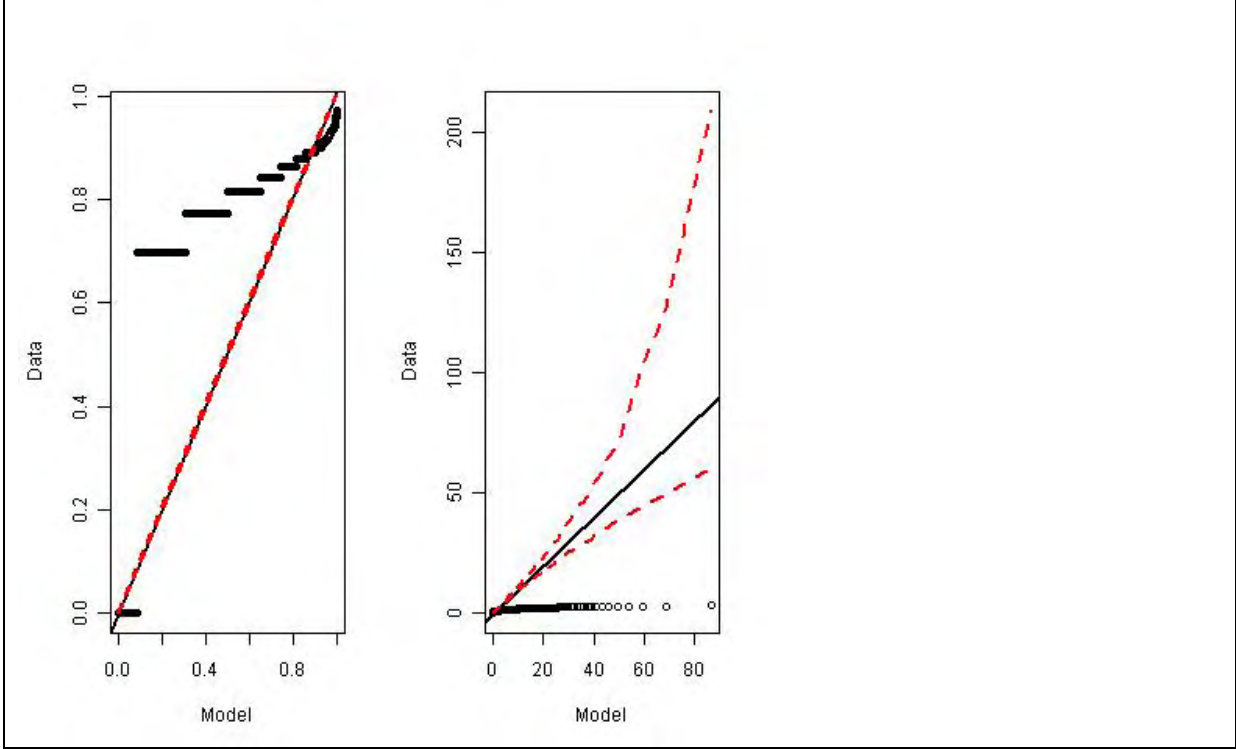
Figure A6.8b – Weibull fit for the swell height (PP and QQ plots) – Test Site GL1946 (the red-dashed lines show 95% confidence bounds)
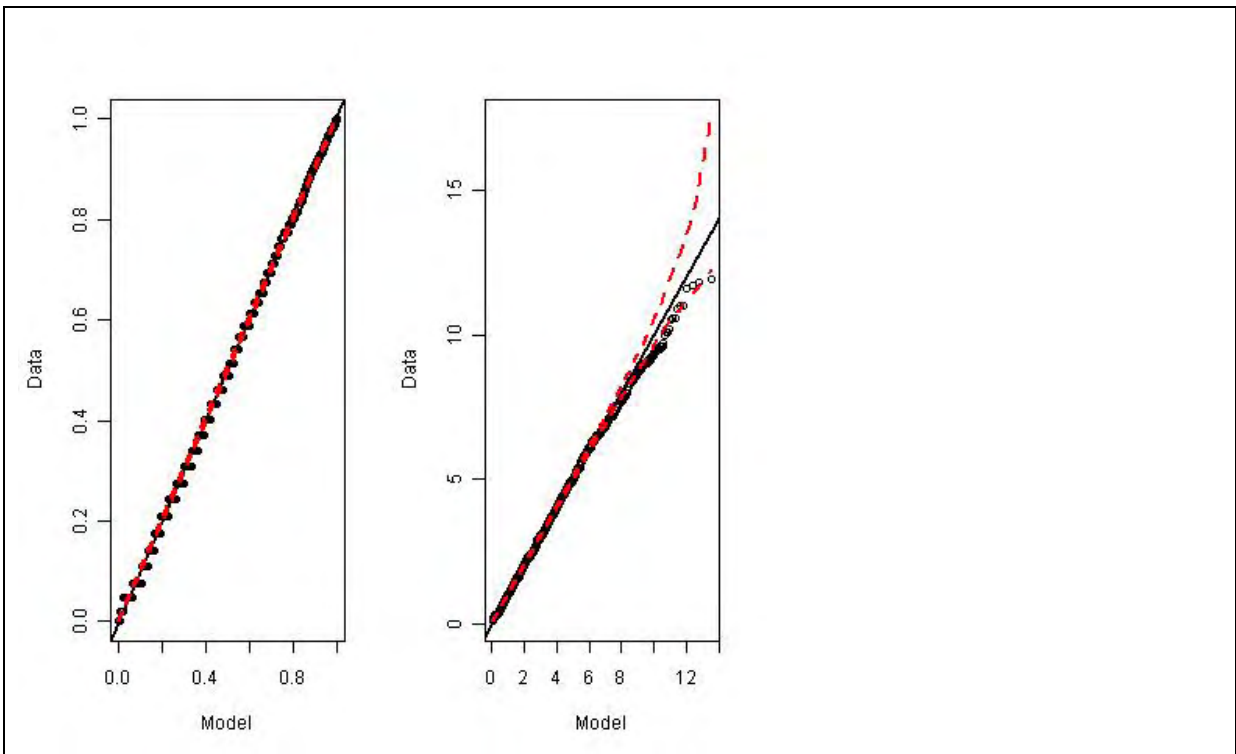
Figure A6.9a – Weibull fit for the wind-sea height (PP and QQ plots) – Test Site GL1276 (the red-dashed lines show 95% confidence bounds)
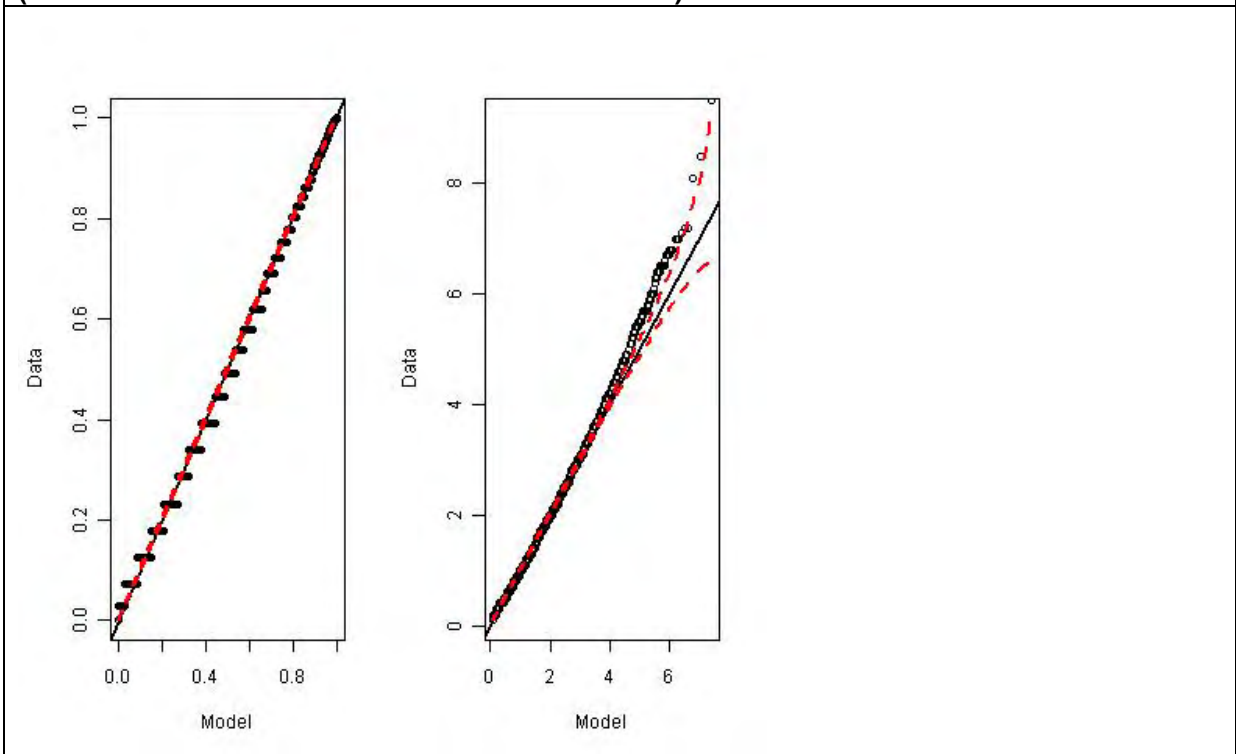
Figure A6.9b – Weibull fit for the swell height (PP and QQ plots) – Test Site GL1276 (the red-dashed lines show 95% confidence bounds)
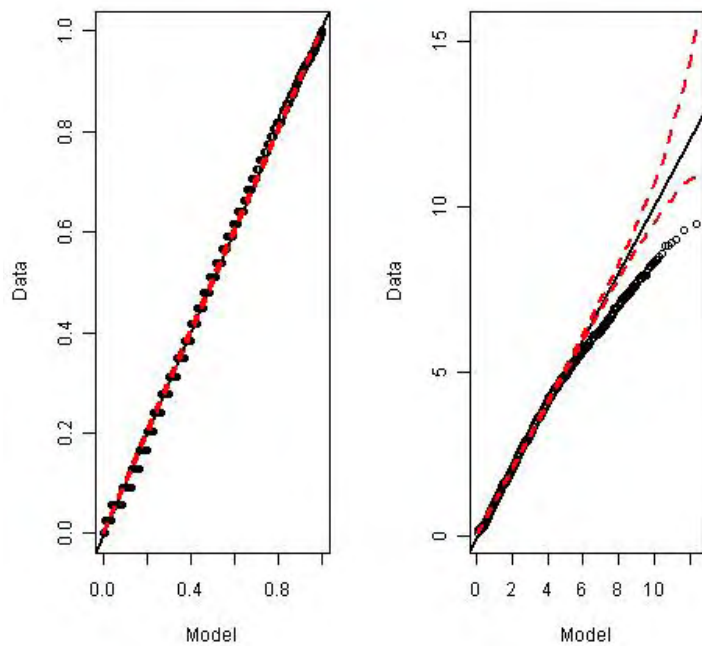
Figure A6.10a – Weibull fit for the wind-sea height (PP and QQ plots) – Test Site GL0531 (the red-dashed lines show 95% confidence bounds)
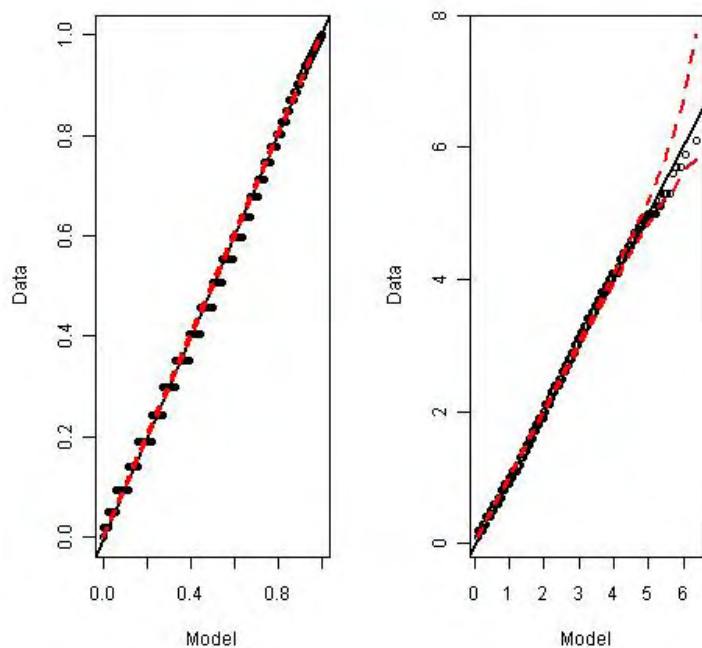
Figure A6.10b – Weibull fit for the swell height (PP and QQ plots) – Test Site GL0531 (the red-dashed lines show 95% confidence bounds)
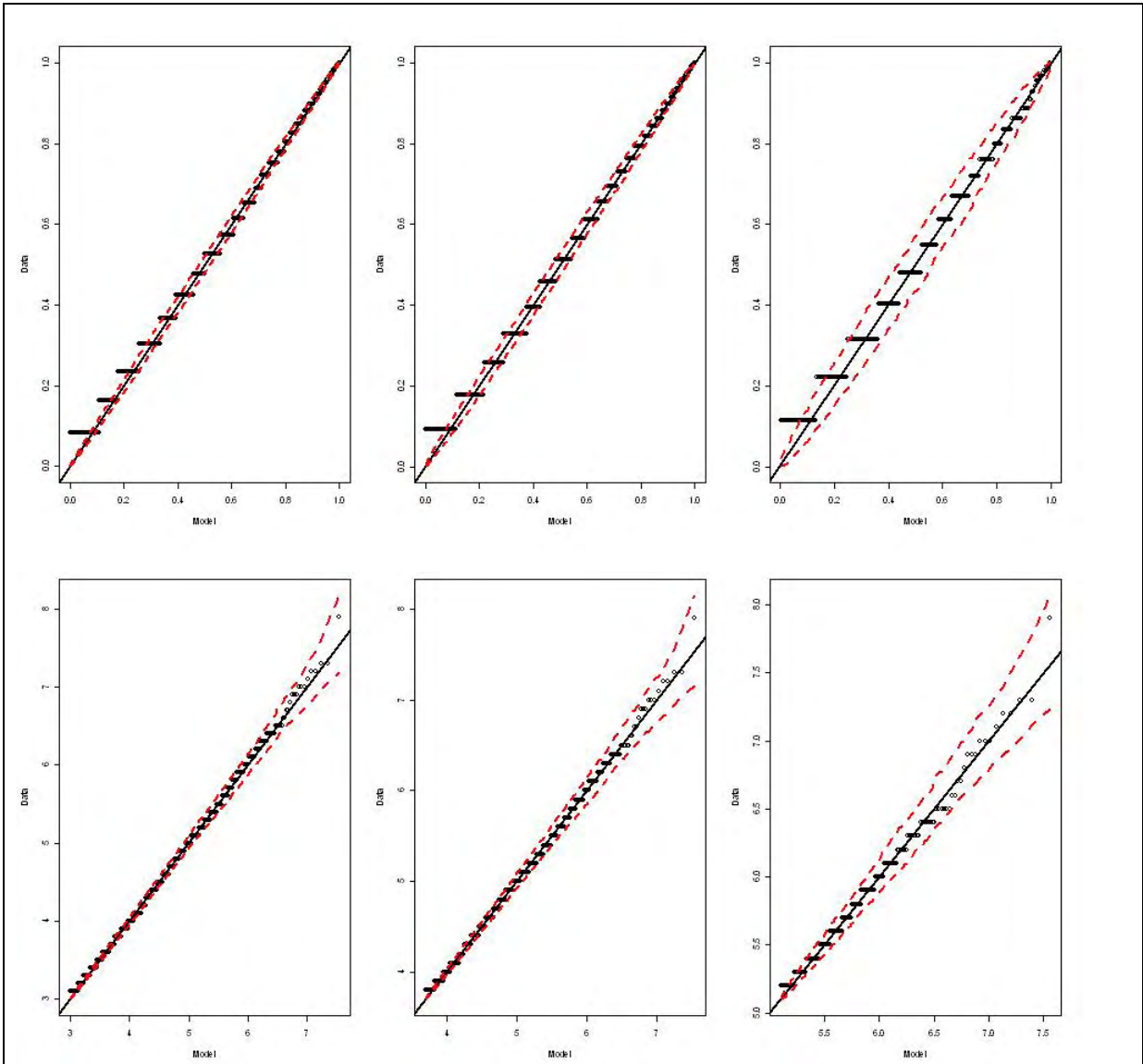
Figure A6.11a – GPD fit to the wind-sea height with the exceedances of 90%, 95% and 99% for thresholds – Test Site GL1104 (above PP plots and below QQ plots; the red-dashed lines show 95% confidence bounds)
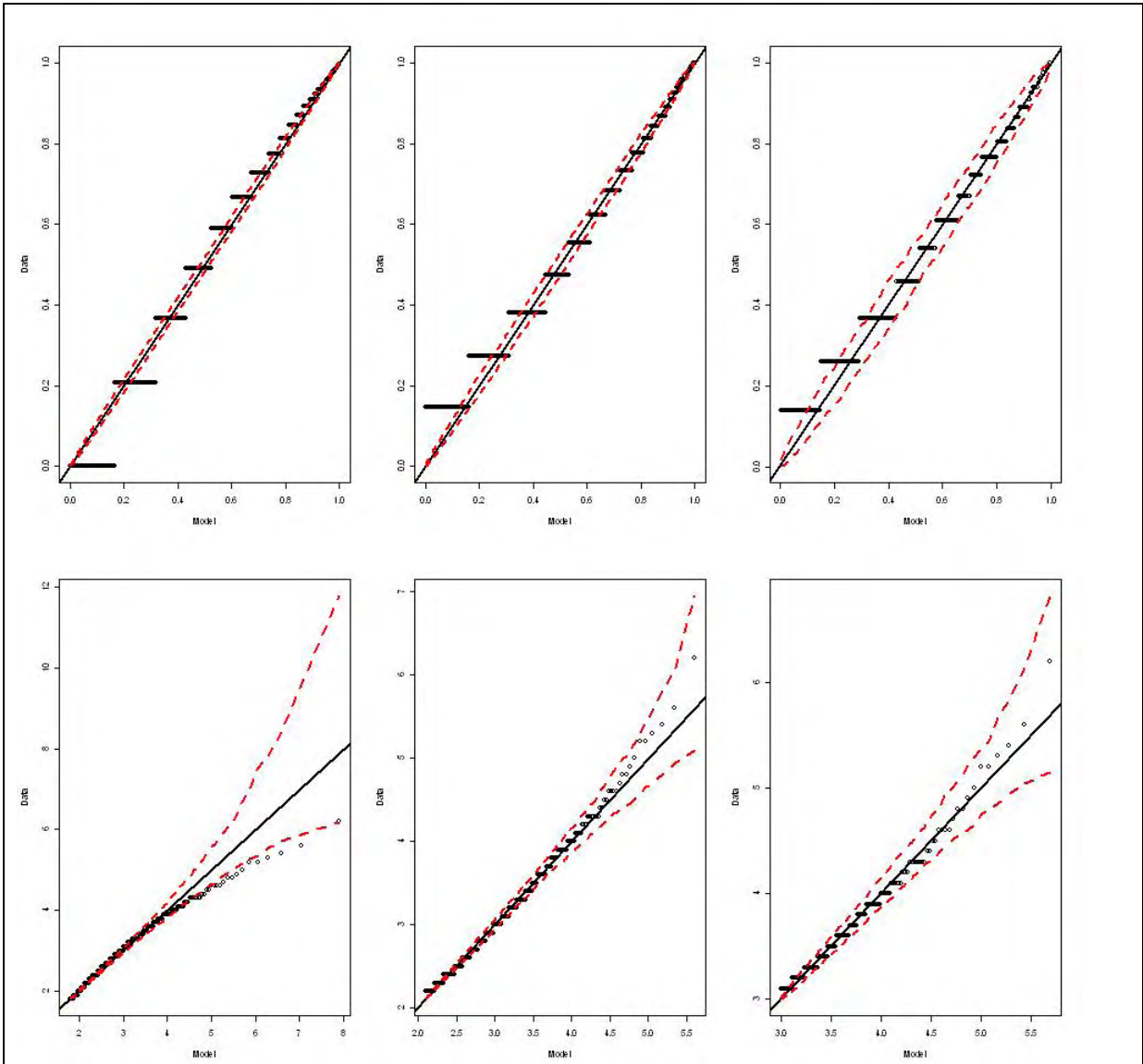
Figure A6.11b – GPD fit to the swell height with the exceedances of 90%, 95% and 99% for thresholds – Test Site GL1104 (above PP plots and below QQ plots; the red-dashed lines show 95% confidence bounds)
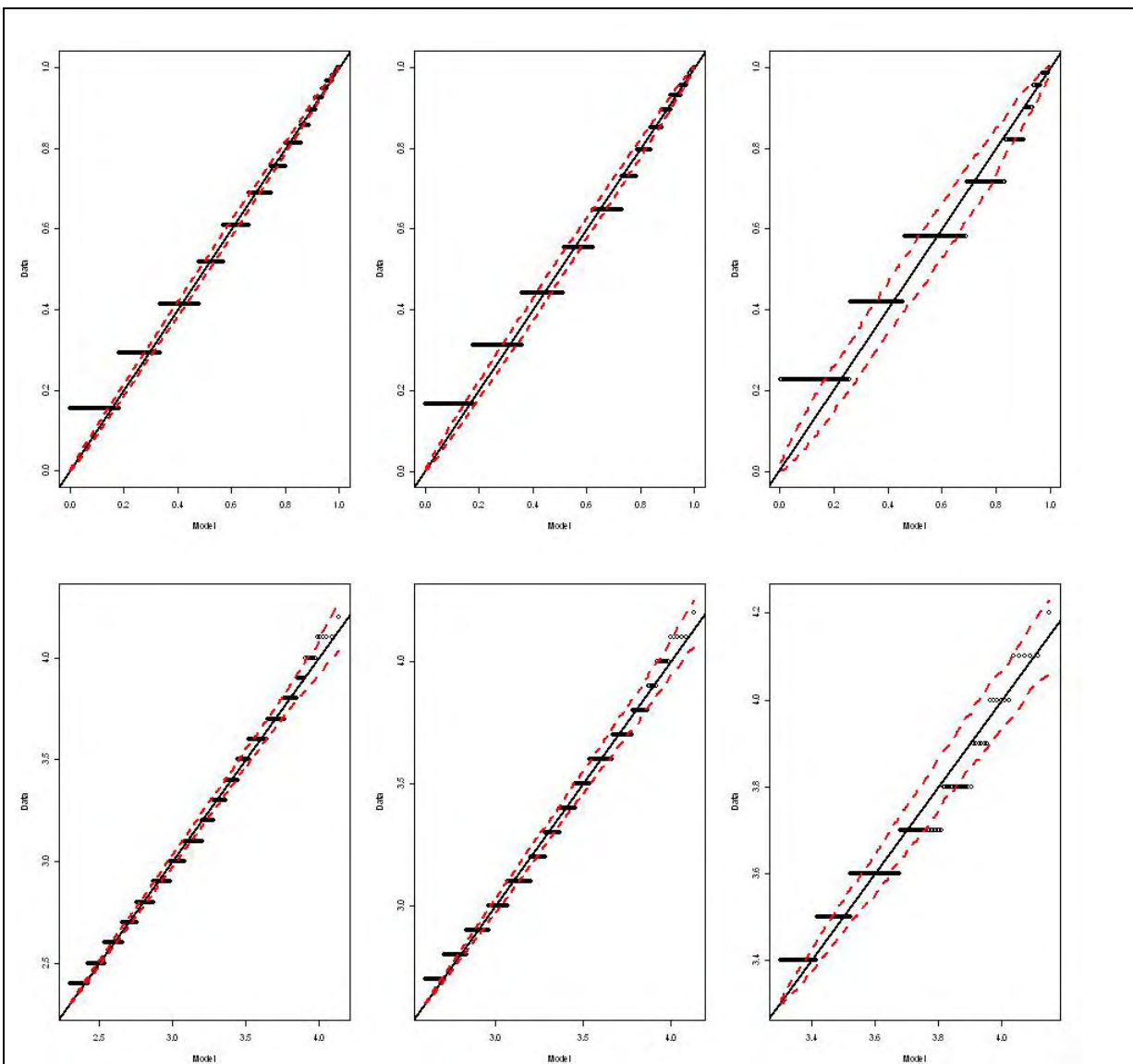
Figure A6.12a – GPD fit to the wind-sea height with the exceedances of 90%, 95% and 99% for thresholds – Test Site GL1993 (above PP plots and below QQ plots; the red-dashed lines show 95% confidence bounds)
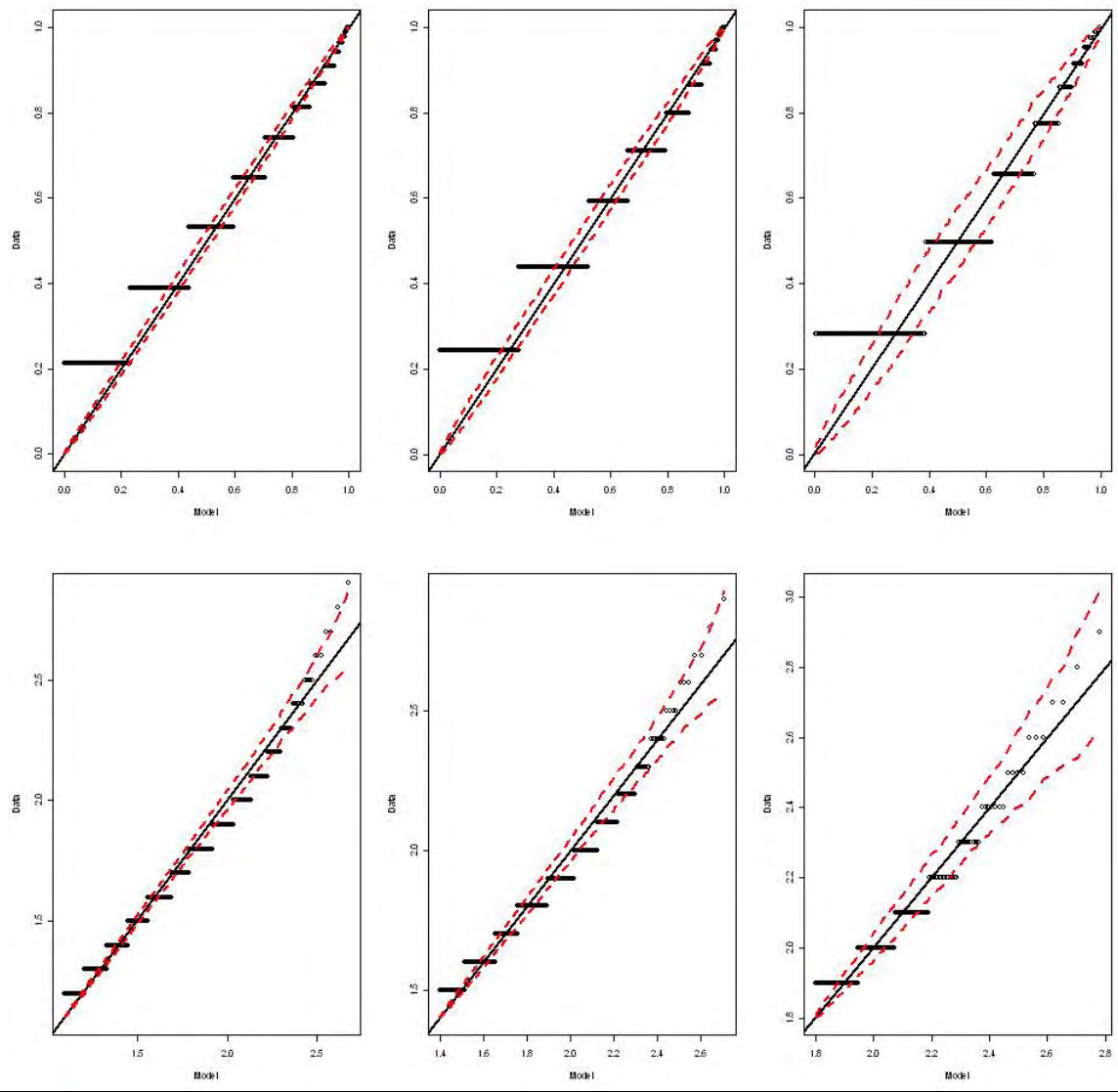
Figure A6.12b – GPD fit to the swell height with the exceedances of 90%, 95% and 99% for thresholds – Test Site GL1993 (above PP plots and below QQ plots; the red-dashed lines show 95% confidence bounds)
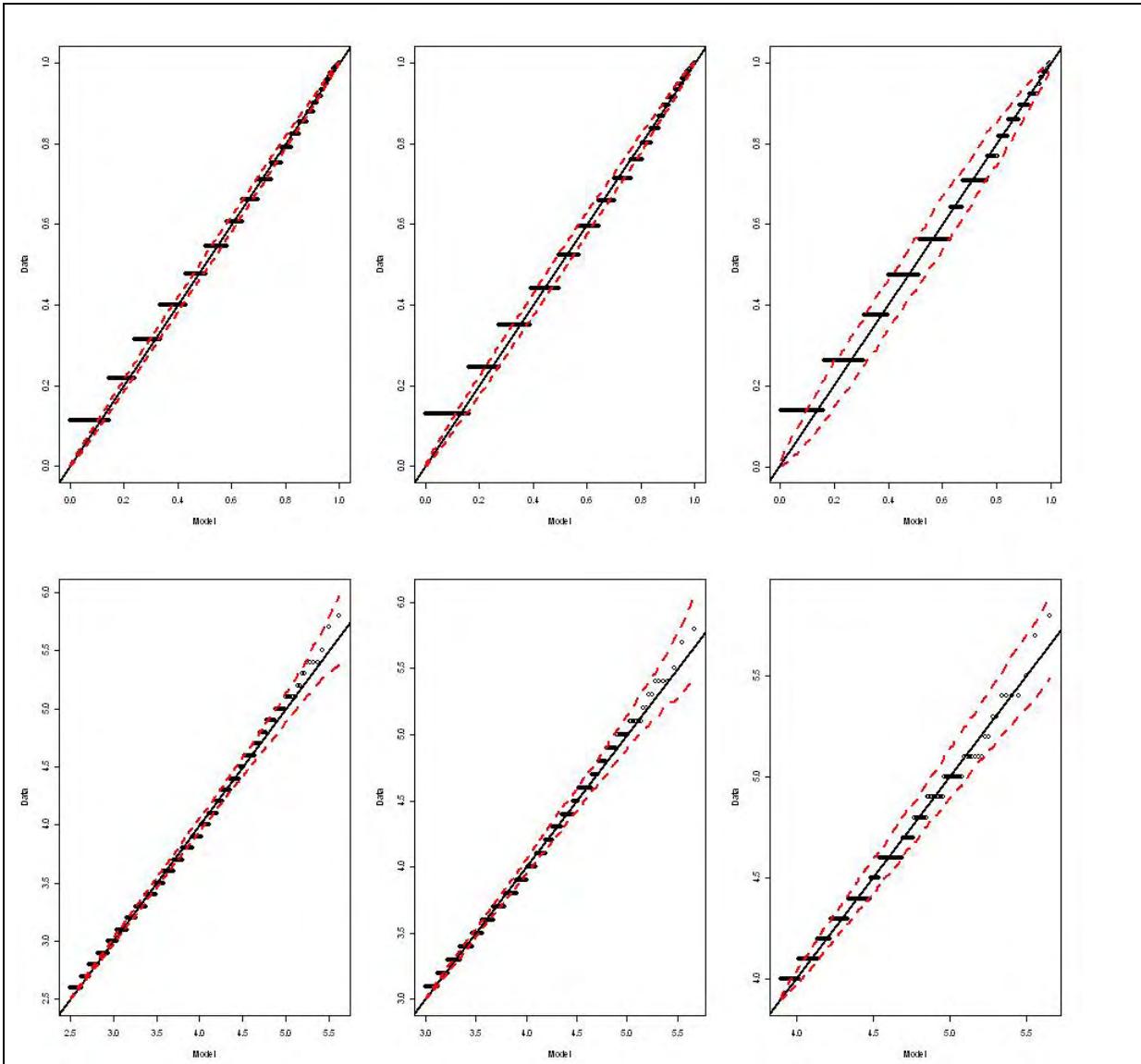
Figure A6.13a – GPD fit to the wind-sea height with the exceedances of 90%, 95% and 99% for thresholds – Test Site GL2645 (above PP plots and below QQ plots; the red-dashed lines show 95% confidence bounds)
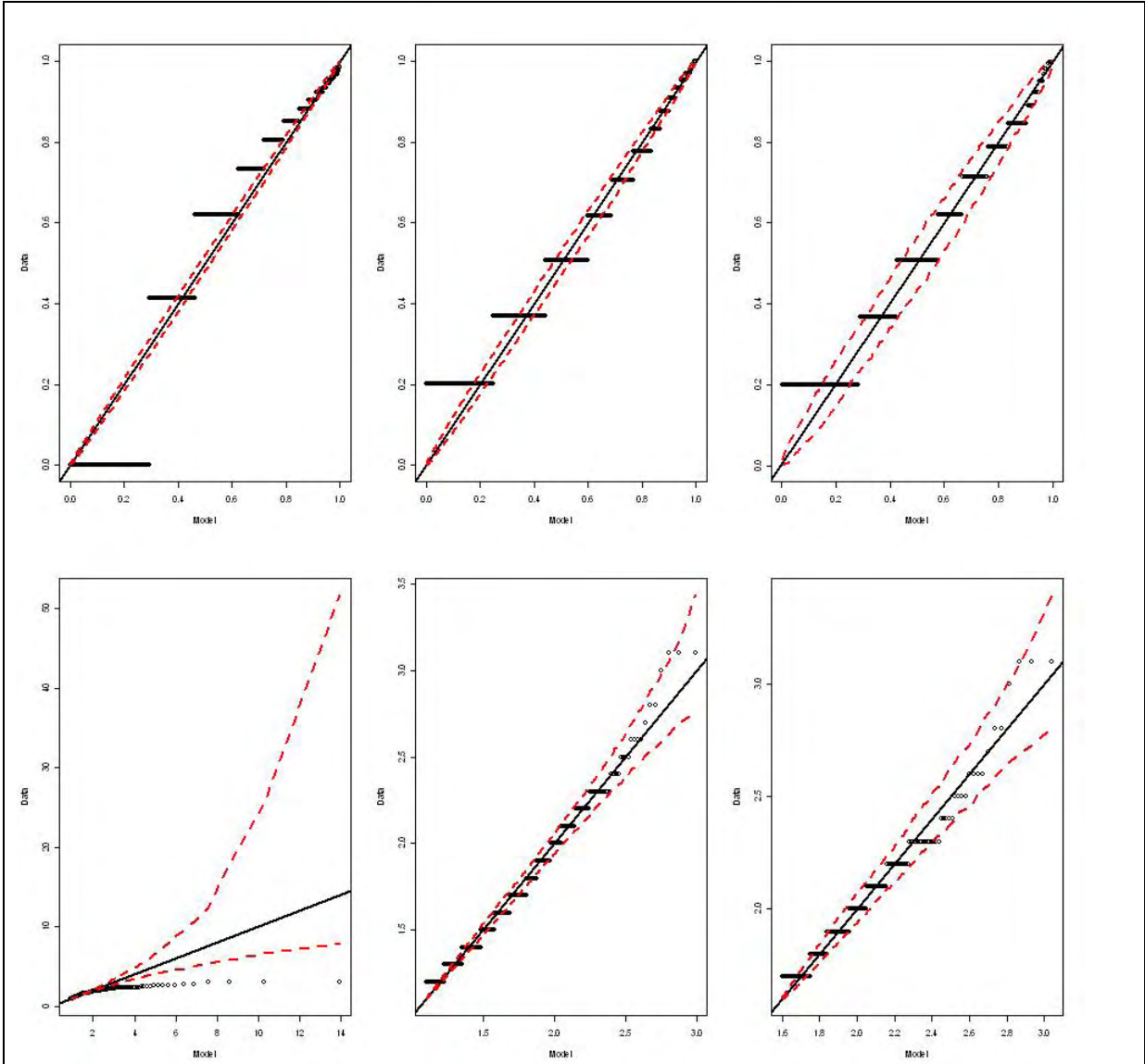
Figure A6.13b – GPD fit to the swell height with the exceedances of 90%, 95% and 99% for thresholds – Test Site GL2645 (above PP plots and below QQ plots; the red-dashed lines show 95% confidence bounds)
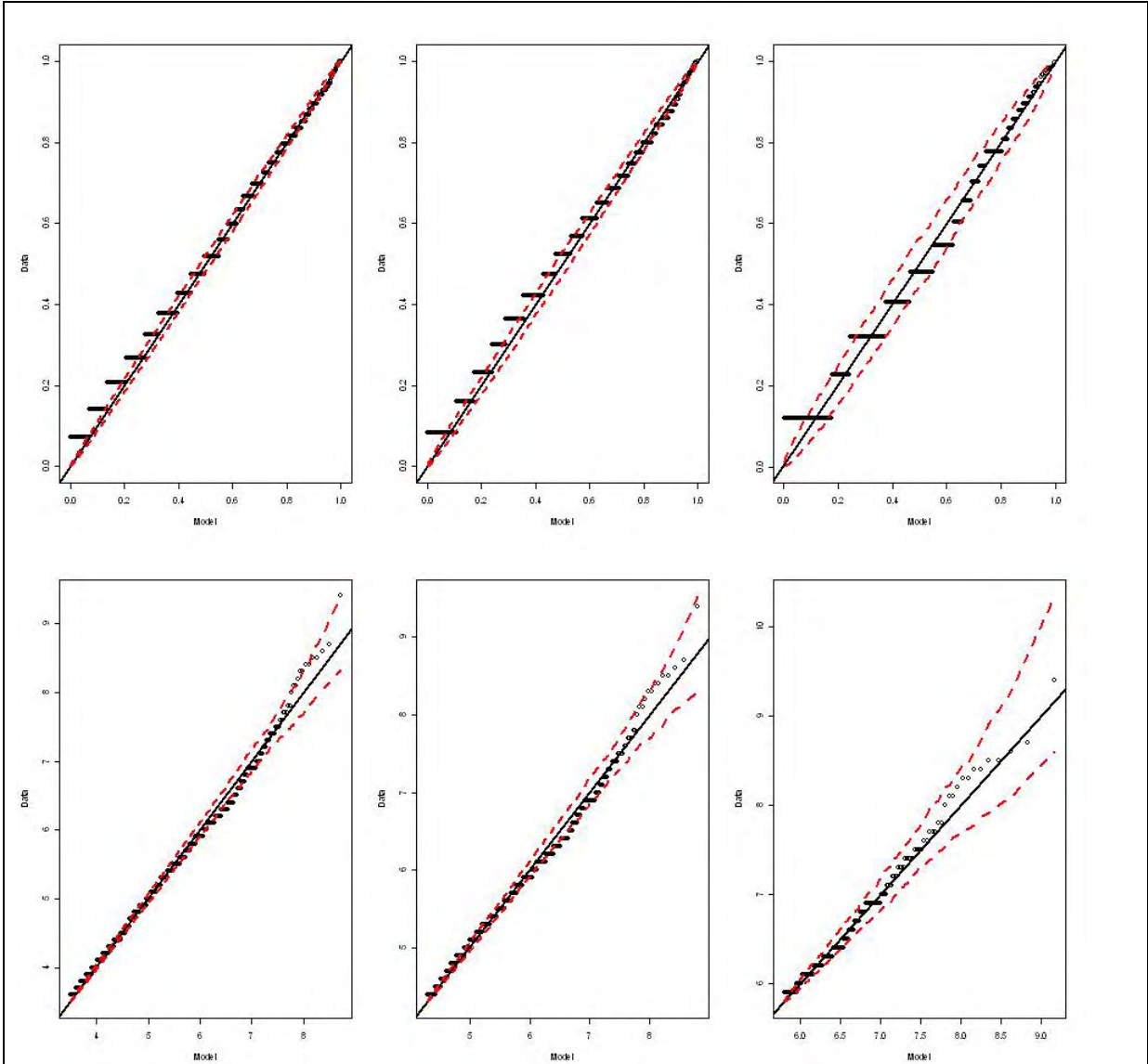
Figure A6.14a – GPD fit to the wind-sea height with the exceedances of 90%, 95% and 99% for thresholds – Test Site GL2849 (above PP plots and below QQ plots; the red-dashed lines show 95% confidence bounds)
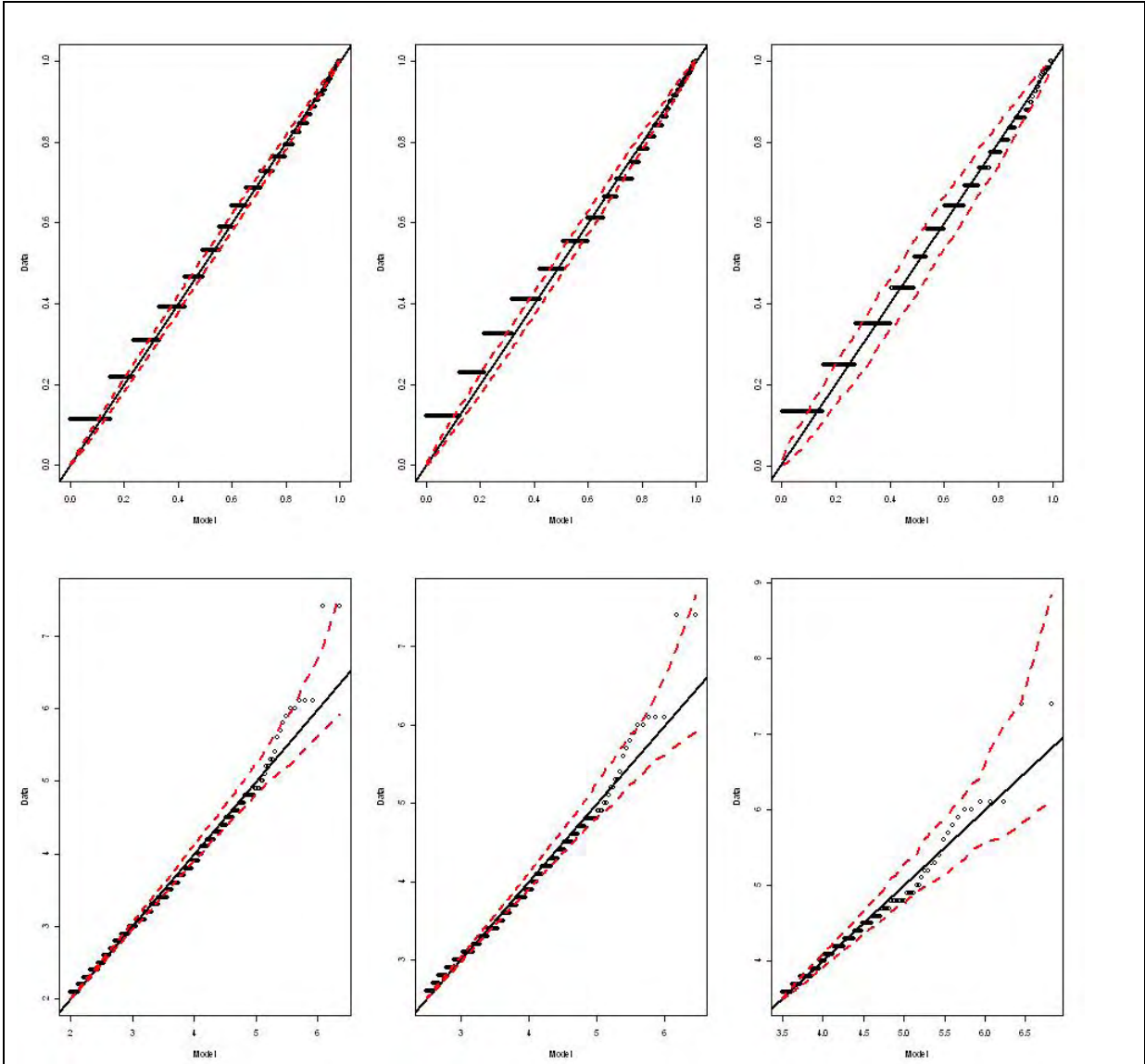
Figure A6.14b – GPD fit to the swell height with the exceedances of 90%, 95% and 99% for thresholds – Test Site GL2849 (above PP plots and below QQ plots; the red-dashed lines show 95% confidence bounds)
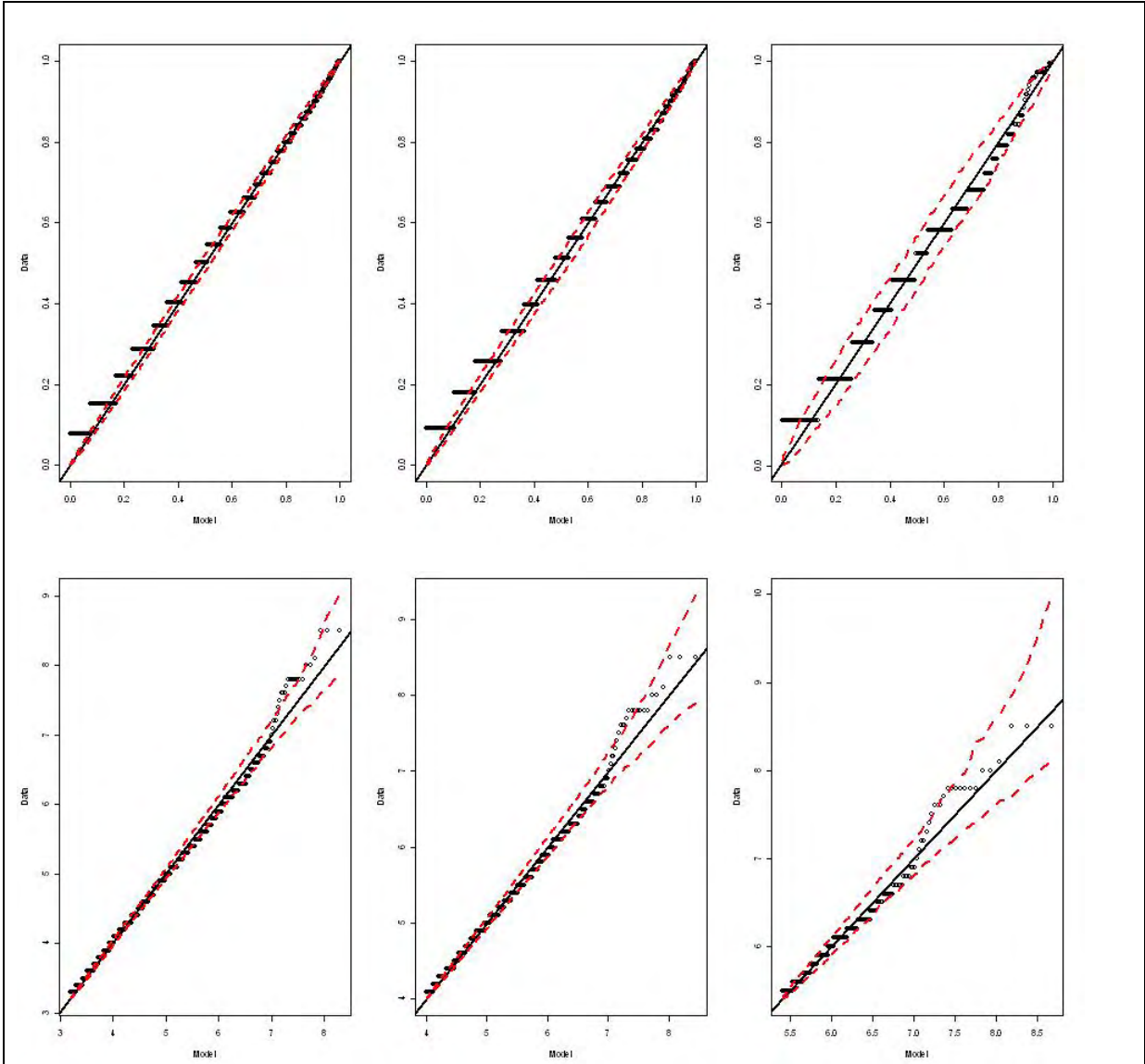
Figure A6.15a – GPD fit to the wind-sea height with the exceedances of 90%, 95% and 99% for thresholds – Test Site GL2523 (above PP plots and below QQ plots; the red-dashed lines show 95% confidence bounds)
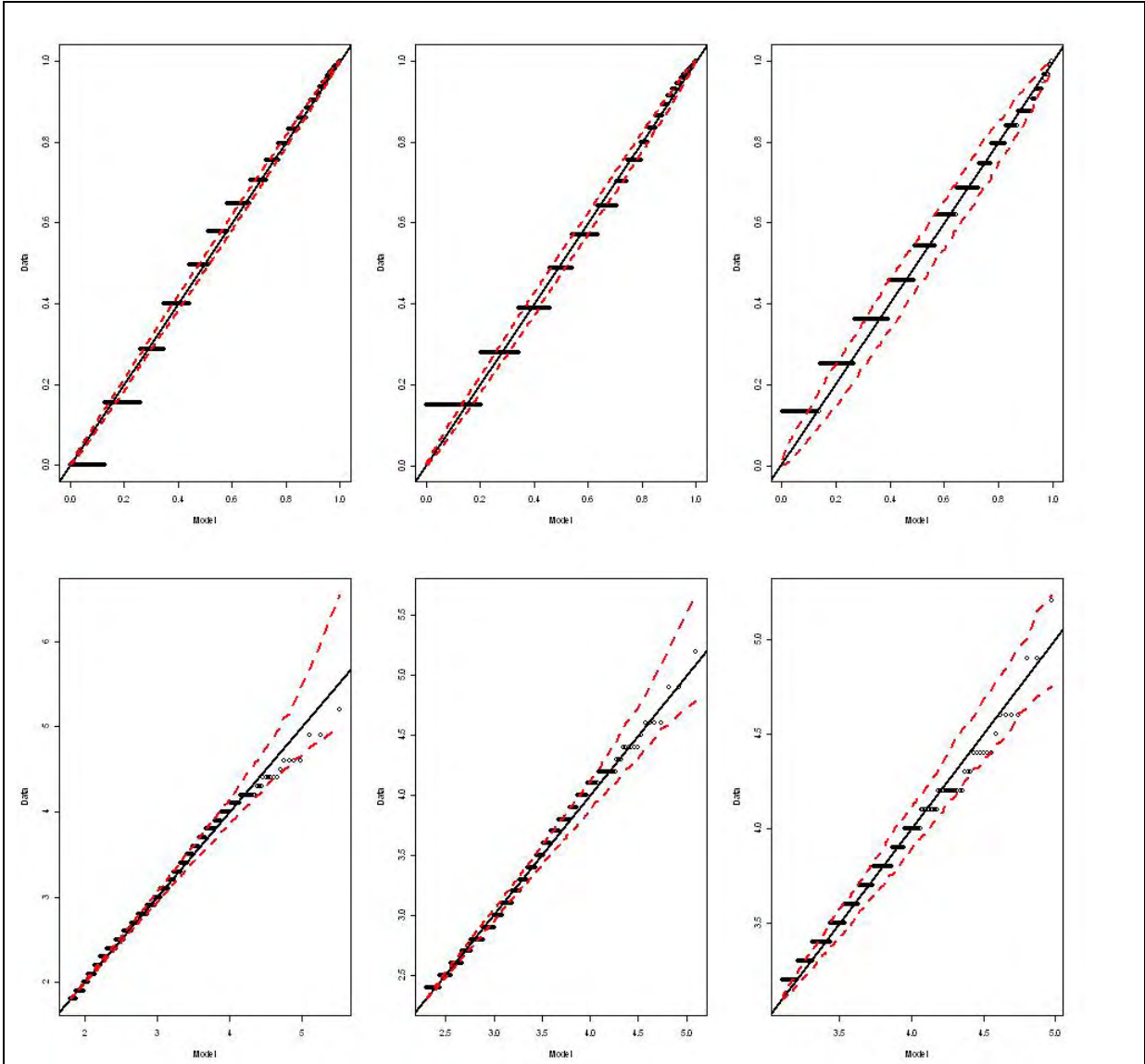
Figure A6.15b – GPD fit to the swell height with the exceedances of 90%, 95% and 99% for thresholds – Test Site GL2523 (above PP plots and below QQ plots; the red-dashed lines show 95% confidence bounds)
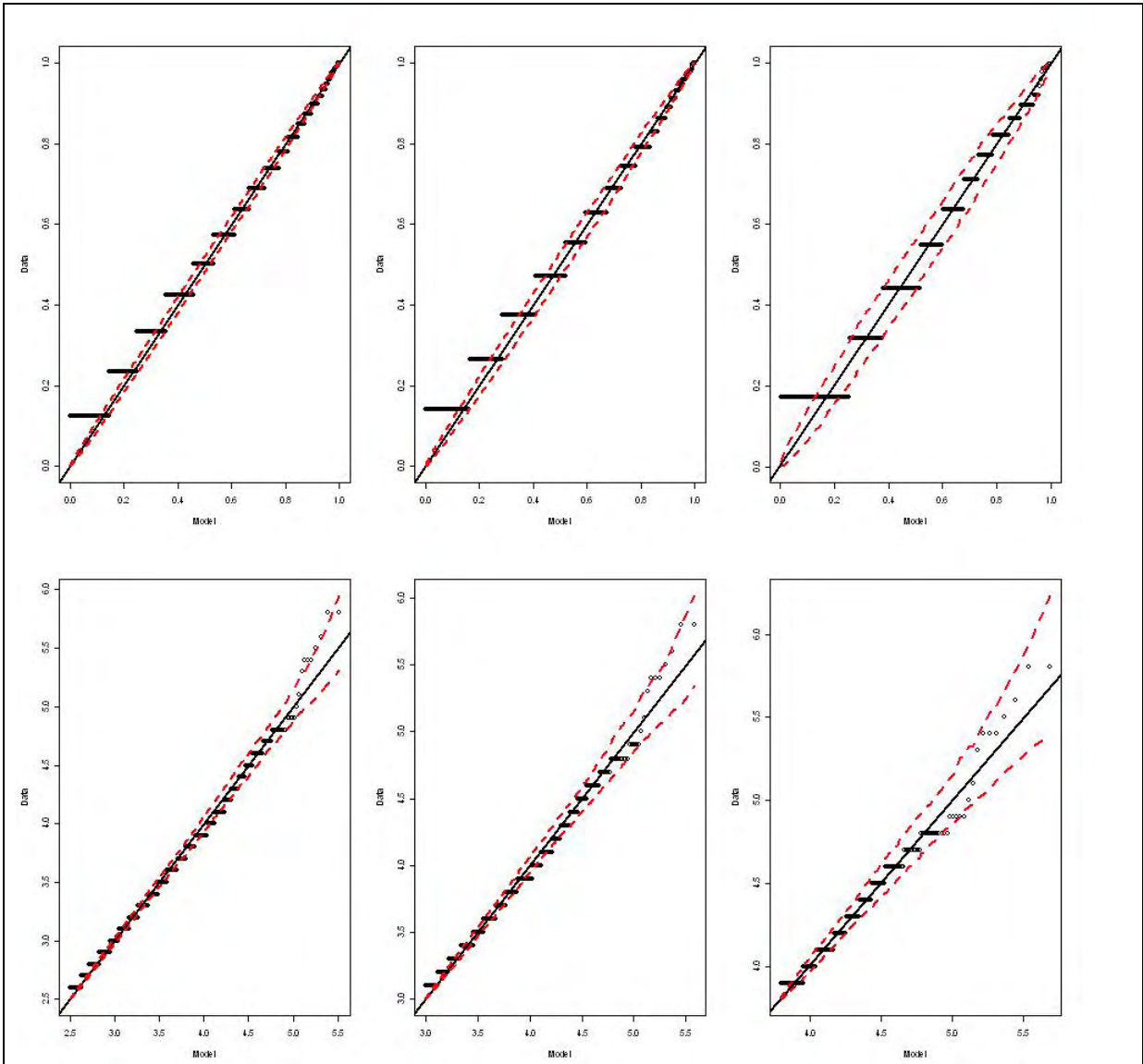
Figure A6.16a – GPD fit to the wind-sea height with the exceedances of 90%, 95% and 99% for thresholds – Test Site GL1946 (above PP plots and below QQ plots; the red-dashed lines show 95% confidence bounds)
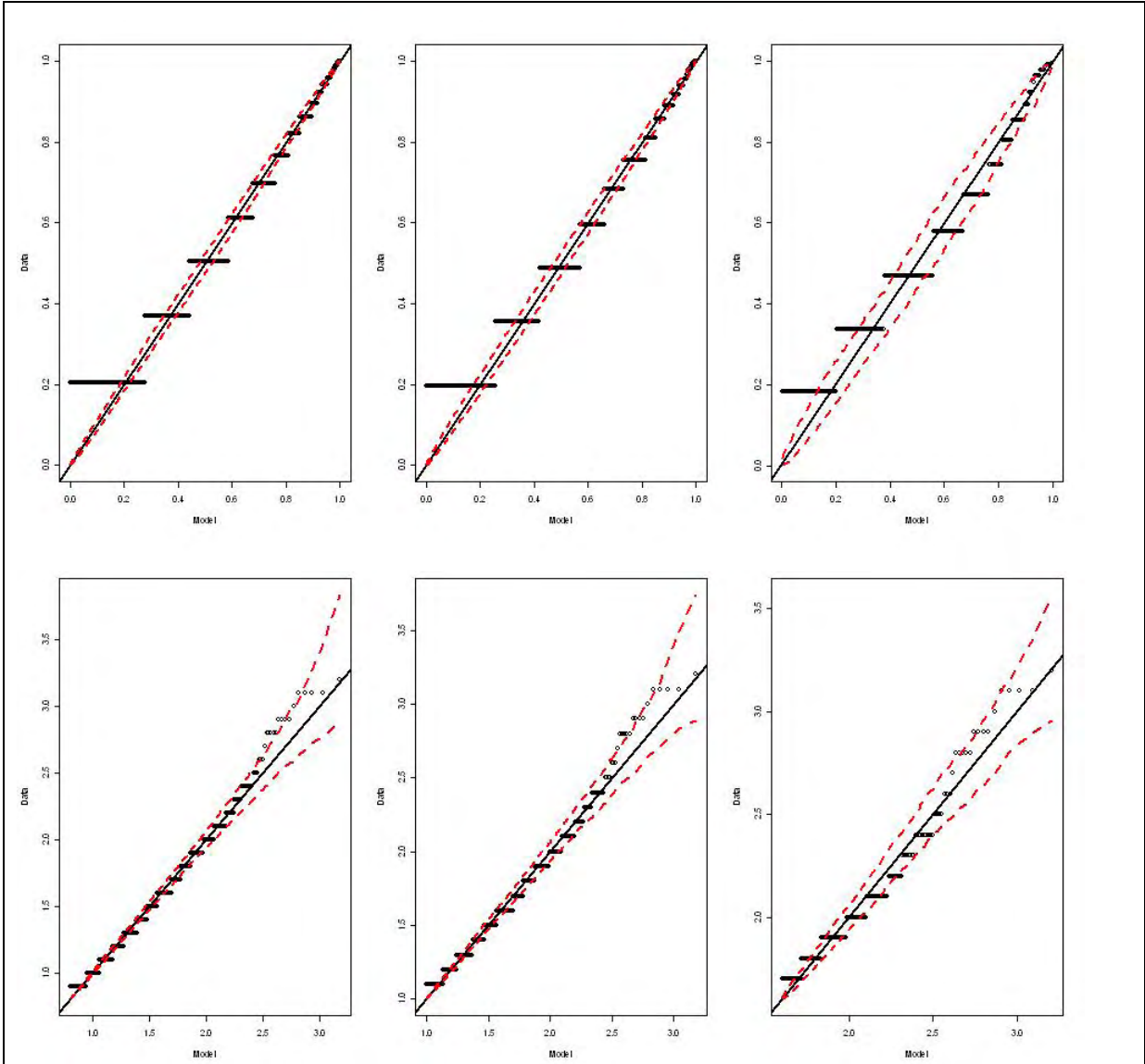
Figure A6.16b – GPD fit to the swell height with the exceedances of 90%, 95% and 99% for thresholds – Test Site GL1946 (above PP plots and below QQ plots; the red-dashed lines show 95% confidence bounds)
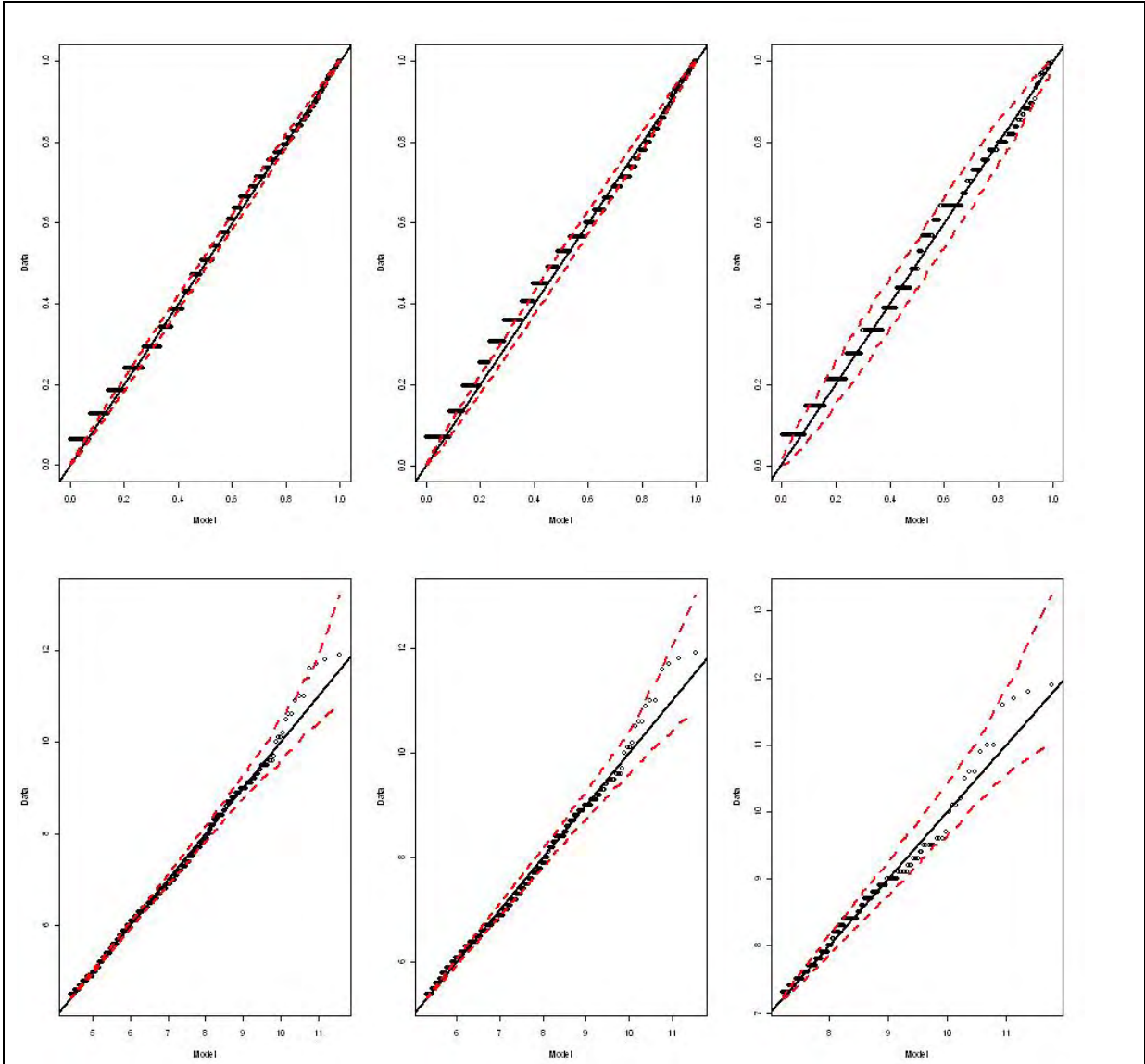
Figure A6.17a – GPD fit to the wind-sea height with the exceedances of 90%, 95% and 99% for thresholds – Site GL1276 (above PP plots and below QQ plots; the red-dashed lines show 95% confidence bounds)
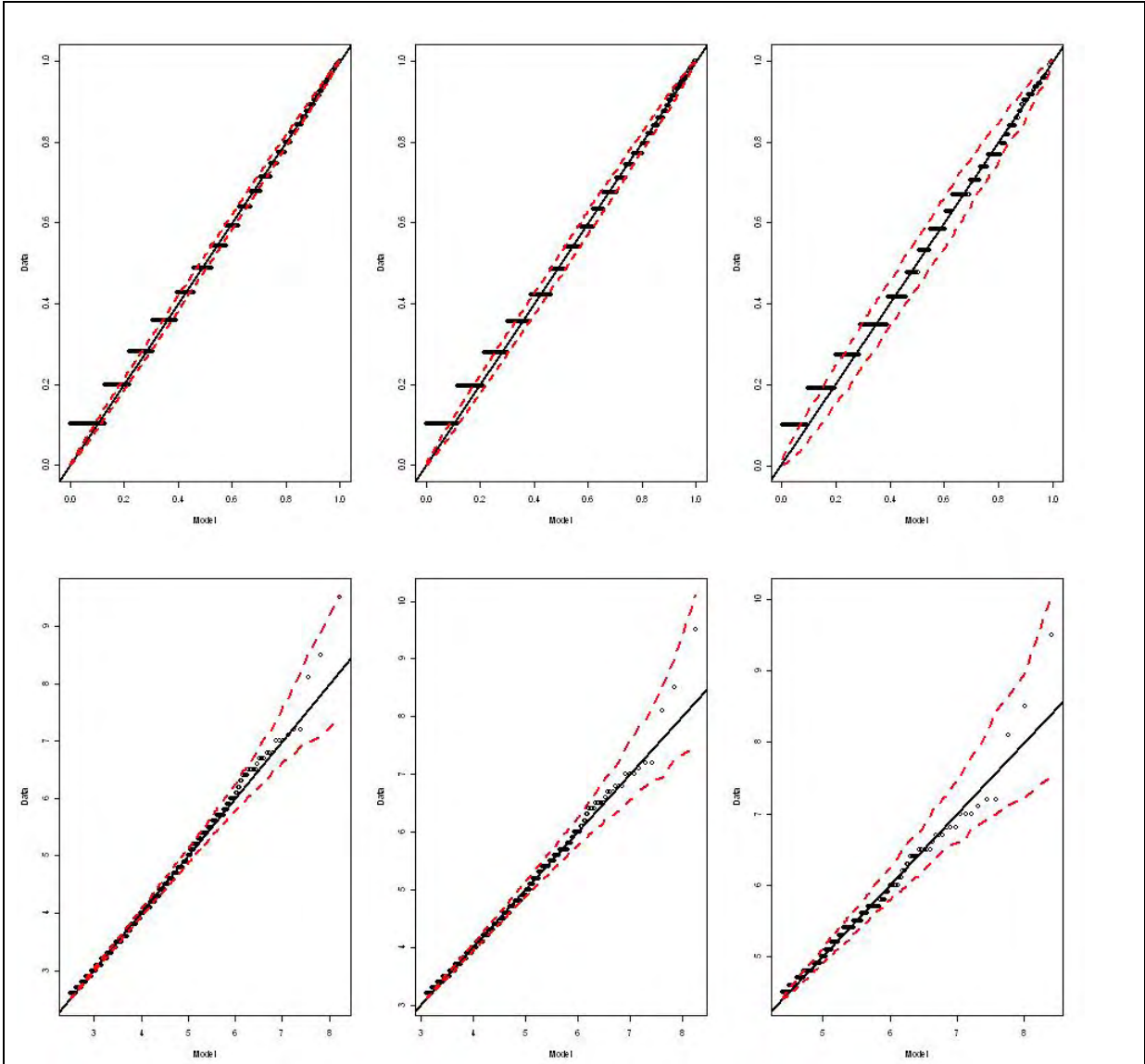
Figure A6.17b – GPD fit to the swell height with the exceedances of 90%, 95% and 99% for thresholds – Test Site GL1276 (above PP plots and below QQ plots; the red-dashed lines show 95% confidence bounds)
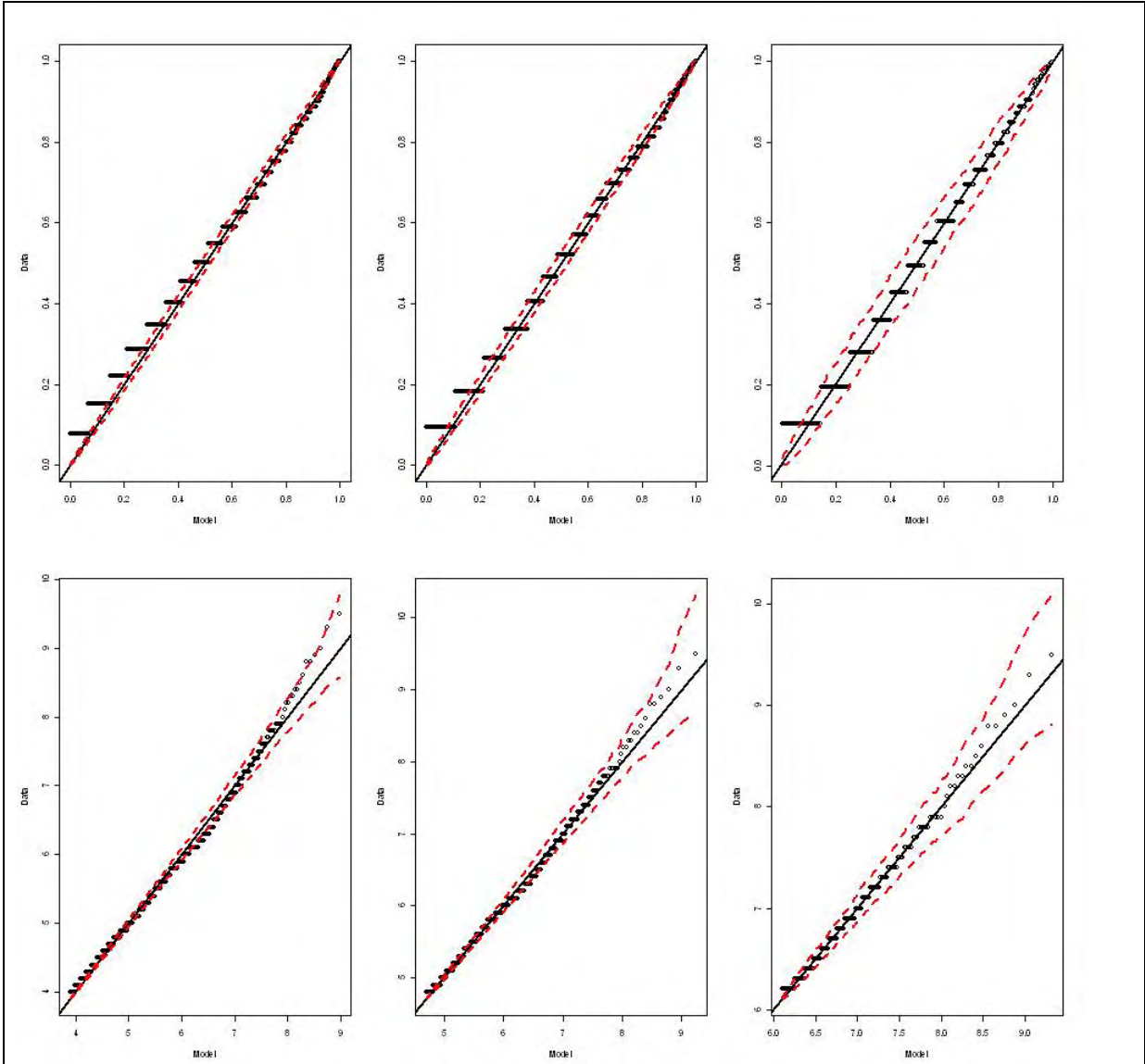
Figure A6.18a – GPD fit to the wind-sea height with the exceedances of 90%, 95% and 99% for thresholds – Test Site GL0531 (above PP plots and below QQ plots; the red-dashed lines show 95% confidence bounds)
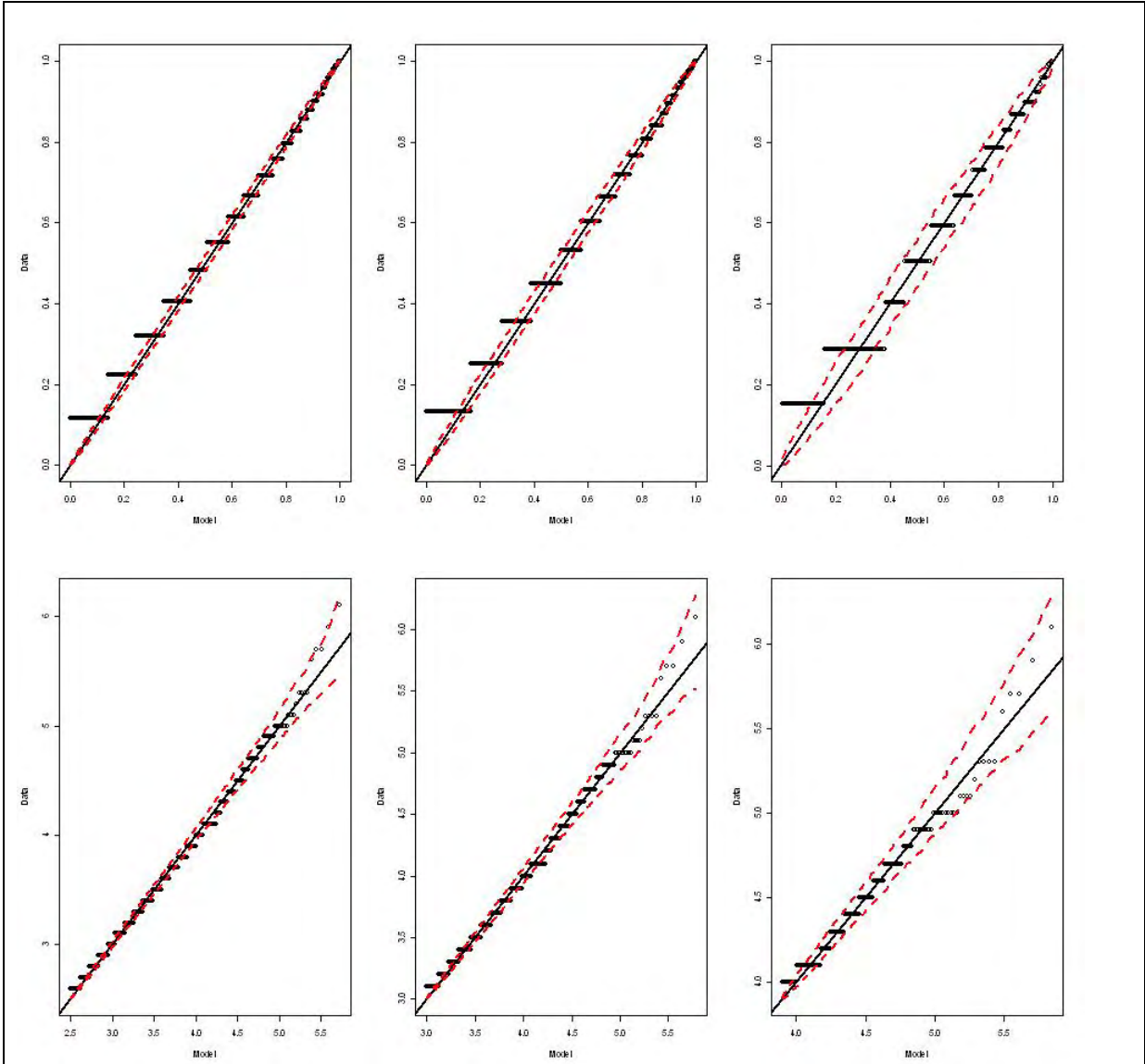
Figure A6.18b – GPD fit to the swell height with the exceedances of 90%, 95% and 99% for thresholds – Test Site GL0531 (above PP plots and below QQ plots; the red-dashed lines show 95% confidence bounds)

Appendix 7   Wind Wave and Swell Interdependence

A7.1   Joint Probability of Wind-sea and Swell Height

This project used the Bivariate Normal distribution (BVN) in the joint probability analysis. For the joint BVN model, only the correlation ρ parameter needs to be estimated. The BVN approach requires the transformation of the data from GPD to the Normal distribution.

Because the model fit is done after both data sets have been transformed to standard normal margins, the same threshold (referenced to the same exceedance) was used for both data sets.

In order to select the threshold(s) for the BVN model fit; the joint distribution of swell and wind-wave heights, were estimated over a range of thresholds. The results are presented in Figures 1-8 which also show the 95% confidence intervals for the estimate of ρ.

The figures presented in this Appendix show the correlation parameter, for a given threshold of wave heights, between wind waves and swell waves.

The figures show negative correlation for low thresholds of 1m except at test sites of GL2849 and GL2523. For high thresholds (above 2m, equivalent to the exceedance of 95.4%), the results of the joint probability analysis demonstrate very weak correlation between wind-sea and swell (either positive or negative correlation).

A strong correlation would be expected to have a ρ>0.5

A7.2   Conclusions:

This study found that the correlation between wind-sea and swell is insignificant so, for practical purposes the two can be treated as independent. This is based on the definitions for swell and wind waves as adopted for this project.
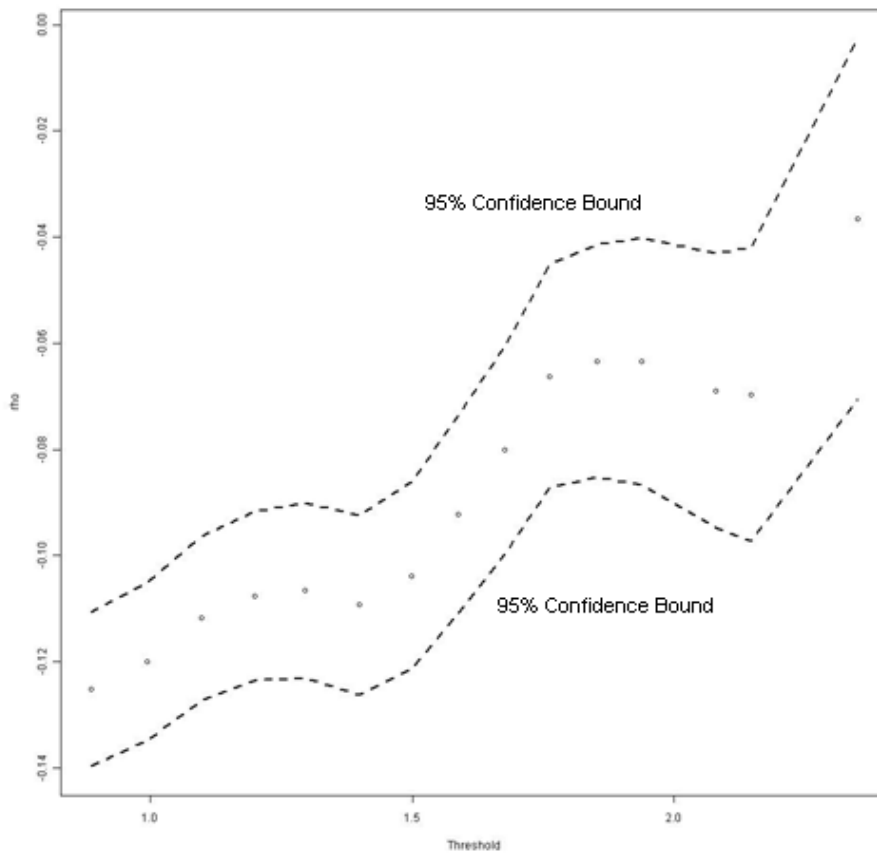
Figure A7.1 – correlation parameter ρ (rho) between wind-sea and swell height (Test Site GL1104)
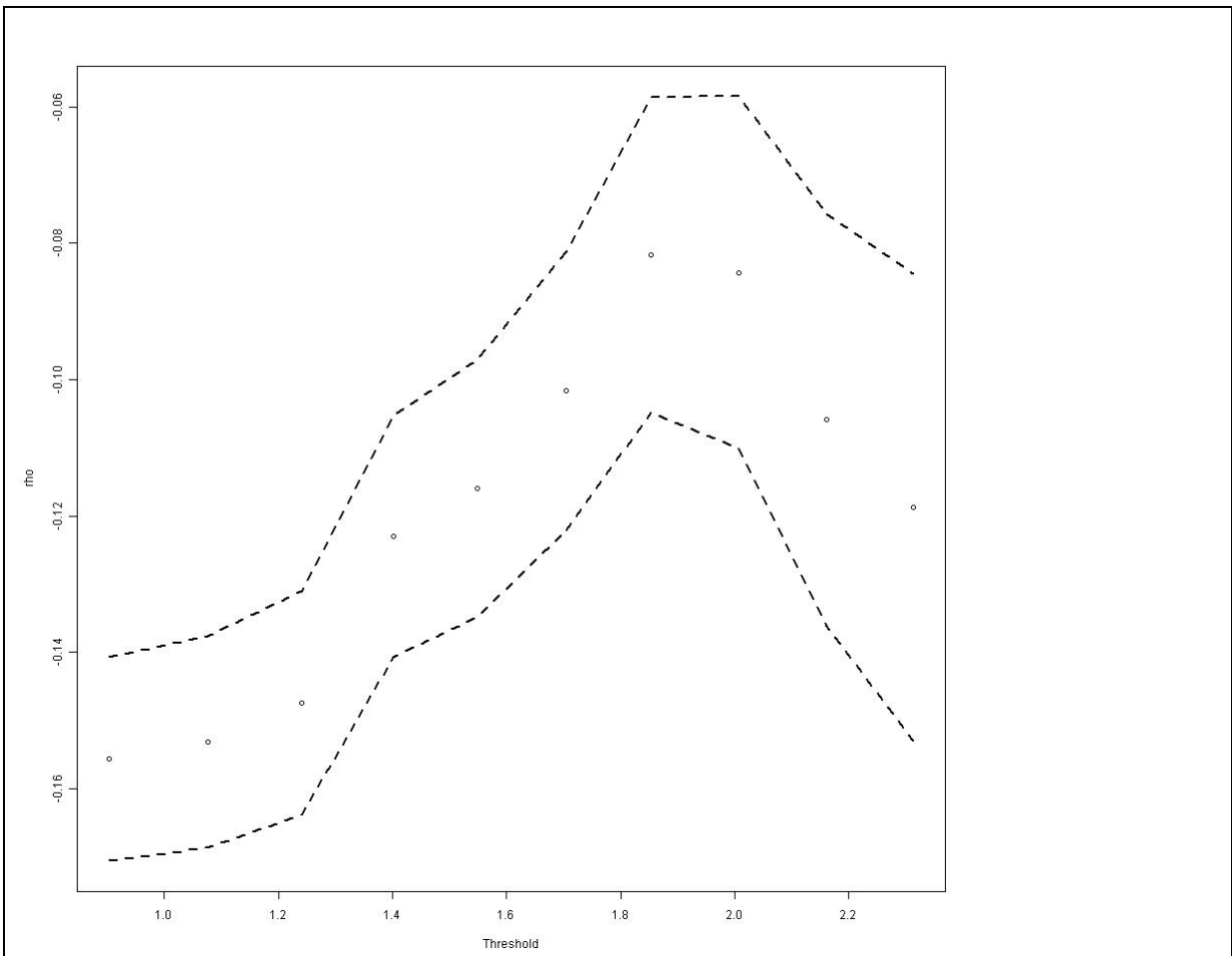
Figure A7.2 – correlation parameter ρ between wind-sea and swell height (Test Site GL1993)
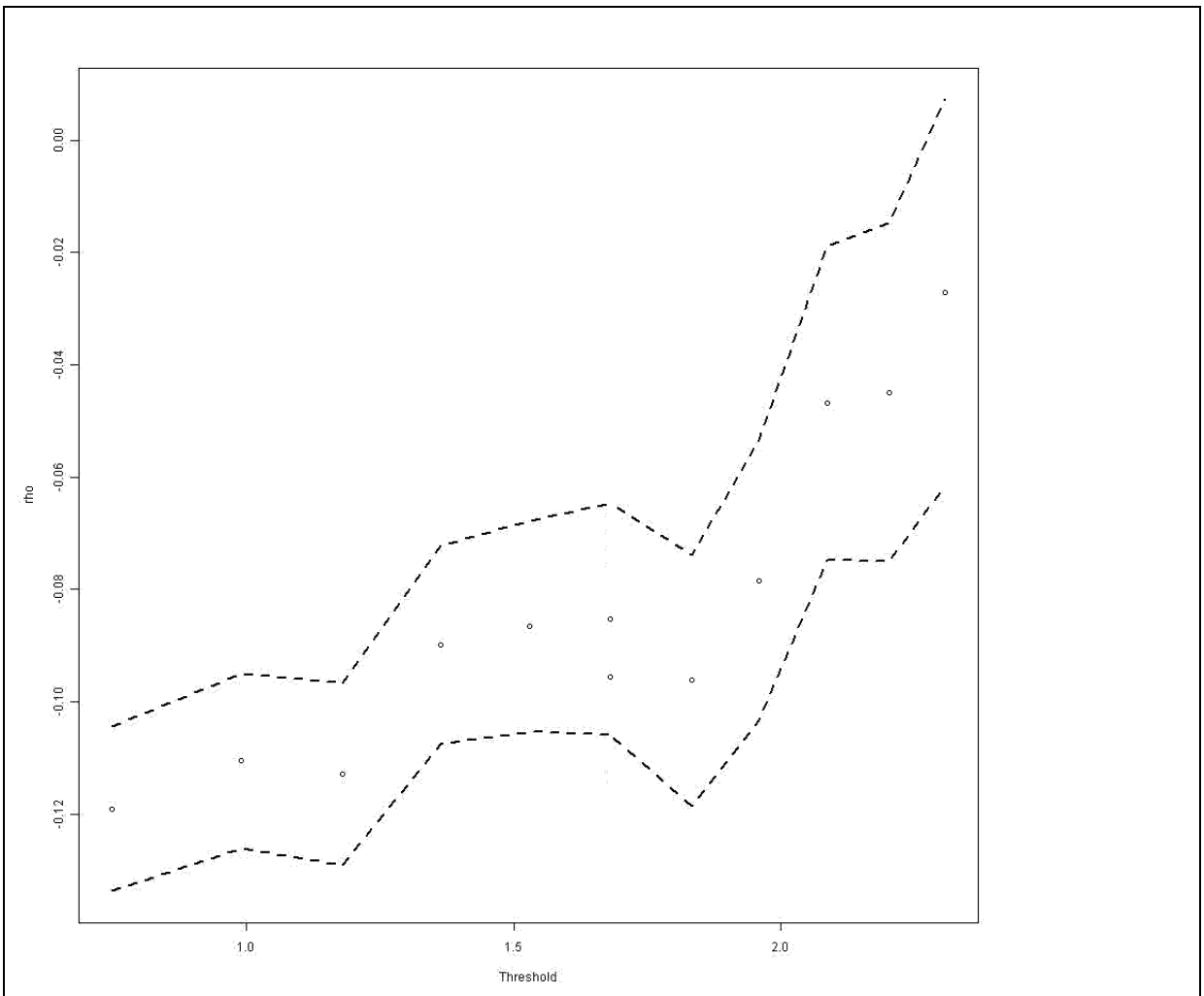
Figure A7.3 – correlation parameter ρ between wind-sea and swell height (Test Site GL2645)
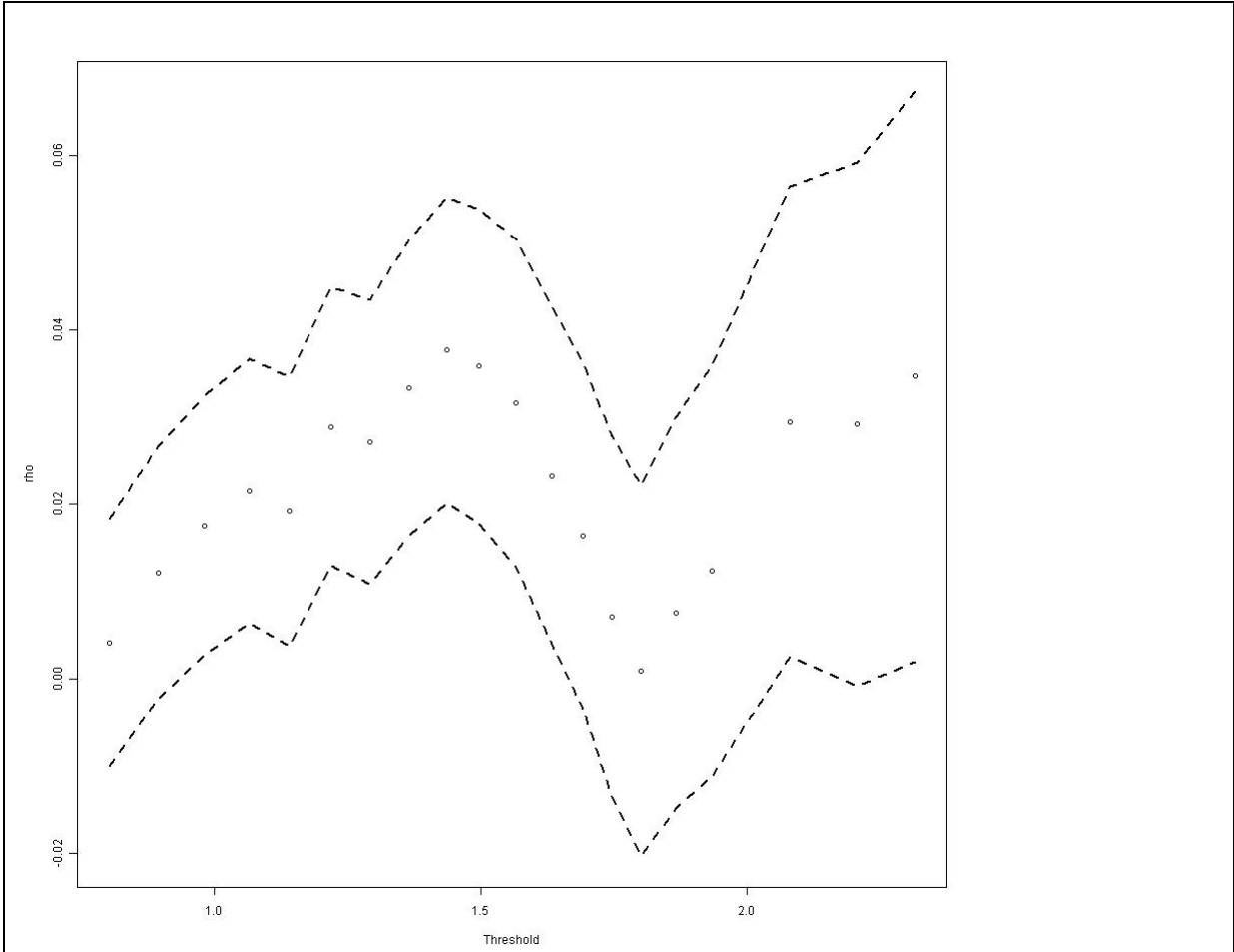
Figure A7.4 – correlation parameter ρ between wind-sea and swell height (Test Site GL2849)
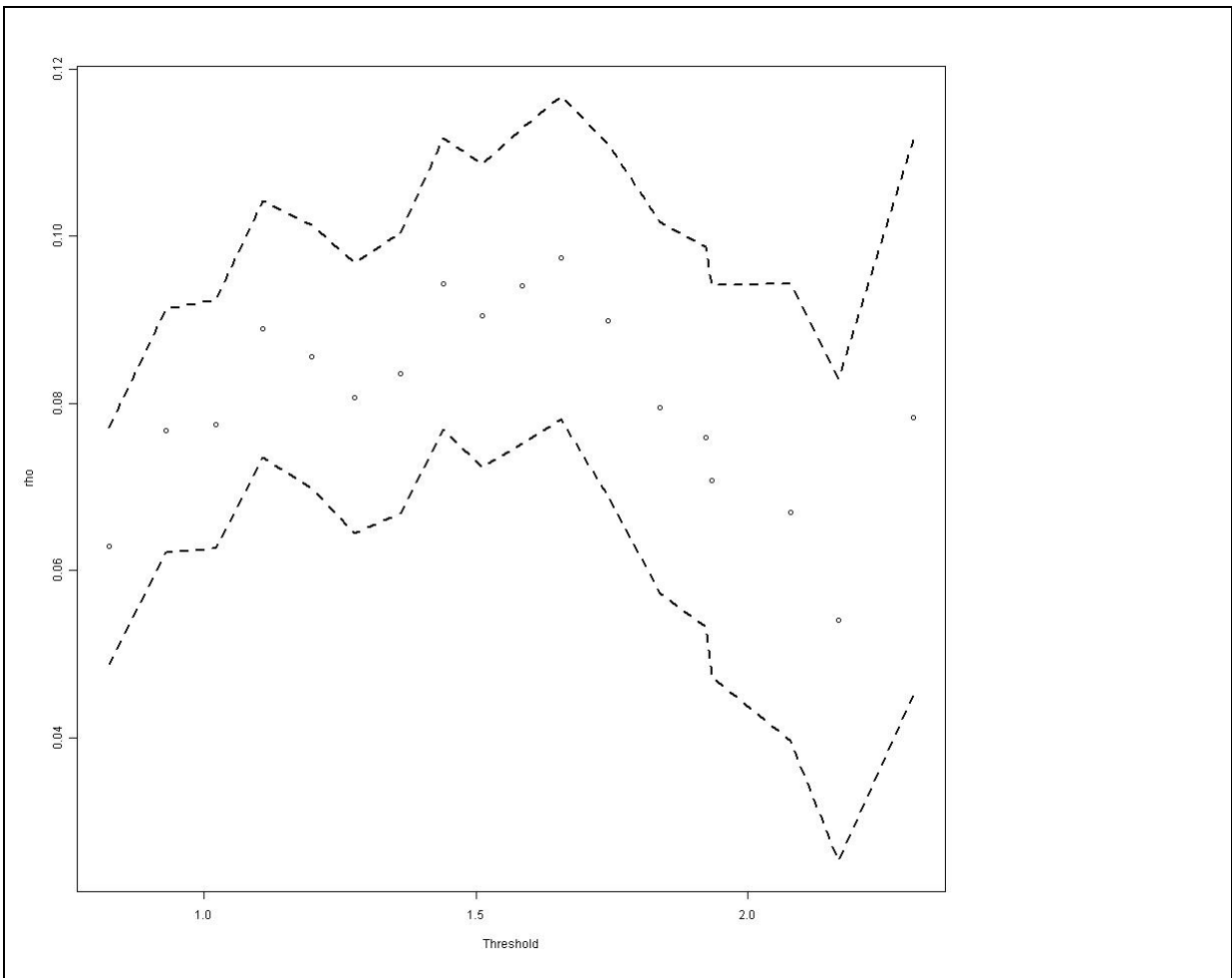
Figure A7.5 – correlation parameter ρ between wind-sea and swell height (Test Site GL2523)

Figure A7.6 – correlation parameter ρ between wind-sea and swell height (Test Site GL1946)
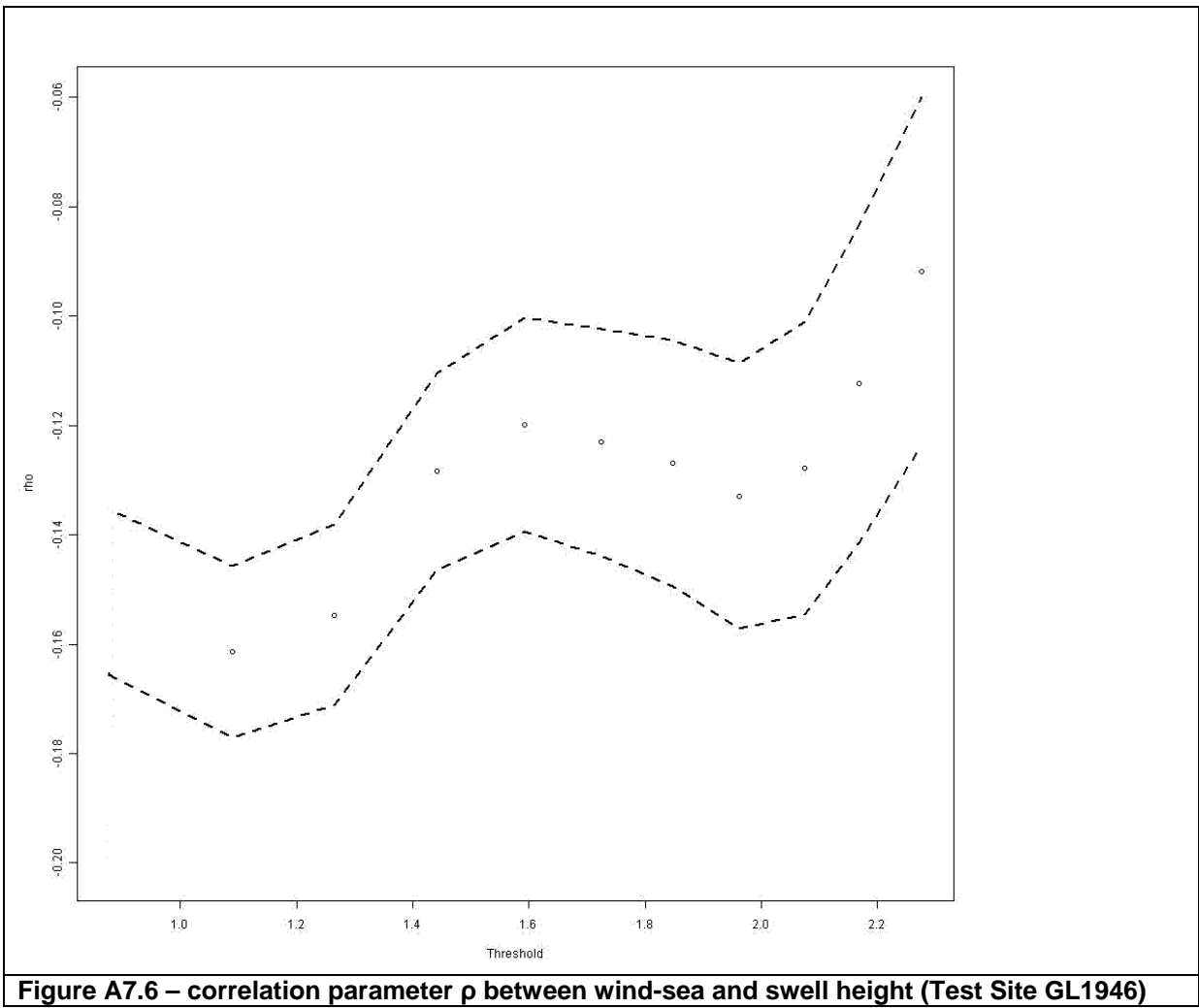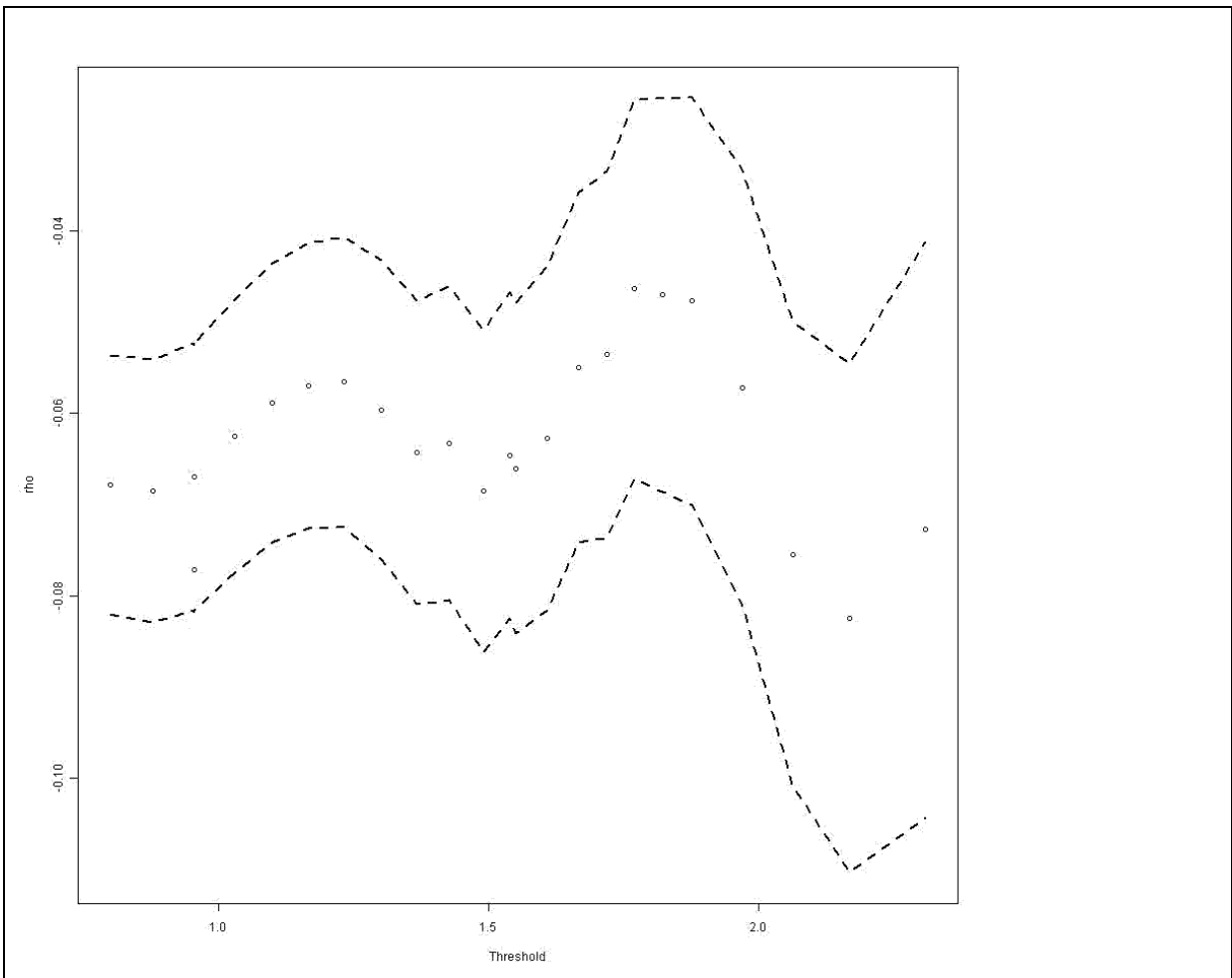
Figure A7.7 – correlation parameter ρ between wind-sea and swell height (Test Site GL1276)
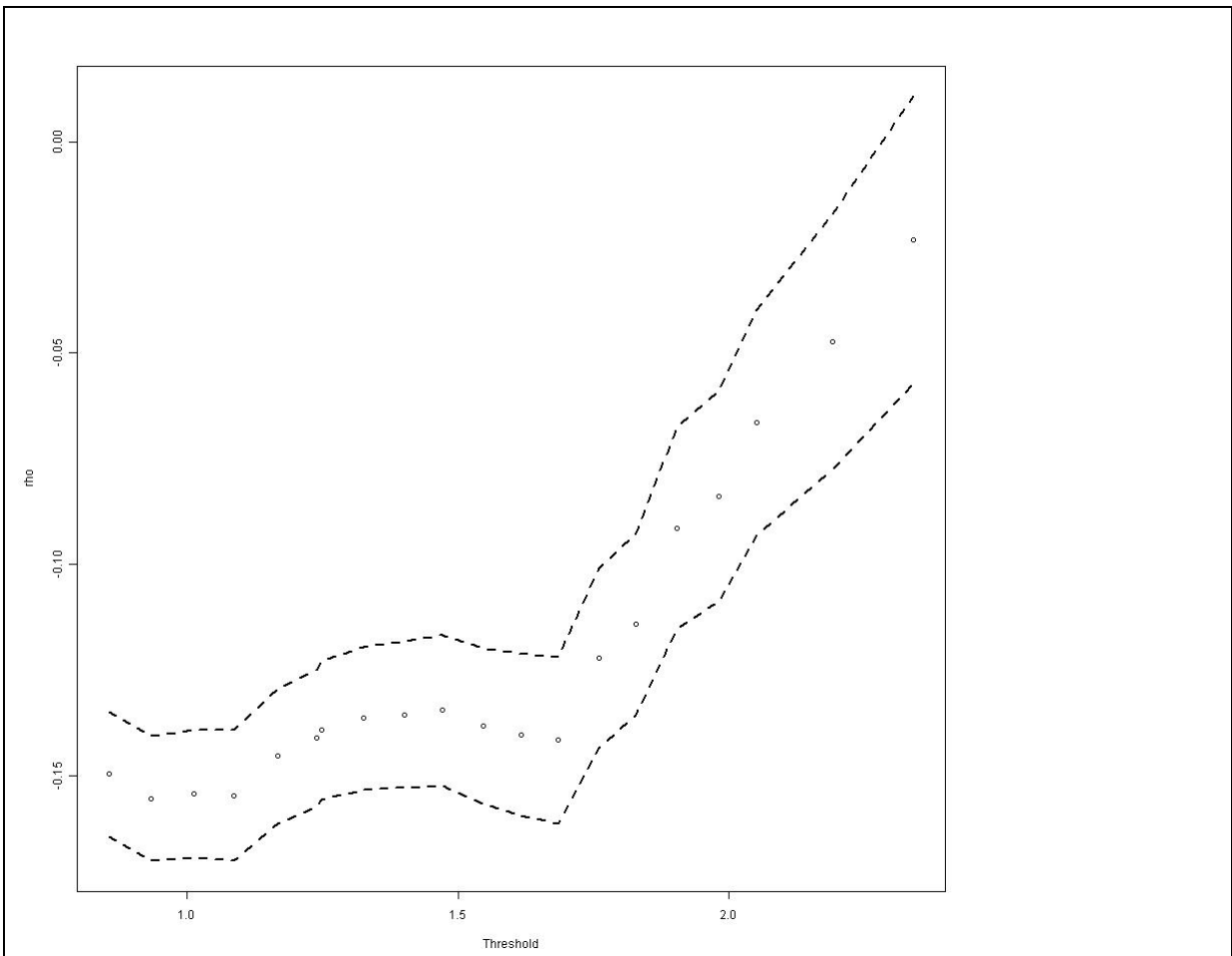
Figure A7.8 – correlation parameter ρ between wind-sea and swell height (Test Site GL0531)

Appendix 8 Confidence Intervals

A8.1   Introduction

This appendix presents an overview of the confidence intervals derived for estimates of swell wave heights. Confidence intervals are an indication of the level of uncertainty in the results provided.

Confidence intervals have been provided for each annual exceedance probability per direction sector. For sites where not enough occurrences (less than 15) of swell were included in the Met Office model data, this was not possible. The file reference for the confidence intervals is contained in the swell wave Shapefile (CFB_Swell_Waves.shp) provided for each output point:

A8.2   Introduction

To provide confidence intervals the standard error for each estimate of swell wave height was calculated. The standard error of a statistic is the standard deviation (spread of values away from the mean) of the sample. Standard errors reflect how much fluctuation within the sample a statistic will show from the mean. The statistics involved in the construction of a confidence interval are based on a standard error. In general, the larger the sample size the smaller the standard error.

As discussed in Section 3 the statistical method used was the Generalised Pareto Distribution. The maximum likelihood method was used to optimise the three parameters used in the GPD: scale, shape and location. The method of maximum likelihood selects the values of GPD model parameters that maximise the likelihood function (the statistical model) to the data.

A confidence bound is a range of values that contain the estimated parameter a high proportion of the time. The confidence bounds are therefore used to indicate the reliability of an estimate. In this project we have provided the 95% confidence. Therefore 95% of the values are within the bounds. This is an arbitrary decision but a common selection in extreme statistics. The maximum likelihood estimators follow a Normal Distribution therefore to calculate the confidence interval from a standard error the following equation is used:

$$\text{95\% confidence bounds} = \bar{x} \pm (S_E * 1.96)$$

$\bar{x}$ = Mean (swell wave estimate)
S_E = Standard Error
1.96 = factor to give 95% confidence bound

In this instance we have expressed uncertainty in terms of confidence intervals, being the distance ($\pm$) of half of the bound with from the mean (swell wave height value).

A8.3   Application of Confidence Intervals

This project has provided estimates of swell wave height from a sample of eight years of hindcast wave data. Confidence intervals have been provided for each of these estimates. **Table A8.1** and **Figure A8.1** shows how the confidence intervals can be applied to the swell wave height estimates to provide an upper and lower confidence bound. Annual exceedance probabilities ranging from 1 to 0.001 (1 year to 1,000 year return periods) are provided for test point GL2849 (offshore from Plymouth), as shown in Figure A8.1. The swell wave heights have been given for the south west direction sector.

Table A8.1 – Applying Confidence Intervals for GL2849 (offshore from Plymouth)

Return Period (years)	1	100	1000
Swell Wave Height (South West Sector) (m)	5.48	7.20	7.79
95% Confidence Interval ($\pm$) (m)	0.19	0.51	0.69
Lower 95% Confidence Bound (m)	5.29	6.69	7.10
Upper 95% Confidence Bound (m)	5.67	7.71	8.48
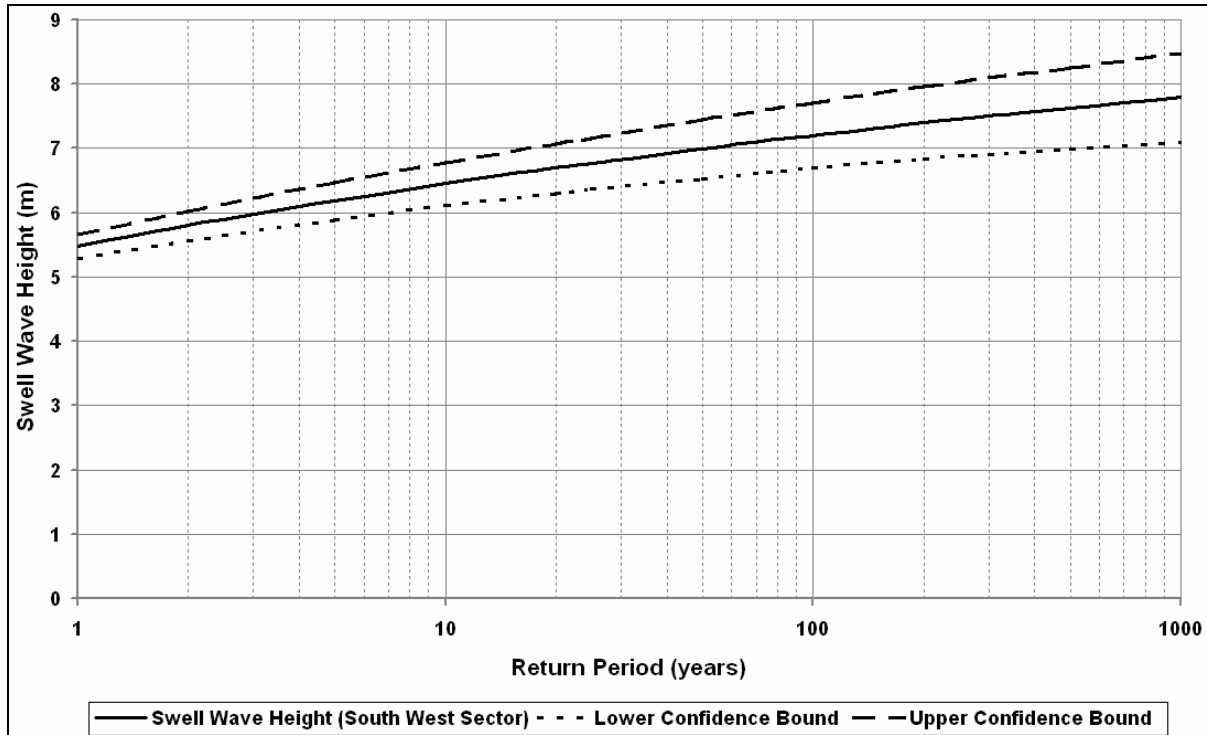
Figure A8.1 Swell Wave Heights and Confidence Bounds for GL2849 (Plymouth)

A8.4   Discussion of Confidence Intervals

As stated in the main report, this analysis has been undertaken using eight years of Met Office model data. We can therefore expect there to be a high degree of uncertainty at the lower annual exceedance probabilities. When selecting a swell wave height to use during design or as part of a study, the user should adopt a practical approach. Where the 95% confidence intervals provide large ranges, for example greater than 1m, this should alert the user to the uncertainty of the results. Therefore there will be a need for sensitivity tests or the requirement to obtain further data to address this uncertainty.

Appendix 9 Results

A9.1   Introduction

This Appendix presents an analysis of the swell wave height results for each region. The results are presented in graphical format with **Table A9.1** preceding the results with a discussion for each figure. **Figure 4.4** shows the regional chainage locations referred to in this Appendix.

The direction sectors are given at sixty degree intervals as shown in **Figure A8.1**.

North - 330° to 30°	**North East - 30° to 90°**	**South East - 90° to 150°**
South - 150° to 210°	**South West - 210° to 270°**	**North West - 270° to 330°**
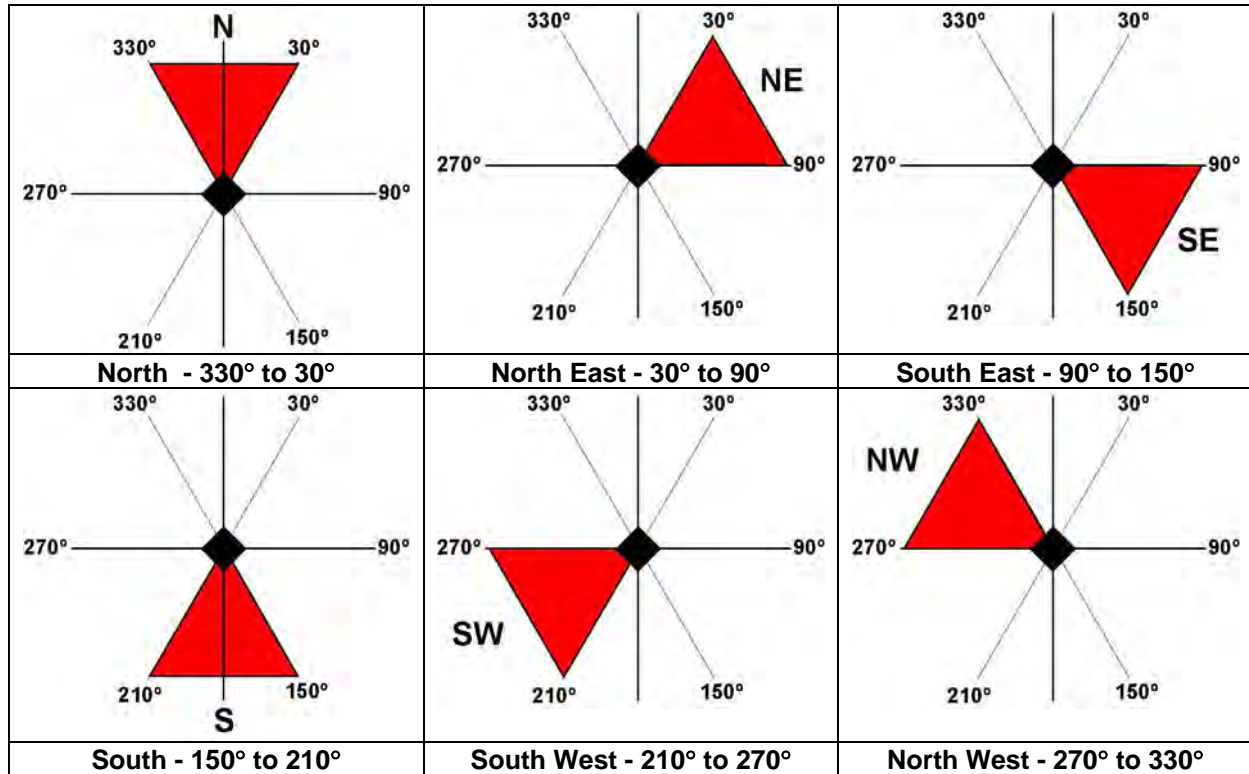
Figure A9.1 – Six Directional Sectors for Swell

Table A9.1 – Comments on the Swell Wave Heights Results

Region	Direction Sector	Comments
North	330-30 (North)	This set of results appear reasonable. There is some natural variation in estimates due to the shape and bathymetry. A turning point is evident at Ch1796 as the chainage turns south round the Orkneys. A point that stands out slightly is at Ch1652, though there is not obvious reason for this and the GPD fit is reasonable.
	30-90 (North East)	There are four noticeable features in this set of results these are a shift in levels around Ch1550, a gap between ch1607 and ch1664, a small set of results at Ch1715 and a peak at Ch 1755. The gap can be explained due insufficient data points to provide an accurate fit which is due to the Sheltering of the points by the Orkneys to the North East. The shift in levels is due to the movement of the chainage points to the next offshore Met Office grid cell, which was necessary to remove shallow water effects. The small set of results appears to have a reasonable GPD fit and enough points, therefore is may be a modelling effect from the limitations of the data being used. The peak is to the north of the Orkneys and therefore representative of the more exposed location.
	90-150 (South East)	There are three features in this set: the lack of results until Ch1705 just north of the Orkneys where the outputs start to become exposed due to the SE. Two points have a reduced level due to the influence of the most northern island in the set. The peak again is at Ch 1765 to the north of the Orkneys which is exposed.
	150-210 (South)	There are several features in this set of results. The results start at Ch1746, NE of the Orkneys where the data points become exposed to the south, with one exception at the top of the Minches the channel between the Inner and Outer Hebrides which is exposed to the south. The remaining points have an expected variation due to exposure, however there are two smaller set of points which is due to the islands to the south.
	210-270 (South West)	The first set of points are now exposed to the south westerly waves and therefore recorded results before the Scottish main land shelter points between Ch1597-1652. The remaining points are variable due to various sheltering and exposed nature of points through the Orkney Islands.
	270-330 (North West)	The waves from the north west provide a clean set of results.
North East	330-30 (North)	The waves from the north provide a good set of results. Three points stand out. Ch2043 just north of Fraserburgh which seams to be a reasonable fit if a little underestimated by the GPD; it is situated in significantly deeper water than surrounding points at 180mCD, similarly Ch2146 is in slightly deeper water. Ch2296 off Eyemouth appears to have a good fit so the variation is likely to be a data effect. Otherwise the shape of the north east coast can almost be seen in the levels.
	30-90 (North East)	The levels provide a consistent set of results except for three points. Ch2093 off Peterhead, Ch2162 off Arbroath, Ch2320 off Eyemouth all appear to be inconsistently high levels, these all appear to have reasonable fits and don't appear to have any depth affect, therefore the inconsistency is put down to an anomaly in the data and best ignored.

Region	Direction Sector	Comments
	90-150 (South East)	The set of results appear good there are two unusually high points and two non fitted points. The two non fitted points at Ch1974 and 1993 are both off the Moray coast and therefore sheltered by land. The two high points at Ch 1933 and Ch2033 are both poor fits and are overestimated by the GPD they are better represented by the 95% thresholds. For this work they should be ignored.
	150-210 (South)	There are three gaps in this set of data corresponding to the Moray Firth, Firth of Forth and the North East coast of England which are all sheltered from southerly waves. There is one peak at Ch2105 off Aberdeen which has a reasonable fit, this may be due longer fetches available to the south or a data effect. Three lower points at Ch2133, Ch2146, Ch2207 appear to be good GPD fits to the data as are their neighbours and therefore an indication of the natural variation in the modelling data.
	210-270 (South West)	The south west direction only provide two data points with a fit due to the sheltering of the land. The two fitted points at Ch2053 and Ch 2081 are off Peterhead and appear to provide a reasonable fit. These may be used to near by locations.
	270-330 (North West)	The are a few points here that are fitted due to swells across the Moray Firth. There is one lone point at Ch2320 open to fetches across the Firth of Forth.
North West	330-30 (North)	There are a few points here that are not consistent. Ch1153 is slightly sheltered from waves approaching from the north. CH1181 expresses slightly higher results owing to a greater depth. CH1300 shows a poor fit. The results are underestimated.
	30-90 (North East)	Most of the data points along this chainage contain less than the threshold (15) occurrences for swell. CH1438 is exposed to swell from the North East of the Shetlands.
	90-150 (South East)	Considering the orientation of the land on this frontage, there are no data points along this frontage owing to the sheltering effect of the land.
	150-210 (South)	Ch1141 - Ch1133 show inconsistent results, the GPD appears to be a poor fit. Similarly at Ch1213 - Ch1238 shows a poor fit, the results are underestimated.
	210-270 (South West)	This set of results generally appear to show a good fit. Ch1382 - Ch1397 demonstrate slightly higher results owing to the deeper conditions.
	270-330 (North West)	These results generally appear to show a good fit.
South	330-30 (North)	There are no data points available for this frontage considering the sheltering effect of the land from swell waves approaching from the North.
	30-90 (North East)	Only 2 data points are available, CH3182 & Ch3193, considering the sheltering effect of the land. However, it would be expected that Ch300 - Ch3200 would experience some swell waves.
	90-150 (South East)	There is not enough data available for points along the chainage between Ch300 and Ch3193. Results at Ch3405 are not consistent, this is due to a greater depth of 70mCD in comparison to the rest of the frontage.
	150-210 (South)	Ch300-Ch3129 and Ch3164 and Ch3182 do not have enough data points available, predominantly owing to the sheltering effect of the land to the south. The data points around Ch3347 at Lyme Bay, yield slightly higher results owing to the influence of a longer fetch distance and deeper water conditions. At Ch3389 and Ch3405 there are significantly lower results owing to the sheltering effect of the headland. The results are not consistent at Ch3559.

Region	Direction Sector	Comments
	210-270 (South West)	The results are generally consistent, with an increase in swell height as the chainage moves further west. There are a few points that can be identified from the graph; Ch3070, displays slightly higher results owing to its situation on the corner of Kent. Ch3359 shows a drop in wave heights as it is situated in the corner of a bay. At Ch3517, Torbay, the results are not consistent and the GPD shows a poor fit.
	270-330 (North West)	Understandably, there are a number of data gaps along the frontage as it is sheltered from swell approaching from the north west. Two peaks in the results at Ch3036 and Ch3559 correspond to a poor fit in the data.
South East	330-30 (North)	There is a gap in the data between Ch2672 and Ch2756, The Wash. This area is sheltered from swell waves incoming from the North and the seabed is significantly shallower at approximately 20mCD. At Ch2789 the results are not consistent, and shows a poor fit which is overestimated.
	30-90 (North East)	There are a limited number of data points available for this frontage, particularly between Ch2830 and Ch3000, where East Anglia is located. The available results generally show a good fit with some underestimation.
	90-150 (South East)	As above, there is a lack of data for the East Anglia frontage. This is owing to the orientation of the land which is sheltered from waves approaching from the south east. The results generally show a good fit.
	150-210 (South)	There are a number of data gaps for swell waves approaching from the South. Between Ch2656 and Ch2721, this corresponds to The Wash, where North Norfolk shelters the frontage from incoming waves. Similar sheltering effects are identified at Ch2867 and for the remainder of the frontage from Ch2921 owing to France. There is one data point that is inconsistent at Ch2756.
	210-270 (South West)	Up until Ch2772, the frontage is not exposed to swell waves approaching from the south west. The results generally show a good fit. At point Ch2772 the results appear inconsistent and the GPD shows a poor fit.
	270-330 (North West)	There are under the threshold value of data points available for all of the frontage with the exception of Ch2801. The results for this data point are plausible considering its location on the top of North Norfolk.
South West	330-30 (North)	There is a gap in the data between Ch292 and Ch390, owing to the sheltering effect of South Wales on waves incoming from the North. Similar sheltering effects of land are identified at Ch490 and Ch560.
	30-90 (North East)	There is sparse data available for this frontage considering the sheltering effect of the land from incoming waves from the north East. For CH48, Ch61 and Ch139, data points situated on the north of Cornwall the data is underestimated.
	90-150 (South East)	With the exception of the South of Cornwall, no data points are available for this frontage owing to the sheltering effect of Cornwall from waves from this direction. One anomaly is located at Ch333 to the north of the Bristol Channel. This shows a poor fit.
	150-210 (South)	A contrast in results can be identified between Ch12 and Ch23-Ch48, this is owing to the results being over and underestimated respectively. Data gaps are identified at Ch156 to Ch280 and Ch449 to Ch490, which correspond to North Cornwall and Cardigan Bay which both shelter the Coastline from swell waves approaching from the South.
	210-270 (South West)	There are a number of data points that show variations in the general trend of results. At Ch121 there is an unexplained drop in the results. Ch345 and Ch560 correspond to high points in the results, these are both poor fits in the GDP.

Region	Direction Sector	Comments
	270-330 (North West)	Two high points in the results can be identified at Ch333 and Ch477 which corresponds to the Bristol Channel and Cardigan Bay. These points show a poor data fit. A low point in the data at Ch544 identifies an underestimate in the data.
West	330-30 (North)	There is a general lack of data for the frontage under this direction owing to the sheltering effect of Scotland. There are 3 points where data has been obtained Ch714 (Liverpool Bay), Ch975 & Ch1035. These generally show a good fit with some underestimation.
	30-90 (North East)	As expected, there is no data available for this frontage owing to the sheltering effect pf Scotland from waves approaching from the North East.
	90-150 (South East)	There is a general lack of data for the frontage owing to its sheltered nature. At Ch843 and Ch919 the data shows a general underestimate.
	150-210 (South)	Data gaps are present between CH637 and Ch752 where the frontage is sheltered by the north of Wales, and at Ch975 to Ch1031 where the frontage is sheltered by the north of Ireland. At Ch805 the results are underestimated and are outside the 90% threshold, similarly at Ch886, the results are underestimated.
	210-270 (South West)	There is a data gap present between CH919 and Ch1008 at South Kintyre where the waves. At Ch843, the drop in the results corresponds to an underestimation. At Ch1035, the peak in results may be attributed to deep water of over 100mCD.
	270-330 (North West)	There are a number of data gaps at sheltered locations between Ch793 and Ch902. Peaks in results at CH764 and Ch776 correspond to a poor fit.
Shetland	330-30 (North)	The results of the waves to the north provide a good fit and reflect the geographic shapes of where each point lies in relation to the Shetland Isles.
	30-90 (North East)	There is a gap in the points for Ch93-133 which are sheltered by the Isles to the NE. Otherwise the results for the waves from the North East are fairly variable. There are no particular points that stand out for particular attention.
	90-150 (South East)	There is a similar gap in data for Ch121-160 due to the sheltering form the land. The data provides a reasonable fit with some variability. The point at Ch 345 appears unusually small the fit appears reasonable and similar to adjacent points, there is no clear explanation but this should be treated with caution.
	150-210 (South)	All the results have a reasonable fit with some scatter, mainly due to the influence of the islands to the north.
	210-270 (South West)	The results of the waves to the north provide a good fit and reflect the geographic shapes of where each point lies in relation to the Shetland Isles.
	270-330 (North West)	The majority of points provide a good fit. There is a gap at Ch360-386 due to the sheltering of waves from the NW. There are two points with levels higher than the rest at Ch145-160 these also have god fits and are likely to be more exposed than adjacent points.
Hebrides	330-30 (North)	The waves form the north provide a good fit with a gap to the south due to the sheltering by the Western Isles. There is one higher point at Ch236 which gives a good fit. There is no particular reason for this to be higher than the points immediately to the north. This is an indication of the accuracy of the data.
	30-90 (North East)	The points are fairly sheltered to the north east and therefore only a few of the points to the north have enough data to fit the GPD. These all appear to be reasonable.
	90-150 (South	No data fits

Region	Direction Sector	Comments
	East)	
	150-210 (South)	The fits are reasonable with a gap due to the sheltering of the mainland.
	210-270 (South West)	The waves from the south west provide a clean set of results.
	270-330 (North West)	There is a good set of results with a gap due to the sheltering of points by the Western Isles. There is also a shift in levels at Ch80 which is again due to the sheltering of points by the Western Isles.
Isle of Man	330-30 (North)	Only provides three points with sufficient data of provide a fit. These appear to be reasonable
	30-90 (North East)	No data fits due to lack of data and sheltering form the land.
	90-150 (South East)	One point provides a reasonable fit
	150-210 (South)	The waves from the south provide a clean set of results.
	210-270 (South West)	The waves form the SW provide a good set of results. There is one point at Ch71 that gives a higher fit than adjacent points which is a overestimated fit to the results and therefore adjacent points are likely to be more accurate.
	270-330 (North West)	One point provides a reasonable fit
Bristol Channel	330-30 (North)	No data fits
	30-90 (North East)	No data fits
	90-150 (South East)	No data fits
	150-210 (South)	No data fits
	210-270 (South West)	The fits provide a good picture of the levels as the travel up the estuary into shallower water and thus get smaller
	270-330 (North West)	The fits provide a good picture of the levels as the travel up the estuary into shallower water and thus get smaller

North Chainage Swell Wave Heights from the North

Legend: ◆ 1yr ◆ 10yr ◆ 100yr ◆ 200yr ◆ 1000yr

X-axis: Chainage (km)

Y-axis: Swell Wave Height (m)

North Chainage Swell Wave Heights from the North East

Legend: 1yr, 10yr, 100yr, 200yr, 1000yr

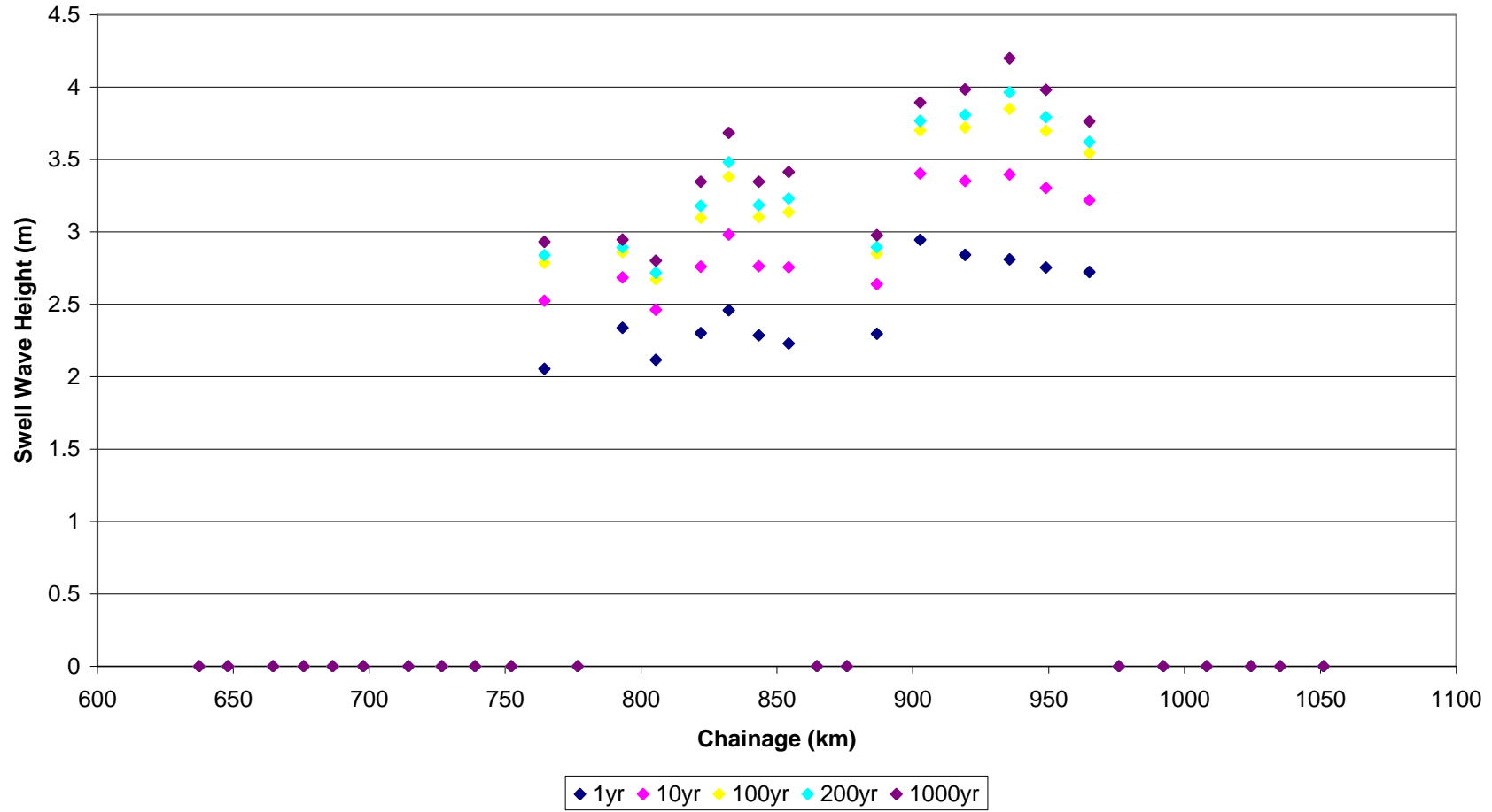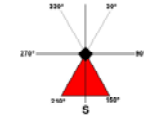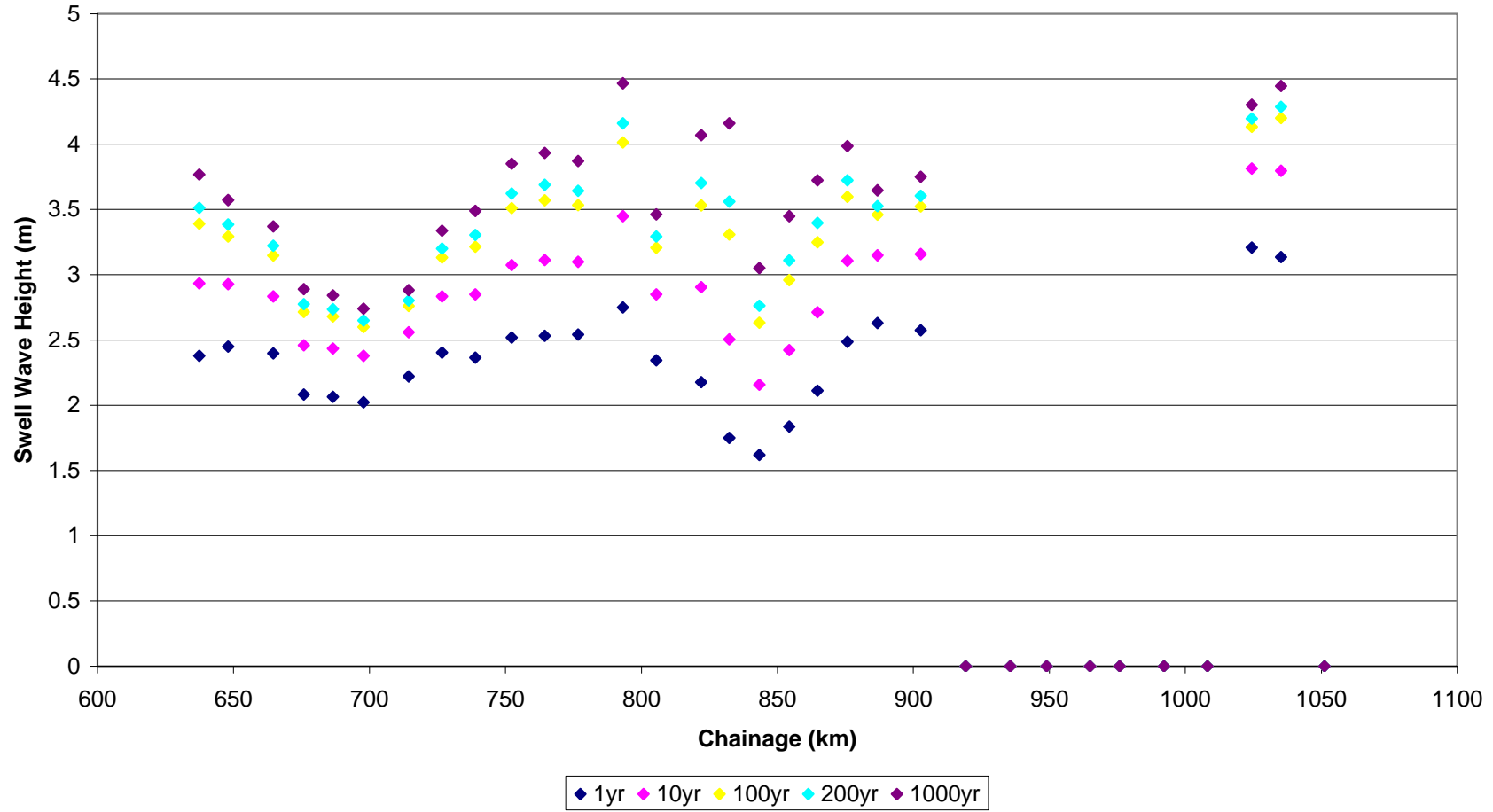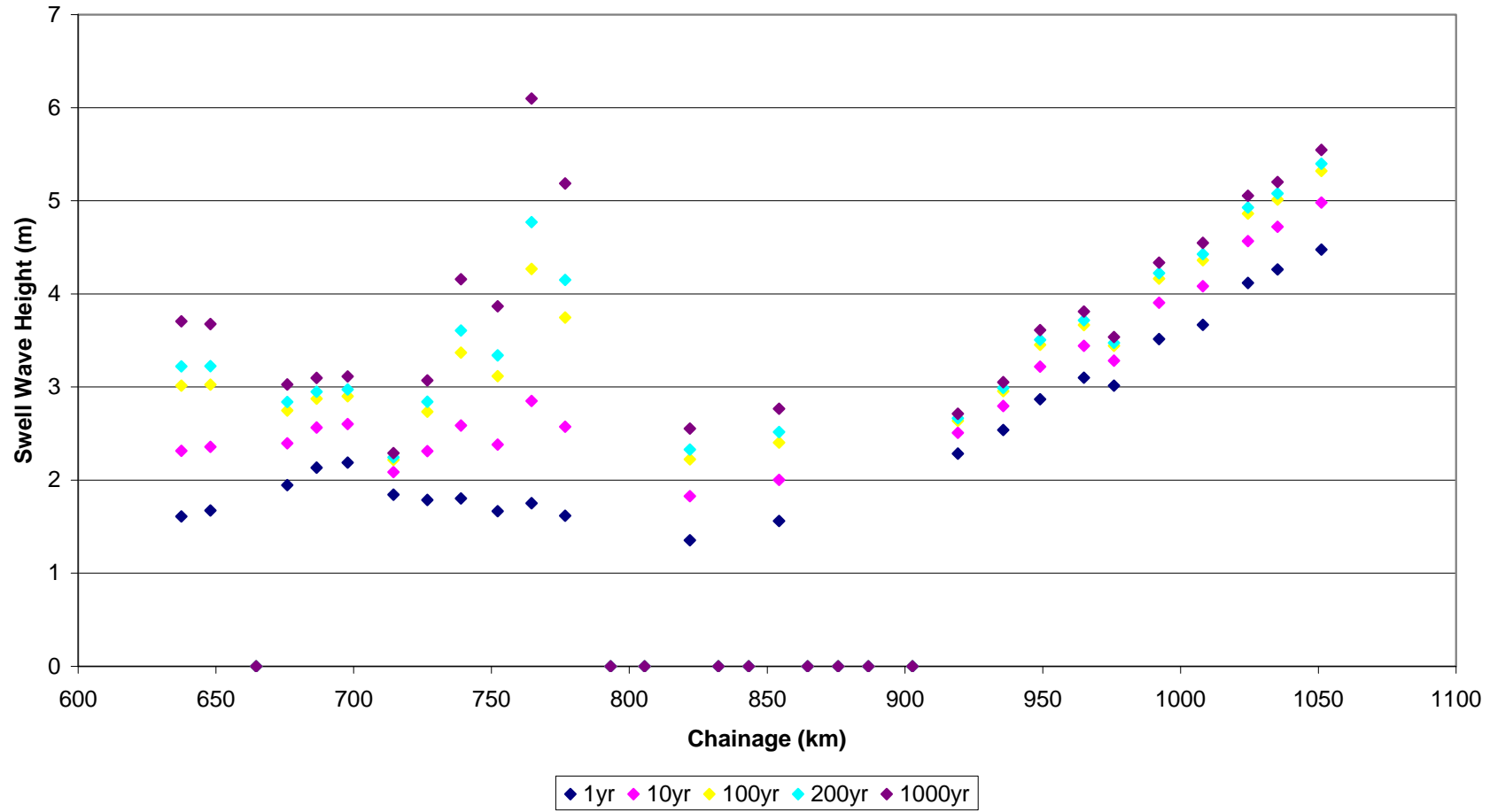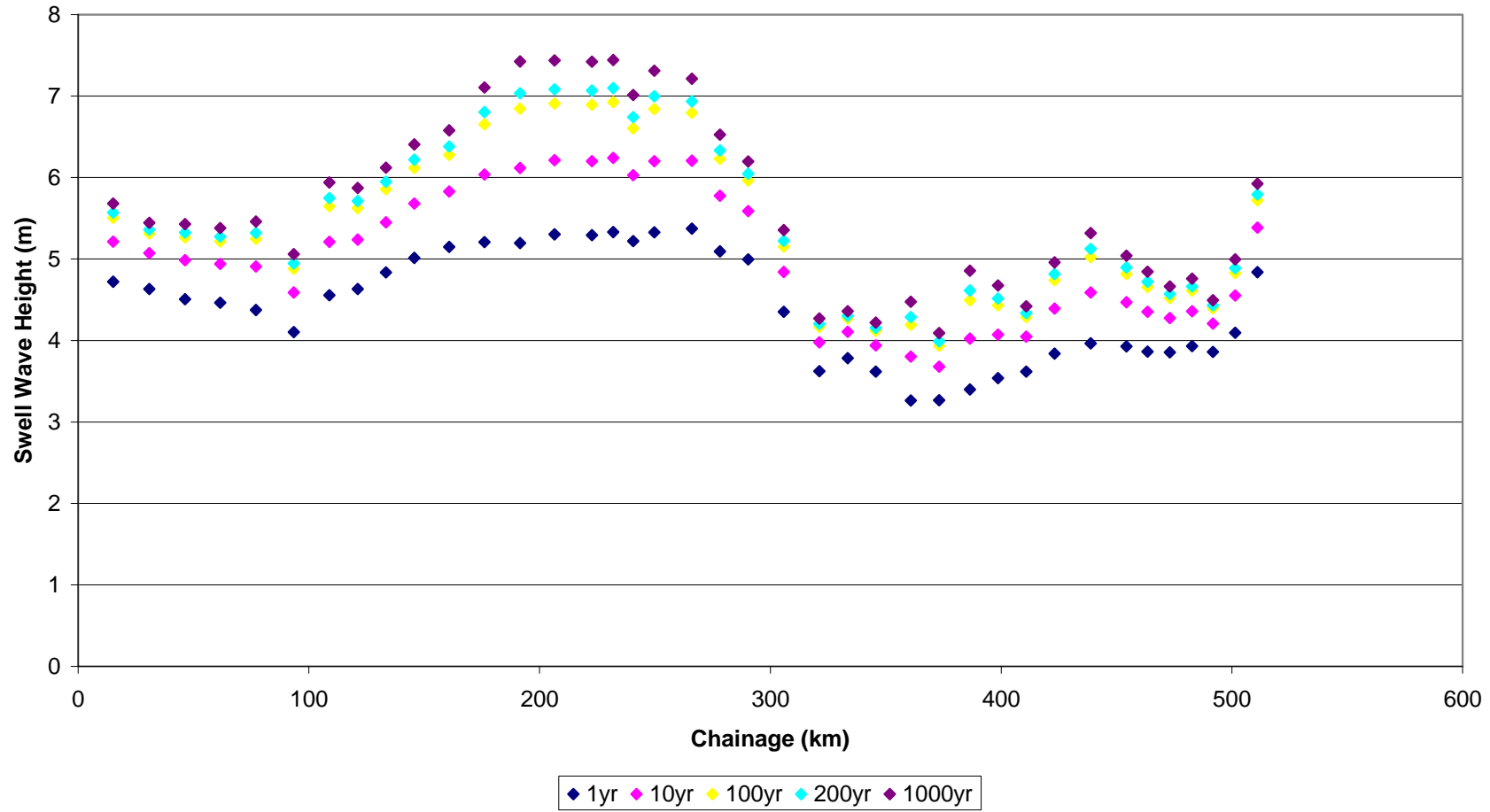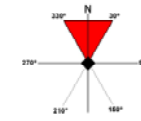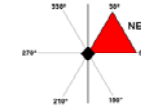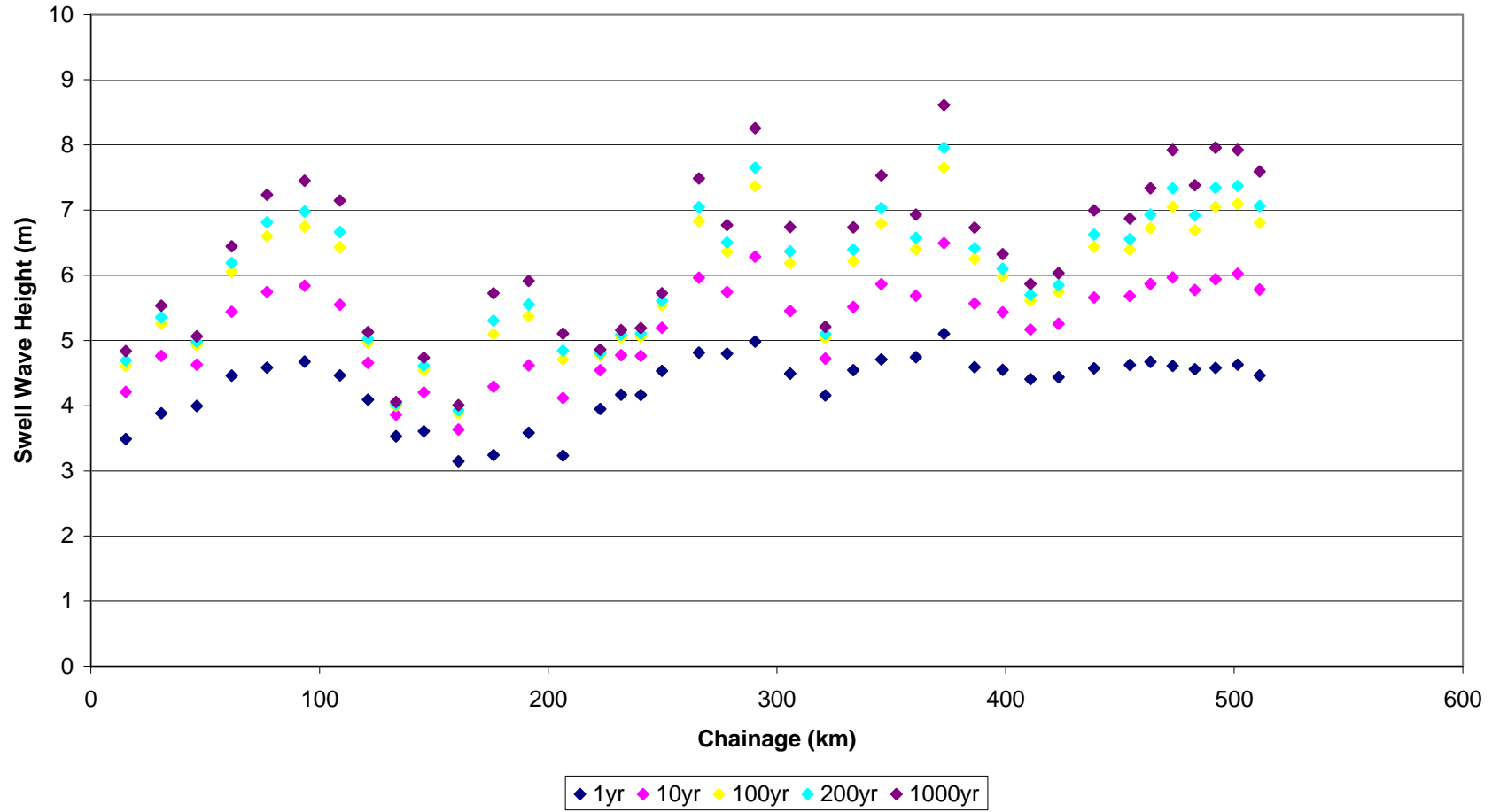Y-axis: Swell Wave Height (m)

X-axis: Chainage (km)
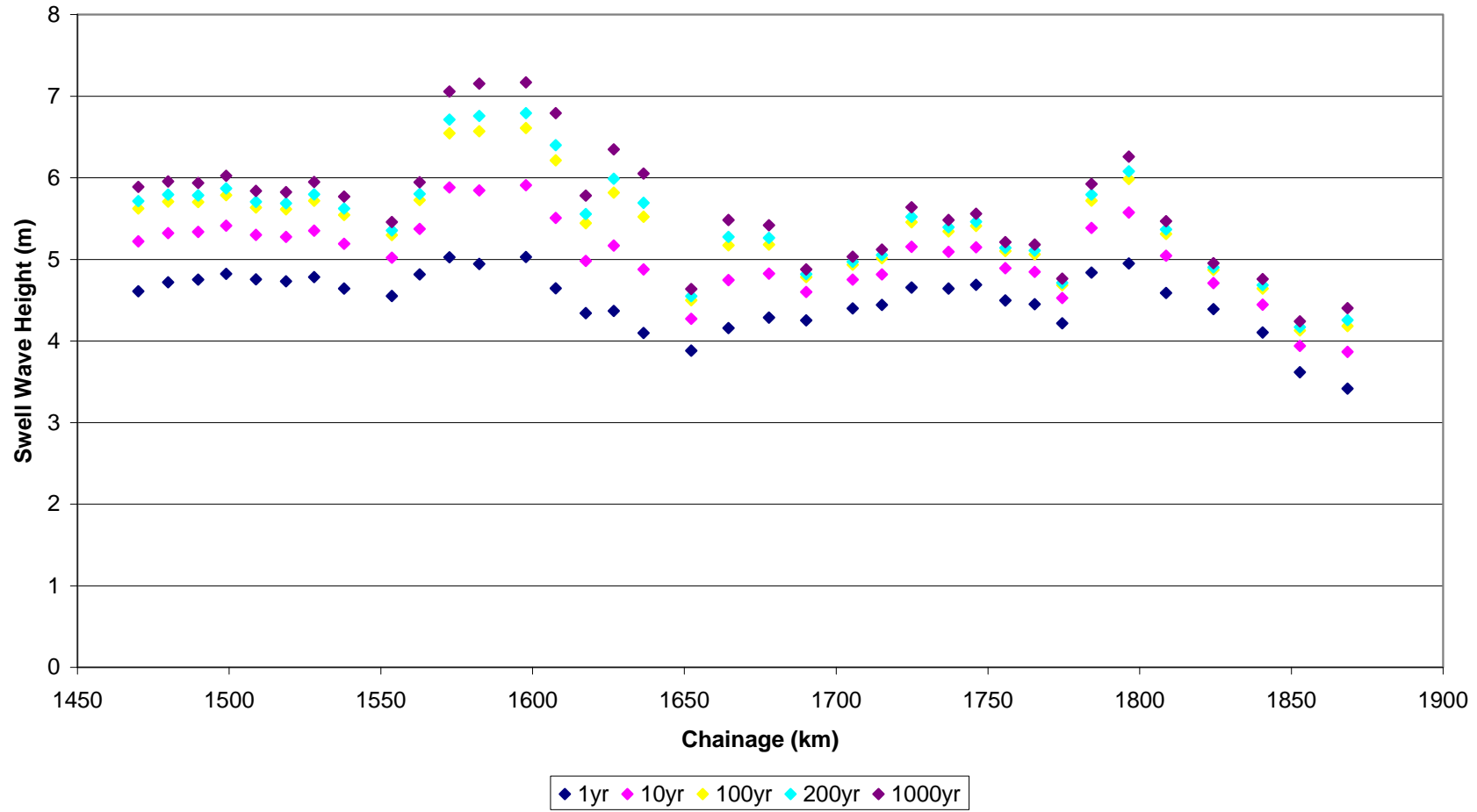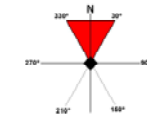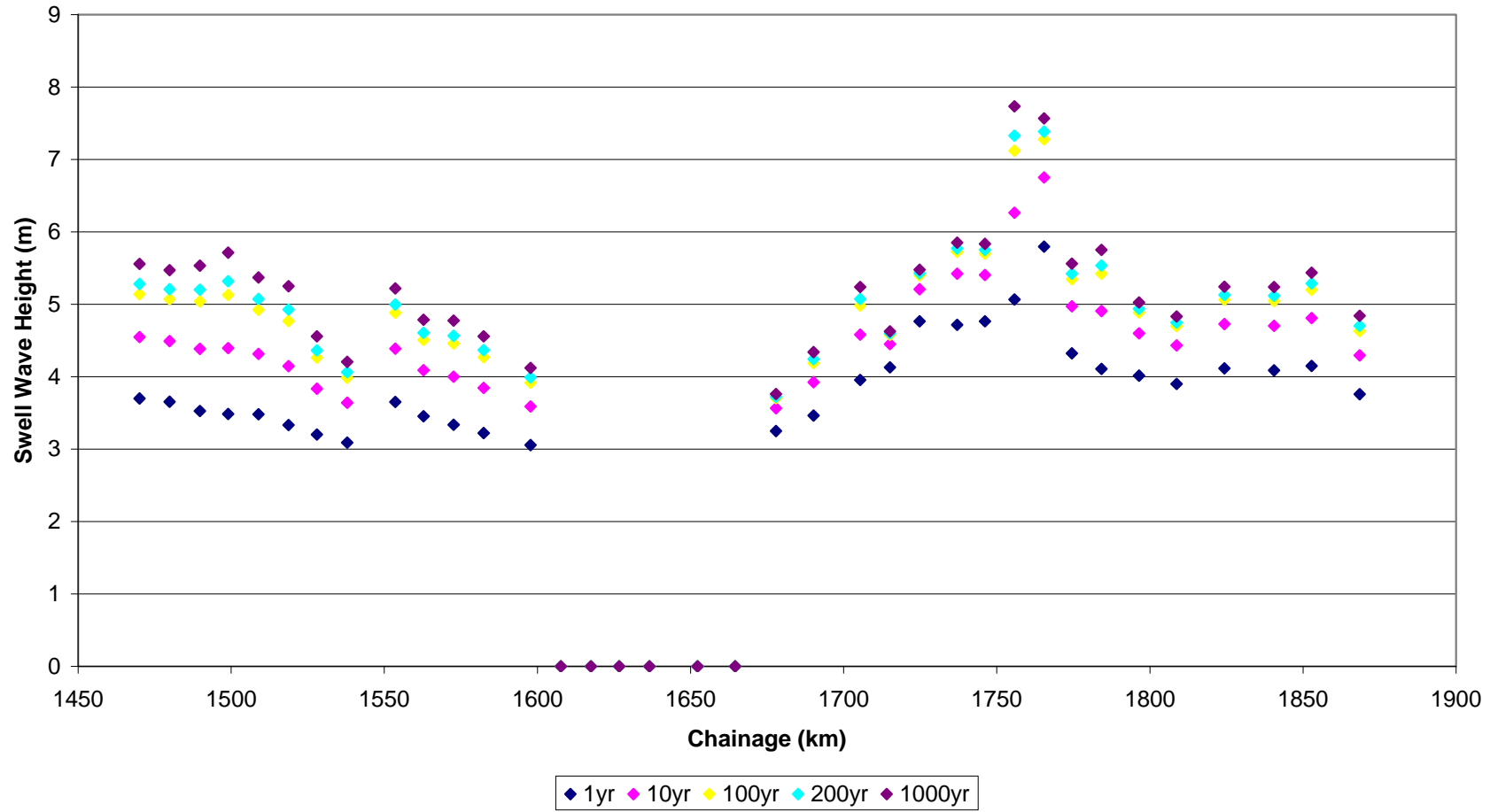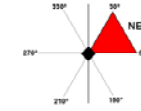
North Chainage Swell Wave Heights from the South East

North Chainage Swell Wave Heights from the South

Swell Wave Height (m) vs Chainage (km)

Legend: ◆ 1yr ◆ 10yr ◆ 100yr ◆ 200yr ◆ 1000yr
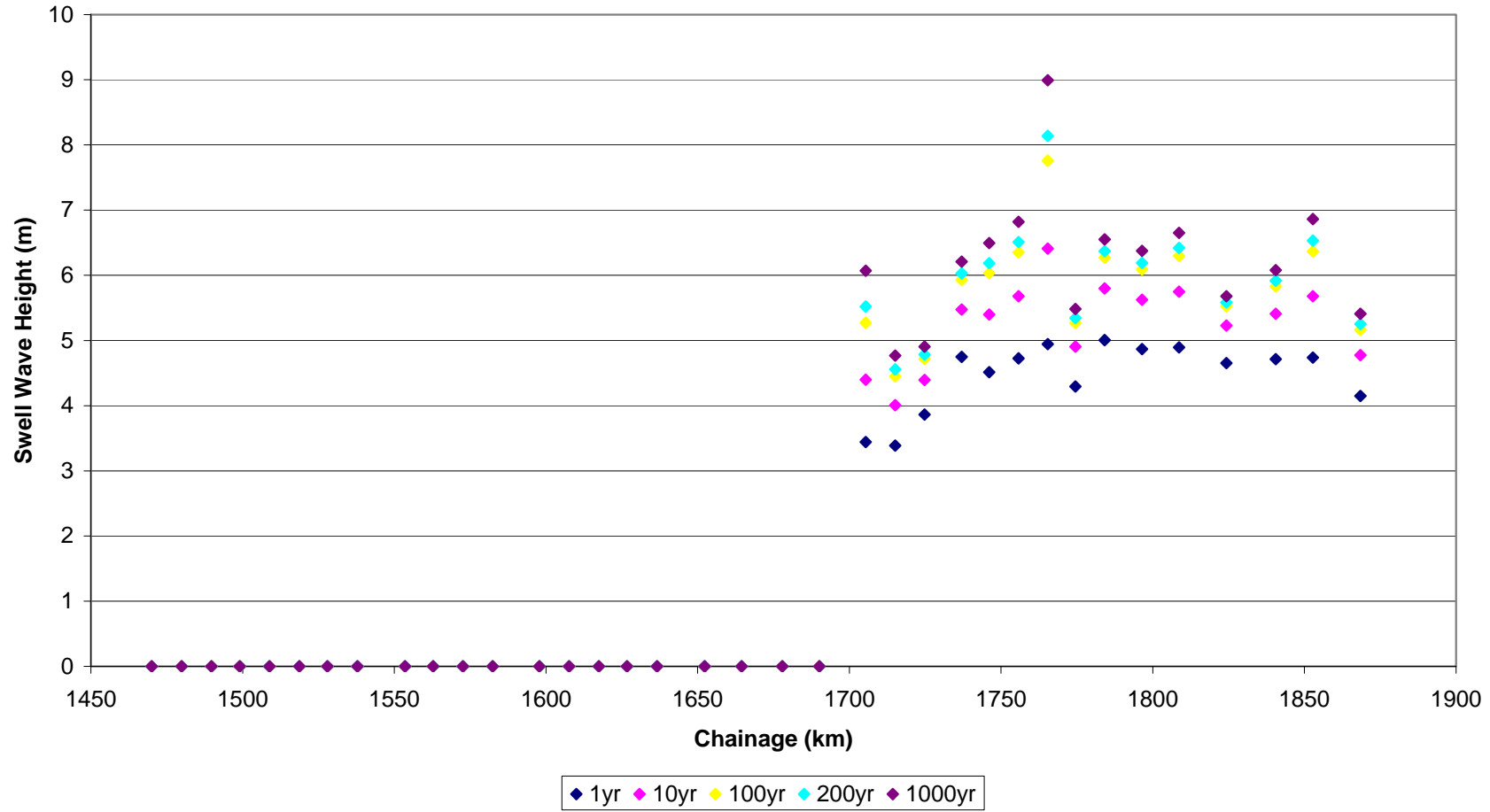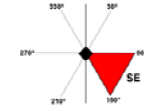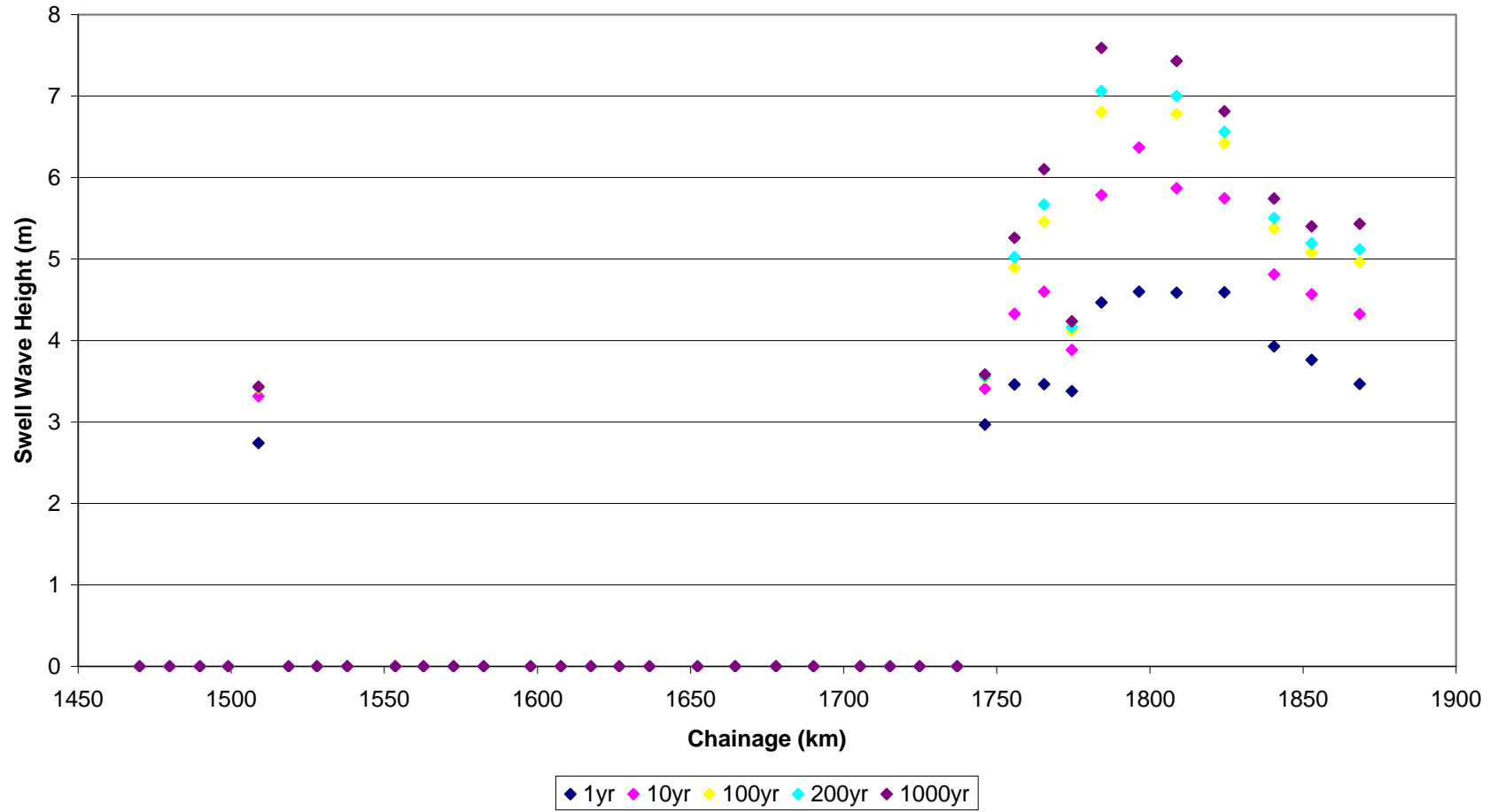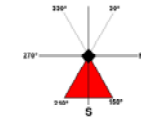
North Chainage Swell Wave Heights from the South West
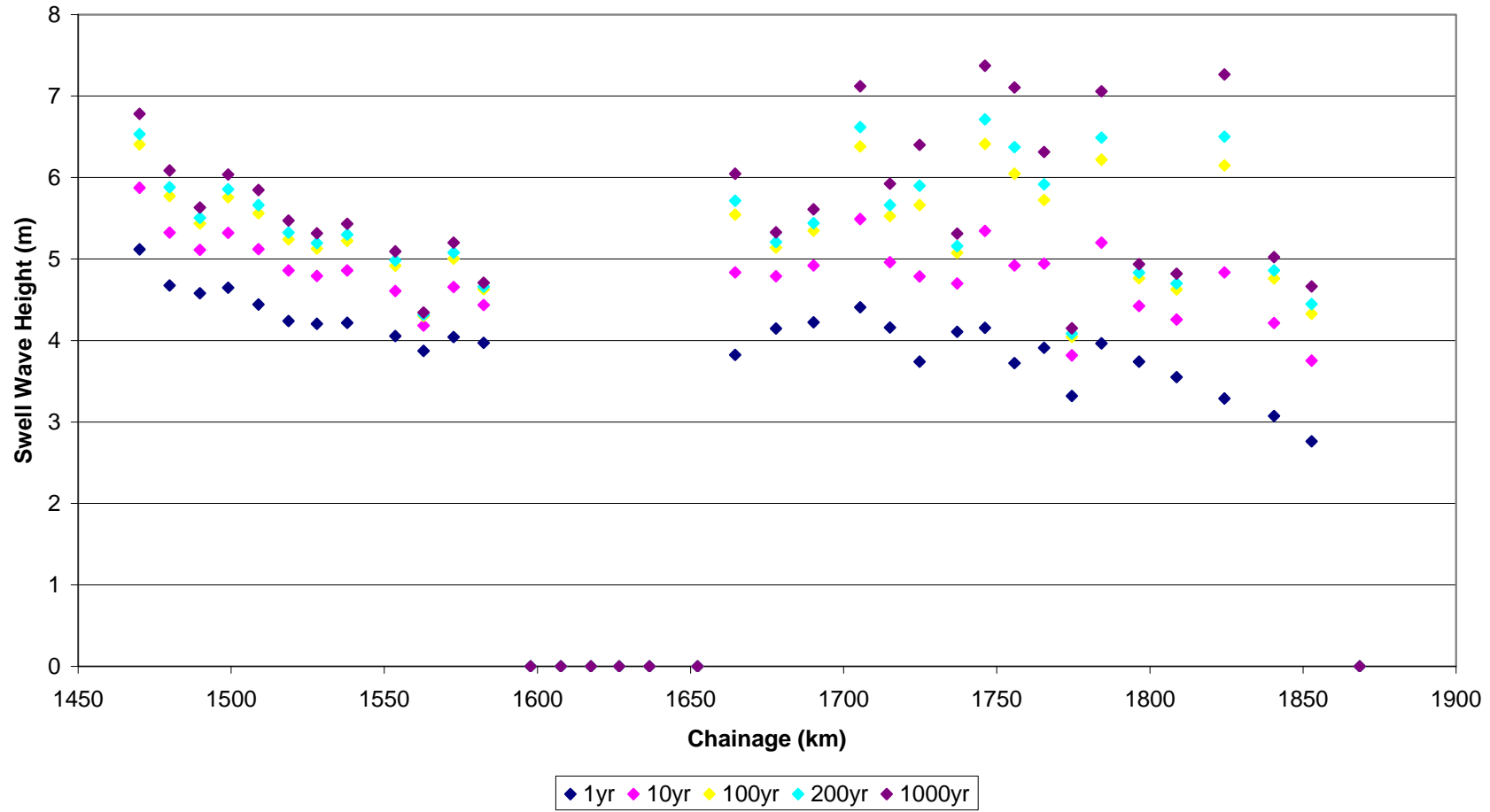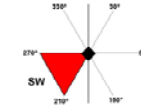
North Chainage Swell Wave Heights from the North West
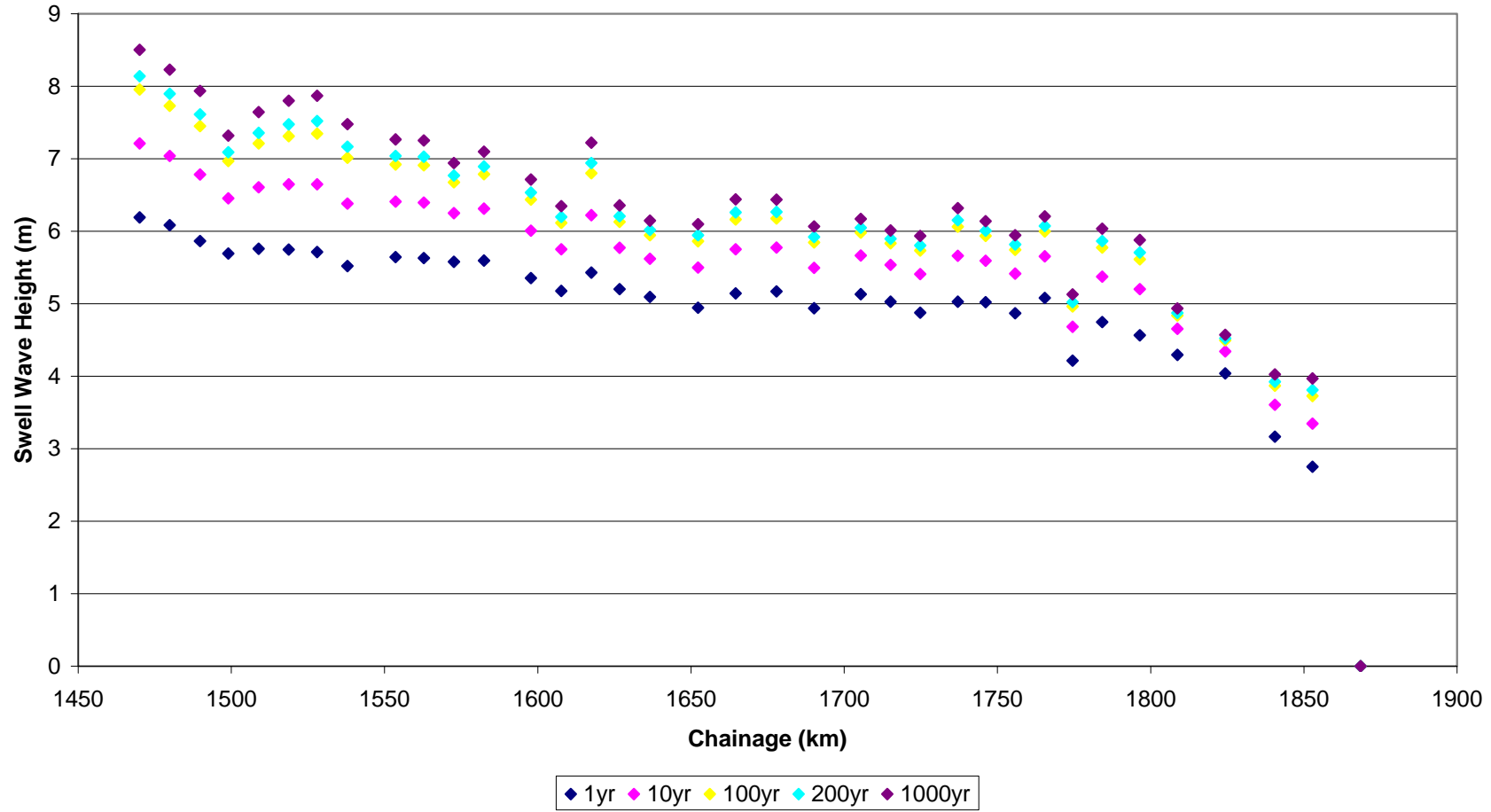
North East Chainage Swell Wave Heights from the North
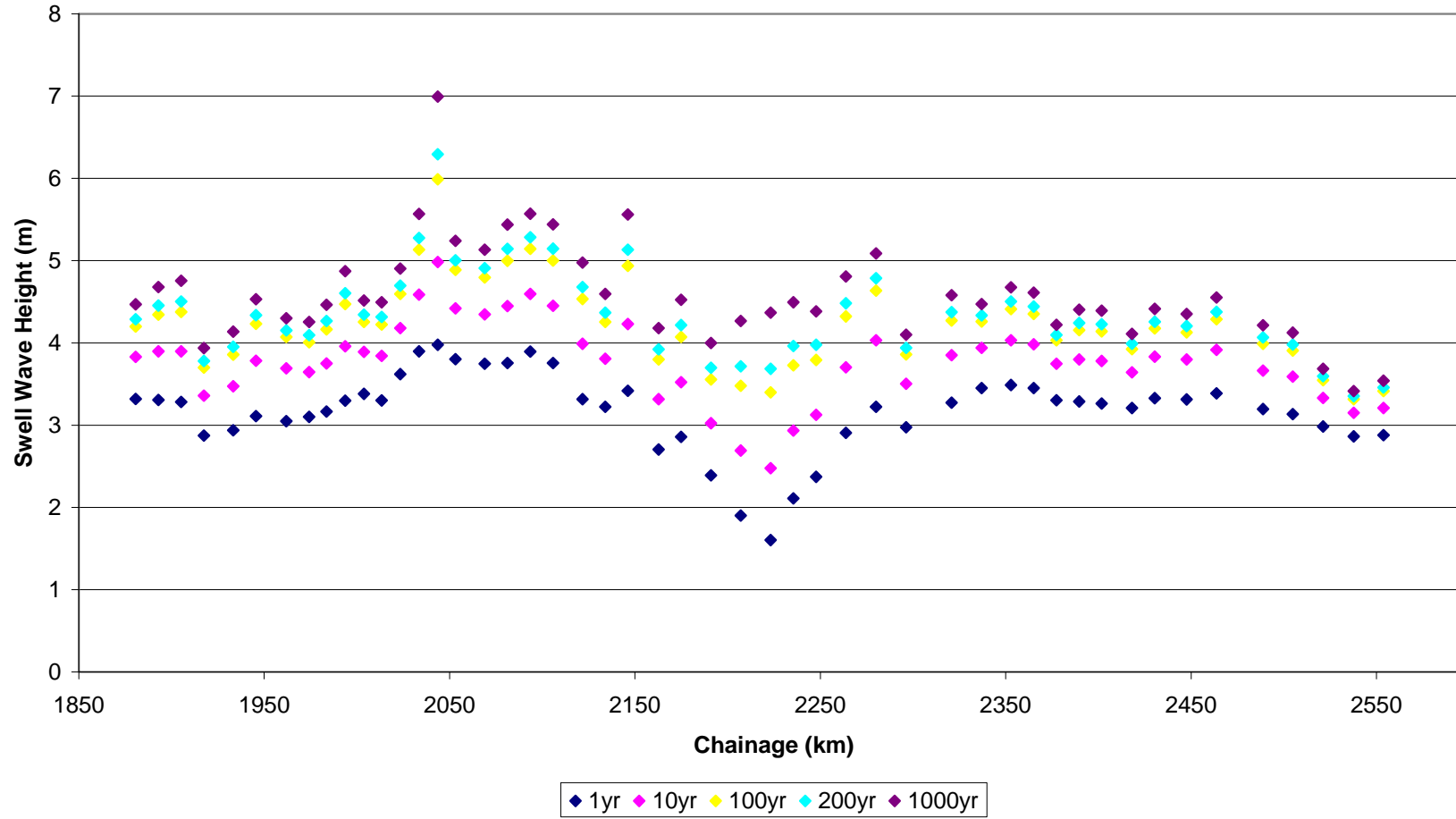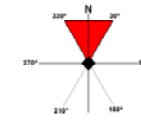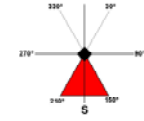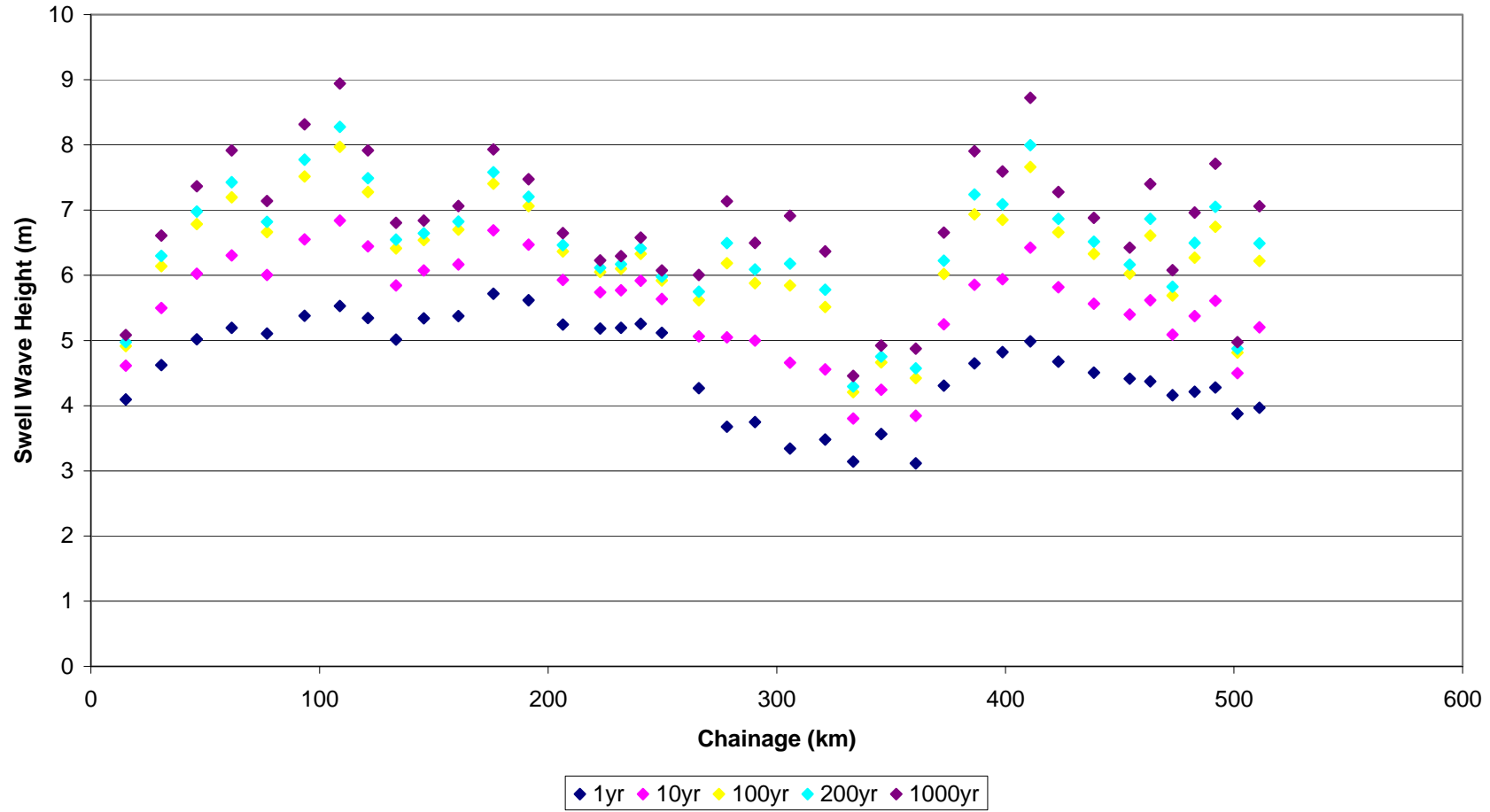
North East Chainage Swell Wave Heights from the North East
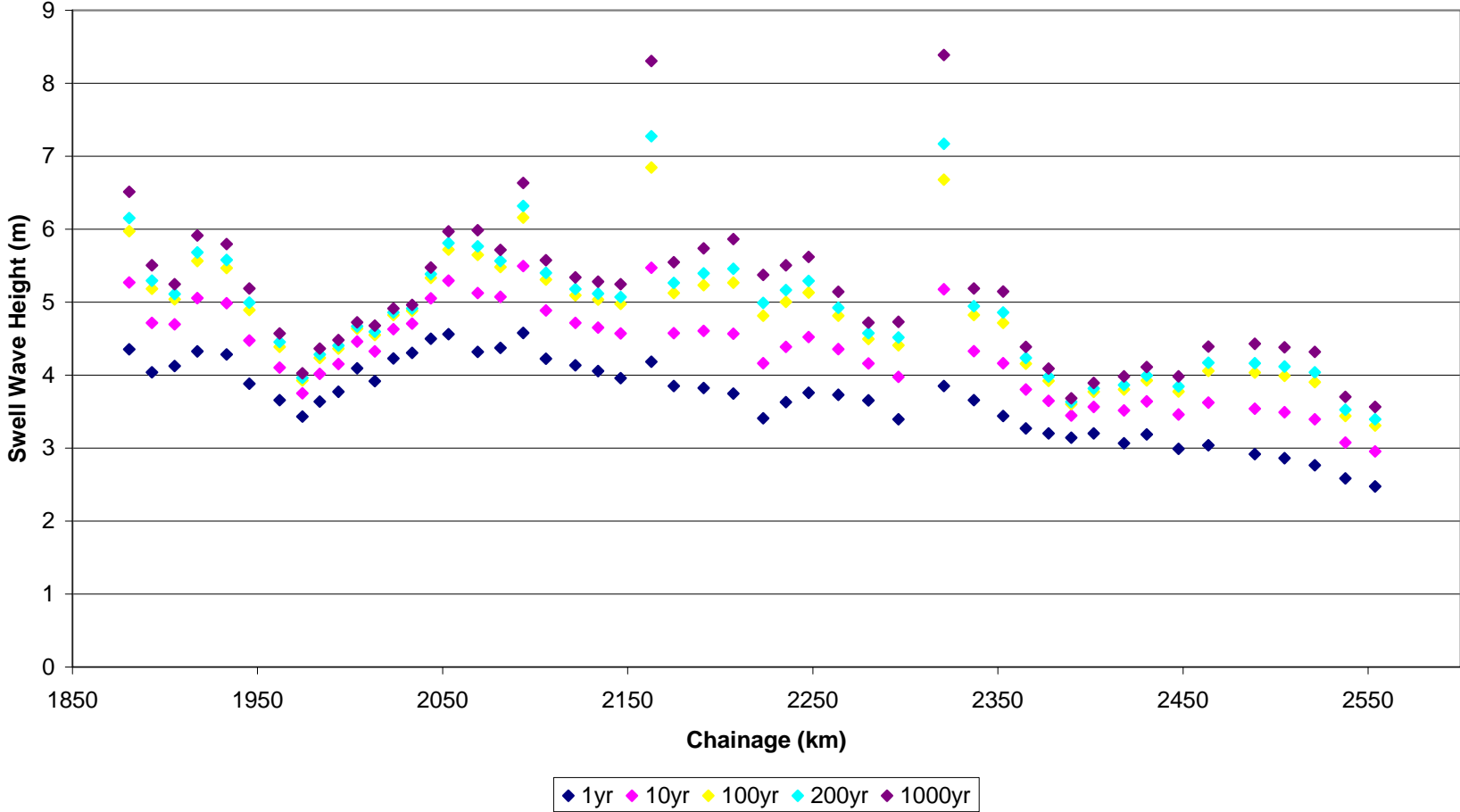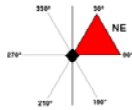
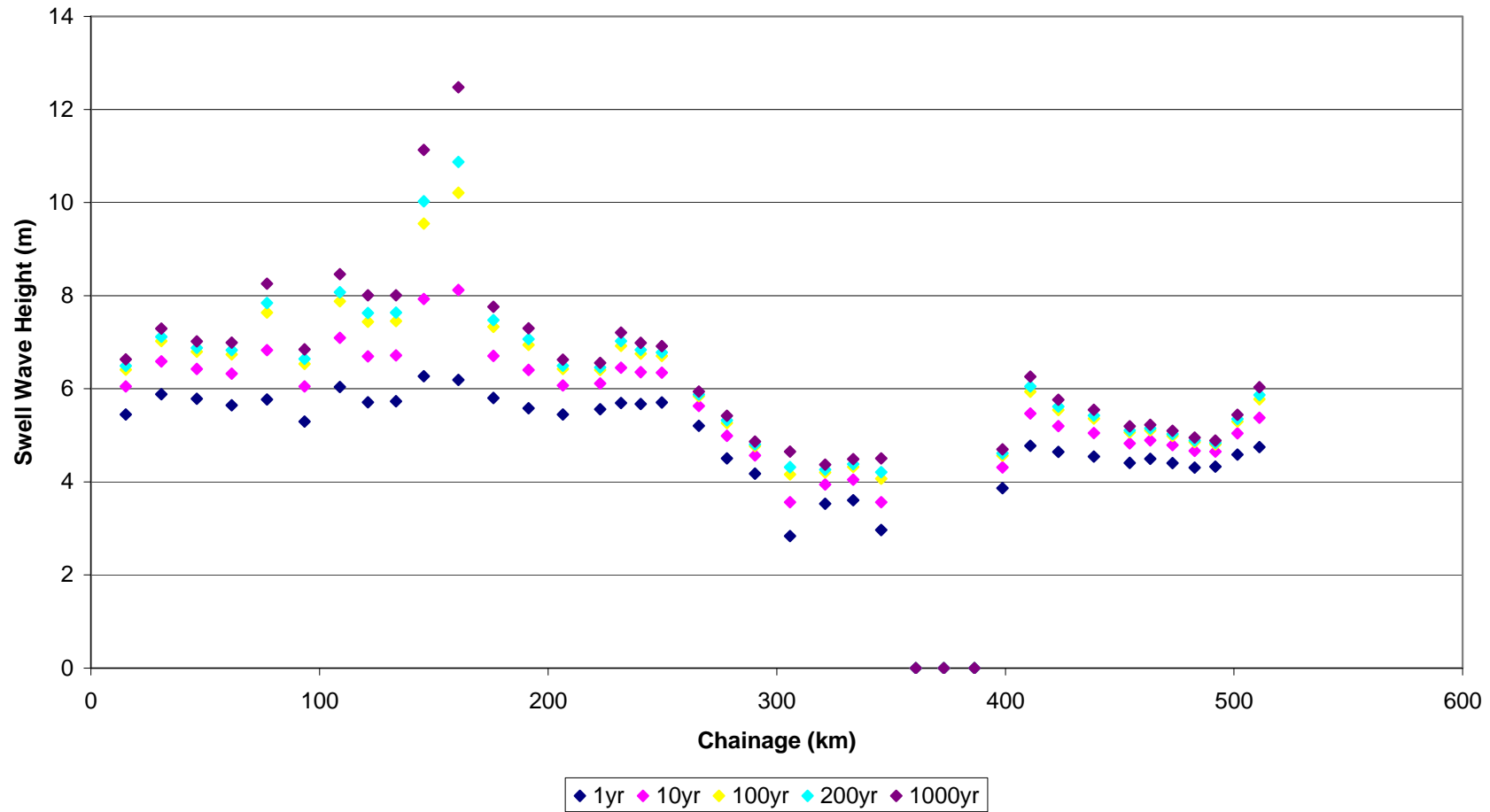# North East Chainage Swell Wave Heights from the South East
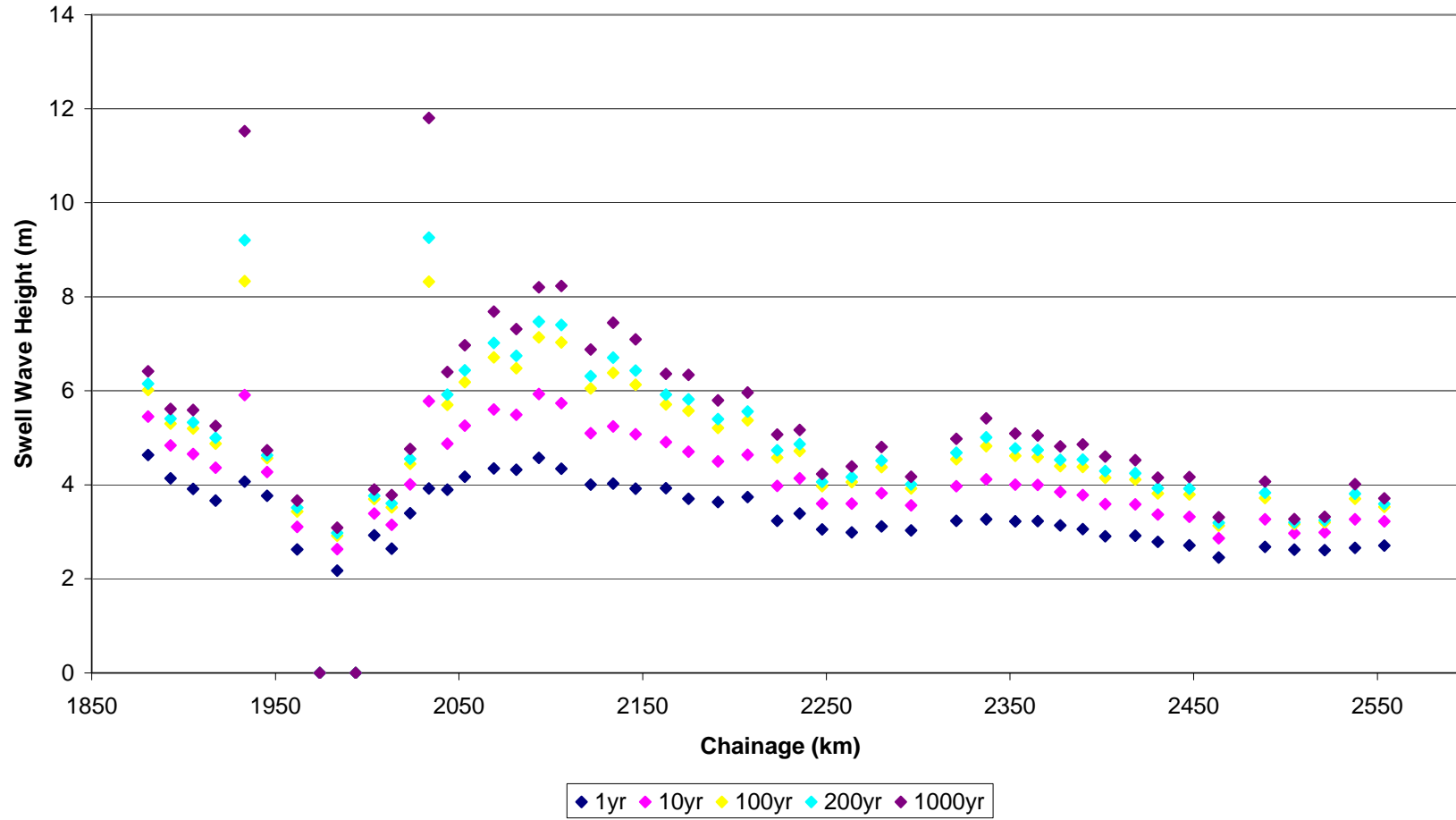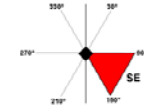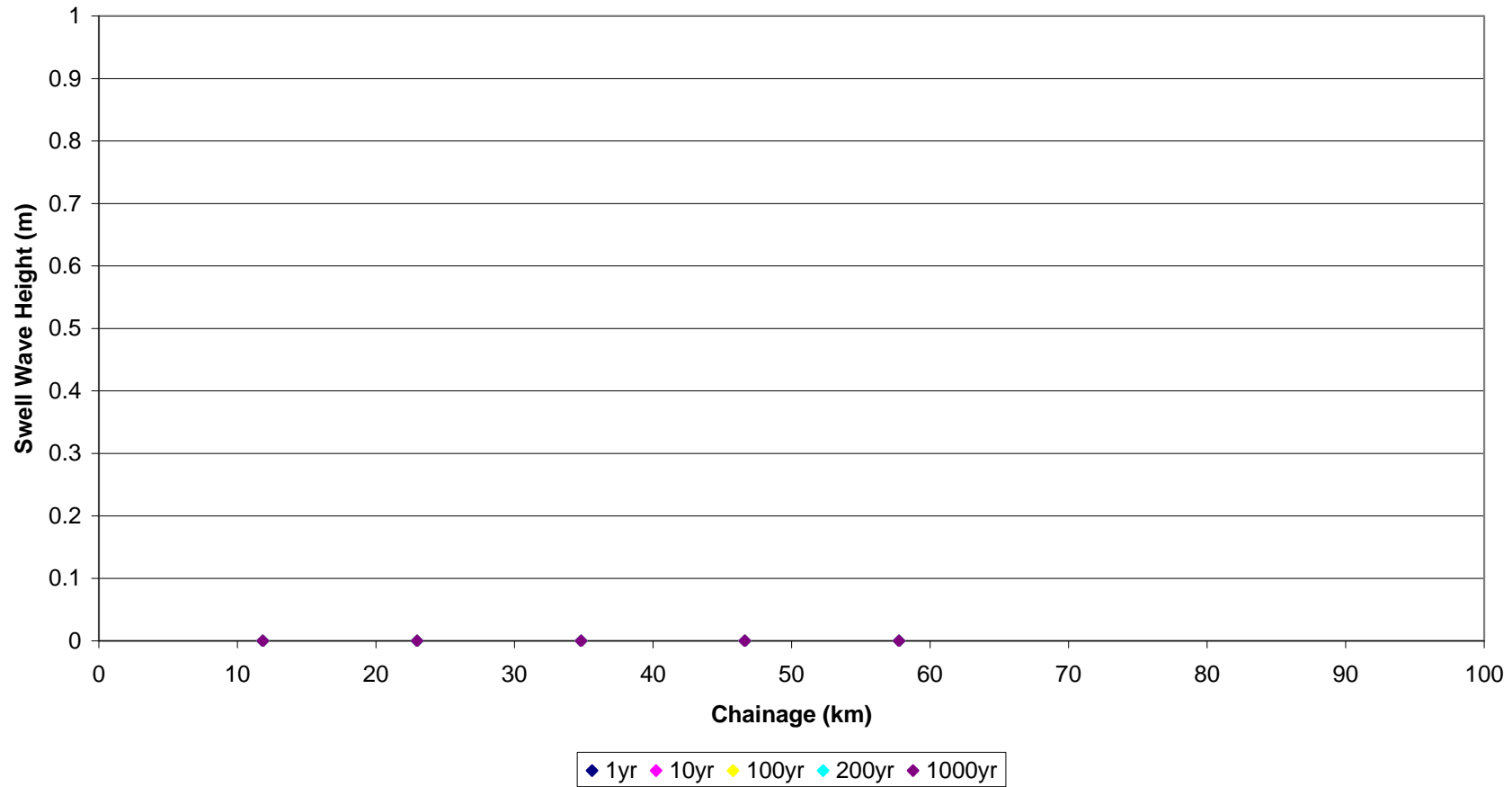
North East Chainage Swell Wave Heights from the South
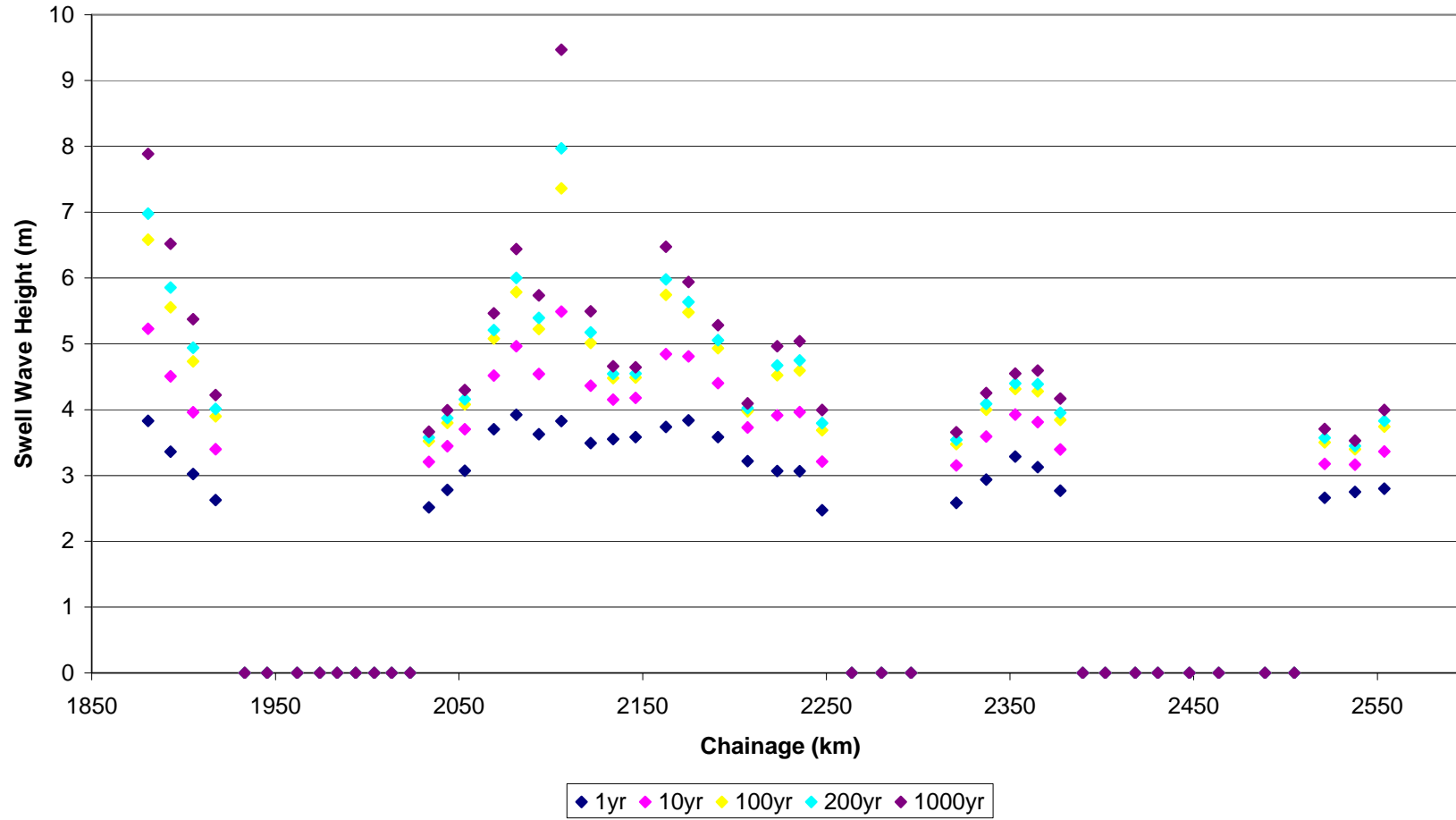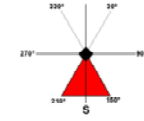
North East Chainage Swell Wave Heights from the South West
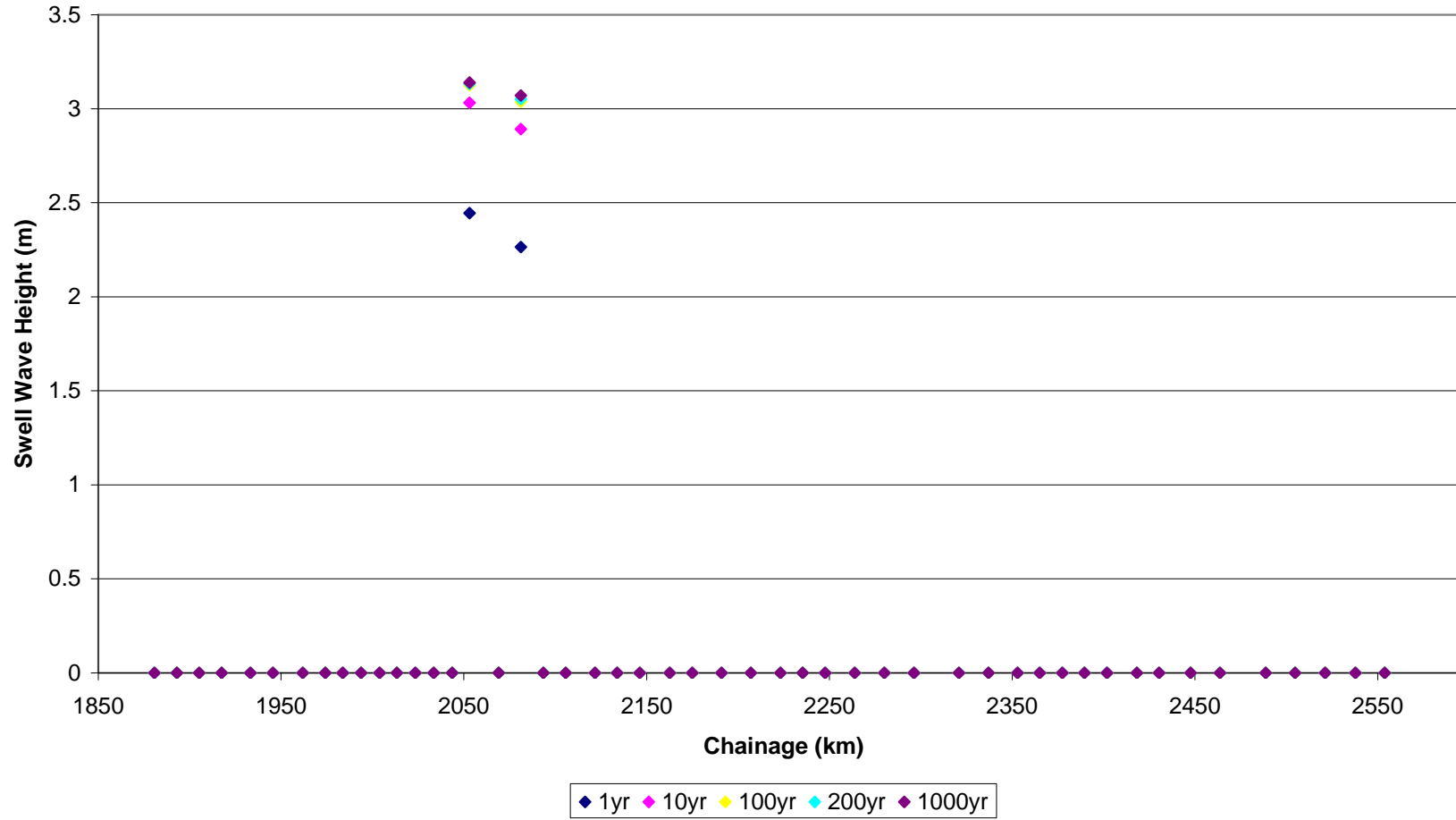
North East Chainage Swell Wave Heights from the North West

Legend: 1yr, 10yr, 100yr, 200yr, 1000yr

Y-axis: Swell Wave Height (m)

X-axis: Chainage (km)
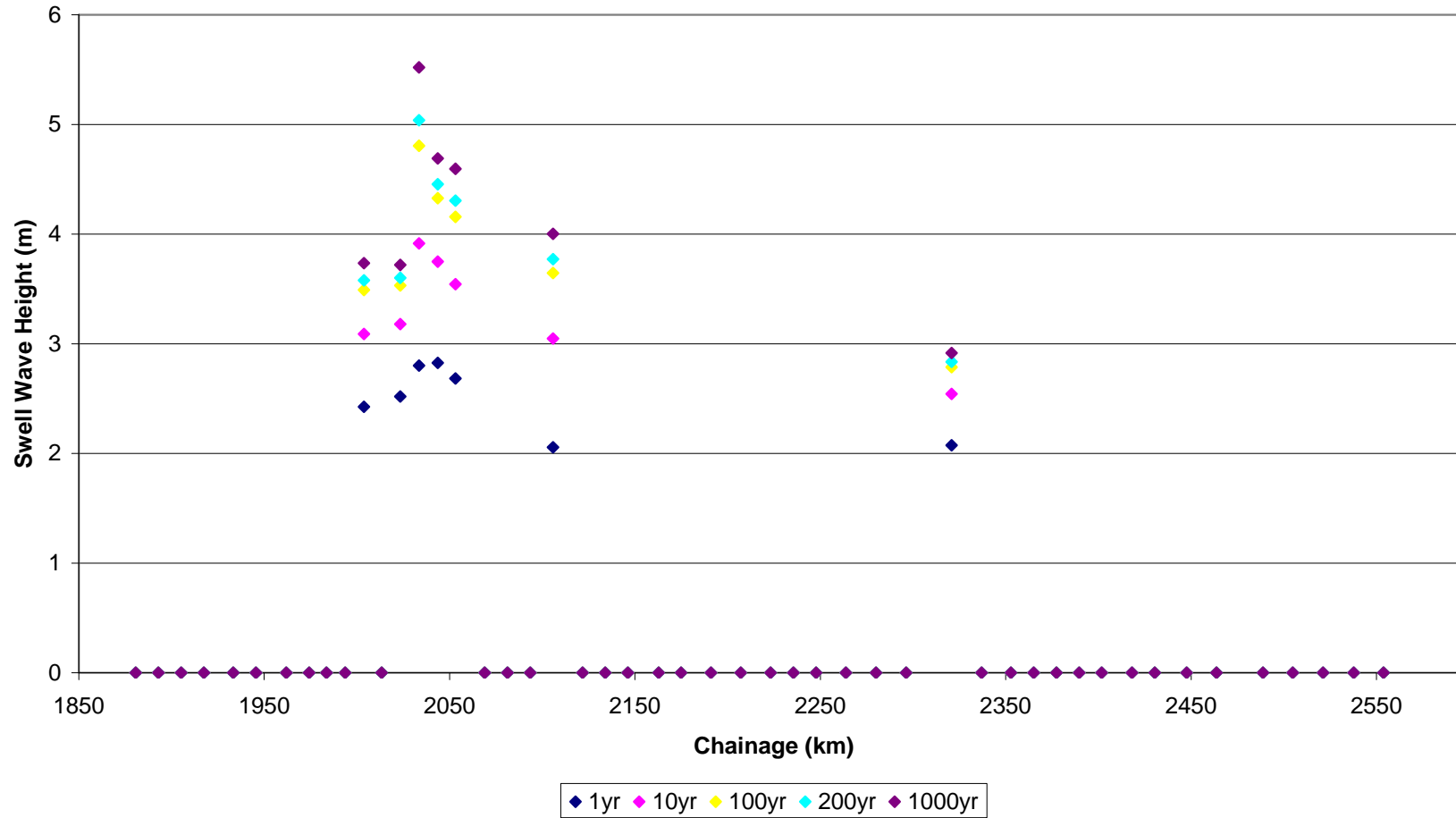
North West Chainage Swell Wave Heights from the North
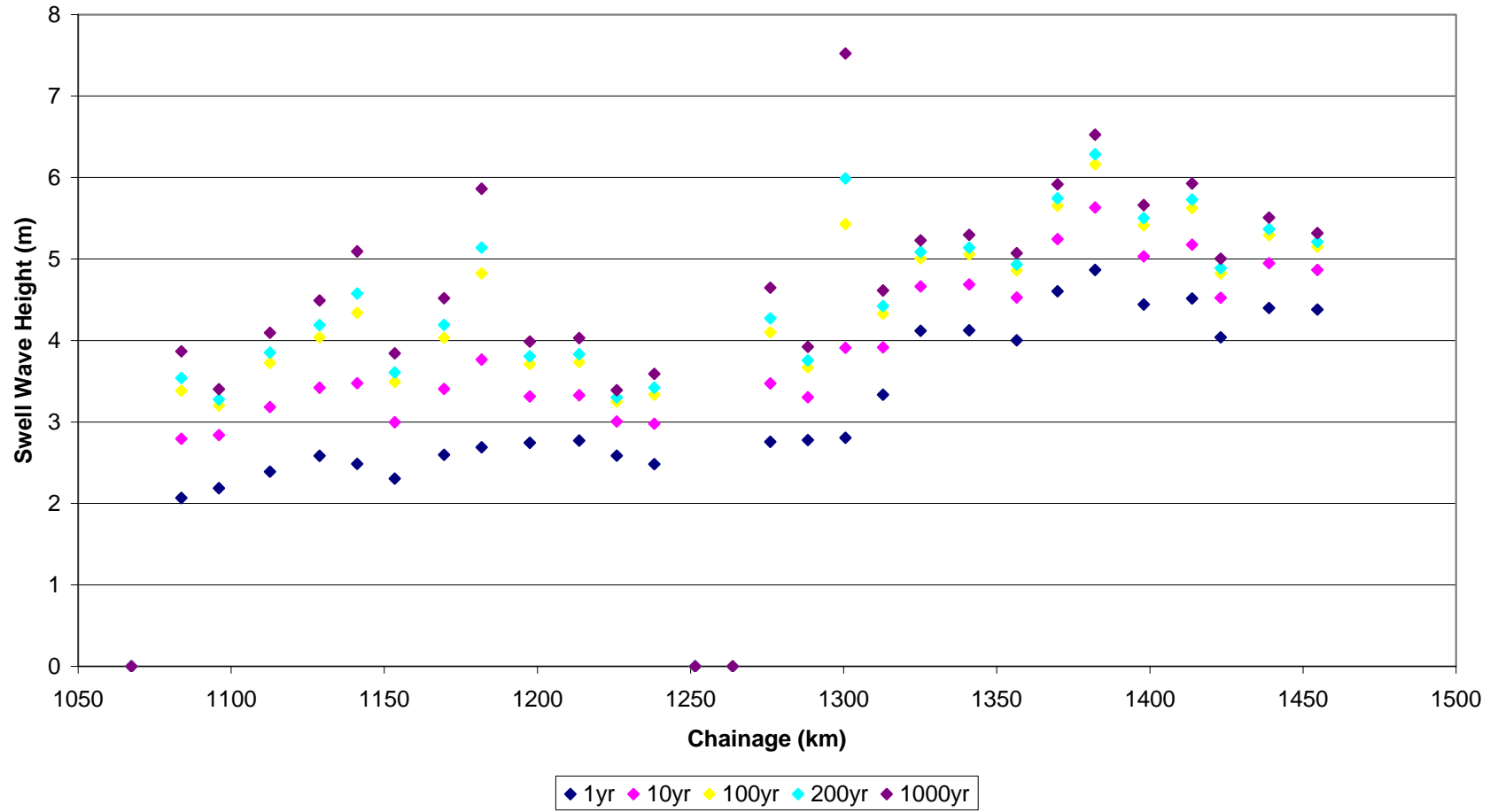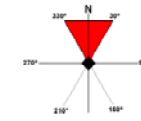
North West Chainage Swell Wave Heights from the North East
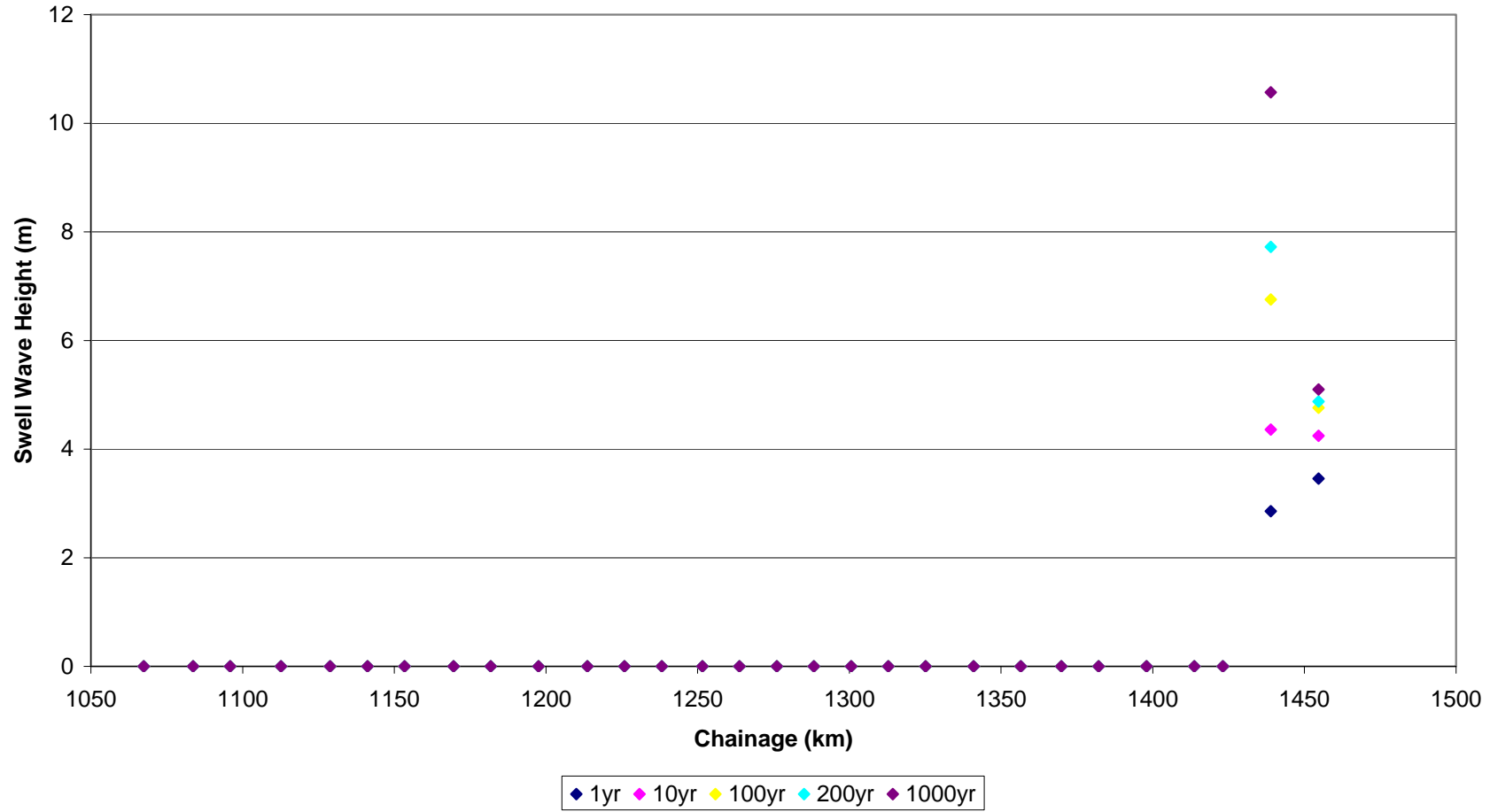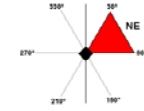
North West Chainage Swell Wave Heights from the South East
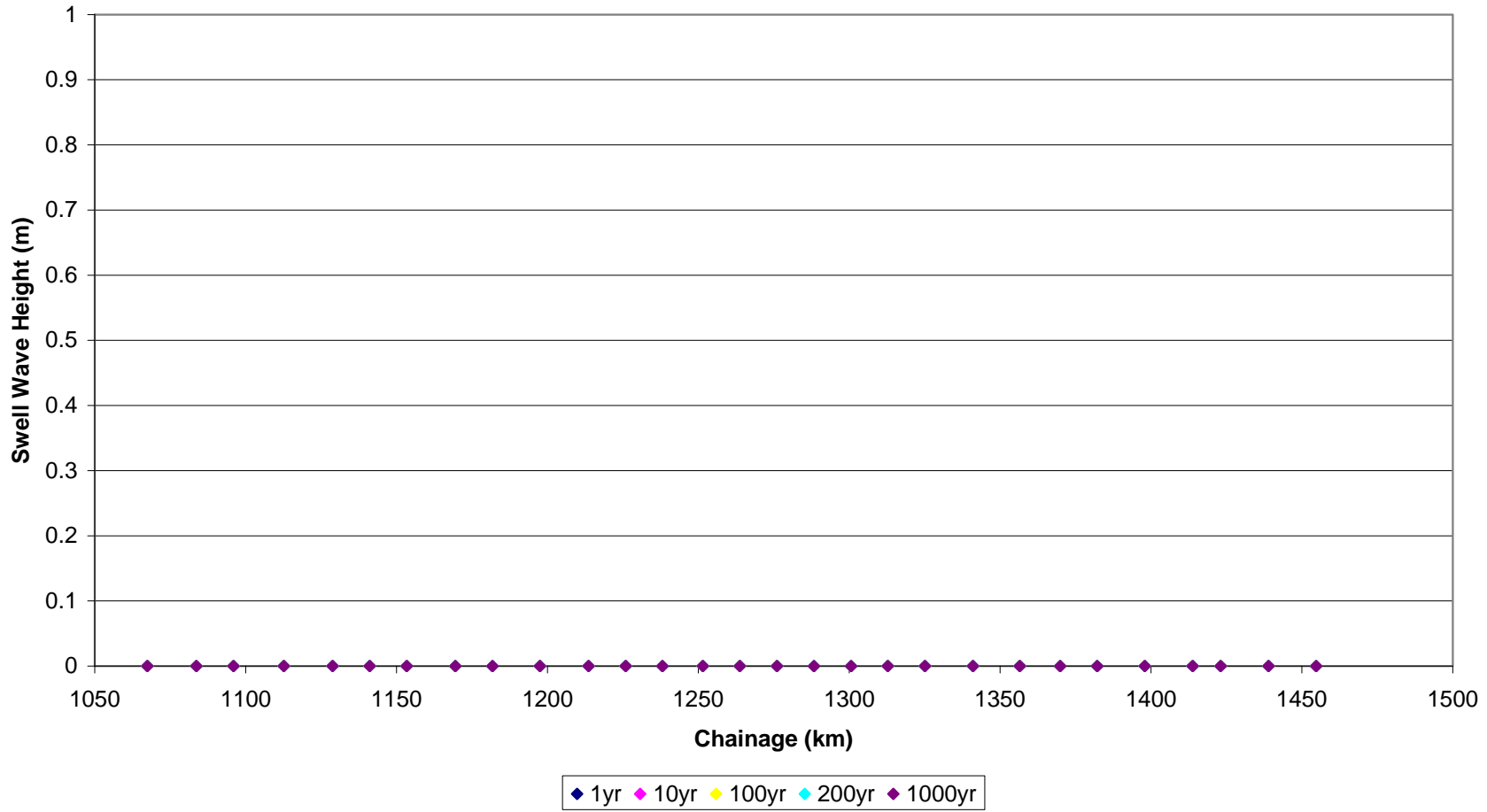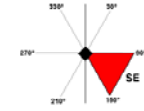
North West Chainage Swell Wave Heights from the South
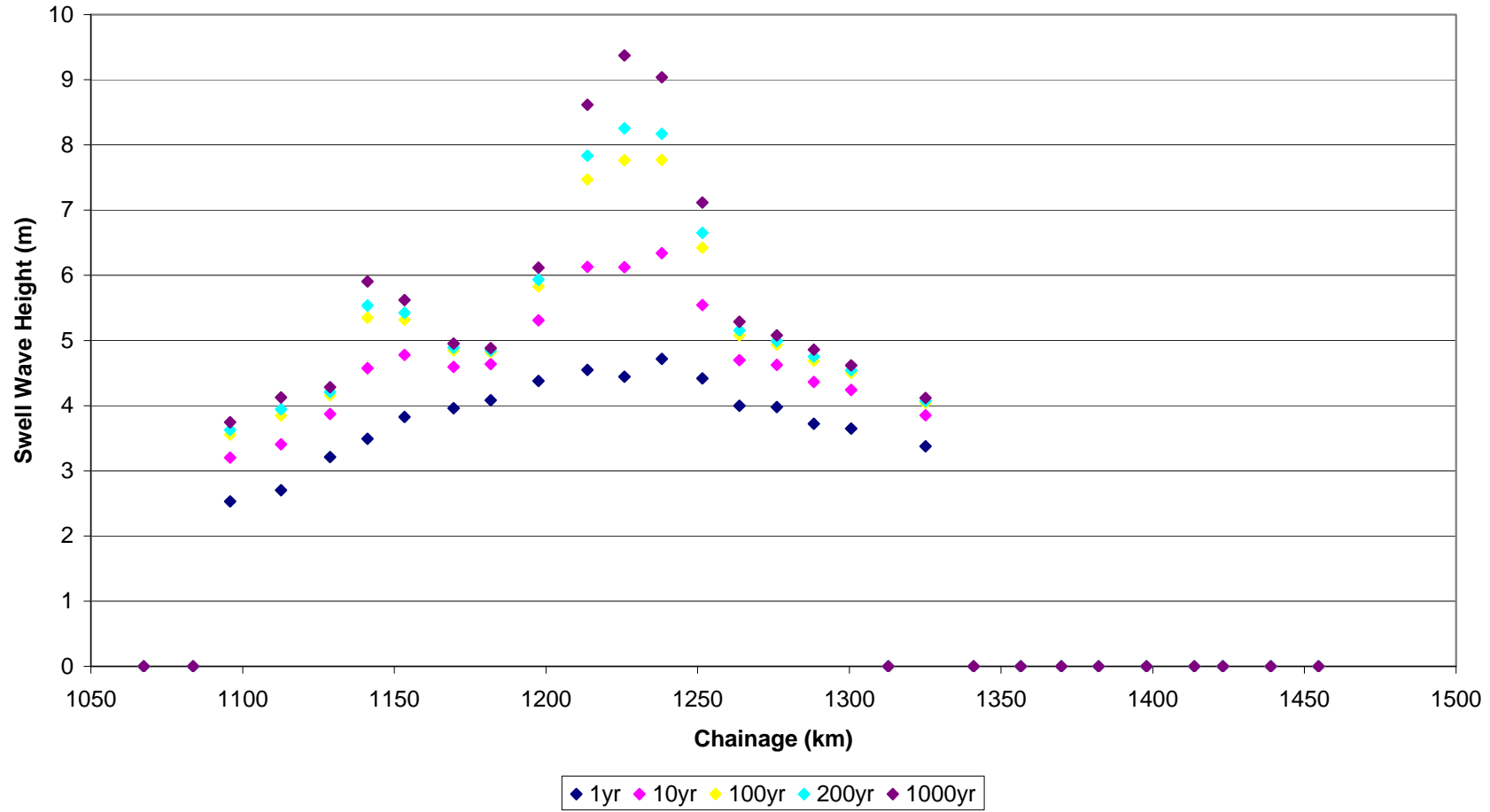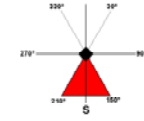
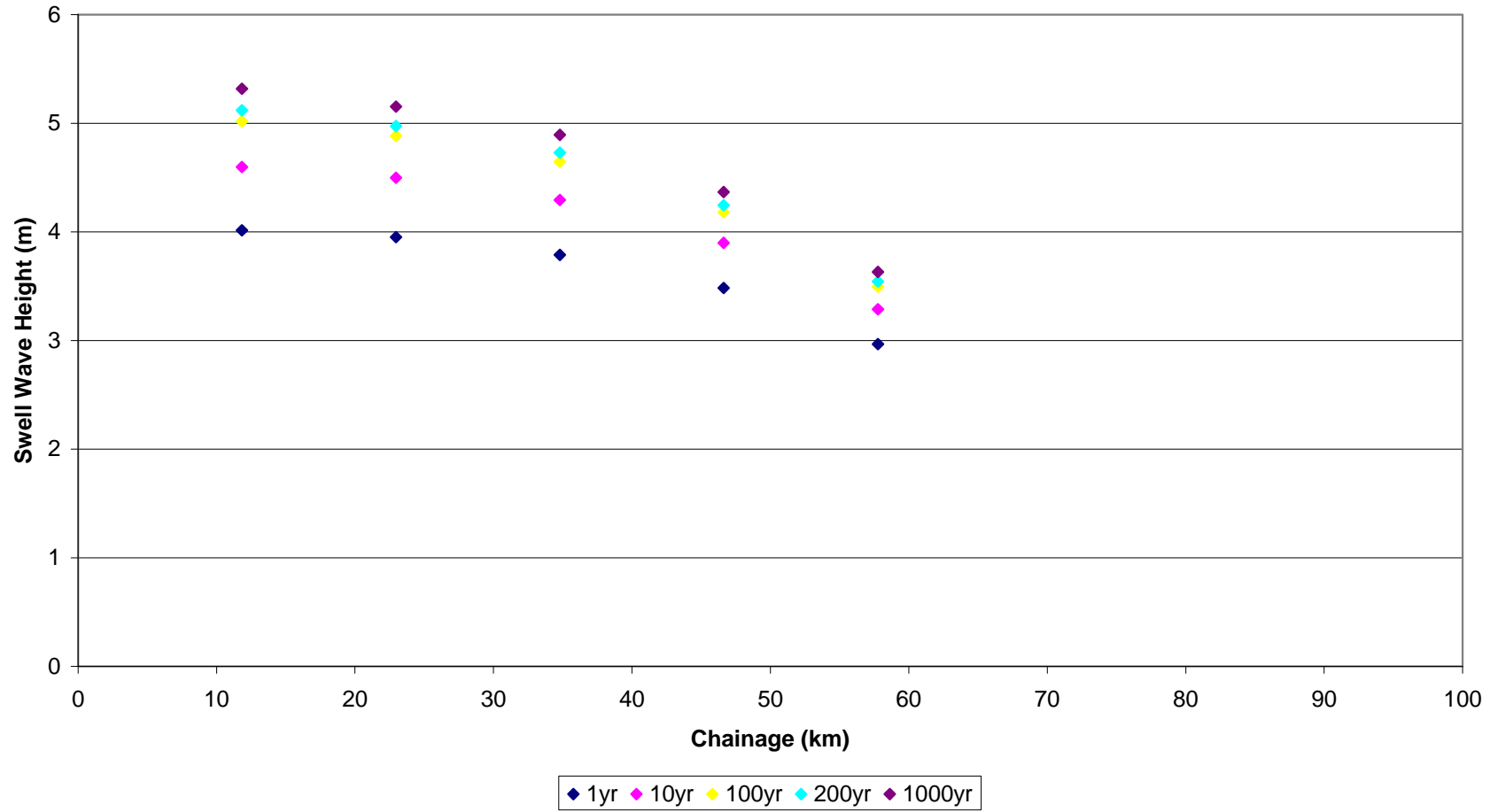North West Chainage Swell Wave Heights from the South West
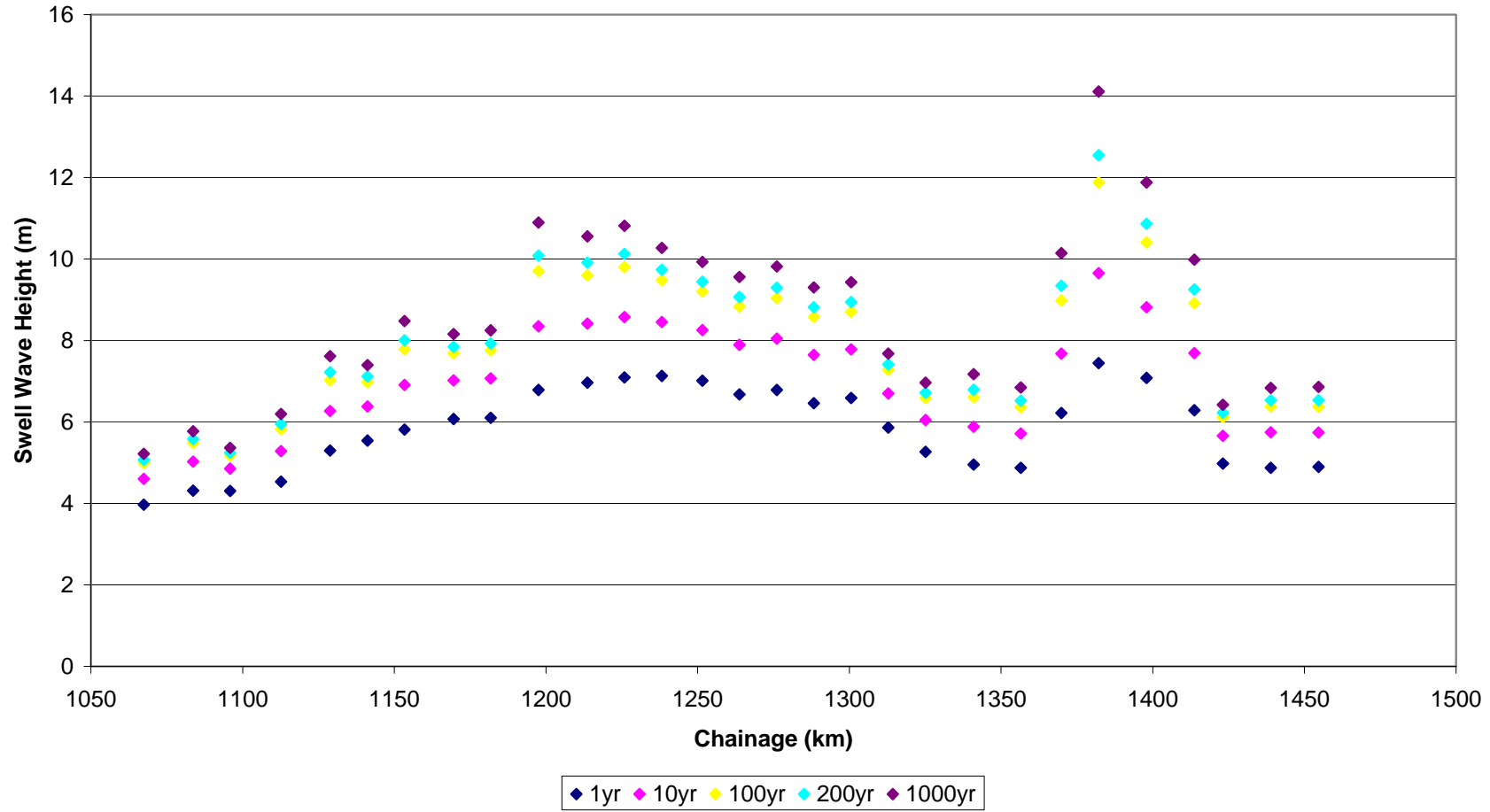
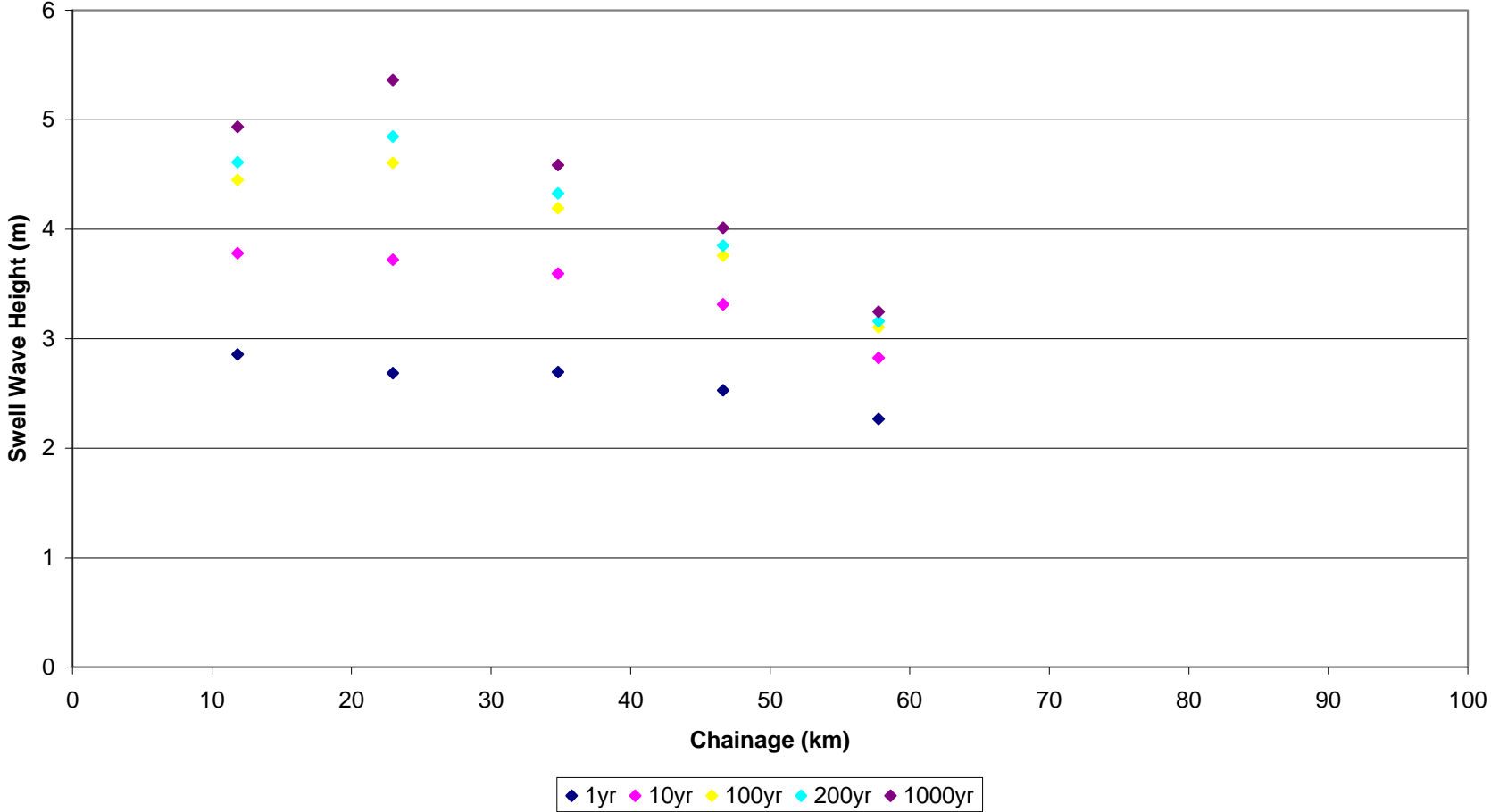# North West Chainage Swell Wave Heights from the North West
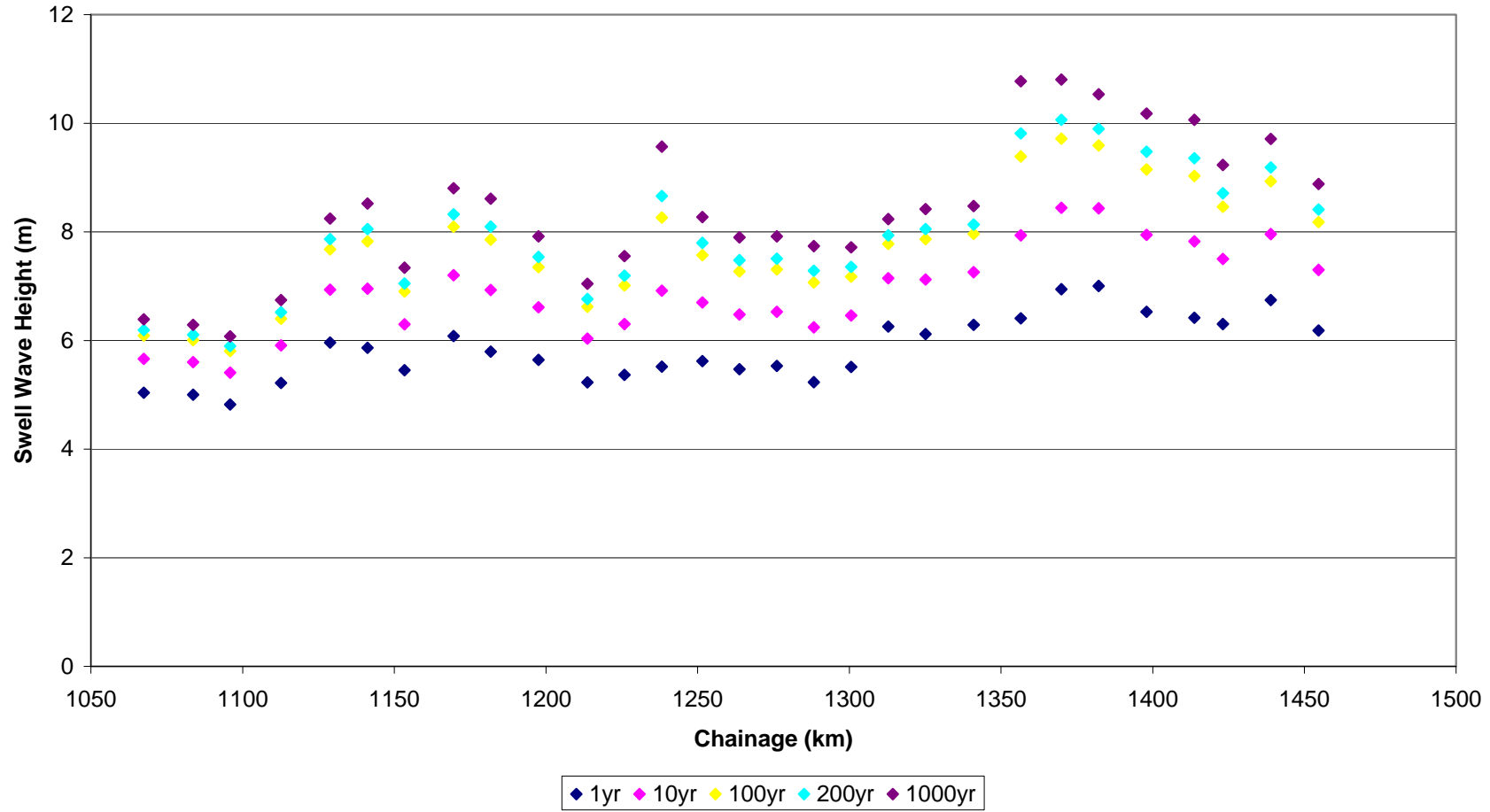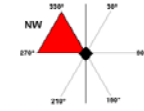
South Chainage Swell Wave Heights from the North

Swell Wave Height (m)

Chainage (km)

◆ 1yr ◆ 10yr ◆ 100yr ◆ 200yr ◆ 1000yr

South Chainage Swell Wave Heights from the North East

Swell Wave Height (m)

Chainage (km)

♦ 1yr ♦ 10yr ♦ 100yr ♦ 200yr ♦ 1000yr
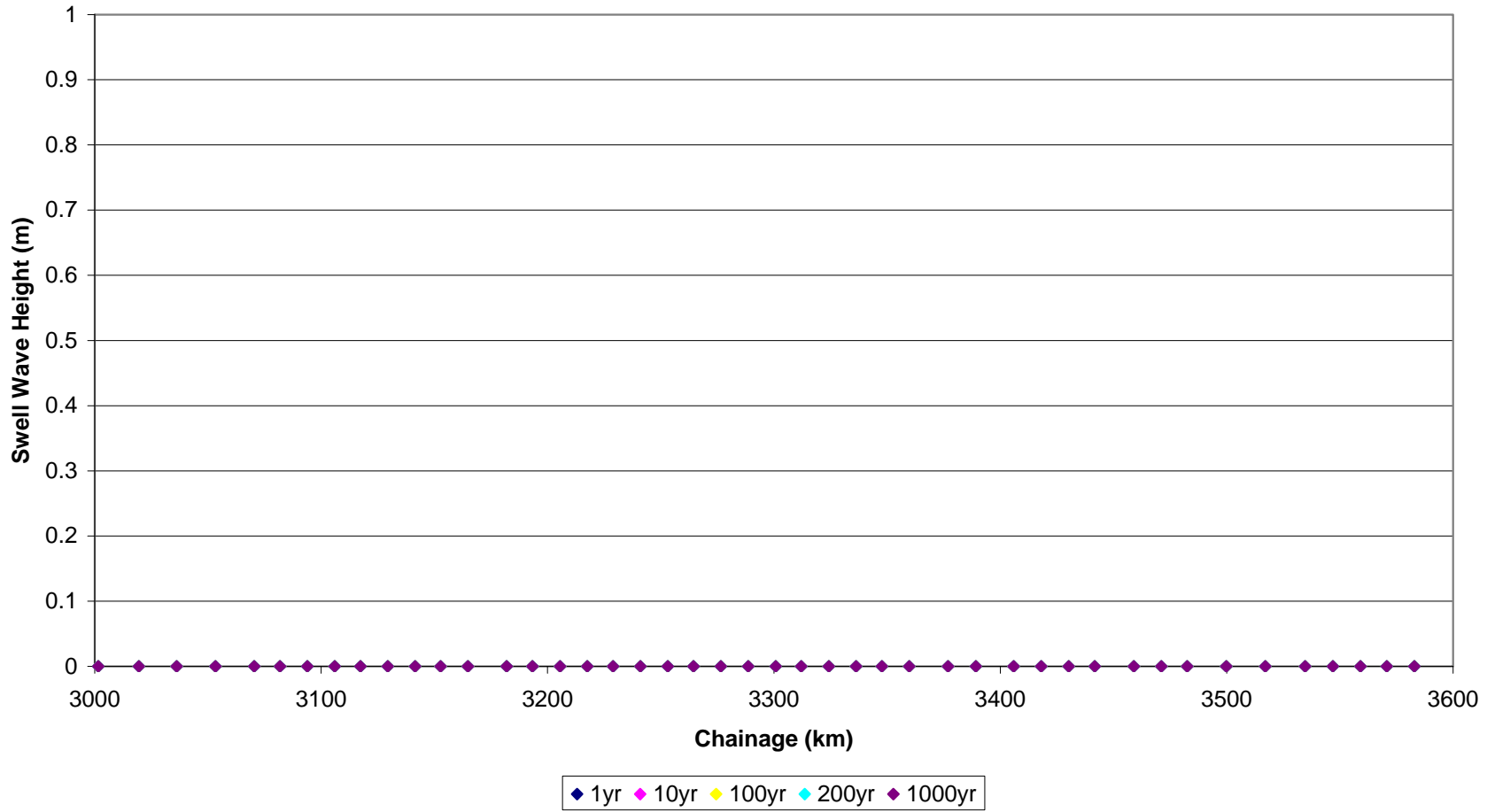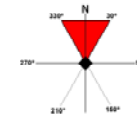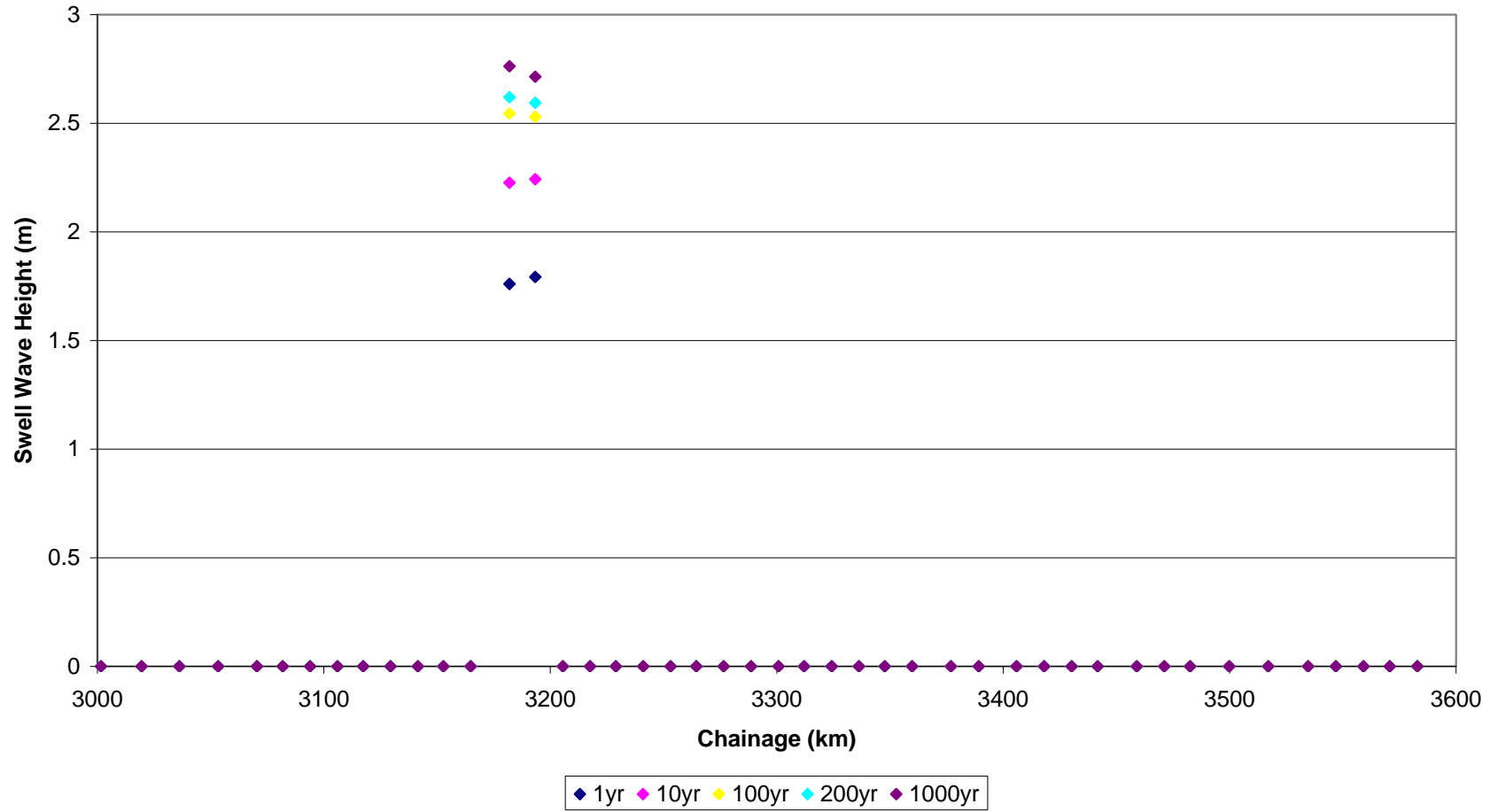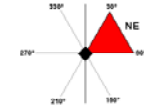
South Chainage Swell Wave Heights from the South East

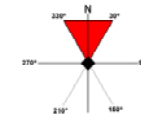South Chainage Swell Wave Heights from the South

Legend: 1yr, 10yr, 100yr, 200yr, 1000yr
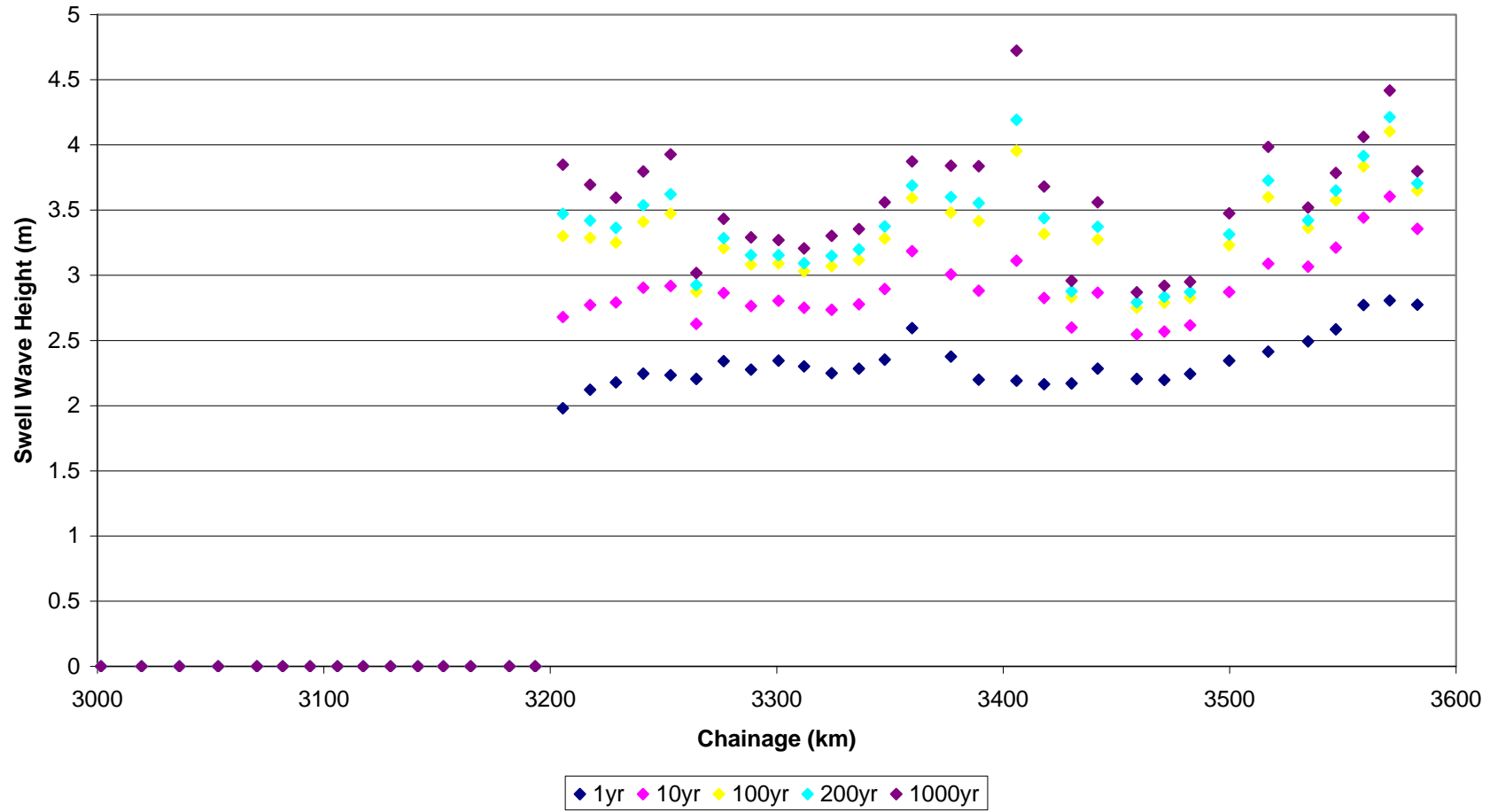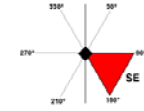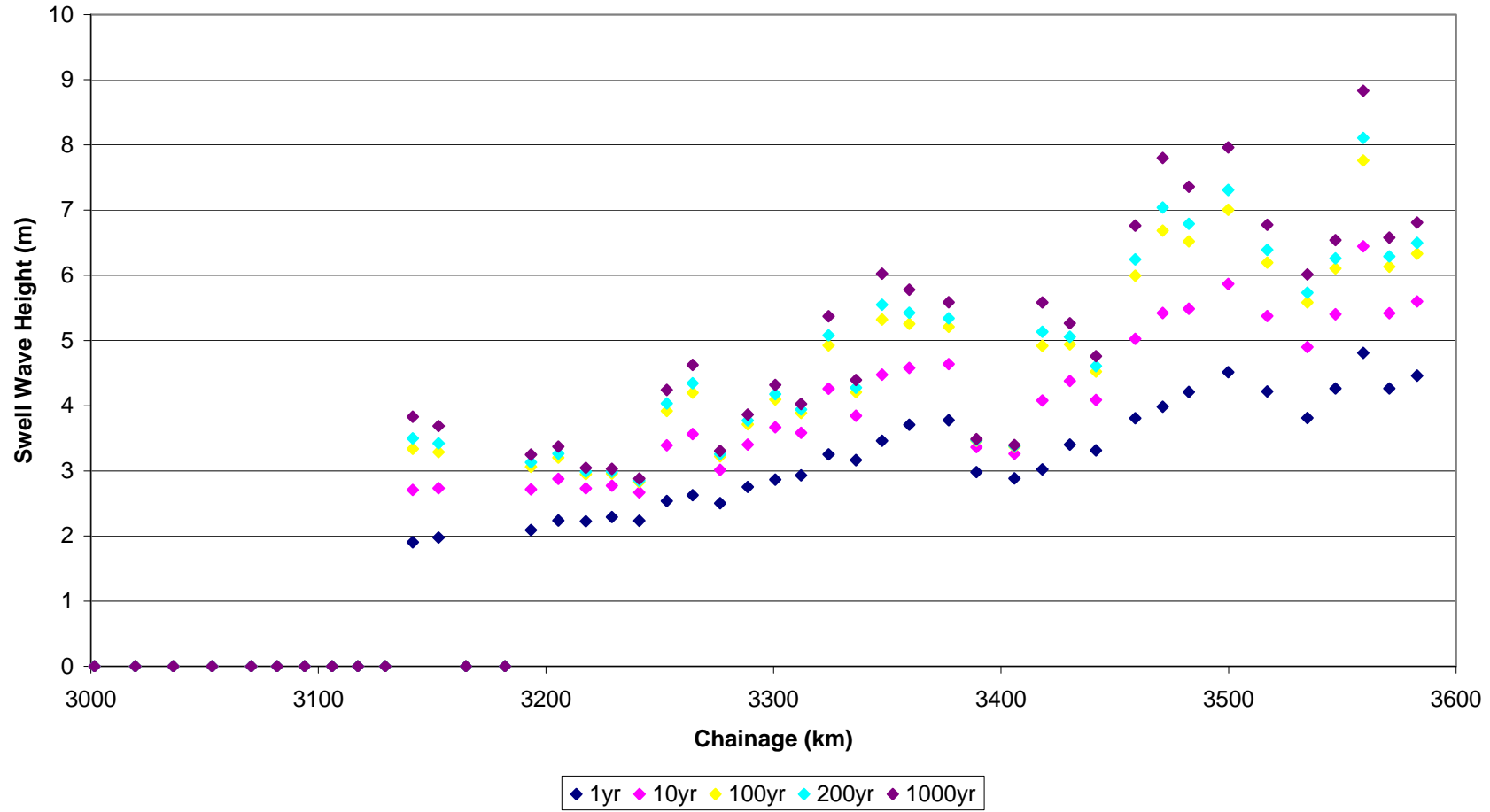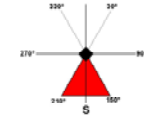
South Chainage Swell Wave Heights from the South West
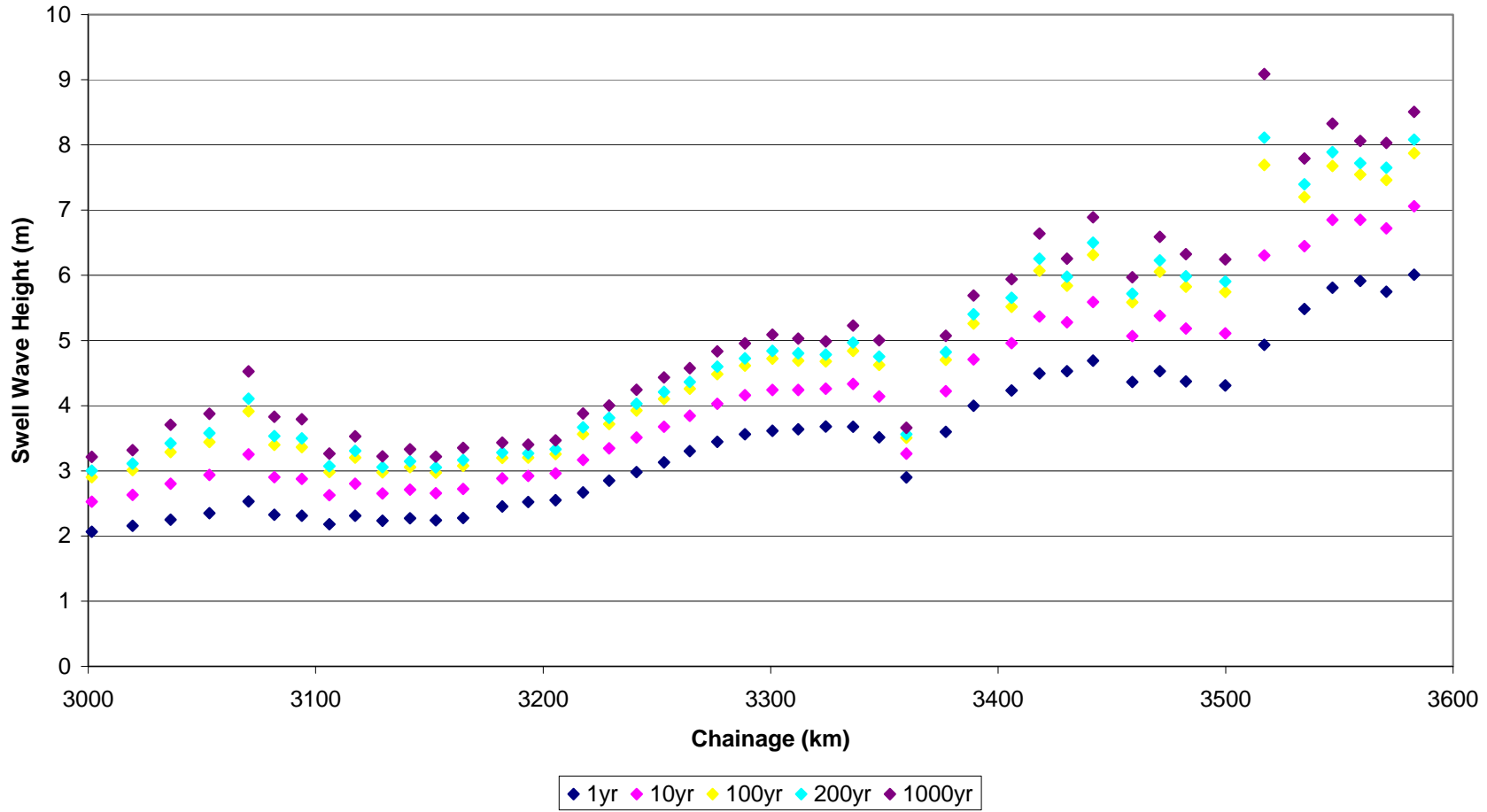
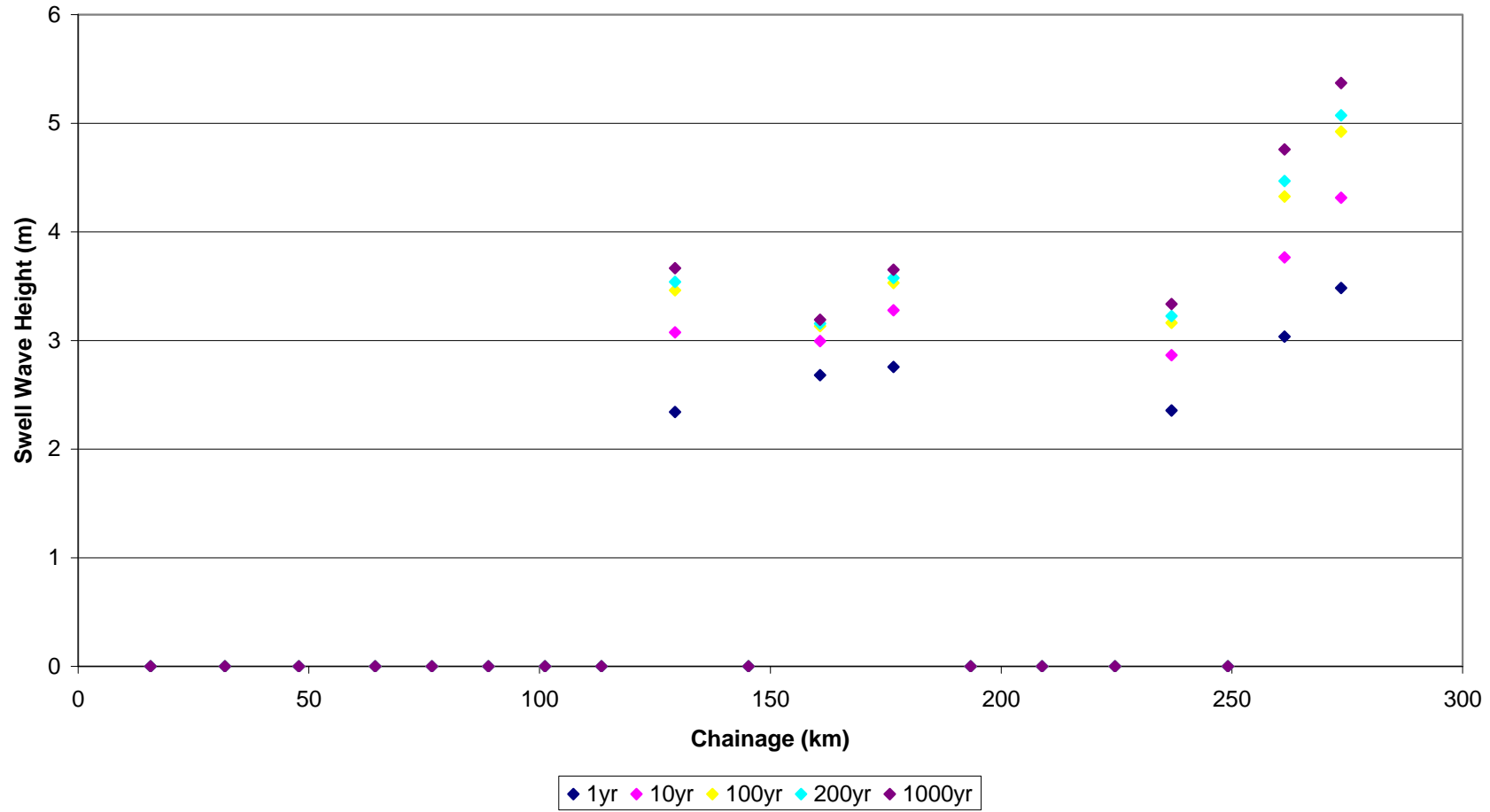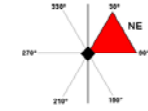# South Chainage Swell Wave Heights from the North West
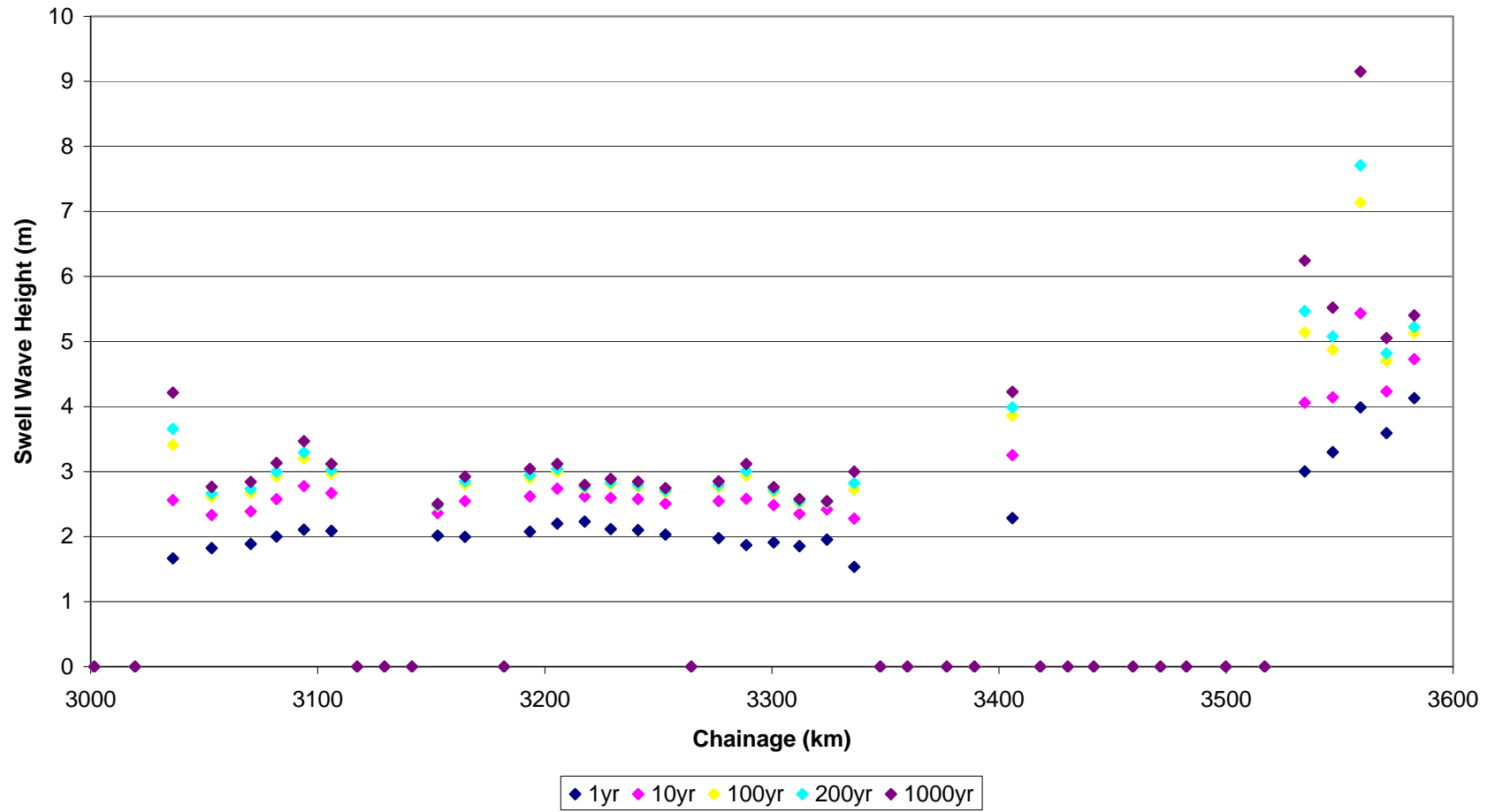
South East Chainage Swell Wave Heights from the North
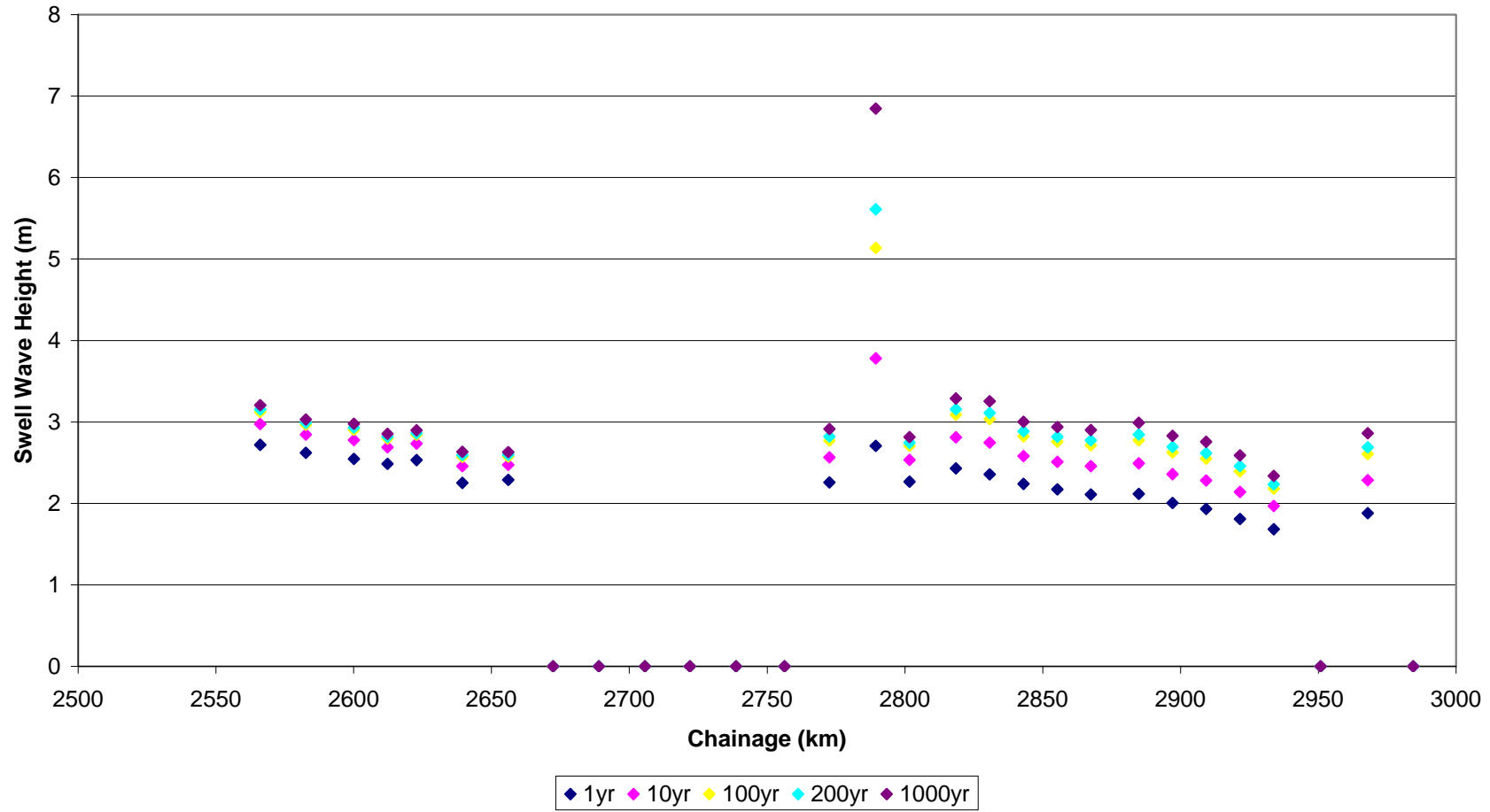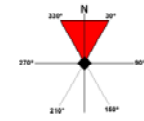
South East Chainage Swell Wave Heights from the North East
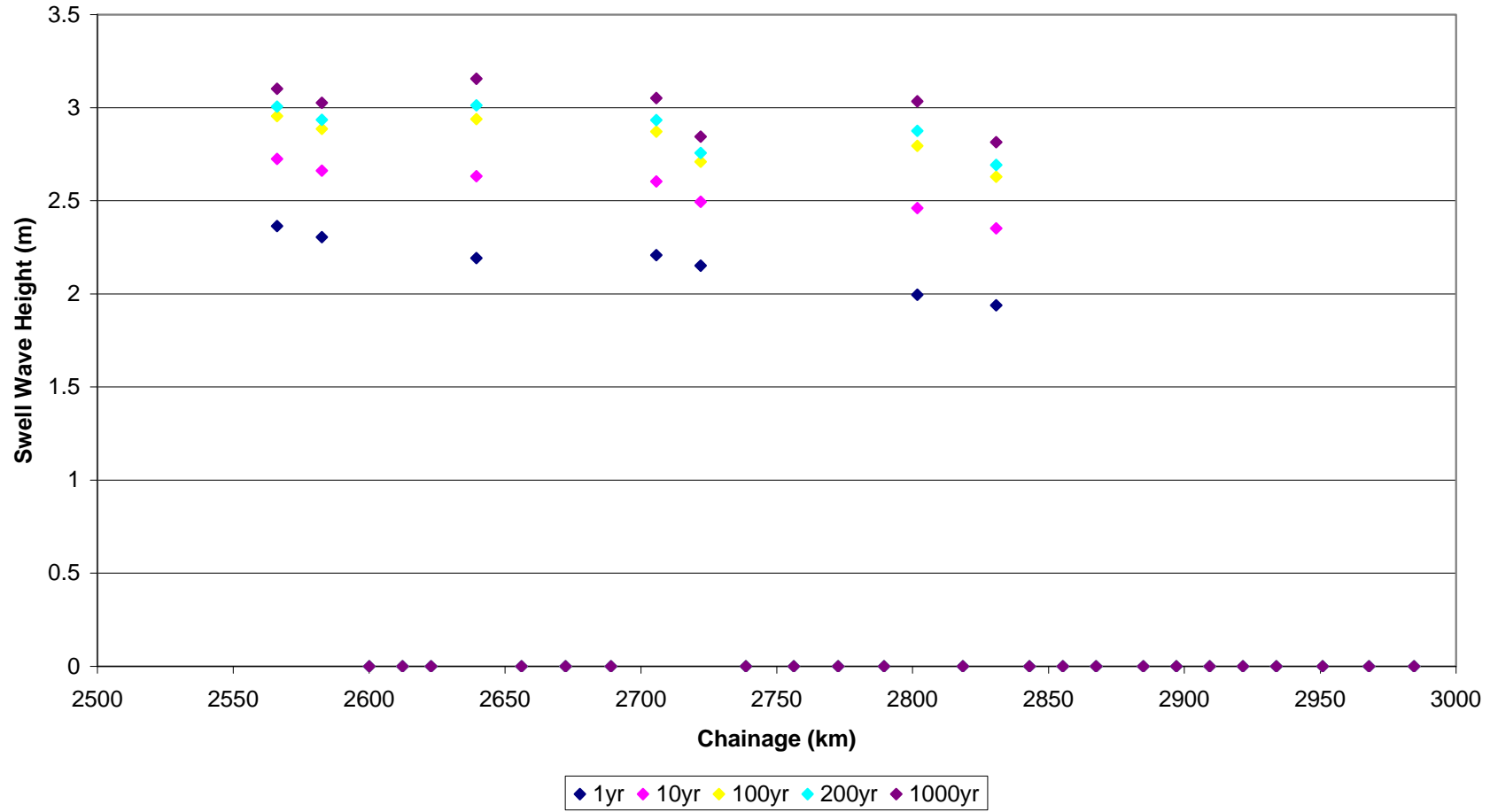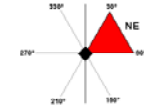
South East Chainage Swell Wave Heights from the South East
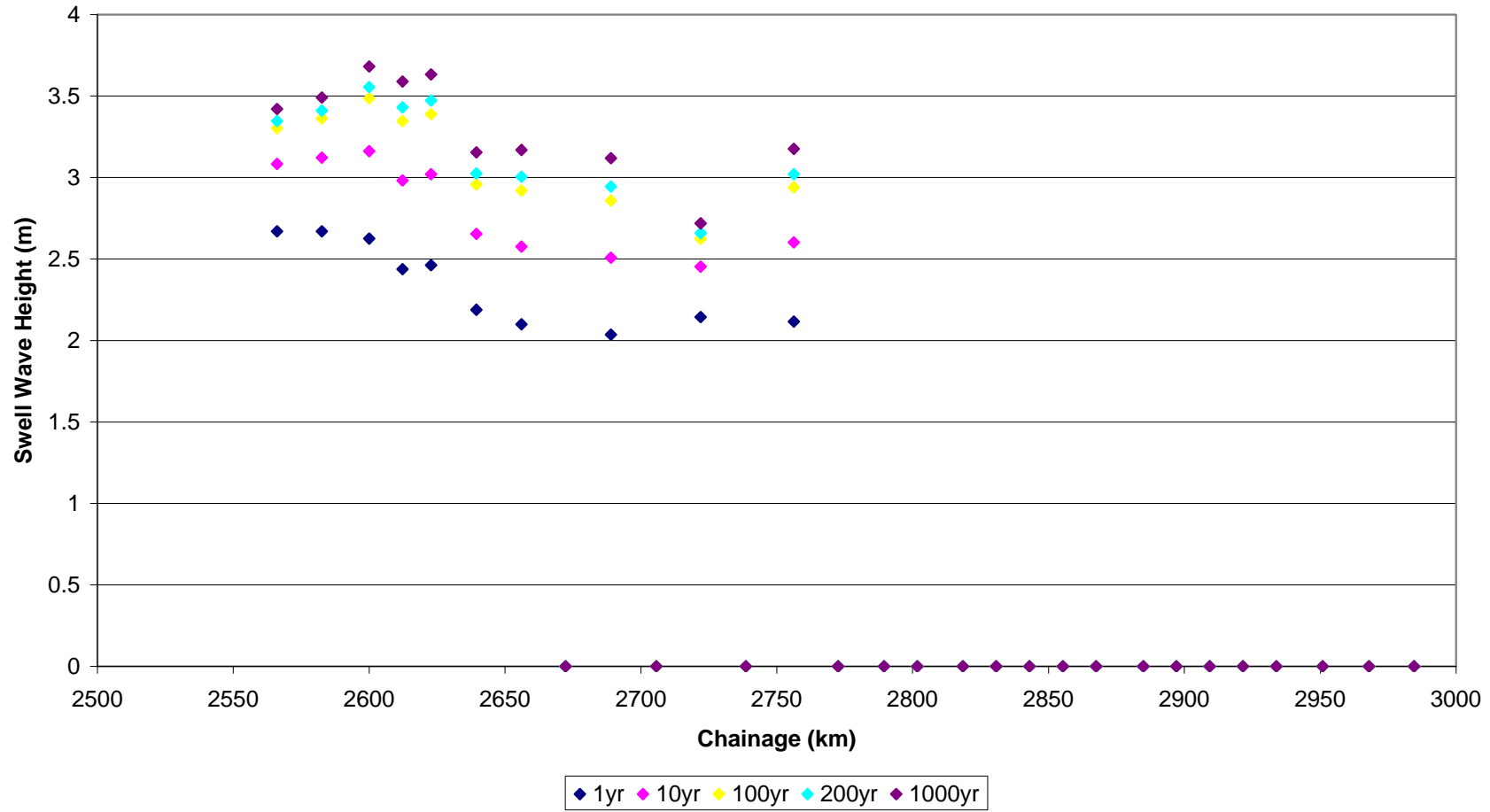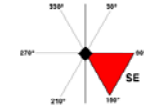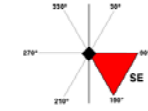
South East Chainage Swell Wave Heights from the South
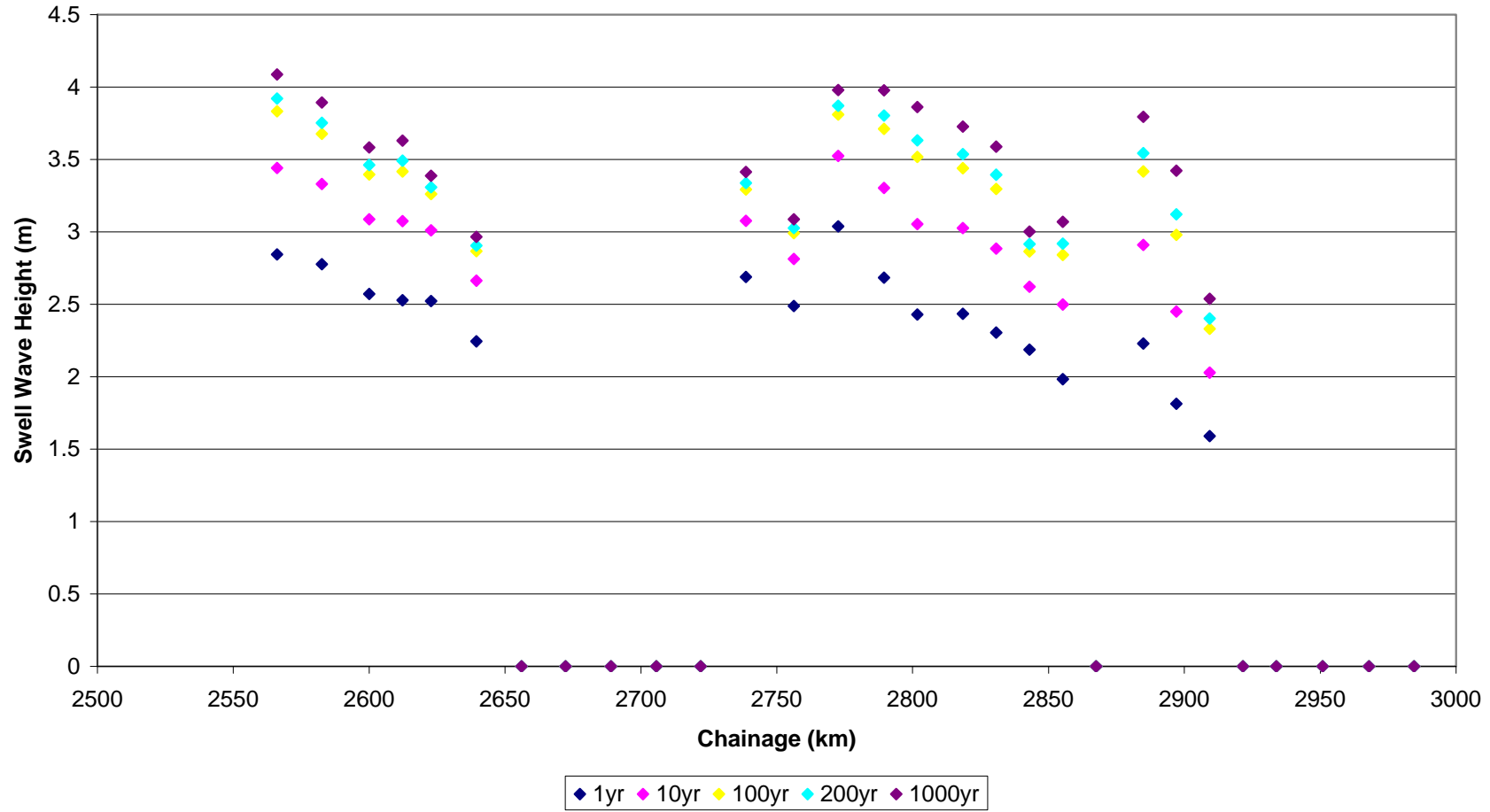
South East Chainage Swell Wave Heights from the South West
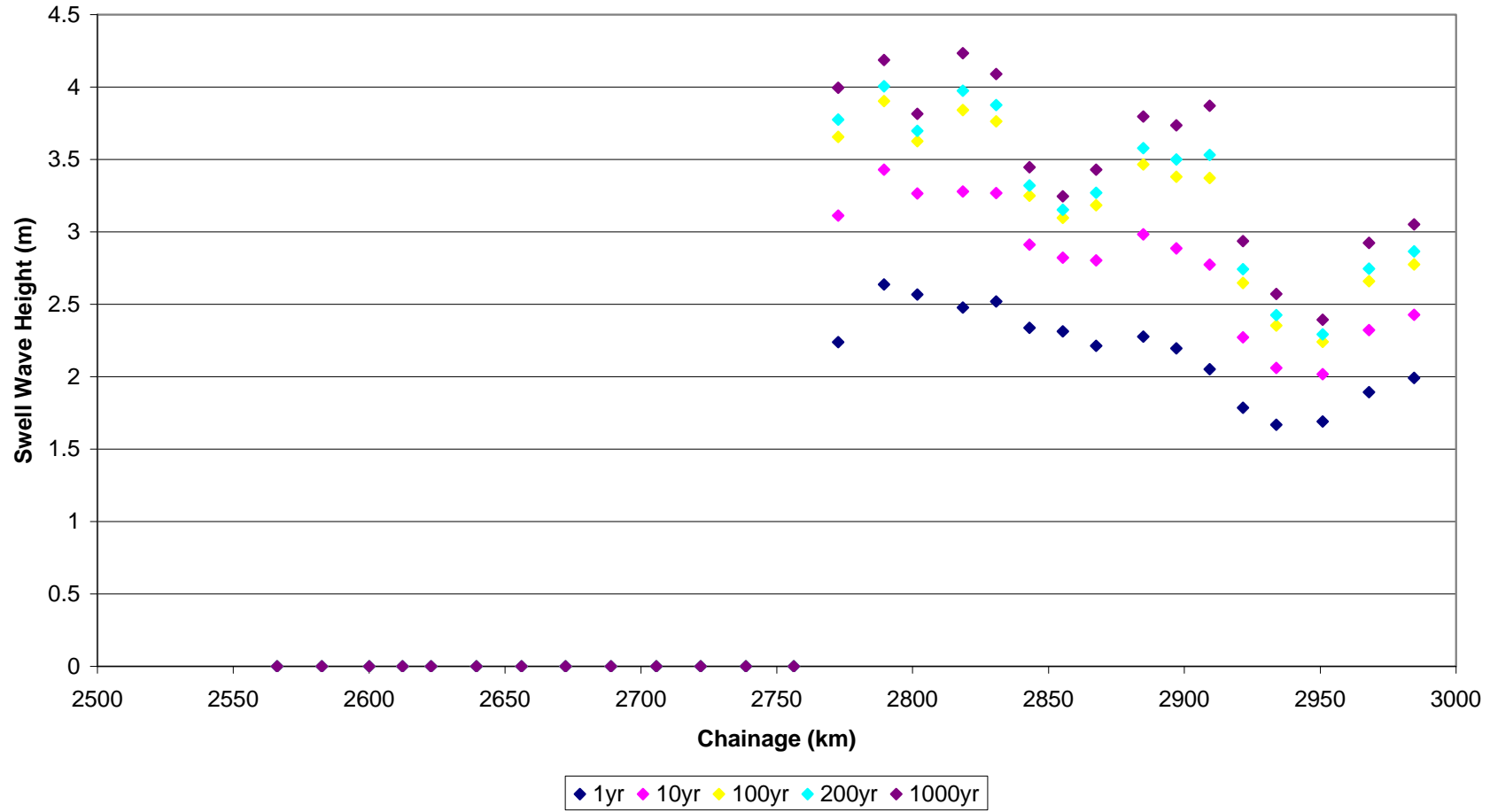
South East Chainage Swell Wave Heights from the North West

South West Chainage Swell Wave Heights from the North

Swell Wave Height (m) vs Chainage (km)

Legend: 1yr ◆ 10yr ◆ 100yr ◆ 200yr ◆ 1000yr
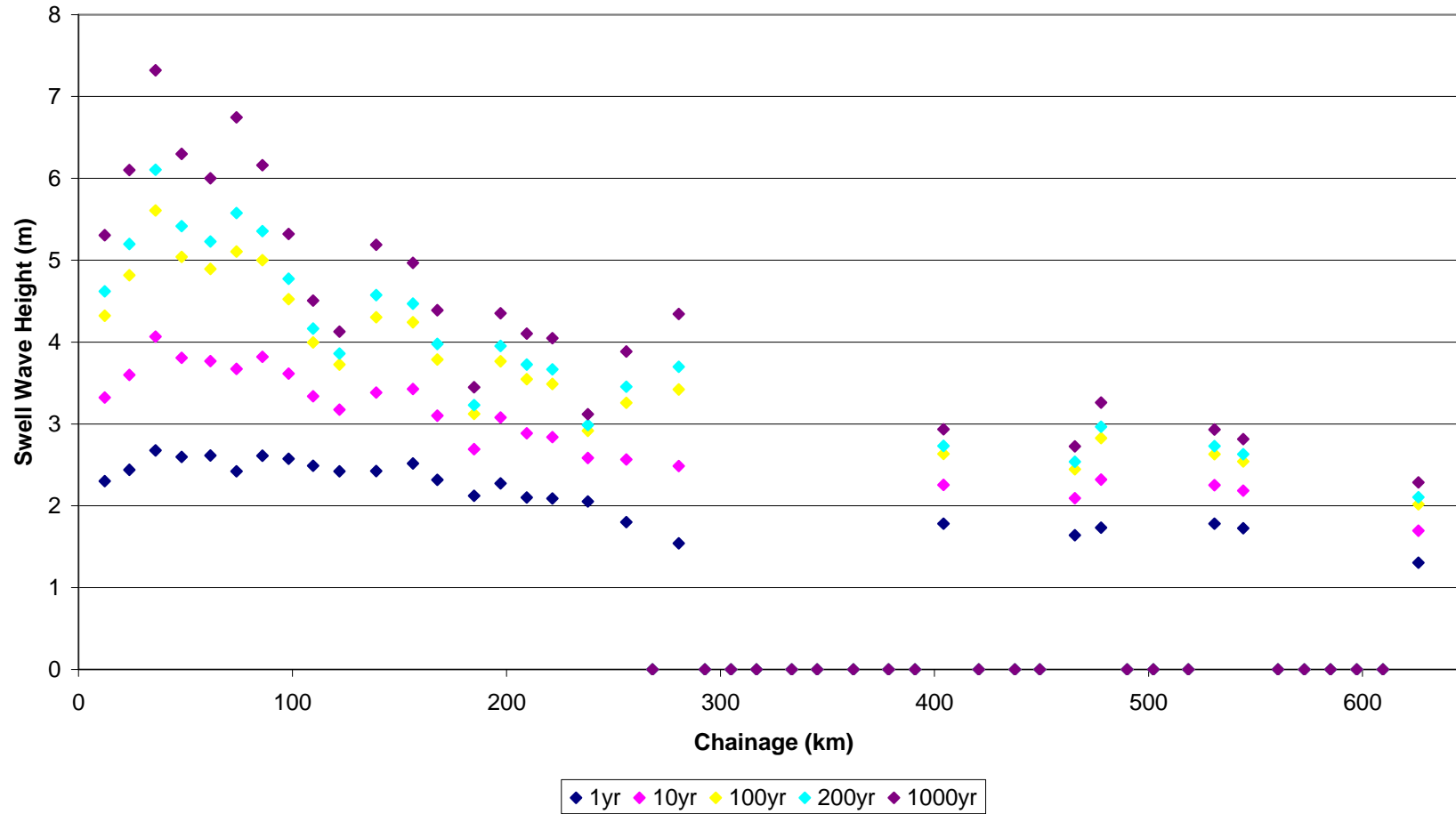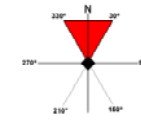
South West Chainage Swell Wave Heights from the North East
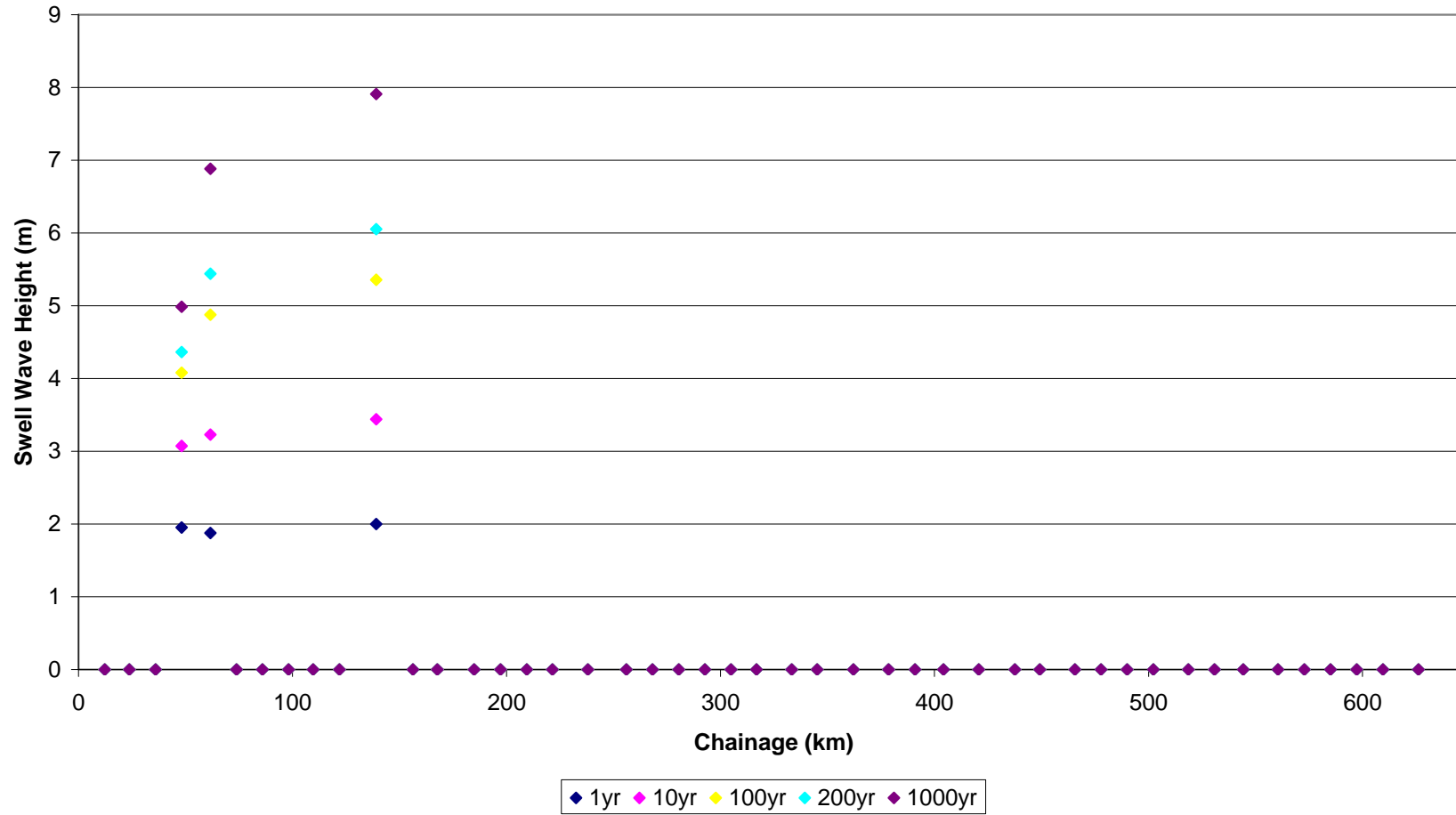
South West Chainage Swell Wave Heights from the South East
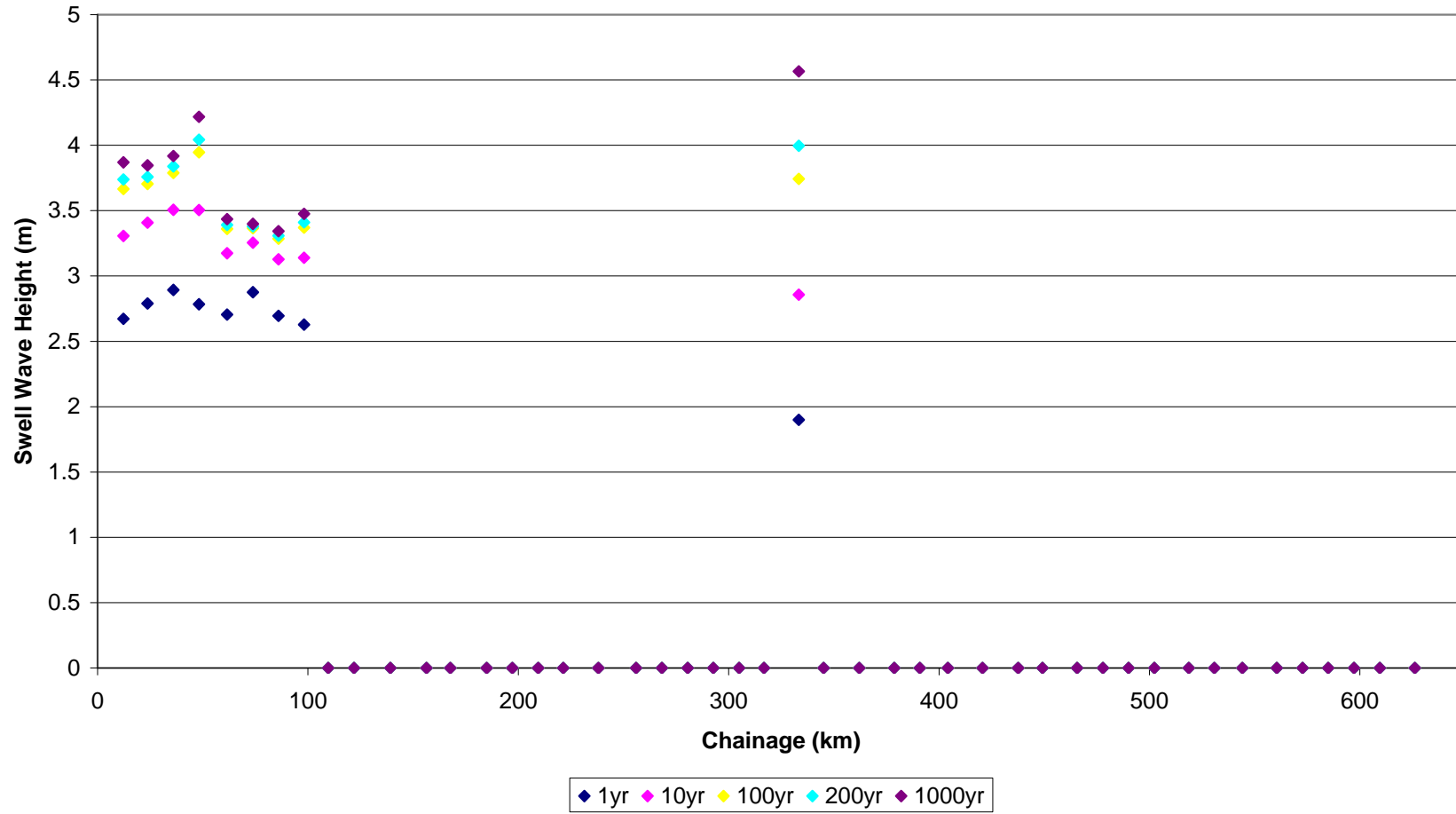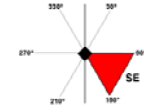
South West Chainage Swell Wave Heights from the South
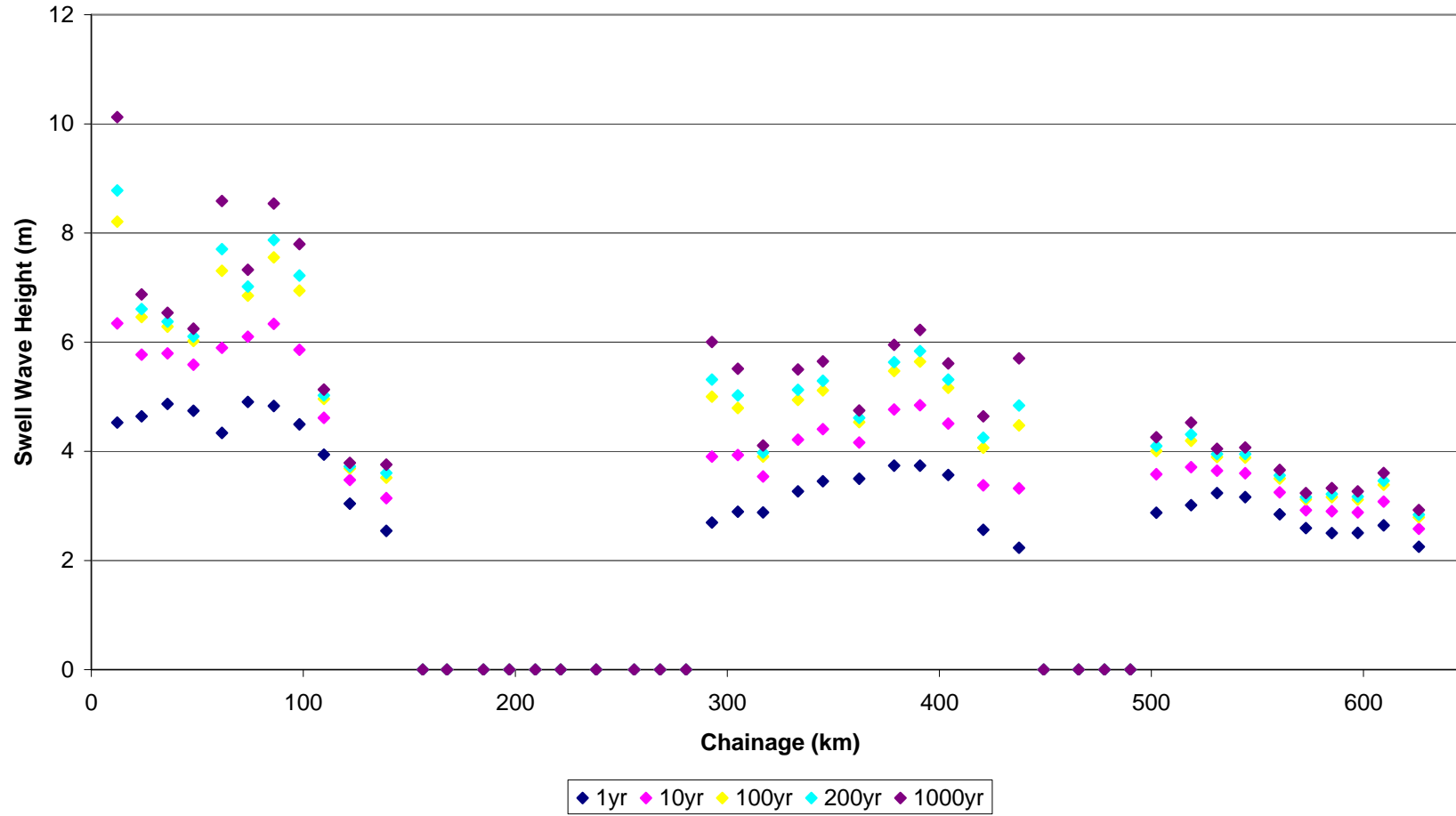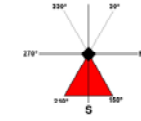
South West Chainage Swell Wave Heights from the South West
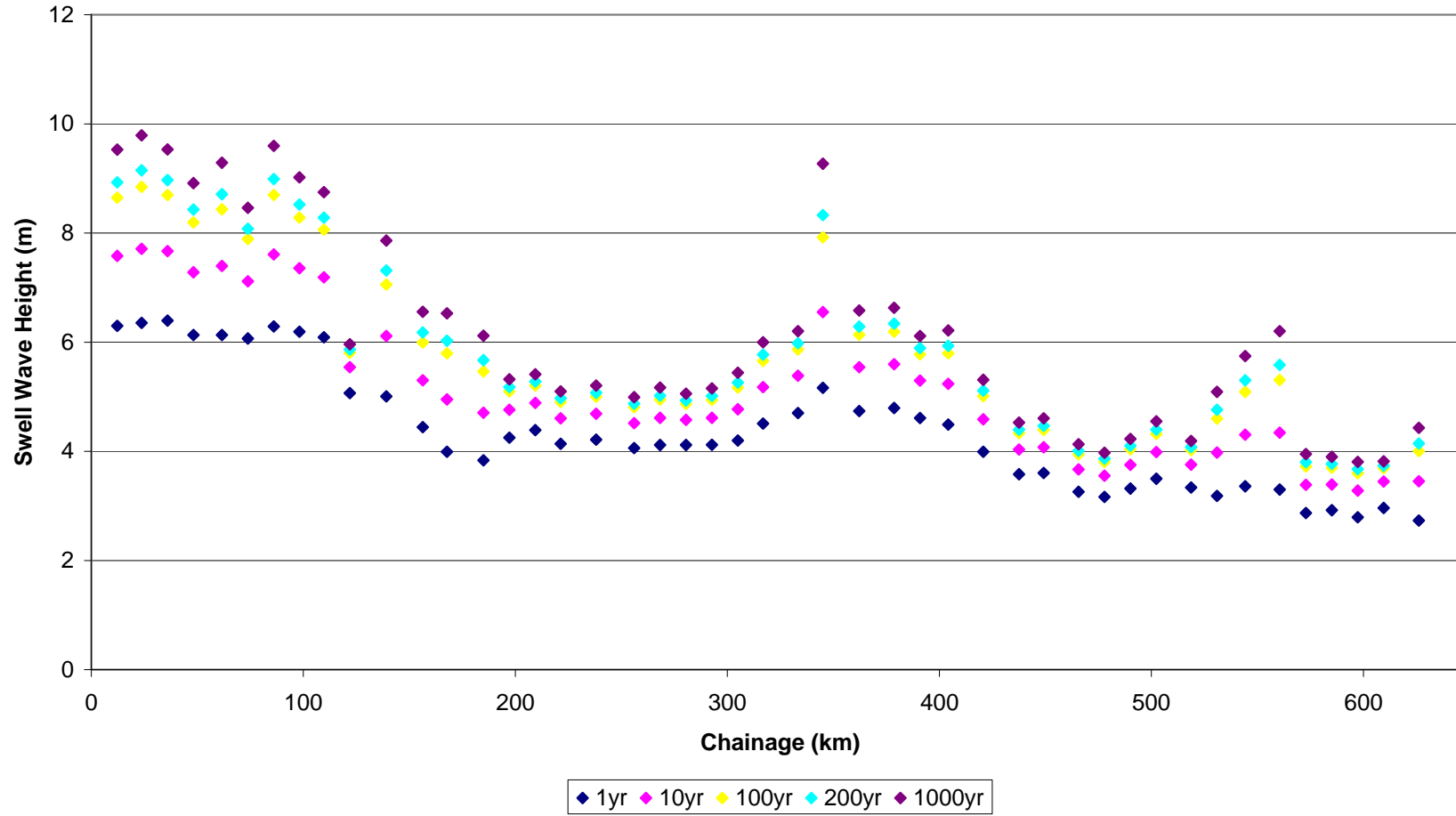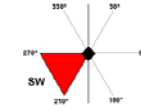
South West Chainage Swell Wave Heights from the North West

Swell Wave Height (m) vs Chainage (km)

Legend: 1yr, 10yr, 100yr, 200yr, 1000yr
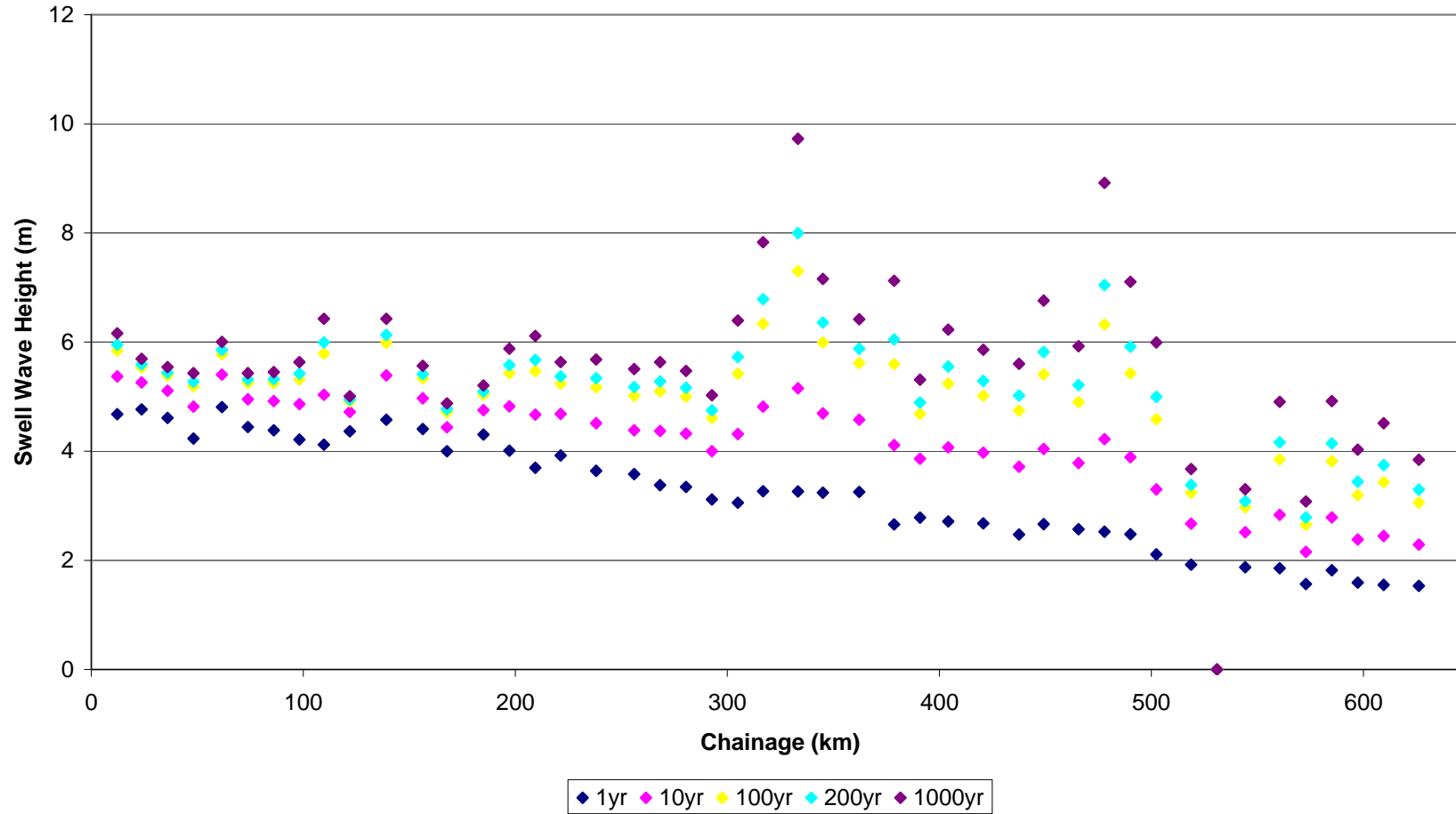
West Chainage Swell Wave Heights from the North
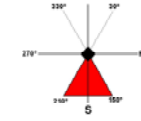
West Chainage Swell Wave Heights from the North East

Swell Wave Height (m) vs Chainage (km)
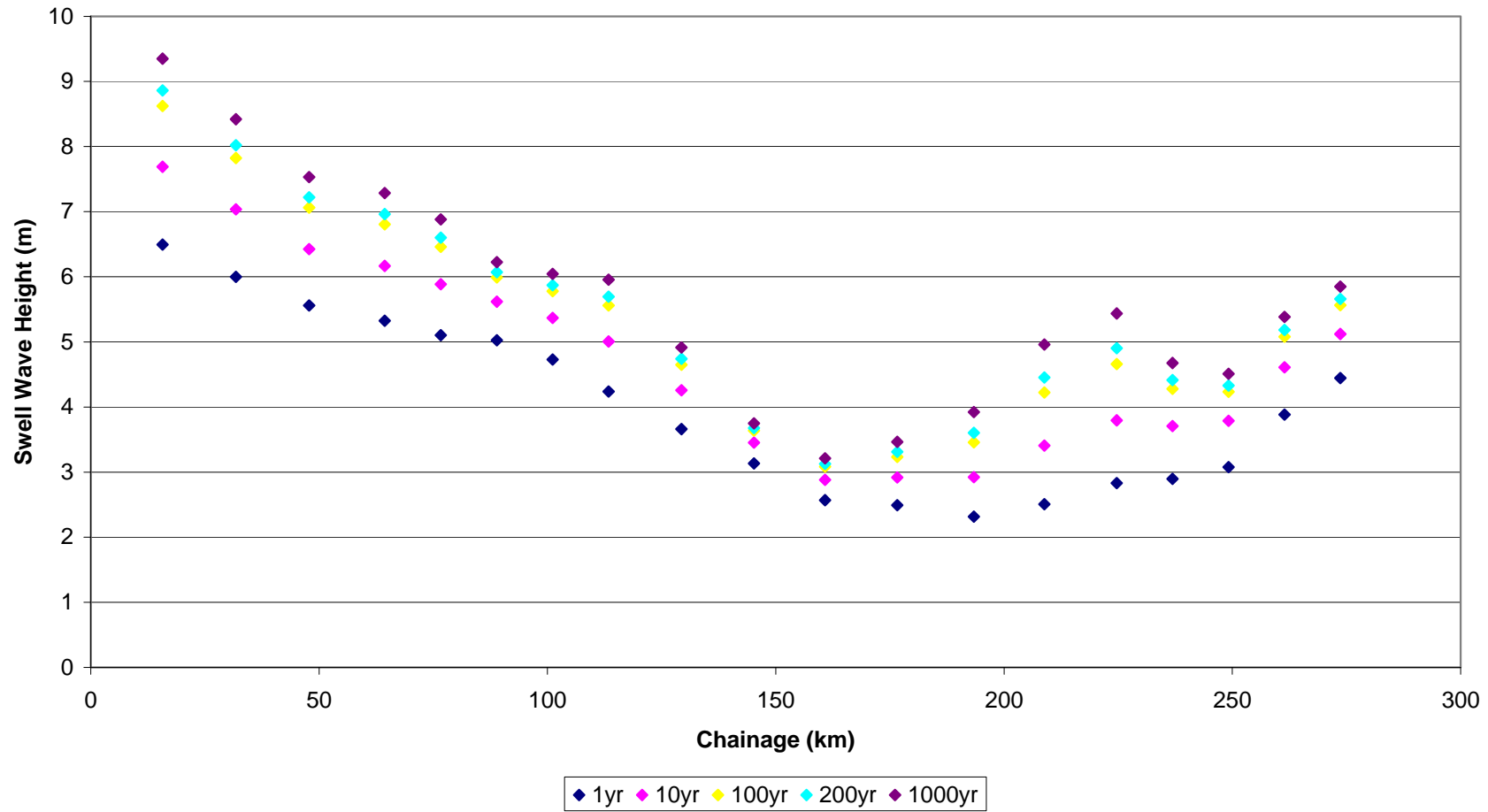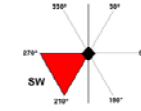
Legend: ◆ 1yr ◆ 10yr ◆ 100yr ◆ 200yr ◆ 1000yr
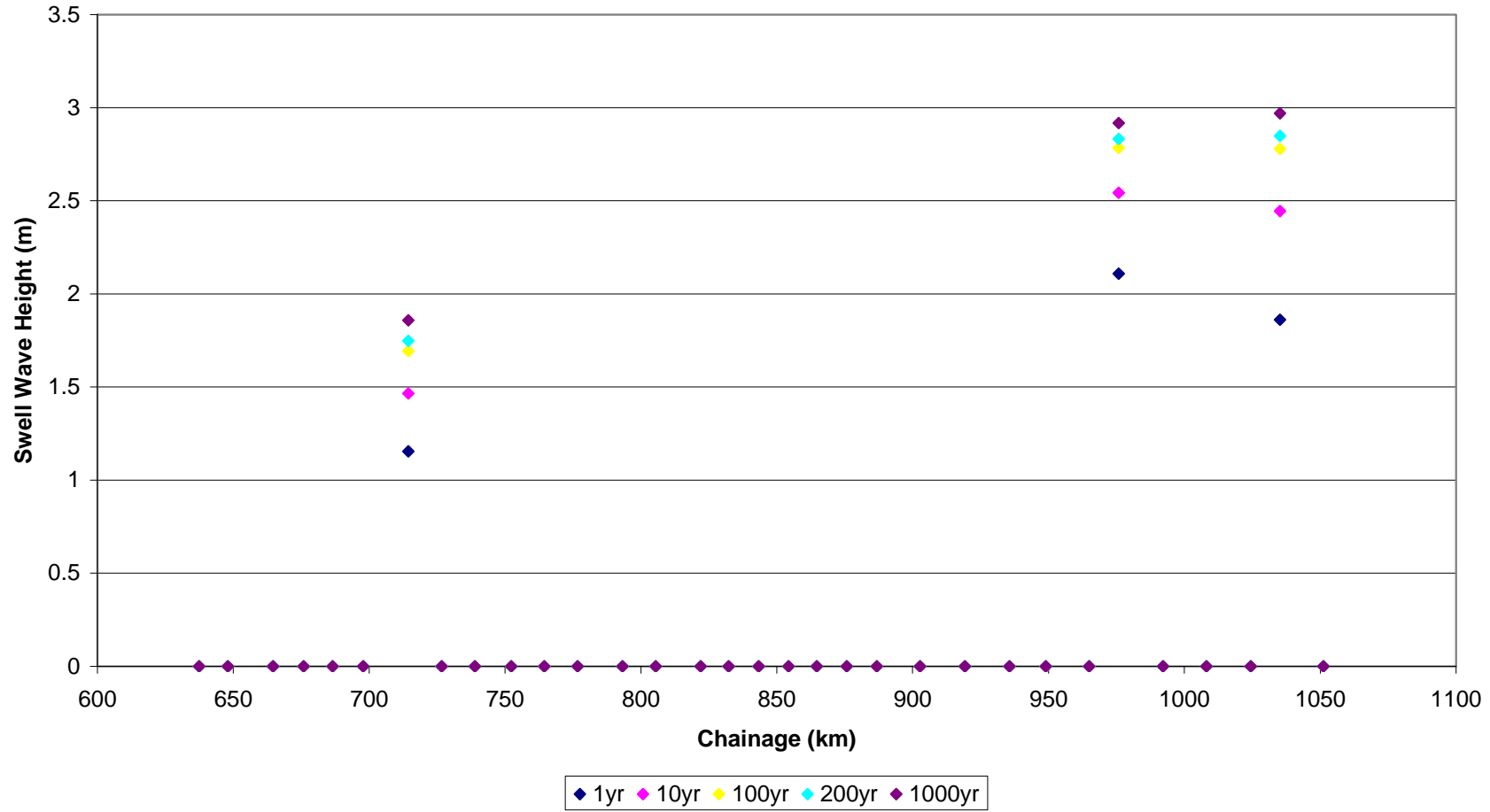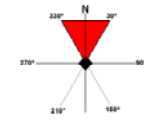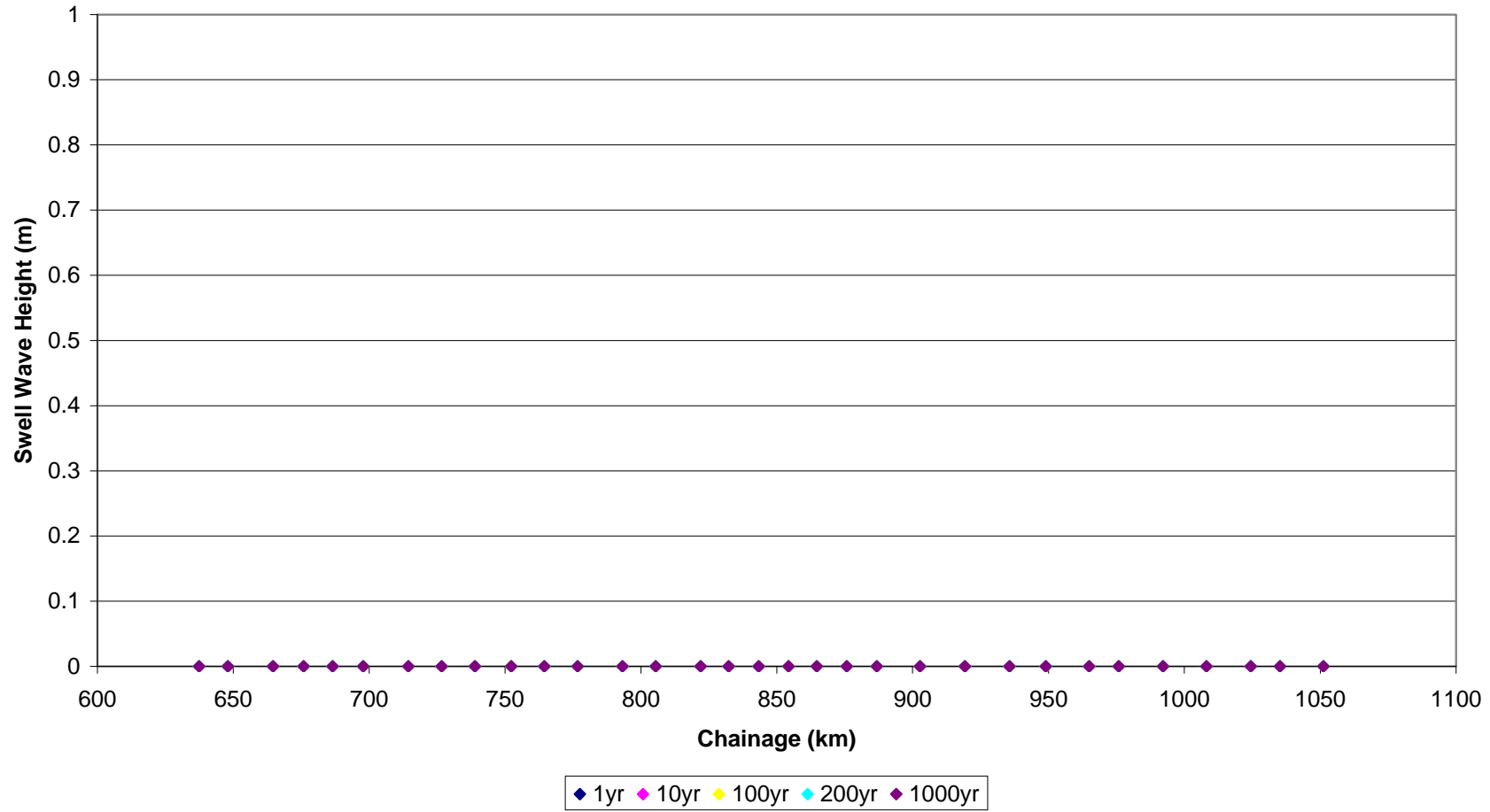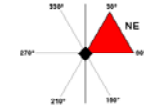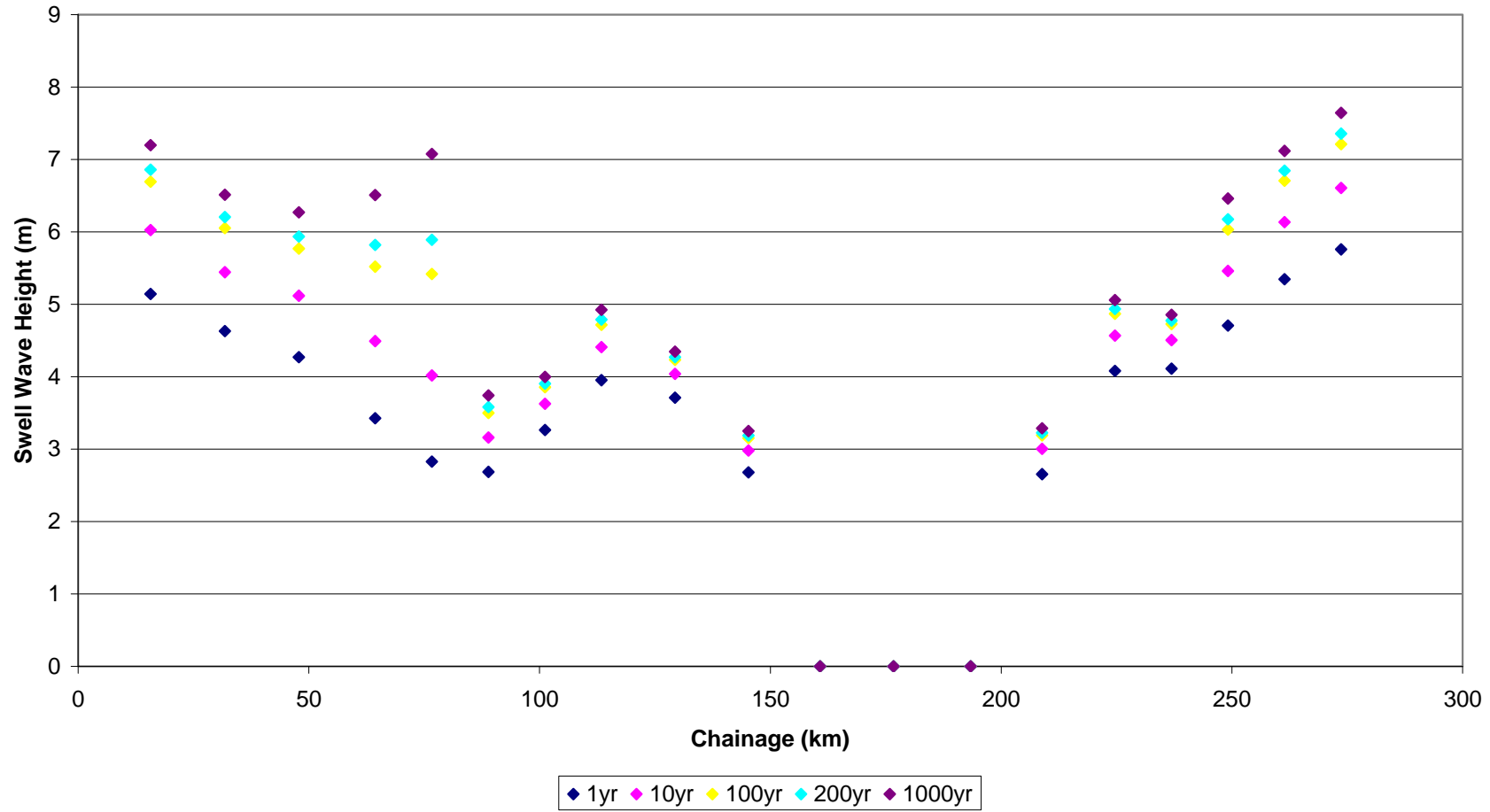
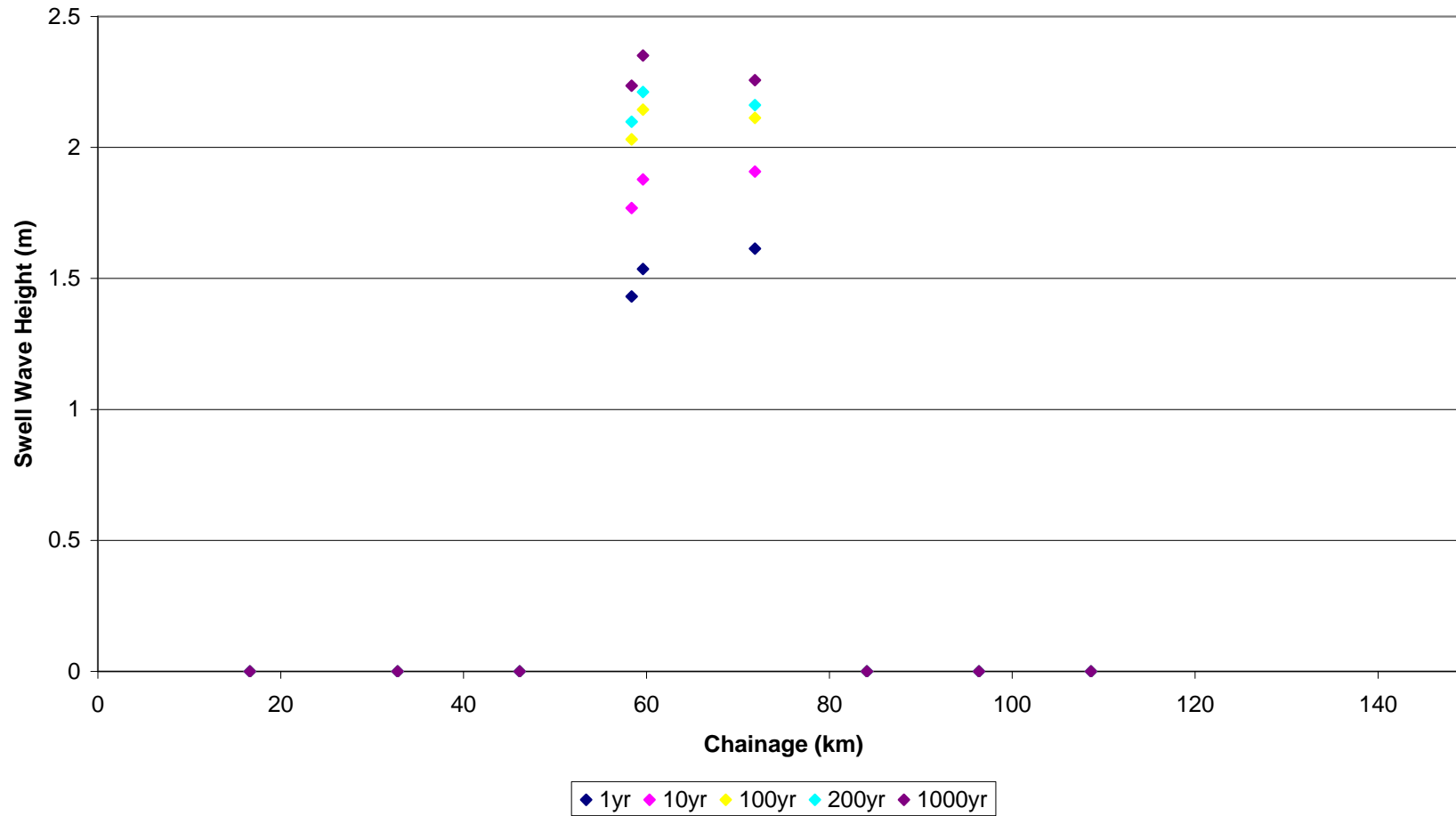# West Chainage Swell Wave Heights from the South East
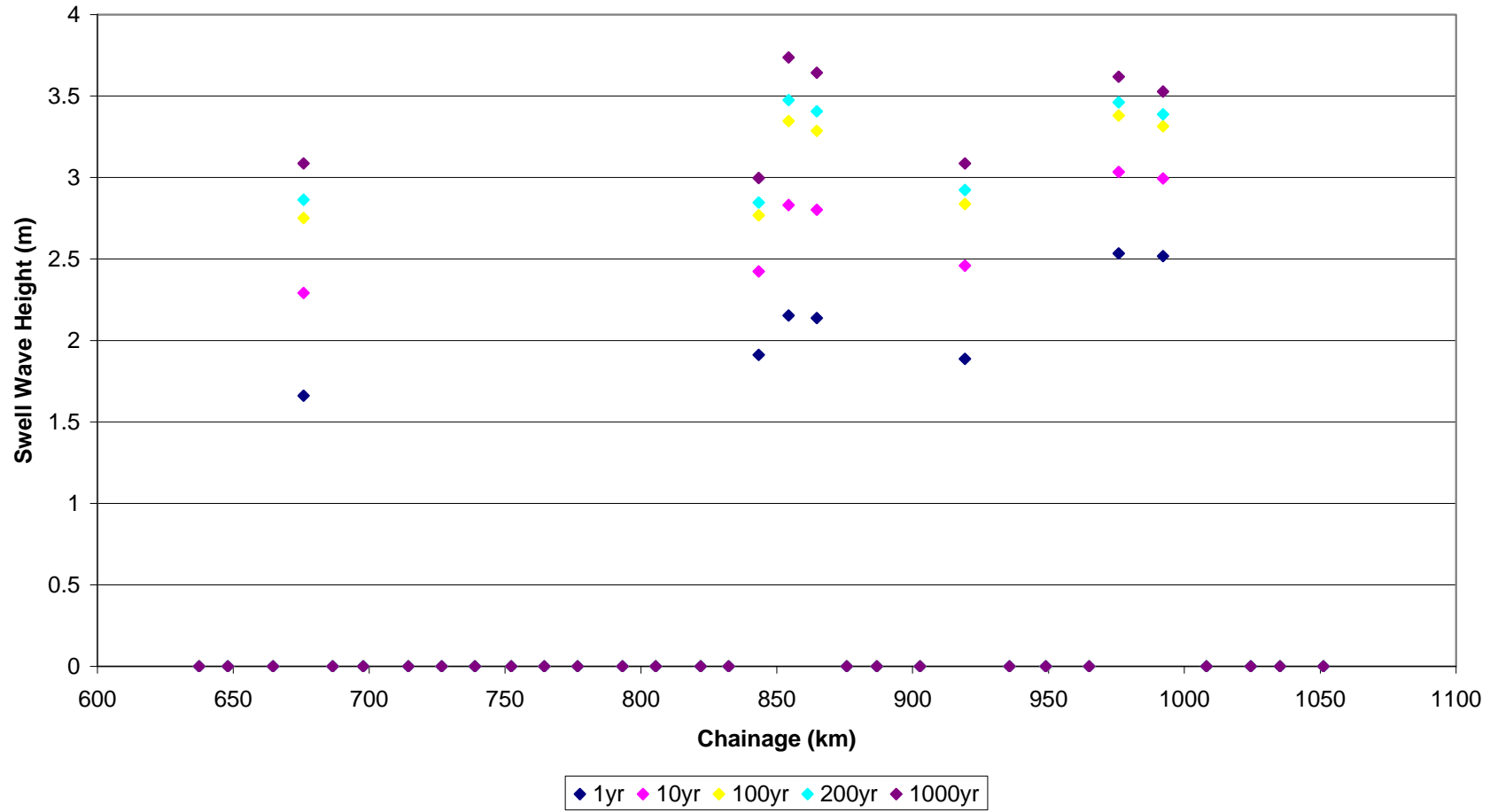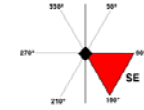
West Chainage Swell Wave Heights from the South

West Chainage Swell Wave Heights from the South West

West Chainage Swell Wave Heights from the North West

Shetland Chainage Swell Wave Heights from the North

Swell Wave Height (m) vs Chainage (km)

Legend: ◆ 1yr ◆ 10yr ◆ 100yr ◆ 200yr ◆ 1000yr

Shetland Chainage Swell Wave Heights from the North East

Swell Wave Height (m) vs Chainage (km)

Legend: ◆ 1yr ◆ 10yr ◆ 100yr ◆ 200yr ◆ 1000yr
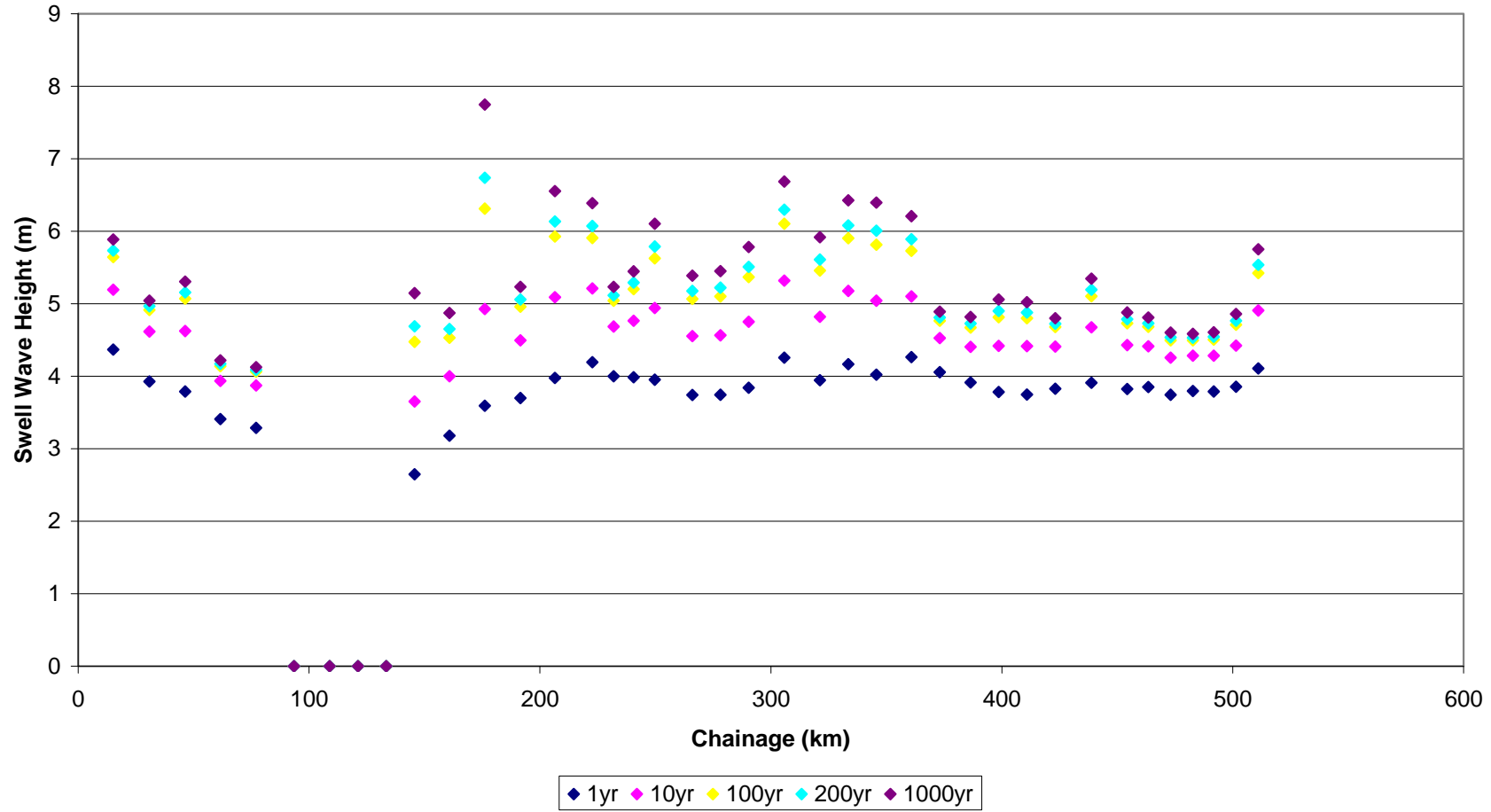
Shetland Chainage Swell Wave Heights from the South East
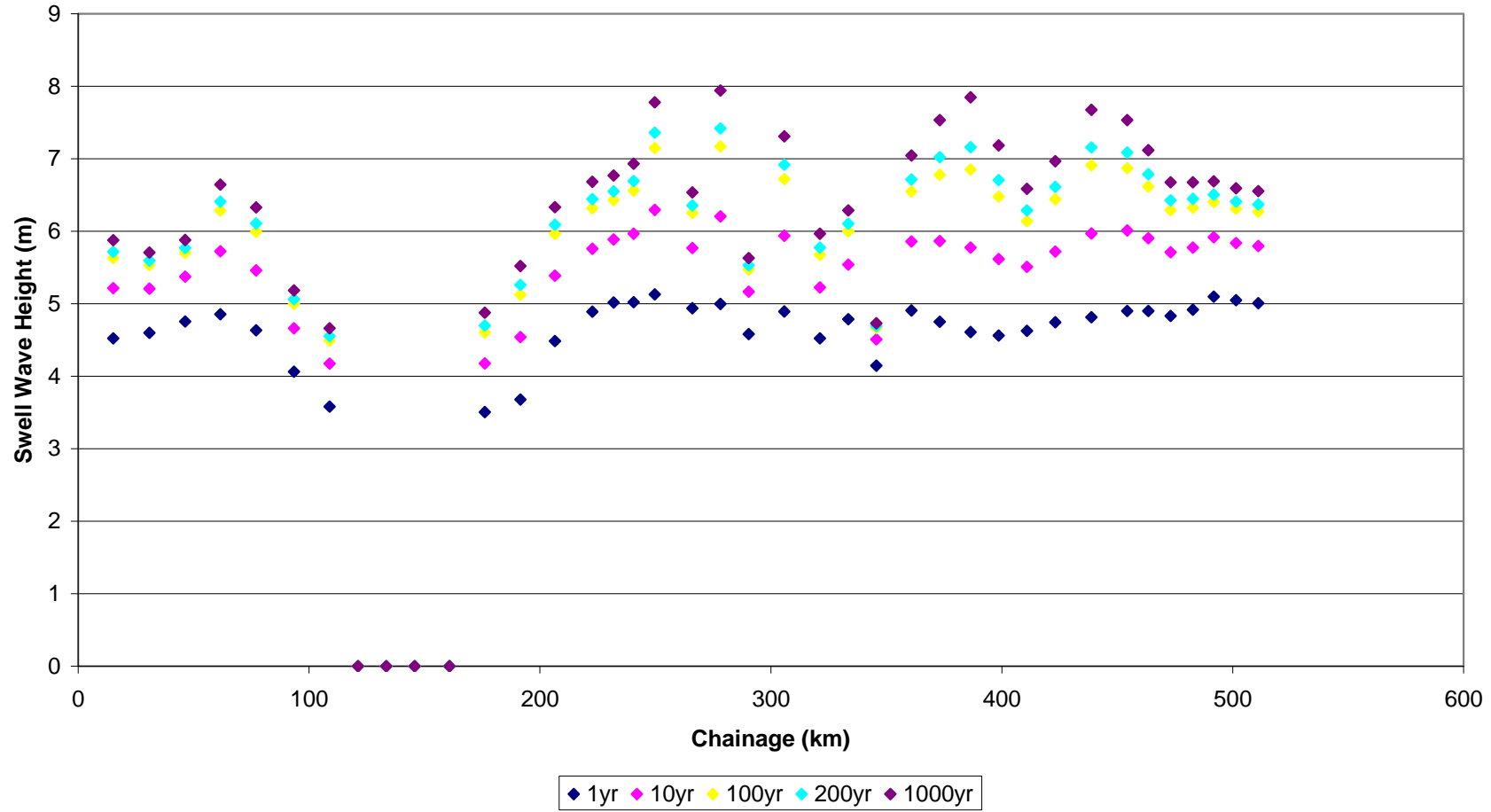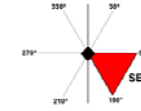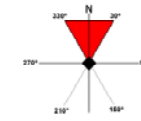
Shetland Chainage Swell Wave Heights from the South

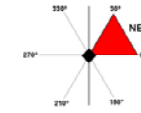# Shetland Chainage Swell Wave Heights from the South West

Shetland Chainage Swell Wave Heights from the North West

Bristol Channel Chainage Swell Wave Heights from the North, Northeast, Southeast and South

Swell Wave Height (m) vs Chainage (km)

Legend: ◆ 1yr ◆ 10yr ◆ 100yr ◆ 200yr ◆ 1000yr

Bristol Channel Chainage Swell Wave Heights from the South West

Bristol Channel Chainage Swell Wave Heights from the North West

Hebrides Chainage Swell Wave Heights from the North
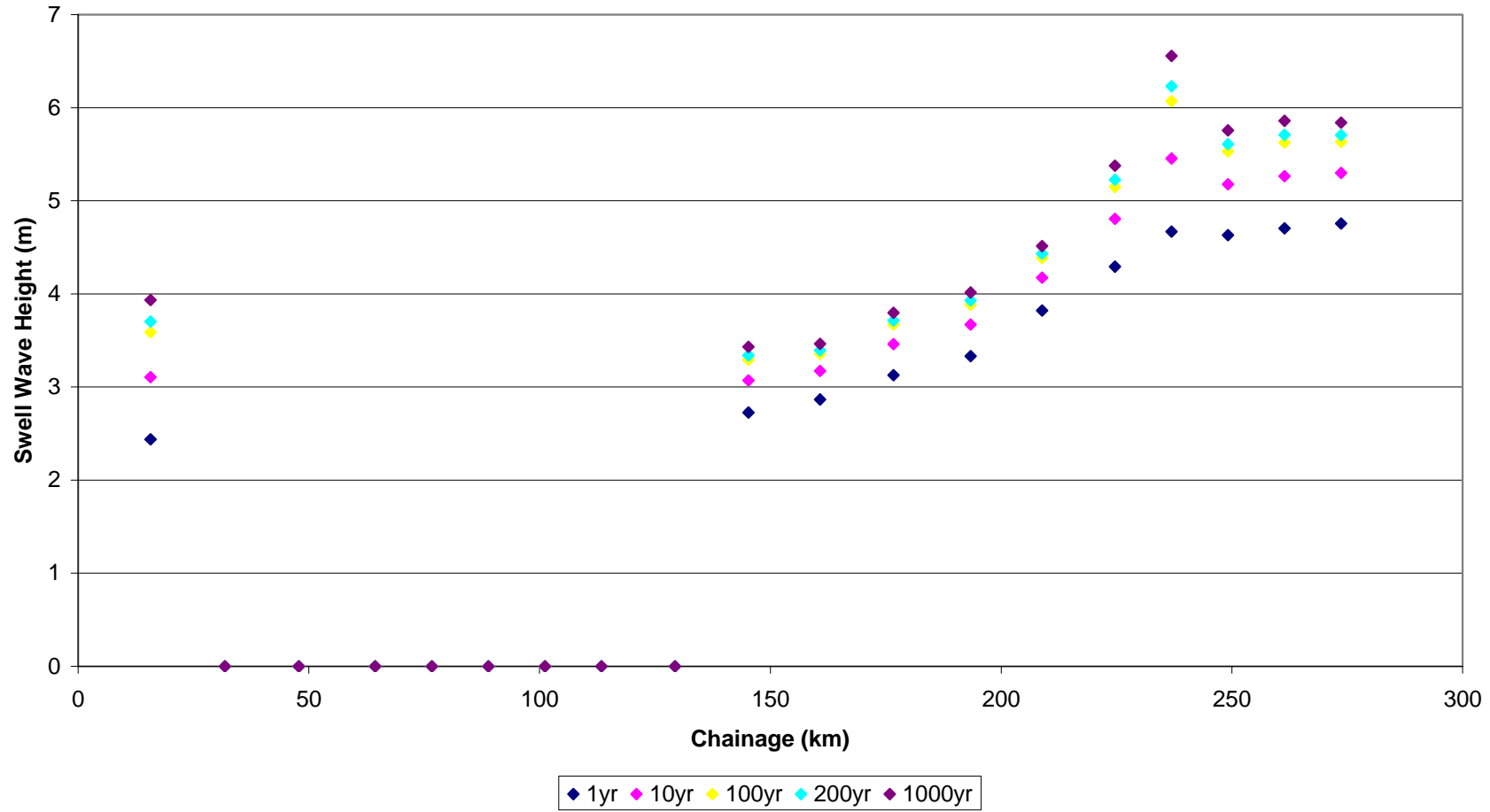
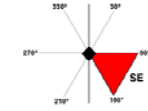Hebrides Chainage Swell Wave Heights from the North East

Hebrides Chainage Swell Wave Heights from the South East
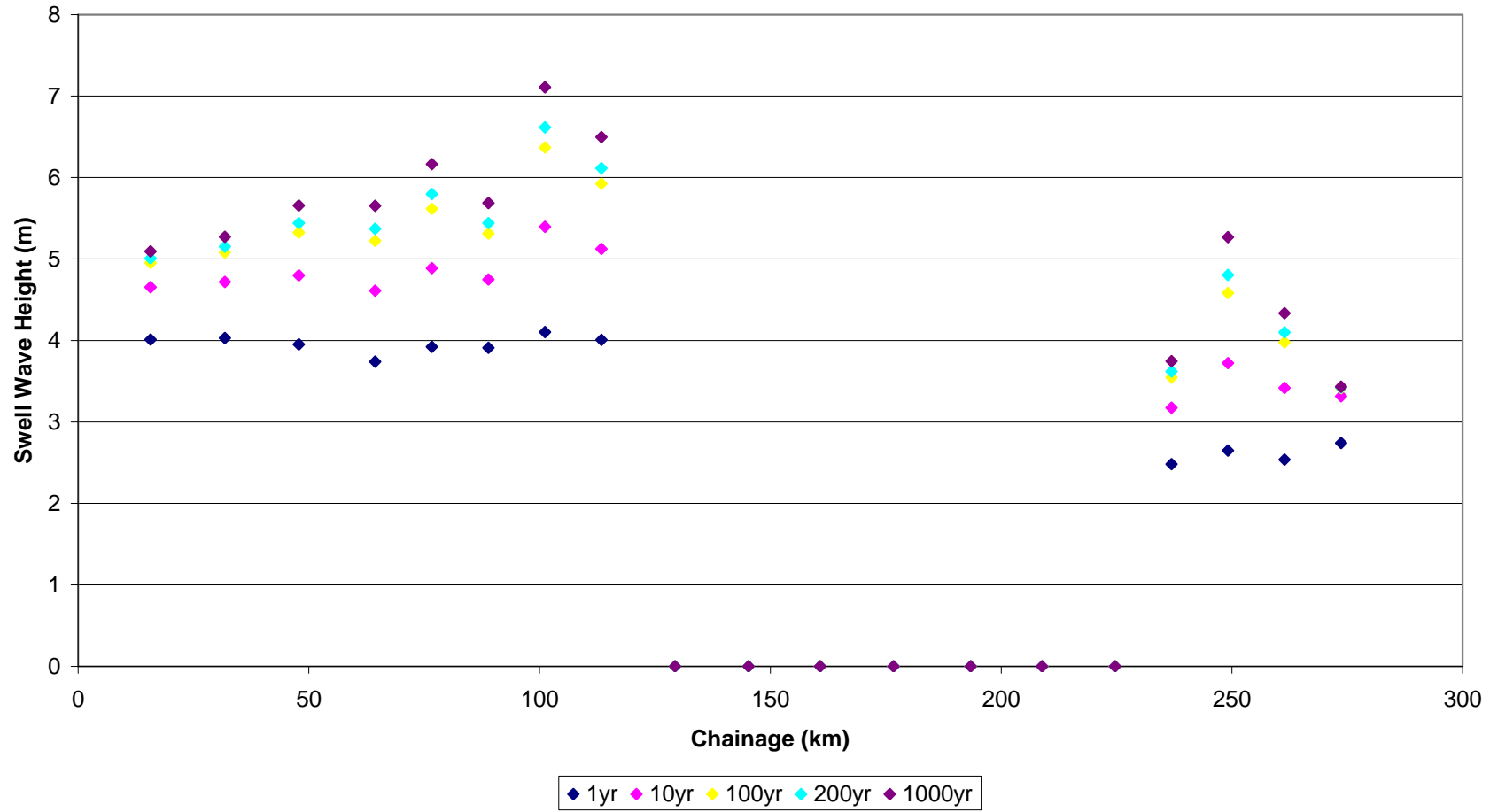
Chart showing Swell Wave Height (m) on the vertical axis (0 to 1) versus Chainage (km) on the horizontal axis (0 to 300). All data points lie along the 0 line.

Legend: ◆ 1yr ◆ 10yr ◆ 100yr ◆ 200yr ◆ 1000yr

Hebrides Chainage Swell Wave Heights from the South

Hebrides Chainage Swell Wave Heights from the South West

Legend: ◆ 1yr ◆ 10yr ◆ 100yr ◆ 200yr ◆ 1000yr

Y-axis: Swell Wave Height (m)

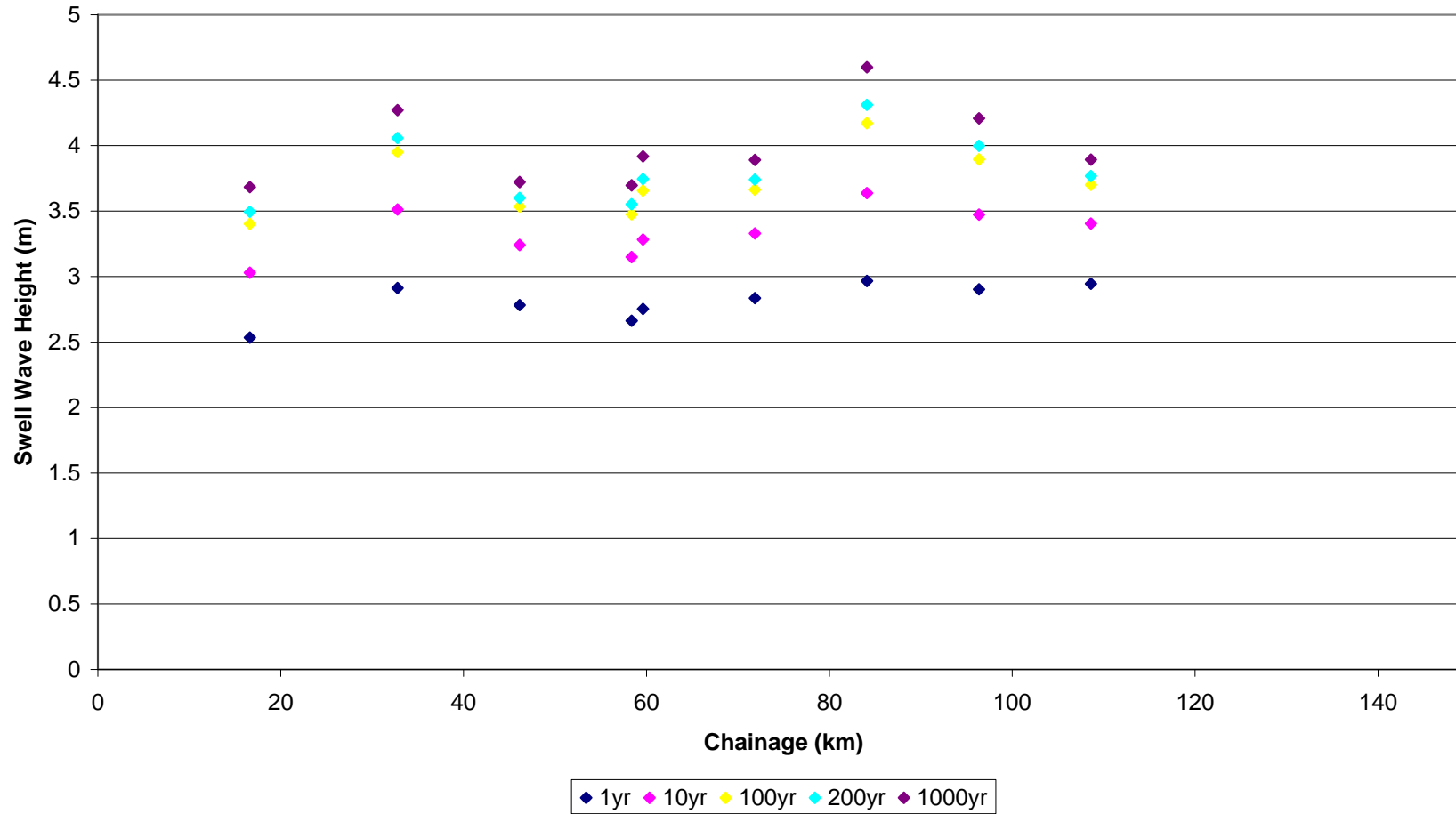X-axis: Chainage (km)

Hebrides Chainage Swell Wave Heights from the North West
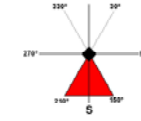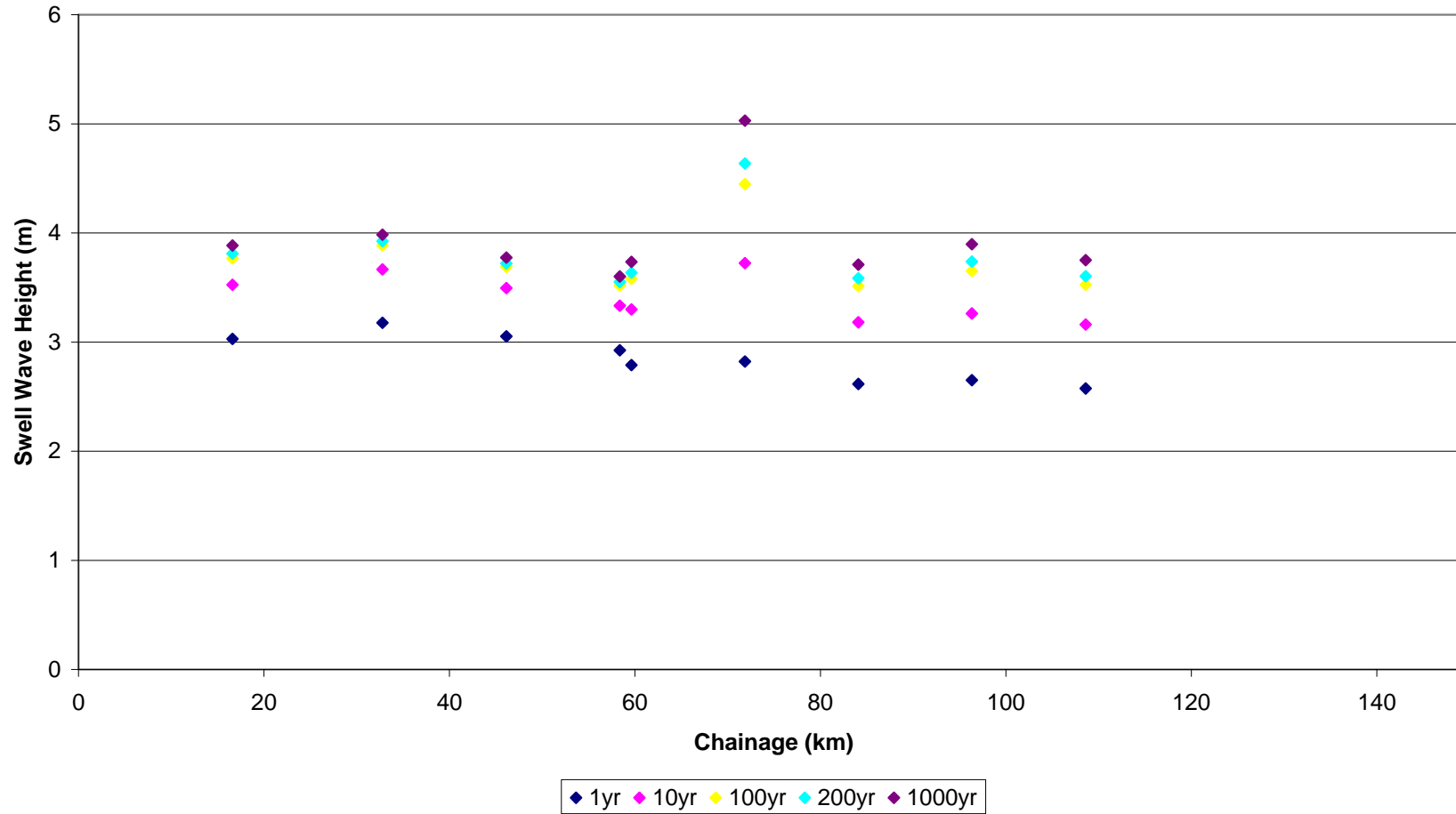
Isle of Man Chainage Swell Wave Heights from the North

Isle of Man Chainage Swell Wave Heights from the North East

Chart showing Swell Wave Height (m) on the y-axis (0 to 1) versus Chainage (km) on the x-axis (0 to 140). Data points for all return periods lie along the zero line.

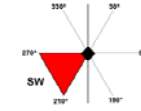Legend: ◆ 1yr ◆ 10yr ◆ 100yr ◆ 200yr ◆ 1000yr
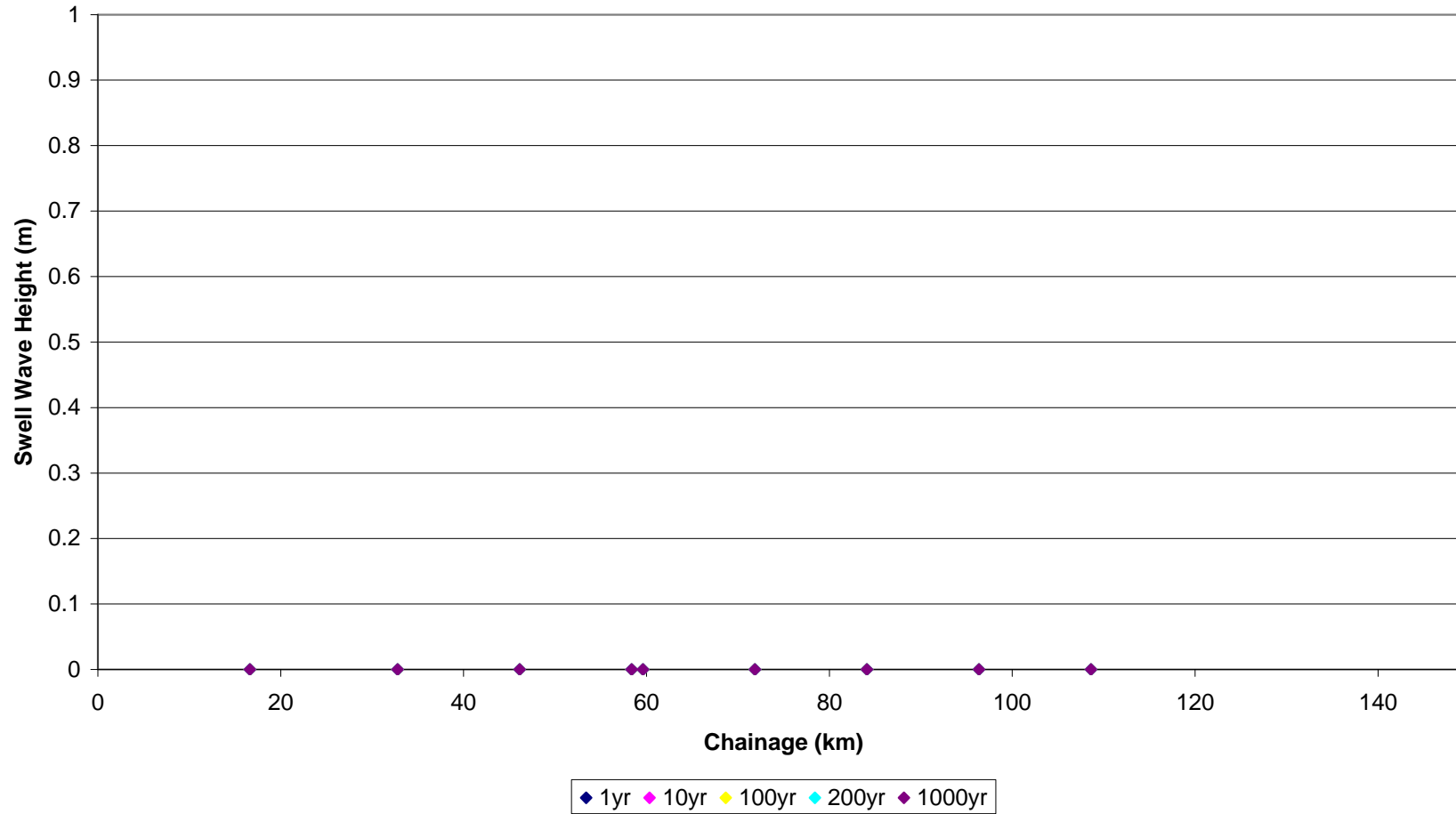
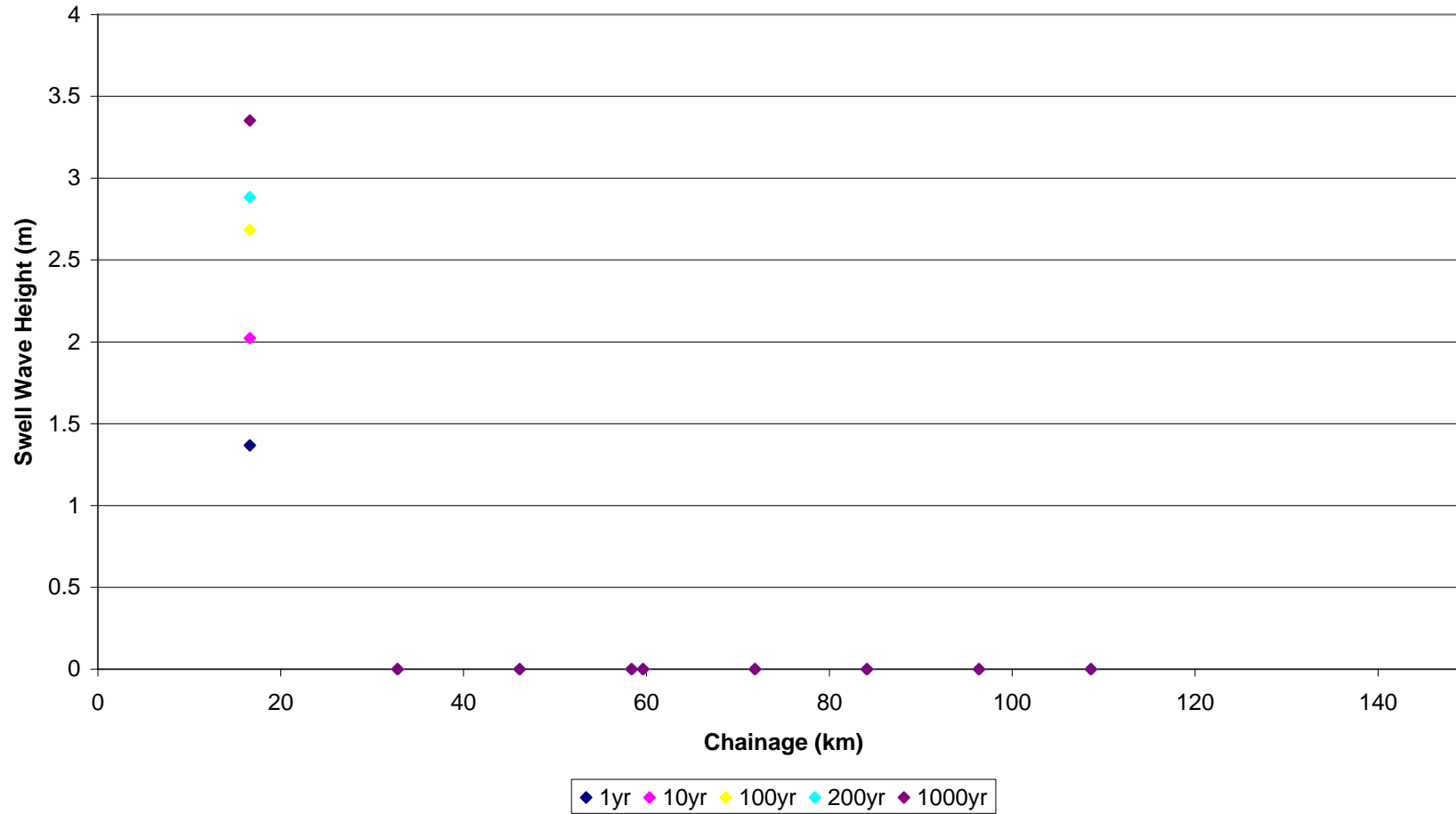# Isle of Man Chainage Swell Wave Heights from the South East
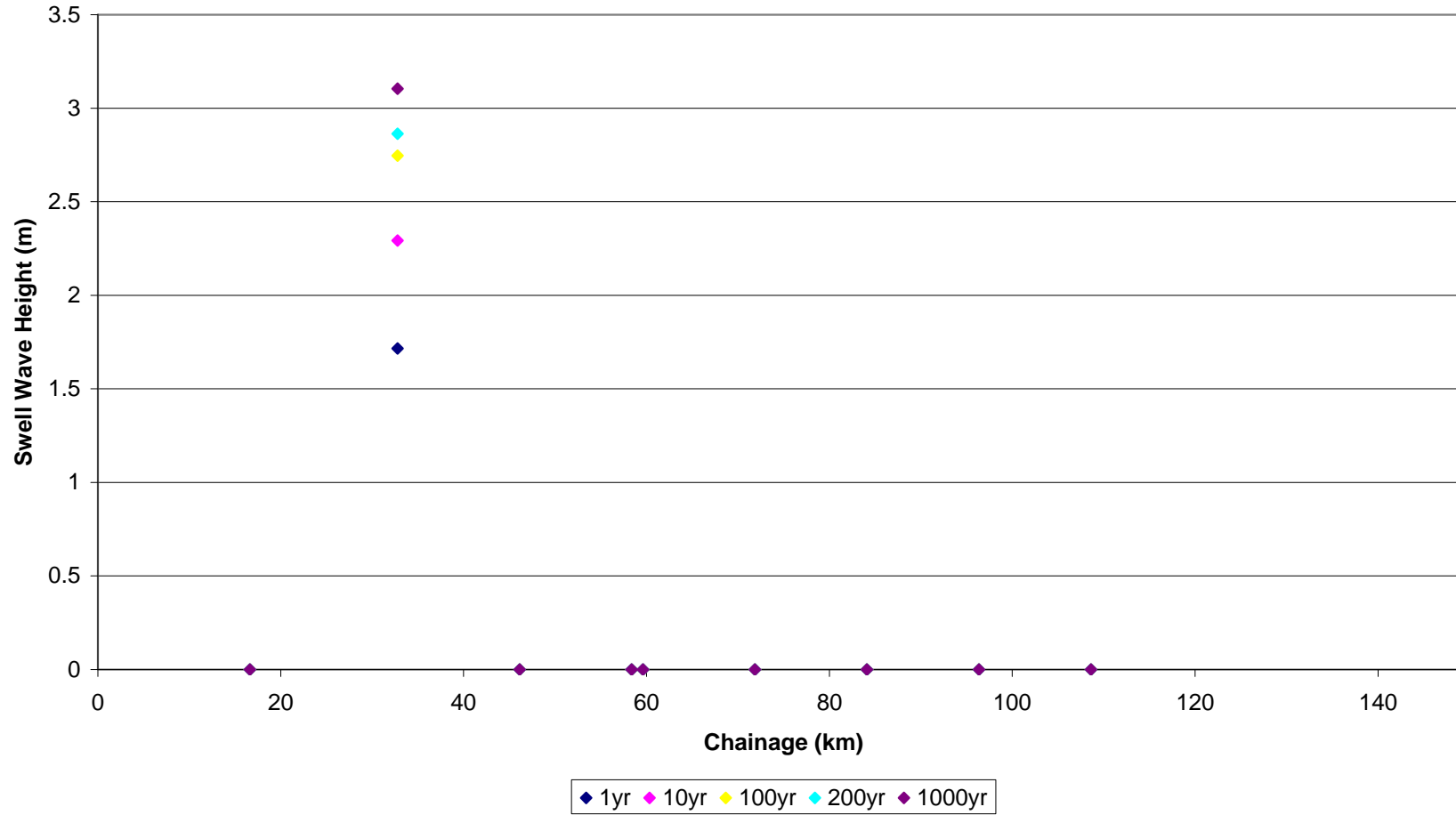
Isle of Man Chainage Swell Wave Heights from the South

Isle of Man Chainage Swell Wave Heights from the South West

Isle of Man Chainage Swell Wave Heights from the North West

We are The Environment Agency. It's our job to look after your environment and make it **a better place** – for you, and for future generations.

Your environment is the air you breathe, the water you drink and the ground you walk on. Working with business, Government and society as a whole, we are making your environment cleaner and healthier.

The Environment Agency. Out there, making your environment a better place.

.

Would you like to find out more about us, or about your environment?

Then call us on
08708 506 506[*](Mon-Fri 8-6)

email
enquiries@environment-agency.gov.uk

or visit our website
www.environment-agency.gov.uk

incident hotline 0800 80 70 60 (24hrs)
floodline 0845 988 1188

* Approximate call costs: 8p plus 6p per minute (standard landline).
Please note charges will vary across telephone providers

Environment first:This publication is printed on recycled paper.